UNIVERSITY OF
LEICESTER

Expression and function of S100A4 in B-cell lymphomas

This thesis submitted for the degree of Doctor of Philosophy at the University of Leicester

By

Zamzam Almutairi

(BSc. MSc.)

Cancer Studies and Molecular Medicine

College of Medicine and Psychology

September 2018

Expression and function of S100A4 in B-cell lymphomas

Zamzam Almutairi

Abstract

B-cell lymphomas are clinically, pathologically and molecularly heterogeneous diseases. Multiple studies have been focused on the analysis of the mechanism of B-cell lymphoma progression, search for novel prognostic markers and development of new treatment approaches. In the current project, the research focus was on the analysis of the expression of S100 proteins in B-cell malignancies. S100 proteins are small, calcium-binding proteins, which are expressed in normal and pathological conditions in cell-specific fashion. They comprise a protein family with more than 20 members. S100 proteins are implicated in various biological processes including cell proliferation and migration, cell signalling, and intercellular communications. S100 proteins don't possess any enzymatic activities, but they participate in transferring calcium signals via interactions with their protein targets. An association between S100 protein expression and cancer was studied in different solid malignancies. Expression of several members of the S100 protein family correlates with the outcome of the disease in different types of epithelial tumours. Therapeutic value of pharmacological targeting of S100 proteins in solid tumours has been discussed. In this study, expression and function of S100 family members was investigated in the peripheral blood and solid tumours of B-cell lymphoma patients. B-cells were purified from the blood samples of healthy volunteers (combined fractions from 5 individuals) and CLL patients. Following RNA isolation, expression of 23 *S100* genes was analysed by RT-PCR. Strong activation of *S100A4* and *S100A6* transcription was detected in malignant B-cells. Western blot analysis of 20 samples prepared from the peripheral blood of the CLL patients confirmed high expression level of S100A4, but not S100A6 in most samples. Therefore, further research was focused on the study of the expression and function of S100A4 protein. Immunohistochemical analysis of 60 blocks of different B-cell lymphomas has demonstrated enhanced expression of S100A4 in the majority of CLL, MCL, DLBCL cases, but not FL. Low or no expression of S100A4 correlated with a longer survival among CLL patients. Although the results were obtained in a relatively small group of patients, data indicate that S100A4 protein may serve as a prognostic marker in CLL. The prognostic significance of S100A4 expression in CLL warrants further investigations. In normal blood and tissue samples, expression of S100A4 was detected exclusively in T-cells and not in B-cells. Immunofluorescent analysis has shown that S100A4 is co-expressed with stem cell markers, CD34, CD133 indicating its potential role in cancer cell stemness. Modulation of S100A4 expression by RNA-interference demonstrated that S100A4 promotes in vitro chemotaxis of B-cells isolated from the peripheral blood of CLL patients. Migratory potential of CLL cells was significantly reduced by two small molecule compounds inhibiting S100A4 function. In conclusion, the data obtained in this study demonstrate for the first time that S100A4 is activated in malignant B-cells, and promotes their migration and invasion. Expression of S100A4 can be considered for the prognostication of CLL patients. Further preclinical studies involving small molecule inhibitors of S100A4 are needed to evaluate their therapeutic potential.

Acknowledgements

First of all, I would like to thank ALLAH almighty for giving me countless numbers of blessings throughout my life. I would like to express my gratitude to the Government of Kuwait for financially supporting me to do the PhD course.

I was greatly honoured to be given the opportunity to work with Dr Marina Kriajevska who to me was not only a supervisor but also a true supporter in so many ways. I have learnt so much from her and I am so grateful to her for leading, teaching and supporting me endlessly. I would also like to thank Prof Simon Wagner for his continual guidance, support and encouragement. I must also thank Prof Kevin West for helping me during slide screening in the Pathology Department of Leicester Royal infirmary. I would like to thank Dr Ildiko Gyory and Dr Eugene Tulchinsky for advice from time to time and Dr Kees Straatman for his support in imaging slides.

I am also extremely grateful to all members of EMT lab, especially Dr Qais Ibrahim and Noura Alibrahim for their support and help. Also, I would like to thanks the staff of Prof Simon especially Dr Sami Mamand and Afaf Alharthi in Toxicology Unit in Hodgkin Building for their technical advice and assistance. Special thanks go to all lovely staff of the routine and immune laboratories in the Pathology Department of Leicester Royal Infirmary. Thanks to Linda Potter and Angie Gillies in Histopathology Department of University Hospital of Leicester for giving their time to cut the paraffin blocks used in this study.

Many thanks go to Dr Nicolas Sylvius and Dr Spencer Gibson for allowing the access to use the qPCR machine in Adrian Building. Special thanks must go to Dr Sandrine Jayne, Prof Martin Dyer and Sheila Porteous for their help in providing the samples from healthy volunteers and CLL patients. Also, many thanks for Michael Martin who is proofreading this thesis and to Leah Officer, a histopathology manager in Hodgkin Building, for her help when needed.

Most of all, I want to thank my family especially my mother, father, dearest husband Dr Jamal Almutairi, and lovely children (Nouf, Noor, Mohammed and Abdullah) for their love and support, which made it all possible.

List of Contents

List of Tables

List of Figures

List of Abbreviations

5-FU	5-Fluorouracil
B2M	B2 Microglobulin
B-CLL	B-Cell Chronic Lymphocytic Leukaemia
BCR	B Cell Receptor
BLNK	B-Cell Linker Protein
BSA	Bovine Serum Albumin
CDK5	Cyclin-Dependent Kinase 5
CLP	Common Lymphoid Progenitor
CSC	Cancer Stem Cell
CSR	Class Switch Recombination
CXCL12	Chemokine Stromal Cell-Derived Factor 12
Cy3	Cy-3 Conjugate
DAPI	4’,6-Diamidno-2phenyl-Indole Dihydrochloride
DLBCL	Diffuse Large B Cell Lymphoma
DMEM	Dulbecco’s Modified Eagle’s Medium
DZ	Dark Zone
EBF	Early B-Cell Factor
EGF	Epidermal Growth Factor
EMT	Epithelial Mesenchymal Transition
ERK	Extracellular Signal-Regulated Kinase
FBS	Foetal Bovine Serum
FFPE	Formalin-Fixed Paraffin-Embedded

FITC	Fluorescein Isothiocyanate Conjugate
FL	Follicular Lymphoma
FLIPI	Follicular Lymphoma International Prognostic Index
Flt3	Fms-Like Tyrosine Kinase 3
GC	Germinal Centre
GEMM	Genetically Engineered Mouse Model
Gra	Granulocytes
HDACs	Histone Deacetylases
HIF1	Hypoxia-Inducible Factor 1
HSC	Hematopoietic Stem Cell
IGH	Immunoglobulin Heavy Chain
IHC	Immunohistochemistry
ITAMs	Immunoreceptor Tyrosine Activation Motifs
LDH	Lactate Dehydrogenase
LH	Light Chain
LSC	Leukaemia Stem Cell
LZ	Light Zone
MALT	Mucosa-Associated Lymphoid Tissue Lymphoma
MBDs	Methyl-Cpg-Binding Domain Proteins
MCL	Mantle Cell Lymphoma
MCL1	Myeloid Cell Leukaemia 1
Meg	Megakaryocyte
Meta-M	Metamyelocytes
MLL-AF4	Mixed Lineage Leukaemia Gene

MMP	Matrix Metalloproteinase
MPPs	Multipotent Progenitor Cells
MRD	Minimal Residual Disease
Mye	Myeloblast
MZL	Marginal Zone Lymphoma
NF-κB	Nuclear Factor KappaB
NHL	Non-Hodgkin Lymphoma
NMZL	Nodular Marginal Zone Lymphoma
NOS	Not-Otherwise Specified
PCR	Polymerase Chain Reaction
PDGF	Platelet-Derived Growth Factor
PFS	Progression-Free Survival
PGE2	Prostaglandin E2
PKA-C	Protein Kinase A Catalytic
Rag-1	Recombination-Activating Gene 1
Rag-2	Recombination-Activating Gene 2
RAGE	Receptor For Advanced Glycation End Products
RPMI-1640	Rosewell Park Memorial Institute 1640
RTK	Receptor Tyrosine Kinase
RT-PCR	Reverse Transcription PCR
SCF	Stem-Cell Factor
SDF-1	Stromal Cell-Derived Factor 1
SHM	Somatic Hyper-Mutation
siRNA	Small Interference RNA

SMZL	Splenic Marginal Zone Lymphoma
T-ALL	T-Cell Acute Lymphoblastic Leukemia
TdT	Terminal Deoxynucleotidyl Transferase
TNF	Tumour Necrosis Factor
TRITC	Rhodamine Conjugate
VH	Variable Heavy Chain
ZAP-70	Zeta-Chain-Associated Protein Kinase 70

Chapter 1. Introduction

1.1 Lymphoproliferative neoplastic disorders

Metastatic cancer is thought to be the leading cause of death worldwide. For instance, in the UK, in 2016, there were around 162,000 deaths from cancer. This means that more than one person dies every four minutes due to cancer (Cancer Research, UK, 2016). It is widely known that cancer incidence is on the rise largely due to lifestyle and health choices. Research development and early detection have assisted in stabilising mortality rates.

Cancer can be classified according to cell origin. For example, epithelial tissue cancers are called carcinoma, while connective tissue cancers are called sarcoma. Moreover, leukaemia and lymphomas are cancers of the blood cells (Jemal et al., 2011).

Clonal neoplastic transformation of mature and immature B-cells, T-cells, and natural killer (NK) cells are referred to as lymphoid malignancies. Lymphoma is the most common form of blood cancer. There are two main types of lymphoma which are Hodgkin lymphoma and non-Hodgkin lymphoma (NHL). Lymphoma occurs when white blood cells called lymphocytes, which are cells of the immune system, grow and proliferate uncontrollably. Cancerous lymphocytes can be located in many parts of the body, including the lymph nodes, spleen, bone marrow, blood, or other organs, and cause a mass called a tumour. The body has two main types of lymphocytes that can develop into lymphomas: B-lymphocytes (B-cells) and T-lymphocytes (T-cells). In many aspects, these cancer cells correspond to the function and differentiation stages of normal lymphoid cells (Tsukasaki and Tobinai, 2014). After considerable efforts extended over many years performed by a number of clinicians and pathologists from different nations, the WHO published the final hematopoietic and lymphoid malignancies classification (Bagg, 2011; Lenz et al., 2008). This classification of lymphoid neoplasms was updated in 2016. The classification based on pathologic parameters including: morphology/histology, immunophenotype, genetic changes, and clinical features. Table 1.1 shows the classification of B-cells neoplasms while the classification of all lymphoid neoplasms is listed in appendix 1 (Arber et al., 2016).

Mature B-cell neoplasms
Chronic lymphocytic leukemia
Monoclonal B-cell lymphocytosis*
B-cell prolymphocytic leukemia
Splenic marginal zone lymphoma
Hairy cell leukemia
Splenic B-cell lymphoma/leukemia, unclassifiable
Splenic diffuse red pulp small B-cell lymphoma
Hairy cell leukemia-variant
Lymphoplasmacytic lymphoma
Waldenström macroglobulinemia
Monoclonal gammopathy of undetermined significance (MGUS), IgM*
μ heavy-chain disease
γ heavy-chain disease
α heavy-chain disease
Monoclonal gammopathy of undetermined significance (MGUS), IgG/A*
Plasma cell myeloma
Solitary plasmacytoma of bone
Extraosseous plasmacytoma
Monoclonal immunoglobulin deposition diseases*
Extranodal marginal zone lymphoma of mucosa-associated lymphoid tissue (MALT lymphoma)
Nodal marginal zone lymphoma
Pediatric nodal marginal zone lymphoma
Follicular lymphoma
In situ follicular neoplasia*
Duodenal-type follicular lymphoma*
Pediatric-type follicular lymphoma*
Large B-cell lymphoma with IRF4 rearrangement*
Primary cutaneous follicle center lymphoma
Mantle cell lymphoma
In situ mantle cell neoplasia*
Diffuse large B-cell lymphoma (DLBCL), NOS
Germinal center B-cell type*
Activated B-cell type*
T-cell/histiocyte-rich large B-cell lymphoma
Primary DLBCL of the central nervous system (CNS)
Primary cutaneous DLBCL, leg type
EBV+ DLBCL, NOS*
EBV+ mucocutaneous ulcer*
DLBCL associated with chronic inflammation
Lymphomatoid granulomatosis
Primary mediastinal (thymic) large B-cell lymphoma
Intravascular large B-cell lymphoma
ALK+ large B-cell lymphoma
Plasmablastic lymphoma
Primary effusion lymphoma

HHV8+ DLBCL, NOS*
Burkitt lymphoma
Burkitt-like lymphoma with 11q aberration*
High-grade B-cell lymphoma, with MYC and BCL2 and/or BCL6 rearrangements*
High-grade B-cell lymphoma, NOS*
B-cell lymphoma, unclassifiable, with features intermediate between DLBCL and classical Hodgkin lymphoma

Table 1.1 Updated classification of mature B-cell neoplasms.
Provisional entities are listed in italics.↵* Changes from the 2008 classification (Arber et al., 2016). Modified from (Arber et al., 2016).

1.2 B-cell lymphomas

Although 2016 WHO classification shows limited changes compared with the 2008 classification, the updated classification helps to distinguish homogeneous groups of well-defined entities and aids the recognition of rare diseases that need additional clarification (Table 1.1). It has been found that B-cell lymphomas are much more common than T-cell lymphomas. Ninety five percent of lymphoma patients are diagnosed with B-cell lymphoma.

A large data base, 596,476 patients diagnosed with NHL, are used to study the distribution of subtypes of B-cell neoplasms. They found that the major subtypes are diffuse large B-cell (DLBCL) (32.5%), chronic lymphocytic leukaemia/small lymphocytic lymphoma (CLL/SLL) (18.6%), follicular lymphoma (FL) (17.1%), marginal zone lymphoma (MZL) (8.3%), mantle cell lymphoma (MCL) (4.1%), Burkitt lymphoma (BL) (1.6%), hairy cell lymphoma (HCL) (1.1%), lymphoplasmacytic (1.1%), and NHL not-otherwise-specified (10.8%) (Figure 1.1) (Al-Hamadani et al., 2015).

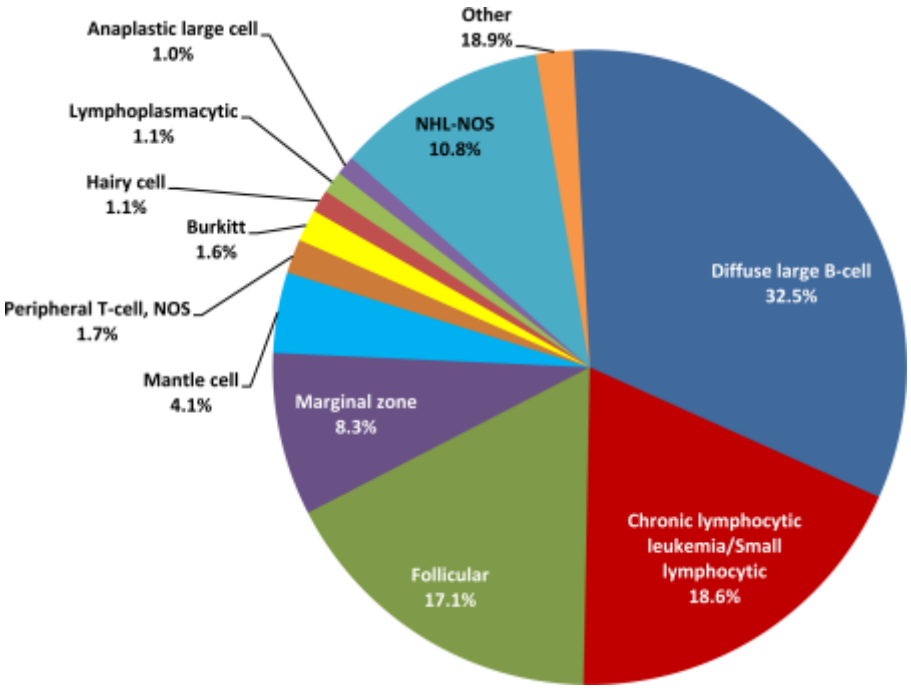

Figure 1.1 NHL distribution from 2009 to 2011 in the National Cancer Database. Copied from (Al-Hamadani et al., 2015)

1.2.1 Chronic lymphocytic leukemia

Chronic lymphocytic leukaemia (CLL) is an incurable disease and also a common type of human proliferative disorder with significant variability in clinical prognosis that is difficult to predict. CLL affects mainly elderly people and the median age at diagnosis is 72 years. CLL is characterized by a malignant expansion of neoplastic mature B-lymphocytes of > $5x10^9$ (Vollbrecht et al., 2015). Moreover, its clinical course usually is asymptomatic and does not require medical intervention (Hsi, 2012). Recently, a biological study of CLL disease shows that molecular inter- and intra-patient heterogeneity of leukemic cells and the possibility of clonal disease evolution over time may cause its variable courses (Landau et al., 2013; Vollbrecht et al., 2015). Genetically, the most common CLL chromosomal abnormalities are deletion of 13q14, 11q, 17q and 7q. CLL patients with deletion of chromosomal region 13q show the best outcome while those with deletion of chromosomal region 17q show the worst (Pekarsky et al., 2010).

Molecular genetic studies have shown that some cases of CLL have been developed from naïve B-cells which carry non-rearranged or unmutated Immunoglobulin Heavy Chain genes (IGVH). Around 35%- 45% of CLL cases have non-rearranged Ig genes related to the high expression of Zeta-chain-Associated Protein kinase 70 (ZAP-70), a protein usually expressed in T-cells and natural killer cells on the cell membrane (Boye and Maelandsmo, 2010). However, other CLL cases arise from memory B-cells from the germinal centre that are carried mutated or rearranged IGVH genes after somatic recombination or hypermutation (Figure 1.2) (Klein and Dalla-Favera, 2010; Mishra et al., 2012). These tumours are more sensitive to treatments and CLL patients have a prolonged survival. IGVH gene analysis is found to have prognostic value. On the other hand, some CLL cases with unmutated IGVH genes show low expression of ZAP-70 and CD38 which is associated with a stable disease form. Despite the fact that ZAP-70 and CD38 are used as prognostic markers for CLL, there are still limitations that restrict their clinical utility (Klein and Dalla-Favera, 2010). So, many attempts have been made to identify new prognostic markers.

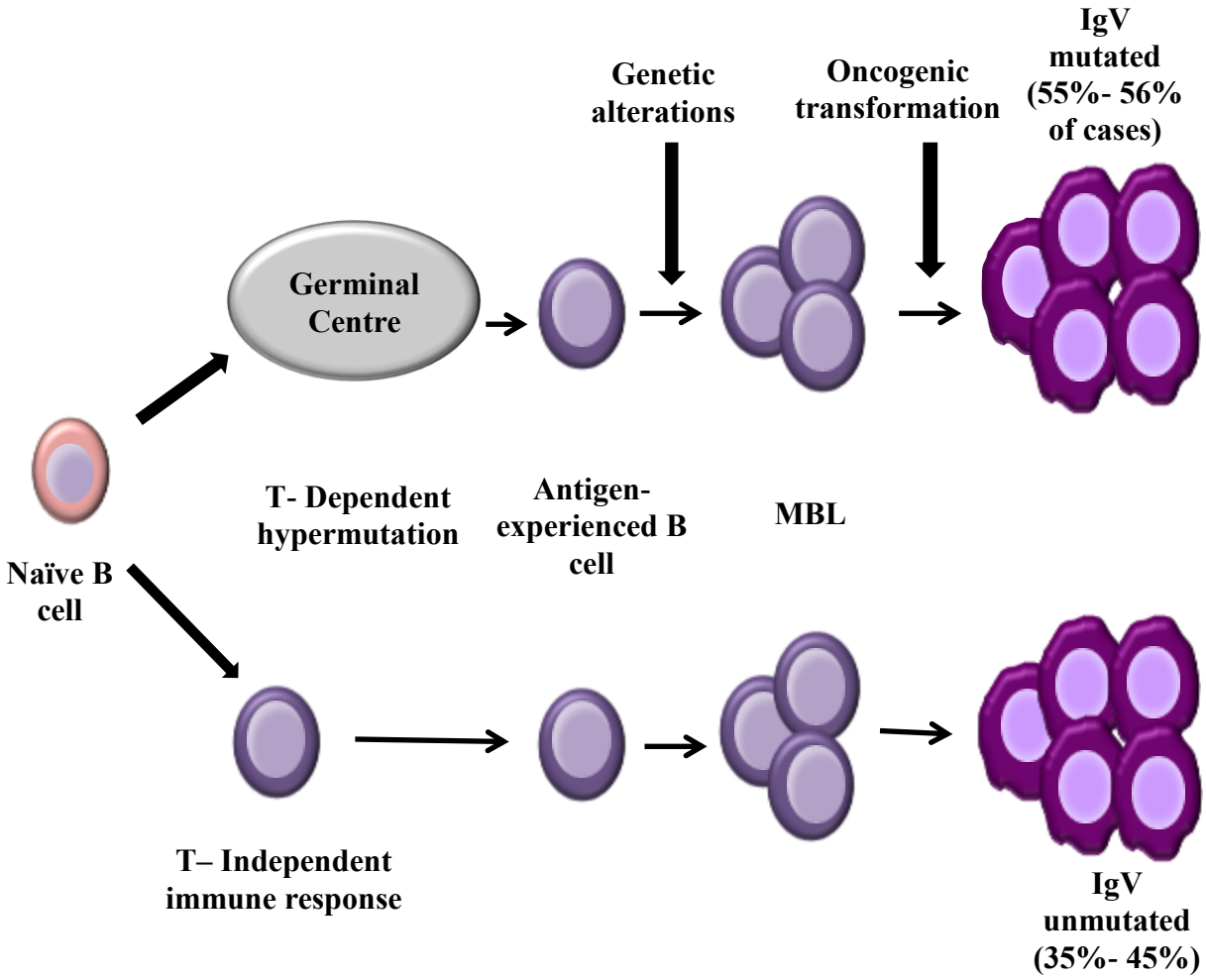

Figure 1.2 The possible cellular derivation of CLL.

Either T-dependent (IgV hypermutation in the GC) or T-independent (no IgV hypermutation) immune responses are driven from naïve B-cells. Once these responses are complete, the cells differentiate into antigen-experienced memory/marginal zone B-cells which may then be continually activated through persisting antigen and acquire genetic alterations that could cause outgrow of clones with amyeloproliferative leukaemia phenotype that finally progress to oncogenic transformation. (MBL= Monoclonal B-cell Lymphocytosis). Modified from (Mishra et al., 2012).

CLL cells have a specific immunophenotype, and they have a characteristic pattern of histological infiltration in the lymph node and bone marrow. It is known that genetic abnormalities cause this difference in clinical appearance. Some patients may present only with lymphadenopathy, organomegaly, and presence of infiltrating monoclonal B-cells with the same immunophenotype as CLL cells, but missing peripheral blood lymphocytosis. This type of lymphoma is called small lymphocytic

lymphoma (SLL) and has been considered for almost 2 decades to be tissue similar to CLL. Both CLL and SLL are currently considered different manifestations of the same entity by the fourth edition of the World Health Organization Classification of Tumours of Haematopoietic and Lymphoid Tissues. It is assumed that differential expression of chemokine receptors (e.g., reduced expression of R1 and CCR3 in SLL cells), integrin (e.g., CLL cells have lower expression of integrin [alpha]L[beta]2), and genetic abnormalities (a higher incidence of trisomy 12 and lower incidence of del(13q) is found in SLL) may explain some of the clinical differences between these 2 types of cancer (Santos and O'Brien, 2012).

There are two different staging systems for CLL including: the Binet staging system and the Rai system. In the UK and Europe doctors use the Binet staging system. The Rai system has 5 stages from 0 to IV and is used commonly in the USA. The Binet staging system has three stages including: stage A which is rare and characterizes by enlarged lymph nodes (lymphadenopathy) and a high white blood cell count, stage B which is common and also characterizes by enlarged lymph nodes and a high white blood cell count, and stage C which characterizes by enlarged lymph nodes or spleen, a high white blood cell count, and low red blood cell or platelet counts.

1.2.2 Diffuse large B-cell lymphoma

Diffuse large B-cell lymphoma (DLBCL) is the most common type of high-grade (fast-growing and proliferating) non-Hodgkin lymphoma. DLBCL is a heterogeneous disease consisting of molecularly different subtypes of tumours. These subtypes differ in gene expression, oncogenic aberrations and clinical outcome. In the UK, approximately 4,800 people are diagnosed with DLBCL each year. This type of lymphoma can occur in people of any age, including children, but researchers found that the risk of developing this type of lymphoma increases with age where most of patients diagnosed with DLBCL are 65 or over. It affects males more than females. Genetically, the most common DLBCL chromosomal abnormalities are alteration in 3q27, 8q24, t(14, 18). There are more than 300 genes mutated in DLBCL and these mutations are different from patient to patient. Some of these genes show a long tail

distribution. The most common mutated gene includes TP53, MYD88, PIM1, BCL6, CREBBP, EZH2 and others (Zhang et al., 2013).

DLBCL originates from the clonal development of B-cells of the germinal center (GC). Also, in this area there is a special microenvironment that forms in secondary lymphoid organs through the meeting of a naïve B-cell with its cognate antigen, in the context of T-cell dependent co-stimulation (Klein and Dalla-Favera, 2008). Because GCs are highly dynamic structures, mature B-cells rapidly proliferate (<12 hours doubling time) and the repetition of the process of somatic hypermutation (SHM), affinity maturation and clonal selection, and class switch recombination (CSR) occur in GC. These processes help in an emergency to produce antibodies with increased affinity for the antigen and are capable of distinct effector functions (Victora and Nussenzweig, 2012). In addition, these processes are classified within two anatomically different parts where B-cells recirculate: the dark zone (DZ), in which centroblasts dividing rapidly, and the light zone (LZ), where smaller non-dividing lymphocytes admixed with a reticulum of follicular dendritic cells are located (Figure 1.3) (Pasqualucci and Dalla-Favera, 2015). A unique biological program in DZ and LZ of B-cells has a critical role to complete a network of transcription factors that required for GC development and have critical role in lymphomagenesis. The development of the DZ is arranged by a transitory expression of NF-κB, IRF4 and MYC, which is a group of regulator genes that act as transcription factors (Calado et al., 2012; Victora and Nussenzweig, 2012). After that their downregulation in the overall DZ population. Specifically, the GC master regulator B-cell lymphoma 6 protein (BCL6) has an effect on MYC, which is an oncogene that contributes to the genesis of many human cancers, transcription and make it silent. During the GC reaction, the transcriptional repressor (in the B-cell lineage) is expressed specifically (Horn et al., 2013; Zeng et al., 2018).

BCL6 has a critical role in GC cells. It supports the DZ phenotype by controlling the activity of a broad set of genes involved in different signaling pathways. Also, it helps to sustain the proliferative status of GC cells while allowing the finishing of the DNA remodeling process that requires class-switch recombination (CSR) and somatic hypermutation (SHM). These are two processes of DNA damage and repair that are required for effective humoral adaptive immunity which create genetic diversity in developing T and B cells, without causing DNA damage responses. Moreover, the

premature activation and differentiation of GC B-cells prior are prevented by BCL6 (Yasui et al., 2017).

Somatic mutations have also been associated in the pathogenesis of DLBCL, for example, regulators of NF-κB signalling, CARD11 (Lenz et al., 2008) and MYD88 (Ngo et al., 2011). Somatic mutations in regulators of the NF-κB pathway were found in 50% of ABC-DLBCL patients and in 22% of cases of GCB-DLBCL (Compagno et al., 2009). Whole genome and exome sequencing has greatly extended the range of mutations detected in DLBCL patients (Lohr et al., 2012; Morin et al., 2011; Pasqualucci et al., 2011). These studies specified novel pathways that might be involved in lymphomagenesis and identified genes involved in chromatin methylation. A deletion in one allele of MLL2 that is involved in chromatin methylation, is mutated in 24-32% of DLBCL patients and is one of the most common causes of mutations (Morin et al., 2011; Pasqualucci et al., 2011).

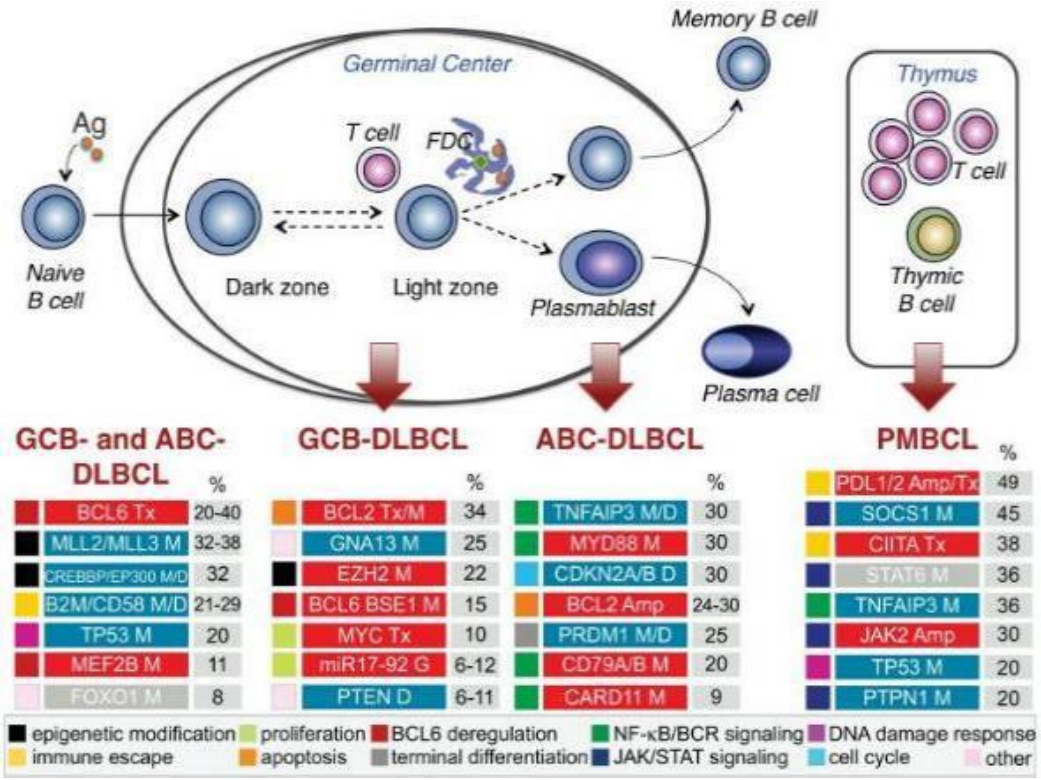

Figure 1.3 Germinal center and DLBCL pathogenesis.

Schematics of the GC reaction and its relationship with the main molecular subtypes of DLBCL show the most common shared and subtype-specific genetic alterations which are presented, with color codes showing the involved biological pathway. Blue, loss of function; red, gain of function. Copied from (Pasqualucci and Dalla-Favera, 2015).

1.2.3 Mantle Cell Lymphoma

Mantle cell lymphoma (MCL) cases are around 3-10% of NHL cases where most patients diagnosed with MCL are 60 or over. MCL affects males more than females. Commonly, MCL is not curable and has the worst outcome of all B-cell lymphomas with a median survival of 3-5 years (Karam et al., 2009). This type of cell lymphoma is derived from the mantle zone where different histological types are seen. Blastoid and pleomorphic types indicate more aggressive variations and are related to the most unfavourable outcome. MCL cells can be distinguished from other lymphoma cell such as CLL cells by their immunophenotype. MCL cells show a positive expression of sIgM/IgD, CD20, CD5, FMC-7 and CD43 and negative or only weak positivity on CD23. In most MCL cases, cyclin D1 is positive. The hallmark of MCL is t(11;14) (Inamdar et al., 2016), with cyclin D1 overexpression (Jares et al., 2012). This abnormality has an important role because it can be used as a marker of minimal residual disease (MRD).

Usually, MCL cells are detected in the peripheral blood, bone marrow or extranodal sites, especially in the gastrointestinal tract where MCL cells are detected in more than 80% of MCL cases. So, the endoscopic examination of the gut is necessary in all MCL cases.

Clinically, there are two forms of MCL: indolent and conventional. The indolent form is mainly categorized by a non-nodal leukemic appearance with bone marrow involvement and splenomegaly (Fernandez et al., 2010). MCL patients with this type show normal performance status, normal serum LDH, and low MIPI score. In addition, indolent MCL characteristic features contain mild to moderate lymphocytosis, hypermutated IGVH genes, a non-complex karyotype, and the absence of Sry-related high-mobility-group box (SOX11) expression. Moreover, this type of MCL is correlated with low Ki67 (≤10%) and expression of kappa light chain contrasting to lambda light chain expression found in aggressive MCL. To date, there are no markers that can confirm the diagnosis of MCL indolent nature although SOX11 shows promise as one of such biomarkers (Inamdar et al., 2016).

1.2.4 Marginal Zone Lymphoma

Marginal zone lymphomas (MZL) which were previously called Mucosa-associated lymphoid tissue lymphomas (MALT) count for 7-8% of all B-cell NHLs through a large national database study. It was found that MZL had a better prognosis compared with diffuse large B-cell lymphoma (Al-Hamadani et al., 2015). As MCL, the median age at diagnosis is 60 and above. However, MZL affects females more than males. Morphologically, mature B-cells appear in MZL slides and these cells cause stimulation of chronic antigenic and involvement of genes in autoantibody formation, VH4, VH3 and VH1. Mature B-cell markers (CD20 and CD79a), marginal zone antigens CD21 and CD35, and sIgM or sIgD show positive expression in MZL cells (Spina and Rossi, 2017).

CT scanning and bone marrow examination are necessary in staging; the procedures of MZL are similar to other lymphomas, however the staging systems themselves are quite complex due to the variation of potential sites. There are different cytogenetic abnormalities which have been associated with MZL, including: t(11;18), t(1;14), t(14;18) and t(3;14) (Spina and Rossi, 2017; Taylor et al., 2017). There are three clinical subtypes of marginal zone lymphomas including extra-nodal, splenic and nodal MZLs. About 70% of marginal zone B-cell lymphomas (MZL) is Extra-nodal MZL while other 30% of MZL cases are classified under splenic and nodal MZLs (Swerdlow et al., 2016).

Extra-nodal MZL presents in a number of organs, for instance the stomach, orbital adnexa, salivary glands, and lungs. Mainly, extra-nodal MZL has been associated with two bacterial infections: *Helicobacter pylori* infection in gastric MZL and *Chlamydia psittaci* in orbital tissues, with geographic difference in frequencies (Sabattini et al., 2010).

Splenic marginal zone lymphoma (SMZL) accounts for 1% of total lymphoma cases. Splenomegaly is main feature of this type of MZL. Splenic hilar nodes are often involved while disseminated lymph node not involved in most cases. In 95% of cases of SMZL, bone marrow involves. On the other hand, circulating villous lymphocytes can

be detected in up to 15% of cases. Usually, SMZL cases are associated with autoimmune hemolytic anemia. And some of them are associated with hepatitis C infection. Some cases may not require treatment for up to 10 years but they need to be checked regularly. Splenectomy is the mainstay of treatment to improve peripheral cytopenias and to reduce marrow infiltration. It performs in the presence of splenomegaly or cytopenias related to either hypersplenism or marrow involvement. Genetically, Neoplastic cells usually in this disease are CD20-positive, CD3-negative, CD23-negative, CD43-negative, CD38-negative, CD5-negative, CD10-negative, BCL6-negative, BCL2-positive, cyclin D1-negative, IgD-positive, p27-positive Annexin A1-negative (Piris et al., 2017).

Nodular marginal zone lymphoma (NMZL) is a small B-cell lymphoma which involves lymph nodes only. It is the least common form of MZL; about 10% of cases. Patients with this type suffer from advanced disease which must be distinguished from extra-nodal MZL with lymph node spread. Cytological and immunophenotypic features are similar in NMZL and SMZL, but have a less favourable prognosis than SMZL. Usually, they occur mostly in adults though there are a few paediatric cases. In NMZL, there are many therapeutic approaches which have been used, but still there is definitive treatment due to the small quantity of patients involved. Future studies are essential to evaluate their therapeutic efficacy for NMZL (Tadmor and Polliack, 2017).

1.2.5 Follicular Lymphoma

20% of cases of NHL are follicular lymphoma (FL). It is rare in those under the age of 20 years and the median age of FL patients is in the sixth decade. It is found that FL is a low grade lymphoma. In addition, it is not currently curable and the median survival is approximately 12-14 years after diagnosis (Czuczman et al., 2004).

Follicular lymphoma cells are derived from follicle centre (germinal centre) B-cells. These cells show clonal control and usually express surface immunoglobulin (sIg) along with the B-cell antigens (such as CD20, CD79a, CD22), BCL-2, BCL-6 and CD10. Up to 90% of cases of FL show the translocation t(14;18) which involves the BCL-2 locus causing interruption of the normal apoptotic pathways. Moreover, there

are other cytogenetic abnormalities which have been investigated and often involve BCL-6, making the distinction from DLBCL difficult. Primary cutaneous follicular lymphoma is usually negative for BCL-2 and t(14;18) (Horsman et al., 2003; Taylor et al., 2017).

40-70% of FL patients having marrow involvement at diagnosis and presenting with advanced stage disease. The majority of FL patients are asymptomatic at diagnosis. FL mainly affects nodal sites, however extra-nodal sites may be involved. A clinical prognostic staging system has been developed: the follicular lymphoma international prognostic index (FLIPI), and is based on 5 prognostic factors including age > 60 years, haemoglobin concentration (Hb) <120g/L, elevated lactate dehydrogenase (LDH), more than 4 nodal areas involved and Ann Arbor stage III/IV(Solal-Celigny et al., 2004). There are three prognostic groups including low, intermediate and high risk. One of the main FLIPI disadvantages is that it was created at the time when rituximab, the standard initial treatment, was not established. Although FLIPI being widely used, there are multiple results within risk groups, confirming disease heterogeneity and pointing to the need for its revision (Sweetenham et al., 2010). So, FLIPI2 was proposed evaluating patients on rituximab-containing regimens, and aiming the function of β2-microglobulin (β2-M), the longest diameter of the largest involved node >6 cm, bone marrow involvement, Hb <12 g/dL, and age as the main factors for progression-free survival (PFS). (Federico et al., 2009; Xu et al., 2017).

1.2.6 Burkitt's Lymphoma

Burkitt's lymphoma, which is an aggressive lymphoma, usually presents as an extra nodal disease or as acute leukaemia. This type of lymphoma has one of the highest cure rates. Clinically, there are three different groups of Burkitt's lymphoma. The first group is endemic Burkitt's lymphoma which has an incidence of 5-10 cases per 100,000 people in Equatorial Africa, and Papua New Guinea (PNG), with a geographical association with endemic malaria (Burkitt and O'Conor, 1961). It is a disease of childhood with a peak incidence occurring in the 4-7 age group and affects males more than females. It has a predilection for the jaw and facial bones. The second group is HIV-associated Burkitt's lymphoma which is present usually in intra-nodal sites.

Patients with this group of lymphoma have a high risk of CNS involvement that occurs in about 6 of every 100 AIDS cases. The third group is sporadic Burkitt's lymphoma which is very rare, occurring in 2-3 per million per year. It is mainly a disease of childhood and early adulthood; with a median age at diagnosis of 30 years, it affects males predominantly. Abdominal disease is the most common feature of this type of lymphoma (Blum et al., 2004).

Histologically, all cases of Burkitt's lymphoma have very similar features including a diffuse architecture, intermediate sized lymphocytes, with round or oval nuclei. Number of tangible-body macrophages and apoptotic cells debris are present due to a high degree of proliferation (Chuang et al., 2007). However, other tests are essential to confirm the diagnosis, including examination for EBV, FISH for typical translocations such as t(8;14), detection of c-myc and there are other translocations involving myc. CD20, CD19, CD10, BCL-6, CD38 are typically positive in Burkitt's lymphoma cells (Van Den Berghe et al., 1979).

1.3 B-lymphocyte maturation

All types of blood cells including B-cells are derived from the haematopoietic stem cells (HSCs) that are located in the bone marrow (BM). BM stromal cells control developing HSC and coordinate their differentiation into B-cells or other type of cells by secretion signalling molecules as cytokines and chemokines. A schematic maturation of HSCs into B-cells is shown in Figure 1.4 (Mårtensson et al., 2010).

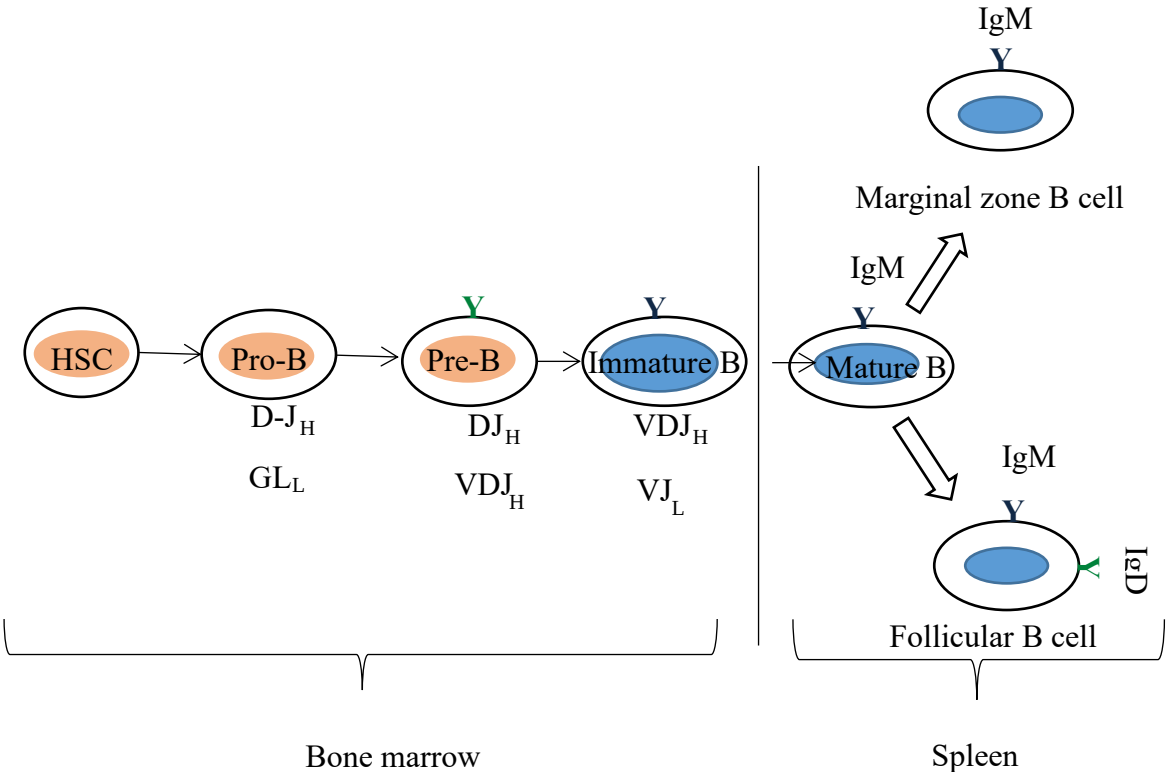

Figure 1.4 Schematic illustration of B-cell development.

Schematic illustration of B-cells development. In adults, B-cells maturation starts in the bone marrow; then immature B cells migrate to the spleen, where the maturation is complete. The differential stages are defined by the recombination status of the IgH and IgL chain loci and accompanied expression of the cell surface specific markers. Adapted from (Abbas et al., 2012, Martensson et al., 2010).

Cell surface specific markers or cluster of differentiation (CD) molecules presented on the cellular membrane of leukocytes are used as specific markers for the identification and characterization of the stage of their maturation (Figure 1.5).

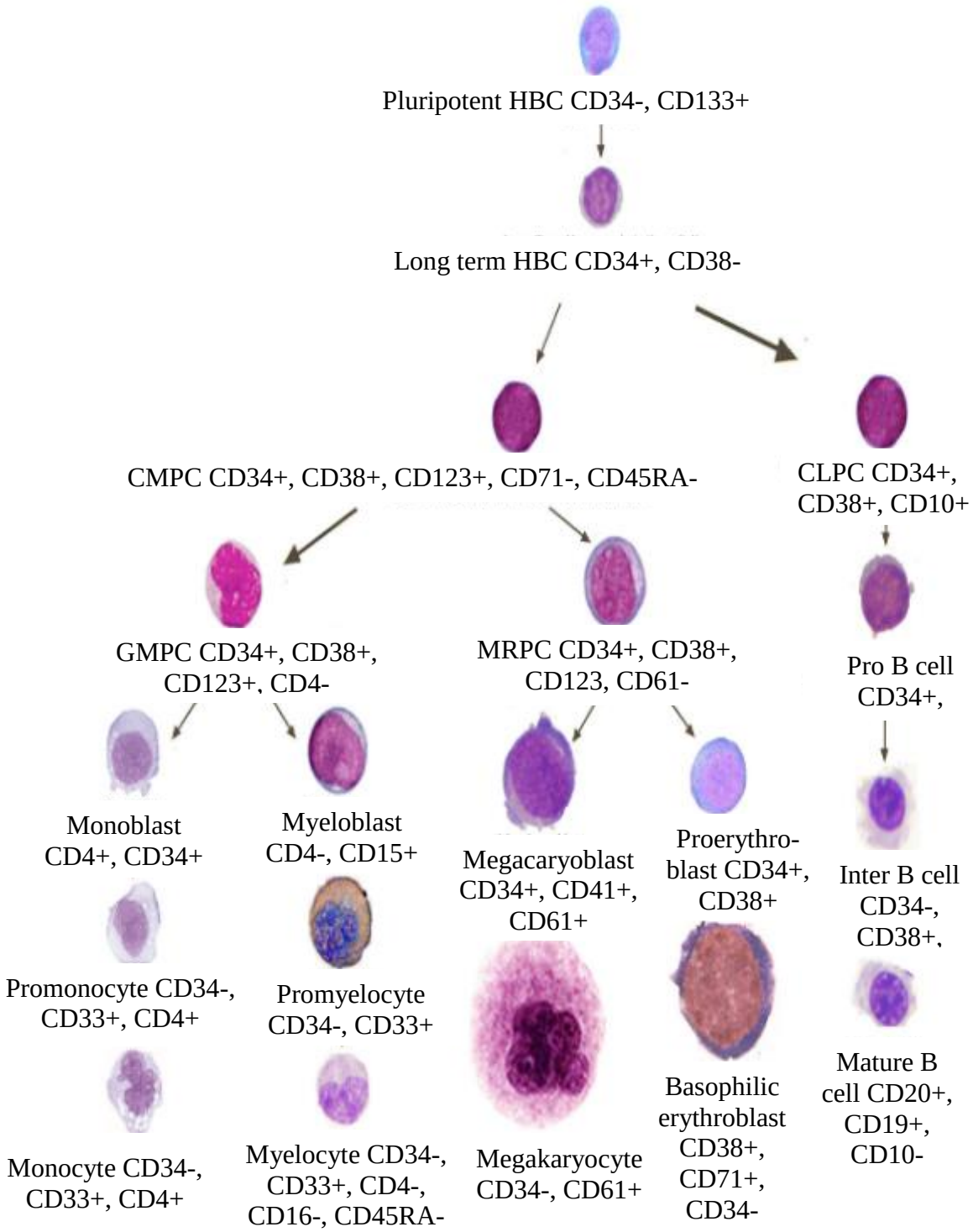

Figure 1.5 A schematic representation shows that different cells within hematopoietic hierarchy express different cell surface markers.

CDs expression during different developmental stages of lymphocyte and myelocytes. CD=Cluster of Differentiation; HSC=Hematopoietic Stem Cells; CMPC=Common Myeloid Progenitor Cells; CLPC=Common Lymphoid Progenitor Cell, GMPC=Granulocyte Monocyte Progenitor Cell; MEPC=Megakaryocyte Erythrocyte Progenitor Cell; Inter B cell= Intermediate B cell. Adapted from (Attar, 2014).

Multipotent progenitor cells (MPPs) refers to a class of HSC that has lost their self-renewal ability, but can still differentiate into different blood cells including B-lymphocytes. MPPs express FLT3, a tyrosine kinase receptor. Activation of FLT3 along with the initiation of expression of PU.1 transcription factor, a protein encoded by the *SPI1* gene, is important for MPPs development further into the common lymphoid progenitor (CLP) (Abbas et al., 2012). Expression of IL-7 receptor, a protein that is encoded by the *SPI1* gene and secreted by stromal cell, also takes part in coordination CLP cells formation and growth. There are other factors that stimulate transition HSC to B-cells such as stem-cell factor (SCF), a cytokine secreted by BM stromal cells that activates the receptor tyrosine kinase c-Kit on precursor cells. Moreover, BM stromal cells produce the chemokine stromal cell-derived factor 1 (CXCL12) or stromal derived factor 1 (SDF-1), which has a significant role to retain B-cell precursors within the BM microenvironment (Chong et al., 2012). Activation of the transcription factors E2A and early B-cell factor (EBF) helps in the transition of CLP to the pro-B-cell stage. E2A expression which is initiated by activation of two transcription factors, PU.1 and Ikaros, induces EBF expression. As a result EBF acts in tandem to initiate the expression of proteins associated with differentiation into the pro-B-cells (Mårtensson et al., 2010).

B-cell development is characterised by the rearrangement of the B-cell receptor (BCR), by which B-cell progresses from the early pro-B cell into the mature B cell. The BCR is composed of two identical heavy chains and two identical light chains which form the surface immunoglobulin (Ig) (Figure 1.6) (Murphy et al., 2012).

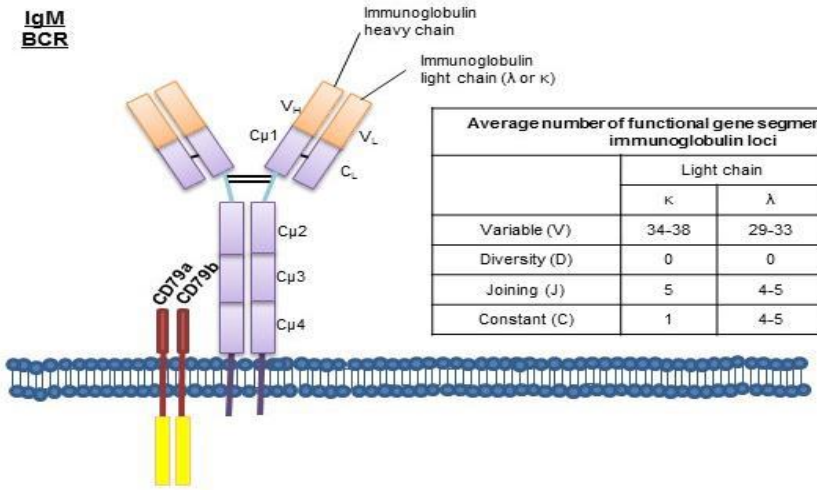

Average number of functional gene segments in human immunoglobulin loci			
	Light chain		Heavy chain
	κ	λ	H
Variable (V)	34-38	29-33	38-46
Diversity (D)	0	0	23
Joining (J)	5	4-5	6
Constant (C)	1	4-5	9

Figure 1.6 Germline rearrangements of the immunoglobulin heavy and light chain loci and BCR structure.
Copied from Murphy. K., 2012.

Gene rearrangement of the BCR is a highly controlled process which prevents self-activation and immune system deregulation. In the diversity (DH) locus of the immunoglobulin heavy chain (IGH) gene, the first rearrangement occurs and D segment links to the joining (JH) segment. The IGH and light chain loci (IGL) of germline rearrangements are derived from an extensive repertoire of different gene segments. Activation of E2A and EBF transcription factors has an important role in joining of D segment with JH by mediated expression of proteins required for gene rearrangement; recombination activating genes (RAG-1 and RAG-2) (Benito et al., 2003; Murphy et al., 2012). PAX5, a member of the paired box (PAX) family of transcription factors, has critical function in B-cell development, without PAX5 expression B-cells development cannot be completed. It requires the development of the pro-B cell stage by targeting CD19, the B-cell co-receptor component, and B-cell linker protein (BLNK) which is essential for signalling from the mature BCR. The transition into the pro-B cell stage occurs by DJH rearrangements. One allele of the variable heavy chain (VH) gene segment will be rearranged to link to the DJH sequence at the late pro-B cell stage. RAG-1 and RAG-2 interact with different enzymes and DNA modifying proteins to form the V(D)J recombinase. They also mediate the endonucleolytic cleavage of the target DNA and introduce double strand breaks. Then, DNA repair machinery results in the binding of the desired segments together. At the pro-B cell stage, the enzyme

terminal deoxynucleotidyl transferase (TdT), which provides non-template nucleotides in between the rearranged gene segments, promotes recognition of multiple BCR-antigens (Calis and Rosenberg, 2014).

A full length of immunoglobulin μ heavy chain is formed after completion of V-DJH rearrangement that occurs in a pre-B-cells. At this stage, a high proportion of developing B-cells are lost as a result of unsuccessful rearrangements of the μ heavy chain. Before the pro-B cell develops further, the structure of the recently formed heavy chain should be functional. In the pro-B-cell E2A and EBF transcription factors signal to produce λ5 and V pre-B-cell: two surrogate light chains. These proteins then interact with the heavy chain to form the pre-B-cell receptor (Murphy et al., 2012). Invariant proteins Igα (CD79a) and Igβ (CD79b) have a critical function in the formation of the pre-B-cell receptor. This protein has the ability to span the cell membrane and their relations with the pre-BCR or BCR are needed to transduce intracellular signals by the kinase activity of the immunoreceptor tyrosine activation motifs (ITAMs) in their cytoplasmic tails. As a result, the pre-BCR clusters on the surface of the cell. Then, intracellular signalling stops RAG-1 and RAG-2 expression, therefore stopping further rearrangement of the heavy chain genes. These cells after stimulation by IL-7, that causes cell proliferation, transform into large pre-B cells (Murphy et al., 2012). Large pre-B-cells then develop into small pre-B-cells by different processes of cell divisions. At this stage, RAG proteins are activated again to induce the light chain genes rearrangement. Although there are two forms of the light chains (κ and λ) only one will be expressed in a complex form with the heavy chain. Rearrangement takes place directly between V and J because the Light chains lack the D segment. Successful rearrangement of the light chain produces IgM molecules which are translocated on the surface of the new immature B-cell. Interaction of surface IgM with Igα and Igβ causes the formation of BCR (Almqvist and Martensson, 2012; Murphy et al., 2012).

There are three ways to prevent self-reactive B-cells from entering the circulating compartment; undergoing apoptosis, developing of a new receptor by receptor editing, or undergoing a permanent state of anergy to antigens, become immunologically ignorant (Murphy et al., 2012). B-cells then develop into mature B-cells that express surface IgD and IgM. These cells then become mature B-cells then migrate from BM and peripheral lymphoid tissues.

1.4 Migration of B cells by amoeboid mechanisms

Leukocytes migrate by amoeboid mechanisms. Reminiscent of the amoeba *Dictyostelium discoideum*, polarized leukocytes develop from a small leading edge consisting of short-lived pseudopods, followed by the cell body that contains the nucleus, and a posterior, near-cylindrical tail of 2 to 10 μm in length termed the uropod (Figure 1.7 a&b). Four steps mediate the amoeboid migration cycle including: the leading edge protrudes one or several pseudopods by actin flow, protruding membrane and surface receptors interact with the substrate, actomyosin-mediated contraction of the cell body occurs in mid-region, and so the rear of the cell moves forward. These four steps occur in a cyclic manner, generating forward movement.

Amoeboid migration is utilized by leukocytes (and likely many stem cells), is fast (up to 30 μm/min), without strong adhesive interactions to the tissue and commonly preserves tissue integrity rather than degrading it (Wolf, 2003).

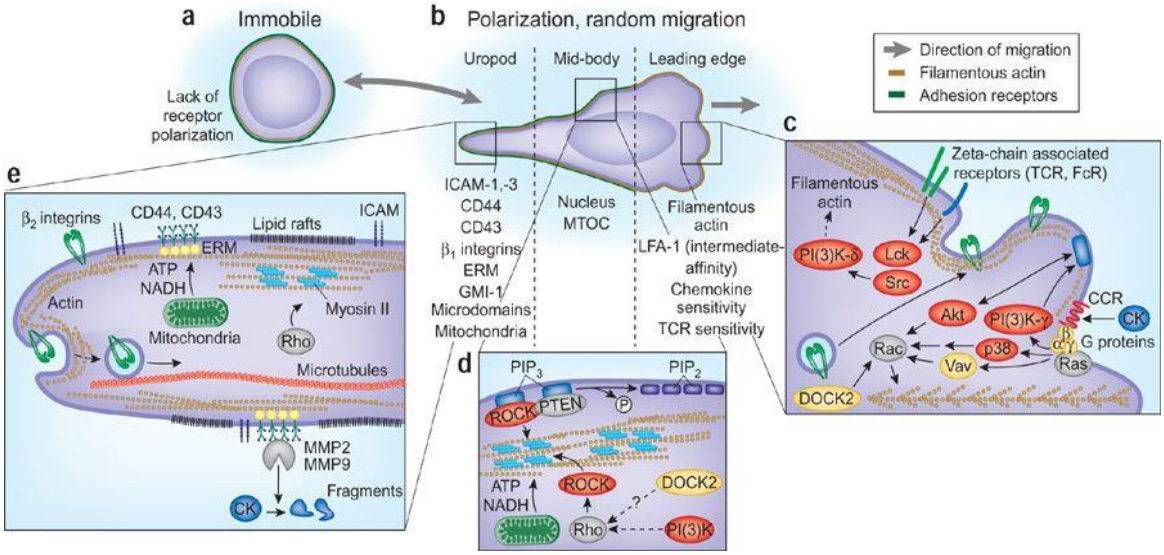

Figure 1.7 Morphology, surface receptors and signalling in amoeboid leukocyte migration.

(a) Immobile or freely floating leukocyte with round appearance, including uniform distribution of surface receptors and cytoskeleton. (b) Amoeboid shape after polarization during random chemotaxis and migration. (c) Surface receptors, cytoskeletal structure and signalling actions in the leading edge, lateral portion of the

cell body and uropod. Class I PI(3)Ks are lipid kinases that phosphorylate phosphatidylinositol-(3,4)-bisphosphate (PIP2) to phosphatidylinositol-(3,4,5)-trisphosphate (PIP3). PIP3 is thought to form multimers at the inner leaflet of the plasma membrane that serve as docking and activation site for pleckstrin-homology (PH) domain–containing proteins, including Akt (protein kinase B). Other pathways directly and indirectly activated by chemoattractant receptors are Ras and p38 and DOCK2. As central effector of these pathways, Rac mediates the formation of actin filaments that move the plasma membrane forward. Other surface receptors, including TCR and FcR, trigger the tyrosine kinases Lck and Src and downstream PI(3)K-δ. (d) The mid-portion contains actomyosin filaments that are controlled by Rho and ROCK. (e) The uropod forms an adhesive and contractile rear that contains microtubules and mitochondria. CK, cytokine; ERM, adaptor proteins of the ezrin-radixin-moesin family; GM-1, monosialotetrahexosylganglioside; MTOC, microtubule-organizing center; Vav, Vav-family guanine-nucleotide exchange factor. Copied from (Friedl, 2008).

The leading edge after polarization immediately making networks of filamentous actin that consist of abundant membrane ruffles indicative of dynamic probing of the environment. The leading edge is sensitive particularly to receptor engagement, including that by Fc receptors (FcRs), T cell antigen receptors (TCRs), chemokine receptors (Wei, 1999) and β2 integrins in intermediate or active state (Stanley, 2008). All these receptor help to initiate contact with other cells, induce signal transduction (Negulescu, 1996) and mediate phagocytosis after binding of bacteria and other particles (Beemiller, 2006). The surface and chemoattractant receptors density on the leading edge is equal to that on other cell parts (normalized to membrane area), at least at the light-microscopic level (Servant, 1999), however, other receptor, such as β2 integrins in neutrophils, show discrete relocation toward the tips of ruffles at ultrastructural resolution (Fernandez-Segura, 1996). The amoeboid cells mid-region contains the nucleus and a relatively immobile cell region that maintains the front–rear axis. The highly glycosylated surface receptors such as CD43 and CD44, adhesion receptors including intercellular adhesion molecule (ICAM)-1, ICAM-3, β1 integrins and ERM adaptor proteins, in addition to GM-1-type cholesterol-rich microdomains found in the trailing edge. The uropod has a putative anchoring function and mediates cell–matrix and cell–cell interactions during migration (Wolf, 2003).

Lamellipod and pseudopod protrusions occur either suddenly or prompted by migration-promoting factors binding to surface receptors, at the leading edge (Figure

1.7 c). In leukocytes, polarization and migration to chemoattractant gradients, known as chemotaxis, are induced by many compound classes. These classes are chemokines and cytokines, lipid mediators, bacterial factors and ECM degradation products including fragments of collagen, fibronectin and elastin (Adair-Kirk, 2003). Various chemoattractants transmit signals through heterotrimeric G-protein-coupled receptors (GPCRs). In leukocytes, most GPCRs transmit through the α subunit of Giα, the subtype of G protein that can be inhibited by pertussis toxin. These GPCRs contain the fMLP (N-formyl-Met-Leu-Phe) receptor and C5a receptor; chemokine receptors including CCR7, CXCR4, CXCR5 and CCR3; the leukotriene B4 receptor BLT1; sphingosine-1-phosphate receptors 1–4 (S1P1–4) and lysophosphatidic acid (LPA) receptors 1–3 (Thelen, 2008). All these GPCRs enhance cell activation and mediate promigratory signals. A key GPCR-mediated pathway is signalling through class Ib phosphatidylinositol-3-kinase (PI(3)K), containing the p110γ catalytic subunit). PI(3)K-γ is recruited to the inner leaflet of the plasma membrane by the G protein βγ subunit, where it becomes activated, and then phosphorylates phosphatidylinositol phosphates (PIPs) and other effectors (Marone, 2008). PIPs act as docking sites for pleckstrin-homology domain–containing proteins, notably Akt (protein kinase B), which is involved in inducing actin polymerization and pseudopod protrusion by phosphorylating downstream effectors, such as the actin-binding protein girdin (Stambolic, 2006). A second pathway related to PI(3)K activation is induced by ζ-chain-associated receptors, including TCRs and FcRs. These receptors signal through tyrosine kinases Lck and Zap-70 to class Ia PI(3)Ks (consisting of p110δ) and activate downstream Akt, in addition to the GTPases Rac and Cdc42 (ref. 30). A third, PI(3)K-independent pathway prompted by the fMLP receptor in neutrophils causes the activation of p38 mitogen-associated protein kinase and downstream Rac activation. Finally, the Rac guanine nucleotide exchange factor DOCK-2 causes Rac activation at the leading edge (Nombela-Arrieta, 2004). Then, Rac prompts actin polymerization through WAVE, which is a member of the WASP family of actin-binding proteins, and Arp2/3. WAVE mediates actin filament formation while Arp2/3 causes sideward branching of actin filament and these activities generate interconnected, branched networks (Ibarra, 2005). Therefore, promigratory signals received at the leading edge cause local Rac activation and actin network protrusion, pushing the plasma membrane outward. At the leading edge, the mechanisms of preferential receptor sensitivity are

likely different and may include local signal amplification mechanisms and the exclusion of counter-regulatory proteins (Charest, 2006).

The mid-region is characterised by actomyosin-based stiffness and contractility, limits lateral protrusions and thus maintains a stable, bipolar cortex (Figure 1.7 d). In the central and rear regions of leukocytes, the cytoskeletal motor protein myosin II promotes actin filament contraction and limits lateral protrusions. Myosin II cross-links actin filaments in parallel, developing the contractile shell needed to hold the extending cell together and propelling the cell nucleus, the most rigid part of the cell, forward (Bendix, 2008). Inhibition of myosin II in neutrophils leads to ectopic lamellae on two-dimensional substrates or the loss of rear-end retraction in three-dimensional tissues, causing impaired migration. Upstream of myosin II, by yet unclear mechanisms, PI(3)K-γ and possibly DOCK-2 suppress lateral protrusions (Lammermann, 2008); deletion of either protein increases cell turning such that overall cell mobility is compromised (Nombela-Arrieta, 2004). The phosphatase PTEN also helps to lateral stability by inhibiting ectopic protrusion formation. PTEN is excluded from the leading edge but active in lateral and rear cell parts, where it dephosphorylates kinases, including PI(3)K and Akt, in addition to phosphatidylinositol-(3,4,5)-trisphosphate, and thus counteracts protrusion formation (Heit, 2008).

The uropod extends rearward from the nucleus and contains the microtubule-organizing centre and rearward-polarized microtubules, the Golgi, and abundant actin-binding ERM proteins (Figure 1.7 e). Mitochondria localize to the rear of the cell and owing to local ATP transport to the region of ATP-dependent actomyosin contraction that essential for proper polarization, uropod retraction and migration (Campello, 2006). Amoeboid polarization therefore makes a bipolar mechanosensory state with a dynamic leading edge to obtain new contacts and signals, a stiff mid-body, and a sticky uropod that is dragged along the substrate and stabilizes the cell position in complex environments (Wolf, 2003).

1.5 S100 calcium-binding proteins

Calcium is a key secondary messenger that has a critical role in cell signalling and metabolism. Calcium regulates multiple cellular processes such as cell migration, muscle contraction and neurotransmitter release (Carafoli, 2002). So, calcium intracellular concentration is strongly controlled by regulation of the balance between the calcium influx and the efflux in order to maintain resting level near 100 nM with a signalling level approaching 1 μM (Berridge et al., 2000). Calcium-binding proteins are responsible for decoding calcium signalling as buffers and effectors. Buffers help to co-ordinate the amplitude and restoration of the calcium concentrations efficiently while effectors are responsible for stimulating different calcium-dependent processes. The human genome encodes more than 200 calcium-binding proteins (Berridge et al., 2003). There are 21 members in the calcium-binding S100 protein family that are similar in their structure but different in function. Most human S100 genes are located as a cluster in the epidermal differentiation complex on chromosome 1q21 (Figure 1.8) (Mishra et al., 2012).

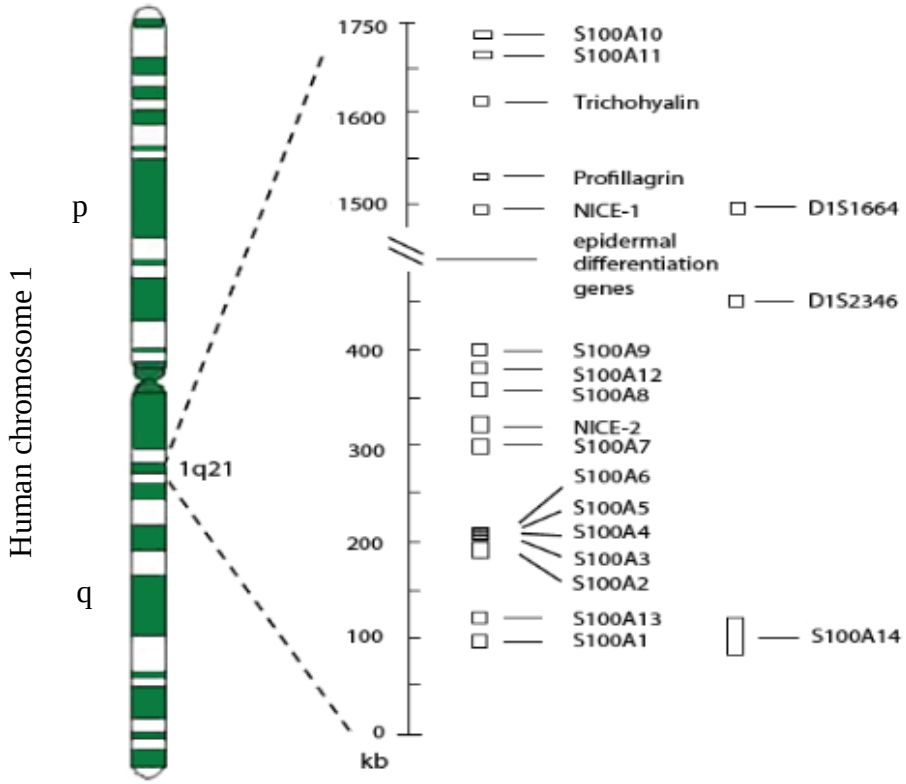

Figure 1.8 The S100 gene cluster on human chromosome 1q21.

Modified from (Heizmann et al., 2002)

1.5.1 Structure of S100 proteins

The S100 genes encode small, acidic, calcium-binding proteins. These proteins have a typical structure that contains a pseudo (N-terminal) and canonical (C-terminal) EF-hand domains, which are connected by a hinge region and end in a C-terminal extension of varying length (Figure 1.9) (Hsu et al., 2009). Alignment of S100 proteins shows common features among S100 proteins including the first EF-hand (containing helices 1 & 2 as well as the linker 1 region), the hinge region, the second EF-hand (containing helices 3 & 4 as well as the linker 2 region), and the carboxy-terminal tail as shown in Hue study (Hsu et al., 2009).

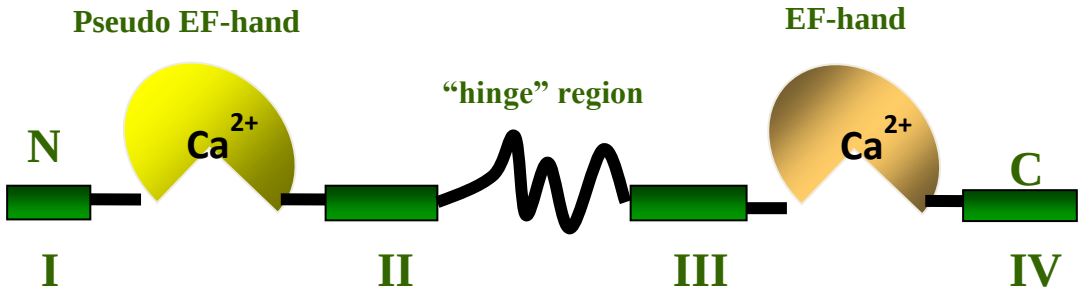

Figure 1.9 Schematic representation of a typical S100 protein structure.

Members of S100 protein family have two EF-hand calcium binding motifs that are held together by hinge region. The N-terminal EF-hand is a pseudo EF-hand comprises of helix I, loop (L1) and helix II, while the C-terminal EF-hand has a canonical structure which is arranged as helix III, loop (L2) and helix IV. Modified from (Rohde et al., 2010).

S100 proteins are typically symmetric dimmers. Each dimmer comprises two identical S100 protein monomers and contains four α-helices (Aggarwal et al., 2015). The S100 proteins play an important role in modulation of cellular responses by acting as intracellular calcium sensors but can also be secreted from cells and serve as extracellular factors (Figure 1.10).

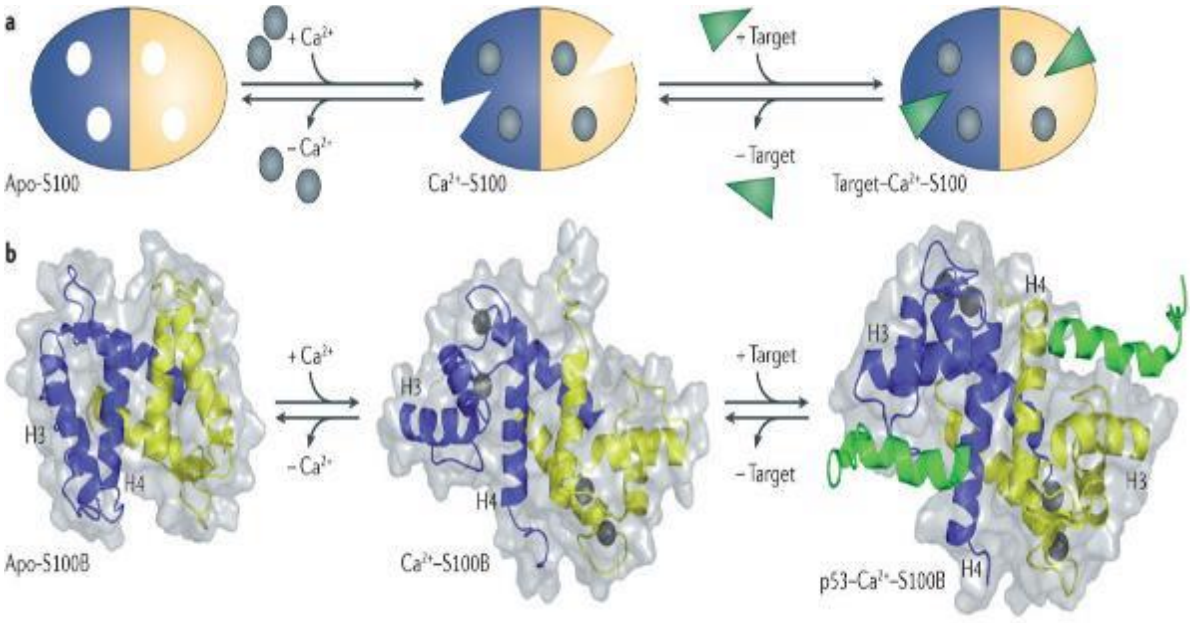

Figure 1.10 S100 protein structural organization and function.

(A) S100 proteins exist in calcium-free or apo-conformation which is shown as a blue and yellow subunits. S100 proteins conformation is controlled by calcium (which is presented as grey circles). They act as calcium sensors and translate alterations in intracellular calcium level into a cellular response. (B) Calcium binding induces a conformational rearrangement by exposing a hydrophobic cleft, allowing S100 proteins to bind to their cellular targets (green) and elicit a physiological response. Ribbon and surface diagrams of apo–S100B, Ca^{2+}–S100B and the Ca^{2+}–S100B–p53 peptide presented. Individual subunits are shown in blue and yellow, the Ca^{2+} ions are presented as dark grey spheres, and the p53 peptide is shown in green. The conformational rearrangements that happen upon Ca^{2+} binding is referred to as the 'Ca^{2+} switch', and contain the reorientation of helix 3 (H3) and the subsequent exposure of hydrophobic remains that participate in target protein binding. Copied from (Bresnick et al., 2015b) .

1.5.2 Expression and distribution of S100 proteins

The expression of S100 proteins has been studied in different cancers. A unique profile (signature) of expression of S100 proteins has been discovered. Since these proteins play an important role in cell proliferation, migration and angiogenesis, they contribute to tumorigenesis (Bresnick et al., 2015b). Furthermore, it has been observed that in various neoplasms such as breast, lung, bladder, kidney, gastric, and prostate cancers, S100 proteins are expressed at different levels and can be considered as potential diagnostic biomarkers (Cancemi et al., 2010).

In addition to the high level of structural homology, S100 proteins show tissue- and cell-specific expression (Donato, 2001). Their expression is modulated by genotoxic stress (Donato, 2003). For example, S100B is not expressed in normal cardiomyocytes but expressed at high level in post-infarction (Tsoporis et al., 2005) while S100A6 is strongly expressed in the adenocarcinoma cell line, HCT116 upon exposure to ionizing radiation (Orre et al., 2007).

Profiles of S100 protein expression can be used to assist diagnosis and/or prognosis, notify best treatment options and monitor patient response to therapy. For example, S100B expression has been used as a diagnostic marker in the primary tumour for malignant melanoma. Also, expression levels of S100P have a diagnostic utility in different cancers linked to their expression in primary tumours (breast, colorectal, pancreatic and ovarian cancer), metastatic lesions (lung cancer), serum (breast and colorectal cancer), saliva (head and neck cancer), bile (cancer of the bile duct) and faeces (colorectal cancer) (Bresnick et al., 2015b). After adjuvant 5-fluorouracil (5-FU) therapy and radical surgery in recurrent colon cancer, the expression of S100A2 and S100A10 is used as a prognostic marker (Yap et al., 1999). Furthermore, autoantibodies directed against S100A7 have been detected in ovarian cancer and may help in diagnosis (Liriano et al., 2012).

A complex regulatory network controls the expression of different members of S100 family in human cancers. This complex includes epigenetic mechanisms and signal transduction pathways, which are activated by chemotherapeutic agents.

Epigenetic changes regulate different S100 family members in different cancer. Studies found that it regulates the expression of S100P in prostate, pancreatic and cervical cancer; expression of S100A4 in different cancer such as pancreatic, endometrial, gastric, breast, ovarian, renal and brain tumours; S100A2 in prostate and breast cancer; S100A6 in prostate and gastric cancer; and expression of S100A10 in pituitary cancer (Day and Bianco-Miotto, 2013; Horiuchi et al., 2012). There are seven S100 genes which are direct targets of histone-lysine methyltransferase MLL2 (also identified as KMT2B and KMT2D) in colon cancer (Guo et al., 2012); but controlled regulation of S100 proteins within a given cancer is specific. For example, the expression of S100A4 is regulated by Wnt–β-catenin signalling (Sack and Stein, 2009), while the expression of S100P is controlled by activation of both the prostaglandin E2 (PGE2) receptor EP4 subtype (PTGER4) and the MEK–ERK–cAMP-responsive element-binding protein (CREB) pathway in colon cancer (Chandramouli et al., 2010). Furthermore, the regulatory mechanisms controlling S100 expression can be cancer type-specific. For example, in prostate cancer, S100A8 and S100A9 expression is controlled by hypoxia-inducible factor 1 (HIF1) and PGE2–protein kinase A catalytic subunit (PKA-C)–CCAAT/enhancer-binding protein-β (CEBPβ) signalling (Grebhardt et al., 2012; Miao et al., 2012); in liver cancer by nuclear factor-κB (NF-κB) signalling (Nemeth et al., 2009); and in skin cancer by ultraviolet radiation, intrinsic ageing and photo-ageing (Lee et al., 2013a).

1.5.3 Epigenetic regulation

It has been demonstrated that S100 genes are epigenetically regulated by DNA methylation (Lindsey et al., 2007). Generally, mammalian genomes are depleted in CpG pairs except for short DNA repeats, known as CpG islands that commonly happen within gene promoters. These regions are often recognised by transcriptional inhibition controlled by DNA methyltransferases that methylate cytosine residues. In the first step, methyl-CpG-binding domain proteins (MBDs) recruit proteins such as histone deacetylases (HDACs) which have important role in modifying chromatin to its repressed state, heterochromatin. The second step, methylation can physically perturb binding of transcription factors to DNA therefore avoiding trans-activation (reviewed in (Robertson, 2005)).

DNA methylation plays an important role in regulation *S100* genes expression. It has been found that in lymphoma cells *S100A4* is activated when DNA methyltransferases are inhibited by 5'azacytidine (Tulchinsky et al., 1995). Another study has shown that DNA methylation of *S100* genes are essential for regulation of their expression (Lindsey et al., 2007) although each S100 gene is likely to be controlled by CpG-specific DNA methylation instead of epigenetic silencing across the entire chromosome band.

1.5.4 S100 transcriptional regulation

S100 proteins, including S100A4, are commonly activated during a number of cell stress events, including chronic osmotic shock (Chen et al., 2011; Rivard et al., 2007) hypoxia (Horiuchi et al., 2012) and inflammation (Schneider et al., 2008). Consequently, different studies have investigated the transcriptional regulation of S100A4 which lead to a conclusion of complex network of response elements and transcription factors controlling its expression (Table 1.2). Generally, S100A4 has been shown to be activated downstream by various types of cytokines and growth factors such as TGF-β (Sato et al., 2010; Xie et al., 2009), FGF (Ryan et al., 2003), EGF (Hugo et al., 2009) and IL-1β (Franco-Barraza et al., 2010). Although the signalling cascades have yet to be fully clarified, it was found that AP-1 and a complex of the NF-κB/ReI specific p50.p50 homo and p50.p65 heterodimers via binding to a κB-like element within the first intron of S100A4 (Tulchinsky et al., 1995). In addition, Cohn found that *cis* elements interacts with transcription factors related to the SP-1 and CBF families (Cohn et al., 2001). Moreover, another *cis* element, fibroblast transcription site-1 (FTS-1), is identified approximately 1000 bps upstream of the TATA box. This element interacted in a complex with the CBF-α subunit/KRAB-associated protein 1 (KAP-1) (Venkov et al., 2007).

S100A4 expression is controlled by an *Erbb2* response element in the promoter (Hernan et al., 2003) and a TCF binding (Stein et al., 2006) implicating in Wnt pathway. Lastly, S100A4 expression is induced by ectopic expression of integrin α6β4 in MDA-MB-45 cells via a NFAT5-dependent mechanism (Chen et al., 2009).

Site	Description	Location	Reference
FTS-1	*Cis* element	1000 bps upstream of TATA box	(Venkov et al., 2007)
Erbb2	Response element	Promoter	(Hernan et al., 2003)
TCF	Binding site	Promoter	(Stein et al., 2006)
CBF	Intronic enhancer	First intron	(Cohn et al., 2001)
SP-1	Intronic enhancer	First intron	(Cohn et al., 2001)
κB-like element	Intronic enhancer	First intron	(Tulchinsky et al., 1995)
AP-1	Intronic enhancer	First intron	(Tulchinsky et al., 1995)

Table 1.2 Transcription factors regulating expression of S100A4 gene.

1.5.5 S100 signaling in cancer biology

Some of S100 family members play an important role in tumour growth, metastasis, angiogenesis and immune evasion. Some of the S100 proteins can act as tumour suppressors in specific cancer type. For instant, S100A2 acts as a tumour suppressor in oral cancer and as a tumour promoter in lung cancer (Bulk et al., 2009; Tesch et al., 2006). Also, S100A7 acts as a tumour suppressor in oestrogen receptor-α (ERα)-positive breast cancer and it helps ERα-negative breast tumour growth (Deol et al., 2011).

1.5.6 S100 function

S100 family members have critical roles in many cellular processes important to the maintenance of cells shape and motility, modulation of signal transduction pathways

and in regulation of calcium homeostasis. These cellular processes can be either intracellularly or extracellularly mediated (Figure 1.11) (Sapkota et al., 2008). The function of extracellular or secreted S100s is less clear because of the lack of an extracellular signal peptide and their export is not affected by the ER-Golgi classical secretion pathway inhibitor. Furthermore, although the receptor for advanced glycation endproducts (RAGE) is interact with some S100s, data regarding the receptor for secreted S100 proteins remain controversial. The biological functions of most S100 proteins are calcium (Ca++) dependent; however some of them have the ability to interact with their target molecules in a Ca++-independent manner. During Ca++ binding, all dimeric S100 proteins, except S100G which exists in monomeric form, producing physiological responses by interaction with target proteins. Some S100 proteins reach extracellular space (by unknown secretion mechanisms) and bind with their receptors, including: RAGE for S100A1, S100A4, S100A6, S100A11, S100A12, S100A13, and S100B proteins; receptors for many S100 members are unknown, and control the respective extracellular functions (Santamaria-Kisiel et al., 2006; Sapkota et al., 2008).

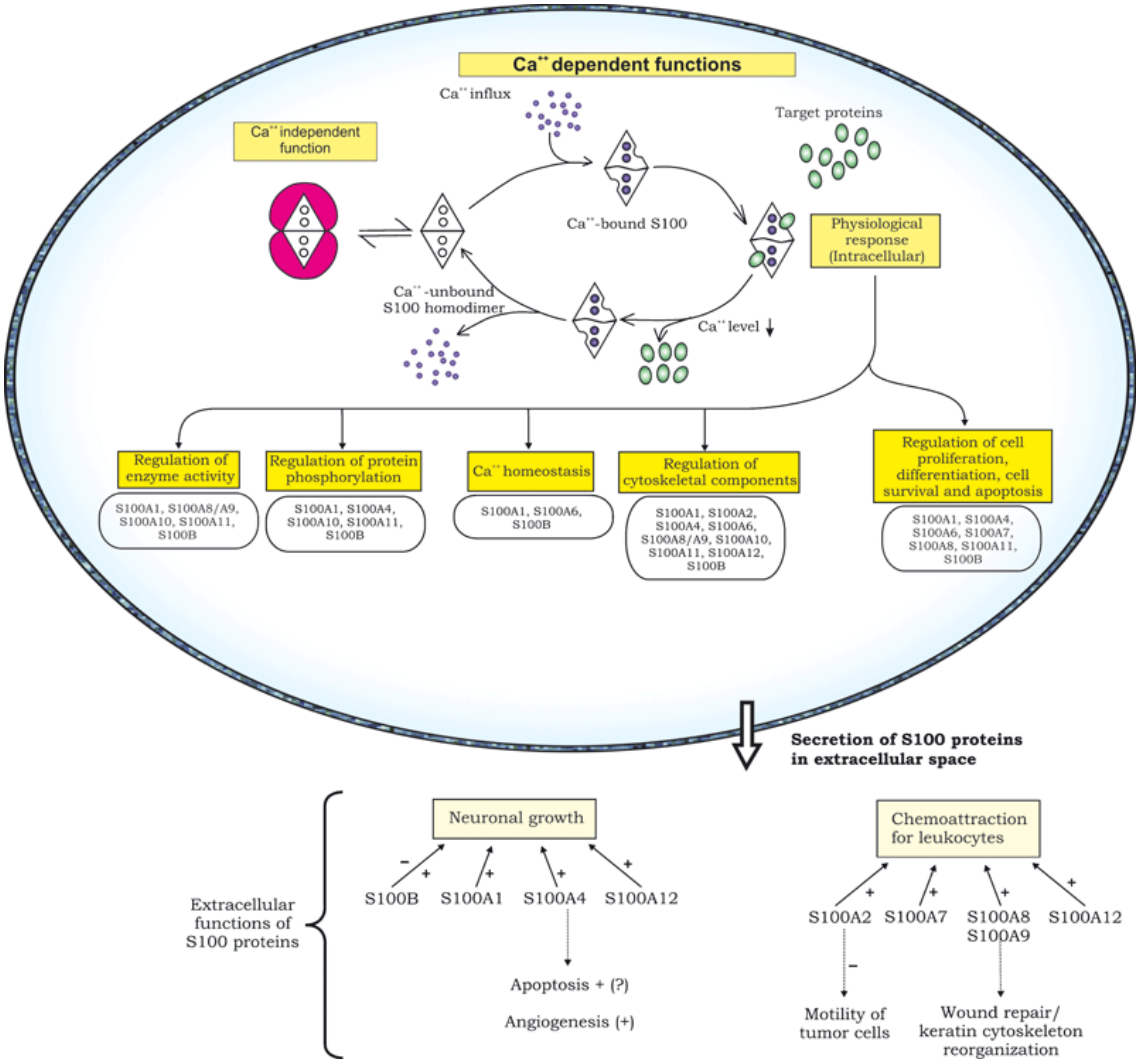

Figure 1.11 Intracellular and extracellular functions of S100 proteins.

Copied from (Sapkota et al., 2008).

1.5.7 S100s in diseases

S100 proteins are expressed in different tissues and cells, and their expression deregulation is related to a multiple groups of pathological disorders which can be categorized into four groups: neurodegeneration, cardiomyopathies, inflammatory diseases and cancer (Marenholz et al., 2004).

In neurodegenerative diseases such as Down's syndrome, Alzheimer's or multiple sclerosis, S100B expression is related to traumatic brain injuries. Thus, S100B can be used as a marker for brain ischaemia and clinical outcome predictive (Donato, 2001).

Cardiomyopathies are strongly related to the expression of S100A1 which controls contractile performance of the heart. Moreover, S100A1 expresses at high level in right ventricular hypertrophy and its down-regulation is associated with end-stage heart failure. S100A1 plasma level links with acute myocardial ischaemia. S100B is not expressed in mature myocardium but its expression is induced after myocardial infarction as a result of apoptosis and progressive deterioration of cardiac function. In damaged myocardium, S100A6 protein has been shown to be upregulated and may be involved in hypertrophy (Tsoporis et al., 2010).

Referring to section 1.4, most of the S100 genes are found on chromosome 1q21 normally, a site known as the epidermal differentiation complex. In cancer cases, such as uterine and bladder adenocarcinomas, this locus is commonly rearranged. Therefore, S100s expression is changed at different levels and many studies have focused to characterise their functions in the context of tumour progression. In the recent decades, usage S100s as a potential prognostic markers has been one of the major interesting research subjects in different malignancy (Fei et al., 2017).

In many human cancers, dysregulation of S100 protein expression is commonly detected. *In vivo* studies have been shown that expression of 10 members of S100 family altered and this may affect the growth, metastasis, angiogenesis and immune evasion process of numerous tumours such as lymphoma, breast, lung and pancreas cancers (Table 1.3) (Bresnick et al., 2015b). Appendix 2 shows the dysregulation expression of S100 in all cancer. In addition, it was found that inhibitions of two family

members, S100B and S100A9, are in clinical trials for melanoma and prostate cancer, respectively. Nowadays, many studies focus on analysis of S100 proteins in cancer diagnosis and treatment. In addition, many reviews have shown that S100 protein inhibitors may use for treating cancer.

Cancer	Family member	Function	References
Lymphoma	S100A9	↑ Growth and ↑ immune evasion	(Kallberg et al., 2012; Cheng et al., 2008)
Breast	S100A1	↑ Growth	(Wang, 2005)
	S100A4	↑ Metastasis	(Lloyd et al., 1998; Grigorian et al., 1996)
	S100A7	↑ ↓ Growth	(Krop et al., 2005)
	S100A8	↑ Metastasis	(Yin, 2013)
Lung	S100A2	↔ Growth and ↑ metastasis	(Bulk et al., 2009)
	S100A4	↑ Metastasis	(Takenaga et al., 1997)
	S100A9	↓ Inflammation	(Ortiz et al., 2014)
	S100A10	↑ Growth and ↑ immune evasion	(Phipps et al., 2011)
	S100A11	↑ Growth	(Hao et al., 2012)
Pancreas	S100A4	↑ Growth and ↑ angiogenesis	(Hernandez, 2013)
	S100P	↑ Growth and ↑ metastasis	(Arumugam et al., 2013; Dakhel et al., 2014)

Table 1.3 Function of S100 proteins in different cancers

1.5.7.1 S100 proteins in haematological malignancy

Yamaguchi (2009) shows that some S100 proteins are ectopically expressed in various hematopoietic malignancies. It is believed that this combination of gene abnormalities is essential for the onset of leukaemia. A study has shown that the synergistic enhancement of S100A6 expression in presence of MLL-AF4 (mixed lineage leukaemia gene) and FLT3 (Fms-like tyrosine kinase 3) plays a significant role in MLL-AF4L-associated leukemogenesis (Yamaguchi et al., 2009). Furthermore, S100P found to be strongly expressed in 51.72% of non-germinal centre of DLBCL cases, and considered as a prognostic marker (All and Abd, 2007). Also, it has been

detected that S100A8 expression is associated with poor prognosis in Acute Myeloblastic Leukaemia (AML), and proposed to be a short survival predictor (Nicolas et al., 2011).

A bioinformatics study of the dataset EGEO-2466 performed in our laboratory shows that there is differential expression of *S100* genes, up/down regulation (Figure 1.12) in CLL versus normal cases. The results from EBI ArrayExpress demonstrated upregulation of S100 genes, including *S100A4, S100A8, S100A9, S100A10, S100A11*, and *S100P*, in CLL samples versus normal samples of the peripheral blood. The microarray data in this study is selected from EBI ArrayExpress (E-GEOD-2466) and NCBI GEO databases (GSE6691 and GSE7905).

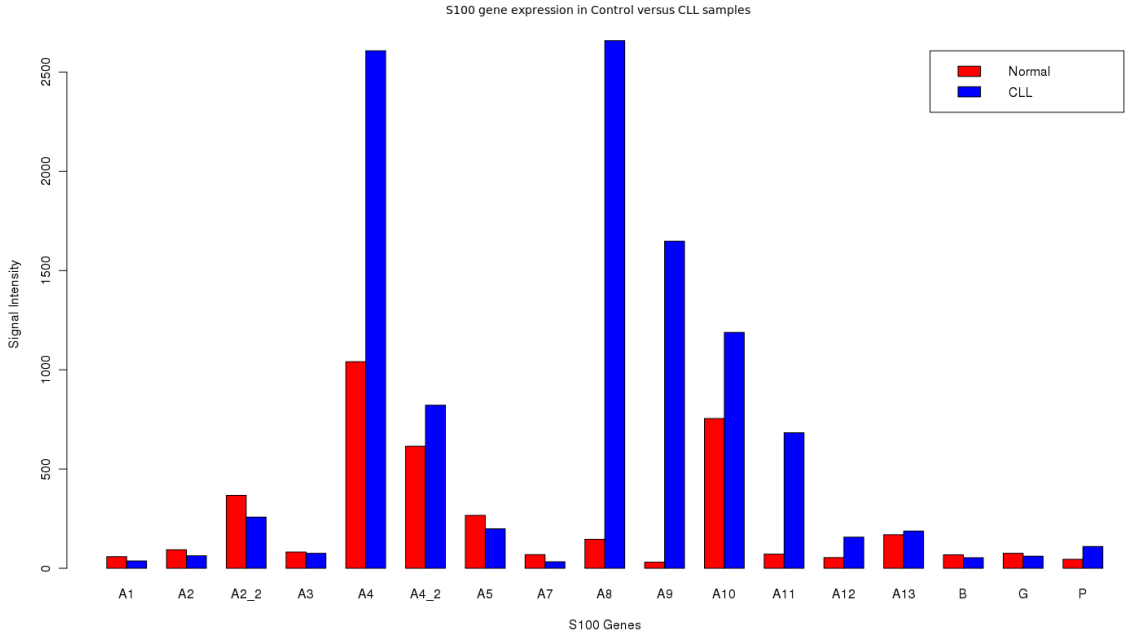

Figure 1.12 Relative expression of S100 genes in normal B-lymphocytes samples versus CLL samples taken from peripheral blood.
The red bar indicates the normal samples and the blue bar indicates the CLL samples. The level of expression of *S100A4, S100A8, S100A9, A100A10, S100A11, S100A12* and *S100P* are relatively higher in CLL samples than other *S100* genes in normal samples (G. Kaithakottil, MSc thesis, University of Leicester, 2010).

In addition, in this study the analysis was performed based on the Pearson coefficient and Euclidean correlation on the GEO dataset GDS2643 using complete linkage algorithm. GSE6691 formed cluster between S100A4:S100A6 (Figure 1.13A), S100A8:S100A9:S100A12:S100P (Figure 1.13B) with Pearson correlation coefficient.

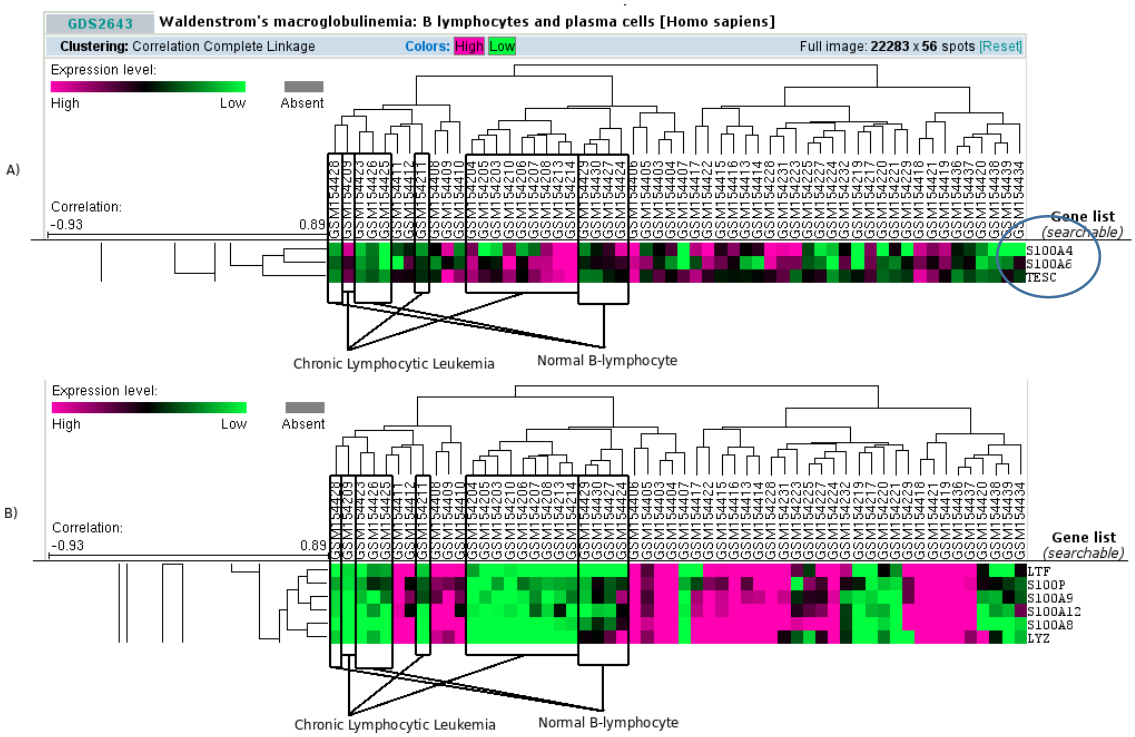

Figure 1.13 Pearson correlation using complete linkage.

The results show clusters of (A) *S100A4* and *S100A6* genes and (B) *S100P, S100A9, S100A12* and *S100A8*. The samples corresponding to B-CLL and normal B-lymphocytes (NBL) are boxed separately. It can also be seen that B-CLL and NBL samples are not grouped separately during clustering.

Also it was revealed from this study that *S100A4* and *S100A6* genes are highly expressed in CLL samples taken from bone marrow in comparison with normal B-lymphocyte samples taken from peripheral blood. This study shows that S100A4 and S100A6 are expressed B-cell lymphomas (Figure 1.14). In a genome wide microarray study they found that CLL cells isolated concurrently from peripheral blood, bone marrow, and lymph nodes show characteristic gene expression profiles which show differential activation of signaling pathways in the various anatomic compartments (Herishanu, 2011). Thus, the microenvironment signals can regulate S100 proteins in CLL.

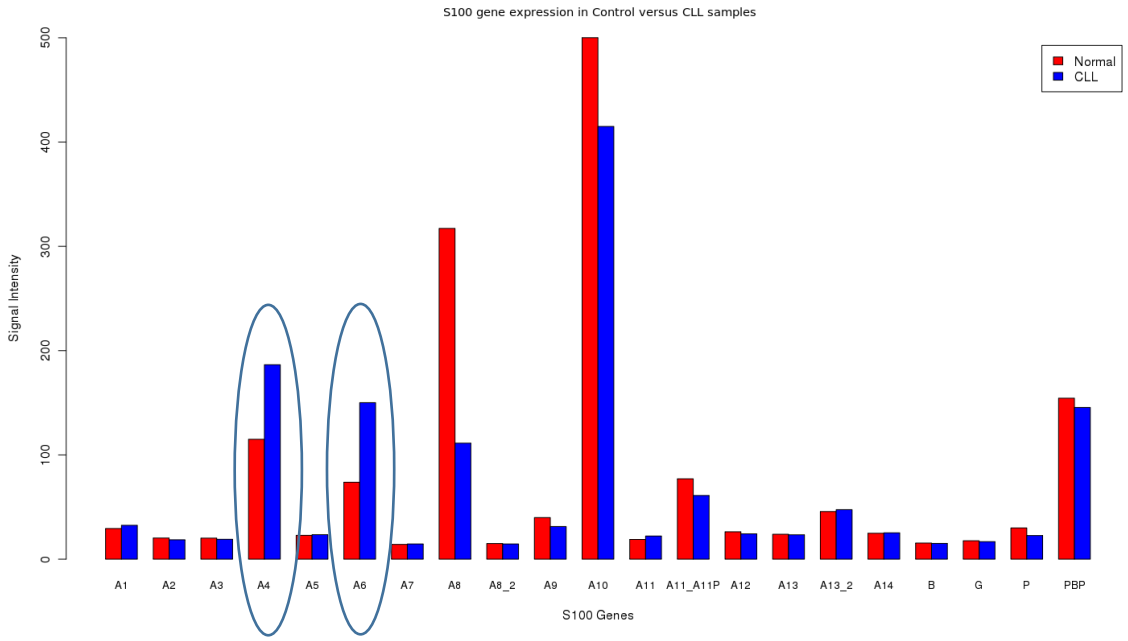

Figure 1.14 Relative expression of S100 genes in normal B-lymphocytes samples taken from peripheral blood versus CLL samples taken from bone marrow.
The red bar indicates the normal samples and the blue bar indicate the CLL samples. Analysis shows that the levels of expression of *S100A4* and *S100A6* are relatively higher in CLL samples than other S100 genes in normal samples.

1.5.7.2 S100A4 in cancer

S100A4 protein is a small protein with a low molecular weight (10-12 kDa) that has no enzymatic activity; but derives its action via interaction with other proteins (Mishra et al., 2012). Several experiments have established the relationship between S100A4 expression and tumour progression and metastasis. Although, its metastasis promoting properties are not fully understood, it is predicted that they occur as a result of their potential role in cells motility, invasion, angiogenesis and apoptosis. S100A4 has also been shown to be a critical regulator in EMT induction, through its interaction and modulation of several intracellular and extracellular targets such as p53, annexin II, receptor for advanced glycation endproduct (RAGE), E-cadherin, NF-κB, and β–catenin (Boye and Maelandsmo, 2010; Mishra et al., 2012).

1.5.7.2.1 S100A4 Expression

S100A4 is expressed in many types of cells such as parietal cells of the stomach, smooth muscle cells, endothelial cells and in many differentiated blood cells (neutrophils, macrophages, T-lymphocytes and platelets) (Strutz et al., 1995). In the research of Osterreicher et al., S100A4 was identified as a potential marker or a fibroblast marker (Osterreicher et al., 2011). This suggestion initiated from a study by Strutz who identified S100A4 as one of five specific transcripts in renal tubulointerstitial fibroblasts when compared to isogenic murine proximal tubular epithelium cells (Strutz et al., 1995).

1.5.7.2.2 S100A4 Function

S100A4 is activated in multi-functional signalling pathways, including Wnt/β-catenin, NF-κB, and E EMT. Recently, researchers found that osteopontin is a down-stream of S100A4 and activated after RAGE stimulation by S100A4. This makes S100A4 an eminently valuable chemotherapeutic target (Buetti-Dinh et al., 2015). In addition, S100A4 has been shown to be linked to EMT by playing an important role in cell cycle, cell proliferation, tumour growth, apoptosis, invasion, motility and intercellular adhesion. Moreover, S100A4 promotes metastatic spread of cancer as demonstrated by gene transfer studies. Its expression has shown a clear correlation with tumour spread to lymph nodes and prognosis (Sherbet, 2014).

S100A4 increases the motility of many cells such as macrophages, neutrophils, and leukocytes and stimulates the recruitment and chemotaxis of these inflammatory cells to regulate inflammation and immune response (Zhou et al., 2015). Moreover, on neurons S100A4 exerts a neuroprotective pro-survival effect by releasing them from brain injury (Doroudgar, 2016) and involves in angiogenesis via its interaction with other target molecules (Xia et al., 2017). Intracellularly, S100A4 binds to several target molecules and this binding causes alterations in cytoskeletal dynamics and increase cell motility and proliferation (Boye et al., 2010). Furthermore, many types of cells, such as fibroblasts, macrophages, and lymphocytes, express and release S100A4 into their

extracellular space as an active extracellular factor; therefore, S100A4 has a great tendency to control gene expression associated with proteolytic activity, angiogenesis, cell survival, and motility by controlling the signaling pathways of mitogen-activated protein kinases (MAPKs), extracellular signal-regulated kinase, p38, Jun N-terminal kinases, nuclear factor-kappa B (NF-κB), and p53 (Schneider, 2007). S100A4 role in human non-tumor pathophysiologies is summarized in figure 1.15.

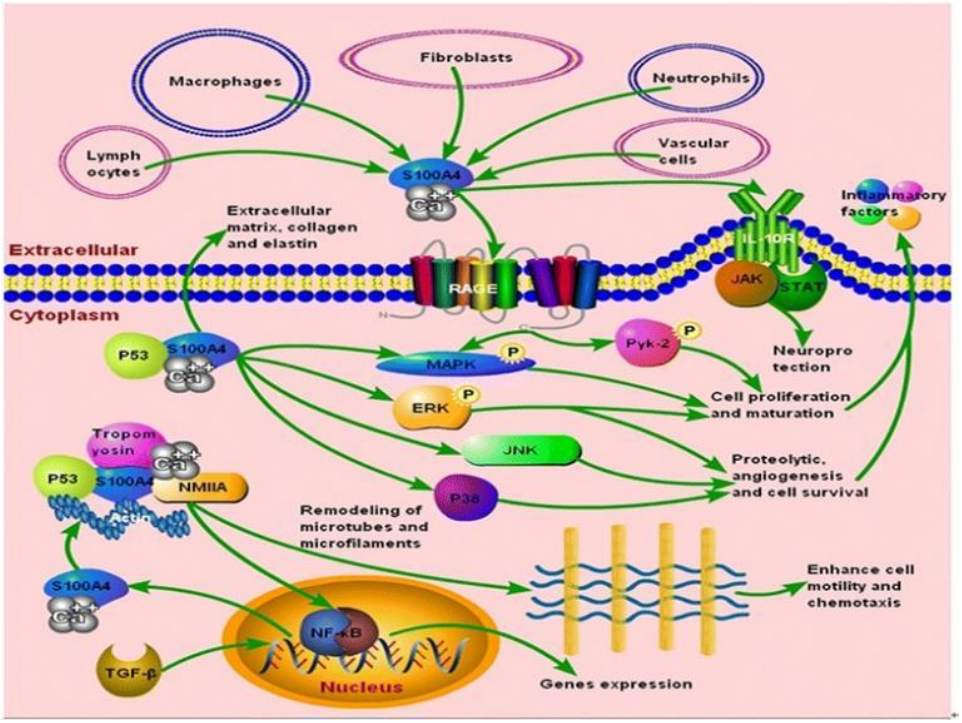

Figure 1.15 The role of S100A4.

The S100A4 interacted with IL-10R exerts a neuron pro-survival effect under many injuries via JAK/STAT pathway. Also, the expression of extra-S100A4 increases phosphorylation of Pyk-2, MAPKs, and activating NF-κB through the RAGE-dependent regulation related with cell migratory abilities and chemotaxis. Moreover, the intracellular S100A4 can interact with numerous target molecules, such as NMIIA, tropomyosin, P53, and actin, forming the complexes that facilitating the remodeling of microtubes and microfilaments to increase cell motility and chemotaxis, contributing to the infiltration of fibroblasts, immune and vascular cells into the affected region releasing inflammatory factors. Furthermore, S100A4 combine with P53 stimulating cell proliferation and collagen expression via MAPK activation and phosphorylation of ERK. The TGF-β-mediated process promotes the up-regulation of S100A4 inducing the generation of extracellular matrix, collagen, elastin and others underlying the basis for the course of inflammation tissue fibrosis. In addition, S100A4 intracellularly controls its upstream and/or downstream gene expression involved in proteolytic activity,

angiogenesis and cell survival by modulating MAPKs, ERK, p38, JNK, NF-κB, and p53signal pathways.

Copied from Schneider, 2007.

1.5.7.2.3 S100A4 in cell migration

Cell migration is an important process required in many steps of the metastatic cascade. A lot of research has been shown as a result of clinical evidence that S100A4 is associated with metastasis. The main functional aspect of S100A4 effect has appeared on its role in enhancing cell migration (Donato, 2001). For example, it was shown that S100A4 is initially correlated with a more motile phenotype in promyelocytic leukaemia cells (Takenaga et al., 1994a). Other study showed that over-expression of S100A4 in the mouse adenocarcinoma cell line, CSML0, also increases cell migration (Ford et al., 1995). Moreover, it was found that S100A4 activates gastric cancer cells proliferation and migration (Guo et al., 2017).

On the other hand, many studies have shown that S100A4 reduction either by RNA oligonucleotides or RNA interference (RNAi) inhibits both cell migration and invasion in Lewis carcinoma cells (Takenaga et al., 1997); breast carcinoma cells (Jenkinson et al., 2004); colon adenocarcinoma cells (Stein et al., 2006); endometrial adenocarcinoma cells (Xie et al., 2009); and osteosarcoma cells (Fujiwara et al., 2011) among others (Tarabykina et al., 2007) (Table 1.4). Further study established the relation between S100A4 expression and cell migration and showed that S100A4 expression is found in highly migratory normal cells such as neutrophils, T-lymphocytes and macrophages (Cabezon et al., 2007).

Cell line	Originating Tumour	Cell Migration Model	Reference
A11	Lewis lung Carcinoma	Transwell assay coated with Matrigel	(Takenaga et al., 1997a)
n/a	Mammary gland tumour of transgenic mice	Transwell assay	(Jenkinson et al., 2004)
HCT116	Colon adenocarcinoma	Transwell assay coated with and without Matrigel	(Stein et al., 2006)
Hec1A	Endometrial adenocarcinoma	Transwell assay coated with and without Matrigel	(Xie et al., 2009a)
LM8	Osteosarcoma	Transwell assay	(Fujiwara et al., 2011)
Bxpc-3	Pancreatic adenocarcinoma	Transwell assay	(Li et al., 2012)

Table 1.4 Correlation of S100A4 expression with increased rates of cell migration.

Overexpression of S100A4 have also been shown to be a significant determinant allowing cellular spreading and distant tumour formation. By its role in cellular motility through its interactions with actomyosin components, S100A4 has also been demonstrated to play important roles in both cellular motility through the interactions with other targets. Both the Wnt/catenin (Zhang el at., 2012) and the AKT/slug (Wang, 2014) pathways have been shown to be capable of regulation by S100A4, effecting cytoskeletal architecture and overall cellular migration. S100A4 can activate other signalling pathways such as the PI3K/AKT/mTOR (Wang, 2014) or the NF-kB (Zhang el at., 2013) route leading to critical alterations in migration but without directly linking this process to cytoskeletal reorganisation. In addition, S100A4 has the ability to

encourage cellular migration and potential chemotaxis relates to its presence in the extracellular matrix, where it is found at concentration as high as 10 μM (Malashkevich el at., 2008). Researchers found that S100A4 regulate the activities of metalloproteinases and RAGE (Schmidt-Hansen el at., 2004). Many approaches have been used to combat the S100A4 motility and invasion inducing ability through inhibitors isolation. The result of this early work has revealed that some of these inhibitors control the interactions of S100A4 with the actomyosin network. For example, trifluoperazine, a phenothiazine-based compound, has been shown to block S100A4 ability to depolymerise NMMIIA filaments (Spiekerkoetter, 2009). Further drugs that can control S100A4 interaction with the actomyosin architecture might be developed as inhibitors of the S100A4 associated cell motility.

1.5.7.3 S100A6 action in cancer

S100A6 (calcyclin) is a 10.5 kDa calcium binding protein, it is highly expressed in various human cells, including: - fibroblasts, epithelial cells, neurons, glial cells, smooth muscle cells, cardiac myocytes, and platelets. There are different factors that regulate the expression of this protein such as platelet-derived growth factor (PDGF), epidermal growth factor (EGF) and tumour necrosis factor (TNFα) (Lesniak et al., 2009).

1.5.7.3.1 S100A6 function

Although the mechanism of S100A6 is not clearly defined, it has been shown that S100A6 is implicated in actin cytoskeleton and membrane dynamics via its interaction with actin binding protein. Moreover, it has an important role in regulation of β-catenin level which done by its binding with CacyBP/SIP (Calcyclin-Binding Protein and Siah-1 Interacting Protein). It is also involved in cellular heat-shock response by inhibiting the interaction between heat shock proteins and Sgt. In addition, it significantly regulates cell growth and apoptosis by its interaction with p53 (Luu et al., 2005). Research has been shown that overexpression of S100A6 protein in several human tumours, such as malignant melanoma, squamous cell carcinoma, colorectal

adenocarcinoma, gastric cancer, pancreatic ductal adenocarcinoma, papillary thyroid carcinoma, astrocytoma and craniopharyngioma are positively associated with tumour metastasis. Also, S100A6 has a negative association with tumour metastasis in another group of cancers, including: osteosarcoma, prostatic intraepithelial neoplastic lesions and medulloblastoma, via enhancing cells adhesion and inhibiting cells motility and invasion (Lesniak et al., 2009).

1.5.8 EMT factors and S100 proteins in haematological malignancies

During malignant progression, EMT has a crucial mechanism for cancer cells because it plays an important role in cell invasiveness, migration capability, stemness, and drug resistance. Also, in normal blood cell development EMT-related factors may also play an essential role. For instance, during lymphocyte differentiation an extracellular signal-regulated kinase-mediated phosphorylation of E2A, which is associated with EMT, controls its degradation in response to Notch signalling. In addition, E2A gene products (E12 and E47) are also targets for G1 cyclin-dependent kinases that regulate B-cell growth and survival during development. Moreover, twist 1 overexpression is correlated with the resistance to imatinib in chronic myeloid leukaemia. Also, twist 1 expression is inhibited by tyrosine kinase inhibitors. However, there is upregulation when the resistance develops (Chou and Yang, 2015).

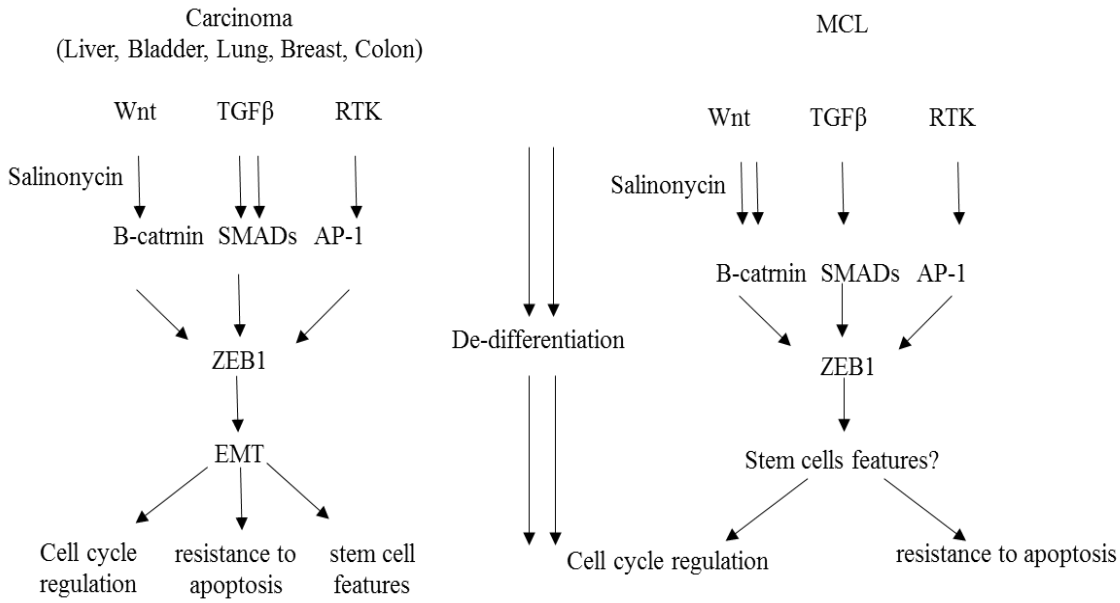

Figure 1.16 Role of EMT-inducing transcription factor ZEB1 in MCL.

Adapted from (Sayan, 2014).

1.5.9 Targeting S100 proteins

Studies have shown that S100 family members can be used as targets for cancer treatment. It was found that genetic deletion has insignificant effects on normal physiology in mouse models. On the other hand, some members of the S100 family can be attractive targets for the treatment of other diseases. For example, the progression of Alzheimer's disease may delay through S100B and S100A1 inhibitors (Afanador et al., 2014; Roltsch et al., 2010). However, in heart disease S100A1 inhibitor delays the development of cardiomyopathy (Rohde et al., 2010).

Many pharmacological approaches have been used to reduce S100 signalling in cancer patients. Some of them are calcimycin (a calcium ionophore), niclosamide (an antihelminth drug) and sulindac (a non-steroidal anti-inflammatory drug) which have all been known as S100A4 transcription inhibitors (Sack et al., 2011; Stein et al., 2011). Transcriptional modulators may have clinically important toxic off-target effects because of their ability to regulate protein expression through the control of other genes. Gene therapy has been used in preclinical animal models, in which it helpfully upregulates expression of S100A1 in heart disease but has not been used to modulate

the expression of S100 family members in patients with cancer (Weber et al., 2014). S100A4 and S100P neutralizing antibodies are other approaches used to modulate S100 protein activity (Dakhel et al., 2014; Hernandez et al., 2013; Weber et al., 2014). In addition, peptibodies (peptide–Fc fusion proteins) directed against S100A8 and S100A9 (Qin et al., 2014). The benefit of these approaches is to reduce tumour growth in murine cancer models. Also, inhibitory peptides can be directed against S100B, which are usually penetrating cells, help to reduce tumour growth in a melanoma xenograft model (Dhar et al., 2014).

S100 proteins inhibitors have the very important function to activate small molecules that block the hydrophobic cleft which required for the recognition of S100 targets, and for stimulating biological effects (Yap et al., 1999). For example, paquinimod (ABR-215757) and tasquinimod (ABR-215050), which are quinoline-3-carboxamide products can block the interaction of S100A8 and S100A9 with RAGE and TLR4, respectively (Bjork et al., 2009; Kallberg et al., 2012). Paquinimod uses anti-inflammatory effects in many disease *in vivo* models, but has not been specifically experienced in cancer models. On the other hand, tasquinimod increases progression-free survival in patients with metastatic castration-resistant prostate cancer, by decreasing the recruitment of MDSCs and inhibiting metastasis (Jennbacken et al., 2012; Pili et al., 2011). Cromolyn is an anti-histaminic drug which stops the interaction between S100P and RAGE and as a result decreasing pancreatic tumour growth and increasing the effectiveness of the chemotherapeutic drug gemcitabine (Arumugam et al., 2013; Kim et al., 2012). Cromolyn binds several other S100 family members, such as S100A1, S100A12 and S100A13, but the biochemical and biological process of these interactions have not been studied. Moreover, Amlexanox which is anti-inflammatory anti-allergic immunomodulatory drug, interacts with some S100 proteins such as S100A1, S100A4 and S100A13 (Mack and Marshall, 2010; Okada et al., 2002). It has the ability to inhibit S100A13 secretion. As a result, it disrupts the interaction of S100A13 with fibroblast growth factor 1 (FGF1) and stop FGF1 mitogenic and angiogenic effects (Rani et al., 2010). Phenothiazines also interact with multiple S100 family members including S100A4. Phenothiazine can mediate S100A4 oligomerization causing the S100A4 sequestration away from its protein targets (Garrett et al., 2008; Malashkevich et al., 2010). 3

1.6 Preliminary Data

IHC of the B- cell lymphomas tissue microarray results confirmed expression of S100A4 in B-lymphoma cell lines (collaboration with Dr Karen Pulford, Oxford University) (Figure 1.17). A high level of S100A4 expression was detected in the majority of CLL and MCL samples and in a proportion of DLBCL (Table 1.5).

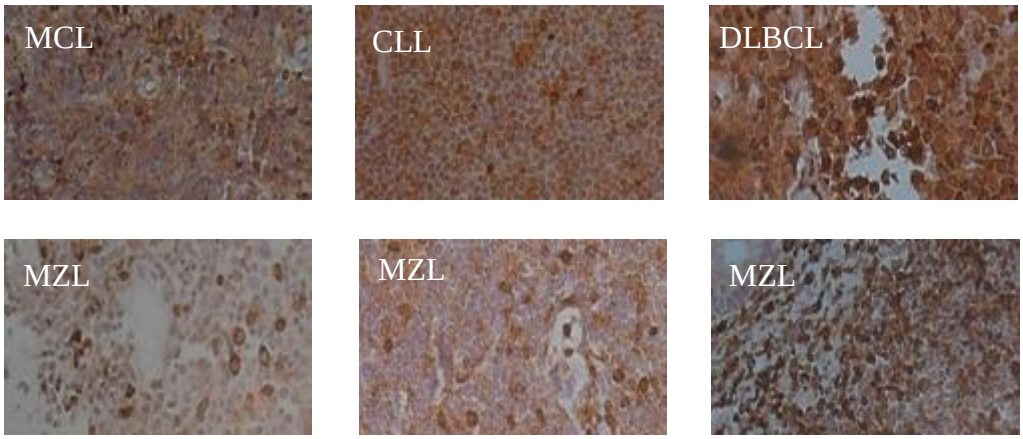

Figure 1.17 S100A4 expression in B-cell lymphomas samples by IHC (Dr Karen Pulford, University of Oxford).

	Analysed	Positive	Negative	Non-interpreted	Scored again
DLBCL	12	5	3	1	3
FCL	9	1 nuclear	8		
CLL	6	5	1		
LPL	2		1	1	
MZL	14	9 cytoplasmic	3	2	
MCL	4	4			

Table 1.5 Expression of S100A4 in B-lymphoma.

IHC analysis shows a high level of S100A4 expression in the majority of CLL and MCL samples and in proportion of DLBCL (Dr Karen Pulford, Oxford University).

1.7 Aims and Objectives

Enhanced levels of S100A4 and S100A6 are linked to poor prognosis in a subset of solid tumours including breast, pancreatic and bladder carcinomas, and the expression of these proteins is activated by EMT programs in epithelial malignancies (Chou and Yang, 2015). We hypothesize that S100A4 and S100A6 are regulated by EMT transcription factors in B-cell lymphomas and their expression is associated with poor prognosis of lymphoma patients. We propose that B-cell lymphoma relapse can be predicted by the analysis of S100A4 expression in bone marrow and in samples obtained from the peripheral blood of the CLL patients.

The main aim of the project is to analyse the expression of S100A4 and S100A6 proteins in B-lymphoma samples. This work focuses on:

1. Characterization of cells expressing S100A4, S100A6, ZEB1 and ZEB2 in tissues of lymphoid organs, including: tonsil, spleen and thymus, and different types of B-cell lymphomas tissue.
2. Study the expression of S1004 protein in mature and immature cells in bone marrow samples of normal and CLL patients.
3. Comparison of the pattern of S100 protein expression in normal B-cells that isolated from normal volunteers and B-cell lymphoma from CLL patients using qPCR analysis in order to investigate which members of S100 proteins overexpressed in B-cell lymphomas.
4. Study the S100A4 expression on 20 peripheral blood samples of chronic lymphocytic leukaemia by Western blotting, IHC and 4-colour immunofluorescence and detection its effect in patient's survival rates using statistical analysis (SPSS).
5. Chemotaxis approach will be used to investigate the role of S100A4 protein on lymphoma cell migration *in vitro*, where S100A4 protein expression will be modulated by RNA approach.
6. Investigation of the effect of cytokines, including: IL-1 alpha, IL-6 and IL-11, on expression of S100A4 protein and its role in lymphocyte invasion.
7. Testing inhibitors of S100A4 activity on cell migration using available cell lines and lymphocytes of the CLL patients.

Chapter 2. Materials and Methods

2.1 Materials

2.1.1 Chemicals, buffers, kits and general equipment

Tables 2.1, 2.2, 2.3 and 2.4 respectively showed chemicals, buffers, kits and equipment and their sources that used throughout this study.

Chemical	Source
Xylene	Genta Medical, UK
Ethanol	Genta Medical, UK
Methanol	Fischer Scientific, UK
Tween-20	Sigma-Aldrich, Dorset, UK
Glycerol	Sigma-Aldrich, Dorset, UK
Mirus buffer	Mirus Bio Ingenio, UK
Cytoblock reagent 1	Thermo Thermo Fisher Scientific, UK
Cytoblock reagent 2	Thermo Thermo Fisher Scientific, UK
Fluromount-G	eBioscience, San Diego, Canada
Haematoxylin	Sigma-Aldrich, St Louis, USA
Tris base	Thermo Fisher Scientific, UK
Ammonium hydroxide, 28–30%	Sigma-Aldrich, UK
RNAscope® 2.0 HD Detection Kit	Advance cell diagnostic, ACD

4’,6-diamidino-2-phenylindole (DAPI)	Invitrogen, USA
DPX	VWR international Ltd, England
Trypsin/EDTA 10X uv inactivated	Thermo Fisher Scientific, UK
Deionized Formamide	Thermo Fisher Scientific, UK
proteinase K solution	Thermo Fisher Scientific, UK
Nuclease-free water	Sigma-Aldrich, UK
Stellaris RNA FISH Hybridization Buffer	Biosearch Technologies
Stellaris RNA FISH Wash Buffer A	Biosearch Technologies, UK
Stellaris RNA FISH Wash Buffer B	Biosearch Technologies, UK
Stellaris RNA FISH Probes, human GAPDH	Biosearch Technologies, UK
Vectashield® Mounting Medium	Vector Laboratories, UK
Ethidium bromide	Fluka Biochemika, Switzerland
Fetal Bovine Serum Gold (FBS)	Seralable, UK
Phosphate Buffered Saline (PBS) tablets	Oxoid Ltd, UK
Rosewell Park Memorial Institute 1640 (RPMI-1640)	PAA Laboratories Inc, UK
Dulbecco’s Modified Eagle’s Medium (DMEM)	PAA Laboratories Inc, UK
PCR Ranger 100bp ladder	PCR Ranger, UK

Pre-stained protein ladder	Fischer Scientific, UK
Trizol	Invitrogen, UK
DAPI	Thermo Thermo Fisher Scientific, UK
Hematoxylin Solution, Mayer's	Sigma-Aldrich, UK
Paraformaldehyde (PFA) 4%	Thermo Fisher Scientific, UK
Super signal west Dura Extended Duration Pierce ECLsubstrate	Thermo Thermo Fisher Scientific, UK
Sodium Chloride Na Cl2	Sigma-Aldrich, UK
Ponceau-S	Sigma-Aldrich, UK
N,N,N',N'-Tetramethylethylenediamine (TEMED)	Sigma-Aldrich, UK
Glycin	Sigma-Aldrich, UK
Triton	Sigma-Aldrich, UK
β-mercaptoethanol	Sigma-Aldrich, UK
Bovine Serum Albumin (BSA)	Thermo Fisher Scientific, UK
Bromophenol Blue	Sigma-Aldrich, UK
Ammonium Persulfate (APS)	Sigma-Aldrich, UK
30%acrylamide/bis acrylamide	Proto Gel, UK
20% Sodium Dodecyl Sulphate solution (SDS)	Fisher Scientific

10X Trypsin EDTA (TE)	Gibco, UK
Dimethyl sulfoxide (DMSO)	Sigma-Aldrich, UK
Doxycycline(DOX)	Sigma-Aldrich, UK
Ethylenediainetetraaceticacid (EDTA)	Sigma-Aldrich, UK
Trypan Blue Solution	Sigma-Aldrich, UK

Table 2.1 General chemicals and their sources.

Buffer	**Chemical composition**
PBS	One tablet of PBS was dissolved in 200ml H_2O
TBS	50Mm Tris pH7.65, 150 Mm NaCl, 0.1% (v/v) Tween 20
20x Sodium citrate buffer	42g citric Acid monohydrate, 1L ultrapure H2O, 20g NaOH. For use diluted 1:20
TE buffer	10 mM Tris-HCl, 1 mM EDTA, pH 8.0
4X Laemmli buffer	4% SDS, 40% glycerol, 20 mM Tris pH 6.8
10X Running buffer	30g Tris base, 144g 99% Glycin and 10g 20%SDS, topped up with 1L distilled water
10X Transfer buffer	30g Tris base and 144g 99% Glycin, topped up with 1L distilled water
1X Running buffer	100 ml 10x running buffer, 200 ml methanol, made up to 1 L with distilled

	water.
1X Transfer buffer	100ml 10X transfer buffer topped up with 900ml distilled water
20X Tris Buffered Saline(TBS)	1 M Tris, 3 M NaCl
1X Tris Buffered Saline-Tween 20 (TBST)	0.05 M Tris, 0.15 M NaCl, 0.001% Tween® 20
5% milk-TBST solution	5g Instant Dried Skimmed milk (low fat) with 100 ml TBST
5% BSA-TBST solution	5g BSA with 100 ml TBST
1X Loading Buffer	2.5ml Tris HCL 1M pH 6.8, 5ml 20%SDS, 5ml 100% Glycerol topped up with 100 ml distilled water
Tris-borate-EDTA 1X (TBE)	20 ml 50X Tris borate-EDTA topped up with 980 ml distilled water
Blocking solution	5g Marvel milk dissolved in 100 ml TBST.
Protein Loading Buffer	1 part 0.4% Bromophenol blue mixed with 1 part 50% v/v β-mercaptoethanol.
Trypsin/ EDTA 1X	500µl/ml Trypsin and 0.22 mg/ml EDTA top up with 45ml PBS
Tris Acetate-EDTA (TAE) 1X	20 ml 50X Tris acetate-EDTA topped up with 980 ml distilled water
Citric Acid	22g citric acid topped up to 500ml distilled water

Paraformaldehyde (PFA) 4%	4g paraformaldehyde dissolved in 100ml distilled water

Table 2.2 Buffers and their chemical content.

Kits	Company
JetPRIME Kit Polyplus Jet prime	Jet prime, France
PCR mycoplasma Test Kit I/C	PromoKine, UK
Pierce BSA protein assay	Fischer Scientific, UK
Pierce ECL Western blotting substrate	Fischer Scientific, UK
Shandon Cytoblock Kit	Thermo Thermo Fisher Scientific, UK
Dynabeads® Untouched™ Human B Cells	Thermo Thermo Fisher Scientific, UK
Maxwell® 16 LEV simplyRNA Cells Kit and Maxwell® 16 LEV simplyRNA Tissue Kit	Promega, UK

Table 2.3 List of Kits used during this study and their sources.

Equipment	Company
Amaxa® Nucleofector® electroporation device	Lonza, UK
Borosilicate glass capillary needles1.0mm OD, 0.78mm ID	Harvard apparatus, USA
Centrifuge 5415R machine	Eppendorf, UK
CL-XPosure film	Thermo Thermo Fisher Scientific, UK
Cover Glass 22 x 22 mm	VWR International, UK
Disposable Neubauer haemocytometers (C-CHIPs)	DigitalBio, Korea
fine surgical forceps 0.1x0.06mm	Fine Science Tools Inc. Canada
Immobilon-P polyvinylidene fluoride (PVDF) membrane	Millipore, Bedford, USA
Microloader 20ml	Eppendorf, UK
Micropipette puller	Sutter instrument .co, USA
NanoDrop ND-1000 Spectrophotometer	Thermo Thermo Fisher Scientific, UK
Picospritzer III injection apparatus	Parker, USA
Pipettes	Gilson, USA
Polysin Slides	Thermo Scientific,UK
Protein gel electrophoresis apparatus	BioRad, UK

Sigma Compact Centrifuge 2-5	SciQuip, UK
StepOnePlus ™ Real-Time PCR Systems	Applied Biosystems, UK
transfection cuvettes, 2mm	GeneFlow, UK
transfection cuvettes, 4mm	GeneFlow, UK
Whatman Filter paper	Whatman, UK
Magnet (DynaMag™)	Thermo Thermo Fisher Scientific, UK
Mixing device with tilting and rotation	VWR International, UK
Lymphoprep® for PBMC preparation	Fischer Scientific, UK
TC20™ automated cell counter	BIO-RAD, UK

Table 2.4 List of general equipment used in this study.

2.1.2 Tissue cultures

2.1.2.1 Cell line

HL-60, Jurkat, MEC1, MEC2, A431, A375, and MIA PaCa-2 cell lines were used in this study. Table 2.5 showed their description. Cell lines were used for the preparation of cytosine, RNA extraction and lysates for various immunological techniques. Some of them were used as negative or positive control for Western blotting.

Cell line	Description	References
HL-60	The cell line was derived from a 36-year-old woman with acute promyelocytic leukaemia at MD Anderson Cancer Centre.	(Birnie, 1988)
Jurkat	The Jurkat cell line was established from the peripheral blood of a 14 year old boy with T cell leukemia by Schneider et al., and was originally called JM.	(Schneider et al., 1977)
MEC1	The cell line was established earlier from explants of blood derived cells of a chronic lymphocytic leukaemia (CLL) patient at different stages of progression to prolymphocytoid transformation (PLL)	(Stacchini et al., 1999)
MEC2	The cell line was established earlier from explants of blood derived cells of a chronic lymphocytic leukaemia (CLL) patient at different stages of progression to prolymphocytoid transformation (PLL)	(Stacchini et al., 1999)
A431-ZEB2	Human epidermoid carcinoma derived from 85-year old female	(Mejlvang et al., 2007)
MIA PaCa-2	Derived from a 65-year-old man with adenocarcinoma	(Yunis et al., 1977)

A375	Derived from a 54 year old female with malignant melanoma. The cell line produces rapidly growing amelanotic melanomas in anti-thymocyte serum treated NIH Swiss mice.	(Kozlowski et al., 1984)

Table 2.5 Names and descriptions of cell lines used in this study.

2.1.2.2 Transfection

Different small interference RNAs (siRNAs) were used during this study. Also, GFP plasmid was used as positive control to check the efficiency of transfection. In addition, pEGFP-C1 plasmid was used as a positive control for gene expression. Table 2.6 showed list of these siRNAs, reagents and plasmid and their sources. siRNA samples were prepared as 5nM solutions, and used as 500x stock according to the laboratory protocol.

siRNA and plasmid	**Company**
siRNA S100A4	Ambion, UK
siRNA S100A6	Ambion, UK
siRNA Non-targeting	Ambion, UK
Mirus Buffer (Ingenio® Electroporation solution)	Bio Ingenio,UK
GFP plasmid	Dharmacon, UK
GFP plasmid	Amaxa
pEGFP-C1 plasmid	Clontech

Table 2.6 List of siRNAs, reagents and plasmid used in this study.

2.1.3 Slides staining

The stains that were used throughout this study were H&E, Immunohistochemistry (IHC), single immunofluorescence, double immunofluorescent and 4-colour immunofluorescence.

2.1.3.1 Primary Antibodies

Different primary antibodies were used in different techniques, including: Western blotting, IHC, immunofluorescence and 4 colour immunofluorescence. Table 2.7 shows the list of primary antibodies, their sources and dilution.

Primary Antibody	Species isotype and clonally	Dilution	Source	Catalogue number
CD3	Rabbit polyclonal	1:1000	Dako	A0452
CD5	Mouse Monoclonal	1:1000	Abcam	Ab193378
CD10	Mouse Monoclonal	1:1000	Abcam	Ab73409
CD19	Mouse Monoclonal	1:1000	Dako	M7296
CD20	Mouse Monoclonal	1:1000	Dako	M0755
CD21	Mouse Monoclonal	1:1000	Dako	IR608
CD23	Mouse Monoclonal	1:1000	Dako	M7312
CD31	Mouse Monoclonal	1:3	Home-made, provided by Dr Karen Pulford, Oxford University	
CD34	Mouse Monoclonal	1:3	Home-made, provided by Dr Karen Pulford, Oxford University	
CD45	Mouse Monoclonal	1:3	Home-made, provided by Dr Karen Pulford, Oxford University	

CD45RA	Mouse Monoclonal	1:3	Home-made, provided by Dr Karen Pulford, Oxford University	
CD68	Mouse Monoclonal	1:3	Home-made, provided by Dr Karen Pulford, Oxford University	
S100A4	Rabbit polyclonal	1:1000	Proteintech group	05-1-AP
S100A4	Mouse polyclonal	1:1000	Prepared in the lab using hyperidoma cells	
S100A6	Rabbit polyclonal	1:1000	Proteintech group	10245-1-AP
ZEB1	Rabbit polyclonal	WB 1:250 1:200	Santa Cruz Biotechnology, Inc, USA	Sc-25388
ZEB2	Rabbit polyclonal	WB 1:5000 1:1000	Dr Eugene Tulchinsky (University of Leicester)	
Tubulin	Mouse Monoclonal	WB 1:30000	Sigma-Aldrich, UK	T6074
p.STAT3	Rabbit Monoclonal	WB 1:1000	Cell signalling, UK	2922

Table 2.7 Different primary antibodies used in this study.

2.1.3.2 Secondary Antibodies

Table 2.8 showed the secondary antibodies that used for immunofluorescence and 4-colour immunofluorescence.

Secondary antibody	Species isotype	Dilution	Conjugated Fluorophore	Catalogue number	Manufactory
Anti-Mouse	Donkey	1:1000	Alexa flour (FITC) 488	A21202	Invitrogen, USA
Anti-rabbit	Donkey	1:1000	Alexa flour (FITC) 568	A21207	Invitrogen, USA
Anti-Mouse	Goat	WB 1:3000	IgG/HRP	P0448	Dako, Denmark
Anti-Rabbit	Goat	WB 1:3000	IgG/HRP	P0447	Dako, Denmark

Table 2.8 Secondary antibodies used in this study.

2.1.3.3 Four colour immunofluorescence

There were special reagents for this type of stain (Table 2.9).

Reagent	Manufacture
OPAL-520	Perkin Elmer
OPAL-570	Perkin Elmer
OPAL-690	Perkin Elmer
DAPI Dilactate	Life Technologies
Sequenza slide clips	Fisher Scientific
VectaShield	Vecta Laboratories
Antibody Diluent/blocking Buffer	Perkin Elmer
Opal Polymer HRP Ms Plus Rb	Perkin Elmer

Table 2.9 Reagents used in 4-colour immunofluorescence.

2.1.4 PCR

2.1.4.1 DNA oligonucleotides

Primers were designed to study gene expression by PCR. Table 2.10 showed the list of PCR primers that were designed using NCBI/Primer-BLAST program.

Primer name	Primer sequences	
	Forward Primer	Reverse Primer
S100A10	ATTCGCTGGGGATAAAGGCT	TATCAGGGAGGAGCGAACTG
S100A11	GTGGGTTGAGGAGAGGCTC	CCAGTTTCTTCATCATGCGGT
S100A12	AAAGGAGCTTGCAAACACCAT	CTCATTGAGGACATTGCTGGG
S100A13	CCACTGACAGAGCTAGAGGAG	TCCGAGTCCTGATTCACATCC
S100A14	ACTCTCACCAAAGGACCAGAC	GCAATTTTCTCTTCCAGGCCA
S100A16	AGTACAGCCTGGTCAAGAACA	GGTCCAGTACTCATCGAAGCT
S100A1	AGACCCTCATCAACGTGTTCC	AAGCACCACATACTCCTGGAA
S100A2	TTCCACAAGTACTCCTGCCAA	CATGACAGTGATGAGTGCCAG
S100A2	GTTTGGTGGGATCAGGTTGAG	TTGGCAGGAGTACTTGTGGAA
S100A3	GGGACAAATACAAGCTCTGCC	CGCACATACTCCACAAAGTCC
S100A4	GCAAAGAGGGTGACAAGTTCA	TTTCATTTCTTCCTGGGCTGC
S100A5	GAGAAGGCCCTGACCACTATG	TCCTTGAAGTCGATCTCCTGG
S100A6	TGGCCATCTTCCACAAGTACT	TACTCCTGGAAGTTCACCTCC
S100A7	AGGTCCATAATAGGCATGATCGA	TGTGGTAGTCTGTGGCTATGT
S100A7A	CTTCCCCAATTTCCTCAGTGC	ATGGCTCTGCTTGTGGTAGT

S100A8	GGCAGGGATAAGGAAGGAGAG	AACTCTTTGAACCAGACGTCT
S100A8	GCATGTCTCTTGTCAGCTGTC	AACTCTTTGAACCAGACGTCT
S100A9	CTGGAACGCAACATAGAGACC	TTGTCTGCATTTGTGTCCAGG
S100B	CCTGGGCAGAGGGAATAAGAG	TTGGTGGAAAACGTCGATGAG
S100B	GGCCGGTGGAAGGATTATGAT	CGTCTCCATCATTGTCCAGTG
S100G	TAGCTGTTTCACTATTGGGCA	TCAGCCTGAATCAATAGCTTCA
S100P	AGGTGGGTCTGAATCTAGCAC	GCAATTTATCCACGGCATCCT
S100Z	GAATCTTCCACCGCTATTCTGG	CATCCAGGTCCTGCACTATCT
ZEB1	ACTCTGATTCTACACCGCCC	AGCGCTTTCCACATTTGTCA
ZEB2	ACTCCTGTCTGTCTCGCAAA	GCTCGATAAGGTGGTGCTTG
ZEB2	TGCCATCTGATCCGCTCTTA	CGAATCAGGGGCAAAAGCAA

Table 2.10 List of PCR primers that designed using NCBI/Primer-BLAST program.

2.1.4.2 PCR amplification

Materials used in RNA extraction, cDNA and PCR amplification listed in table 2.11.

Material	Source
50X Acitate Borate EDTA	Thermo Thermo Fisher Scientific, UK
Agarose Hi-Res Standard	Thermo Thermo Fisher Scientific, UK
Chloroform	Sigma-Aldrich, UK
Ethanol	Thermo Fisher Scientific, UK
Fast SYBR Green Master Mix	Applied Biosystems, USA
Isopropanol	Thermo Fisher Scientific, UK
ReverAid H minus First strand c DNA synthesis kit	Thermo Thermo Fisher Scientific, UK
RNeasyPlus mini Kit	QIAGEN,UK
TRIZOL	Invitrogen, UK

Table 2.11 Materials used in RNA extraction, cDNA and PCR amplification.

2.1.5 Samples collection

Samples were collected under ethical approval UHL-10588 (Investigation of protein expression in normal B-cells and cells from haematological malignancy) leaded Professor Martin J S Dyer.

2.1.5.1 Tissue Blocks

2.1.5.1.1 Tonsil, spleen and thymus samples

To compare the expression of S100A4, S100A6, ZEB1 and ZEB2 in normal and malignant lymphocyte, slides of paraffin embedded normal tonsil spleen and thymus tissue were collected from the Department of Pathology at Leicester Royal Infirmary. These sections examined to investigate the expression of different CD Markers, S100A4, S100A6, ZEB1 and ZEB2 in B-cell. Tonsil tissue slides were used also as a control of some experiments and to optimize antibodies for IHC, double immunofluorescence and 4-colour immunofluorescence.

2.1.5.1.2 Lymphoma samples

In order to evaluate the expression of CD markers, S100A4 and S100A6 in malignant B-cells, 60 lymphoma tissue blocks were collected from the Department of Pathology at Leicester Royal infirmary. The malignant cases in this project were diagnosed by the Histopathology Department on Leicester Royal Infirmary and Haematoxylin and Eosin (H&E) sections were examined to confirm the viable tumour.

2.1.5.1.3 Bone Marrow samples

12 samples of normal bone marrow sample and 4 of CLL patients were collected from the Department of Pathology at Leicester Royal infirmary and cut by Histopathology Department on University Hospital of Leicester (UHL).

2.1.5.2 Peripheral blood of CLL patients

Samples of peripheral blood of CLL patients were collected from The Ernest and Helen Scott Haematological Research Institute, Leicester Cancer Research Centre,

University of Leicester to study the correlation between S100A4 expression and survival rate. Data collections were done entirely.

2.1.5.3 Peripheral blood of healthy volunteers

Under ethical approval, 15 fresh blood samples were collected from normal volunteers in MRC building.

2.1.5.3.1 Buffy coat preparation

Ficoll histopaque (17-1440-03, Ficoll-Paque PLUS) was performed as the standard procedure to separate of white blood cells (WBCs) from fresh whole blood in a suitable cell culture facility.

2.1.6 B-cell isolation

Dynabeads™ Untouched™ Human B Cells Kit were used to isolate B-cells in normal blood samples and in samples of CLL patients.

2.1.7 Chemotaxis assays

Chemotaxis assay was used to investigate the role of S100A4 protein in B-cells migration. Materials used for this protocol were listed in table 2.12.

Materials	Source
Transwell chambers with 8-μm polycarbonate membrane	Kennebunk, USA
Fibronectin	Sigma-Aldrich, UK

HEPES buffer	Thermo Thermo Fisher Scientific, UK
Haemocytometer counter	Thermo Thermo Fisher Scientific, UK
Trypan blue solution	Sigma-Aldrich, UK
BSA	Thermo Fisher Scientific, UK

Table 2.12 List of materials used for chemotaxis assay.

2.2 Method

2.2.1 Cell culture

Used cell lines were taken from liquid nitrogen. Cells were warmed up directly in a water bath at 37°C to be completely thawed. Cell suspensions then were transferred into a tube containing 10ml of prober medium and re-suspended very well. After centrifugation at 1000 rpm for 5 minutes, the supernatant was discarded; the plate was re-suspended again with 1ml fresh medium, transferred into T-25 flask and topped up with 4ml media. After 24 hours of incubation in 37°C with 5% CO_2 oven, cells growth was observed.

2.2.1.1 Cell resuscitation

All working steps were carried out in a laminar flow cabinet. Cell lines were grown in Dulbecco's Modified Eagle's Medium (DMEM) with high glucose (the amount of glucose in cell culture formulations ranges from 1 g/L (5.5 mM) to as high as 10 g/L (55 mM) according to culture requrements) and L-glutamine, supplemented with 10% Nu Serum and 1% Penicillin/Streptomycin (PT) or in Rosewell Park Memorial Institute 1640 media (RPMI-1640) with glutamine. To induce EMT, cells were usually grown in the presence of Doxycycline (2 μg/ml). All media used for cell lines were adjusted to contain 10% Foetal Bovine Serum (FBS) and 1% PT were incubated under

the same conditions, 37°C with 5% CO_2. Sterile conditions were maintained at all times in a laminar flow hood.

2.2.1.2 Cell culture media

Culture media and Trypsin/ EDTA (TE) were stored at 4°C and warmed up to 37°C before using. A431, A375, HL-60, MEC1, MEC2 and MIA PaCa-2 cells were grown in DMEM with high glucose and L-glutamine. Jurkat was cultured in RPMI-1640 media with glutamine. RPMI-1640 media also was used for peripheral blood of lymphoma patients.

2.2.1.3 Cells culture technique

In this study, there were two types of cells. Suspension and non-suspension cells. Firstly, for non-suspension cells, cells were split when quantity of cells extend approximately 70-80%. They were not sub-cultured more than twenty times. Cell passaging was performed by removing media from the flask, washing with 1X Phosphate Buffer Saline (PBS) twice, and incubating at 37°C for 10 to 15 mins after adding proper amount of 1X TE to detach monolayer cells from the surface. After that, fresh media was added to neutralize the trypsin. The mixture of cell and media was then transferred into 15ml tube and pelleted at 1000rpm for 5mins. The cells pellet was mixed with 1ml of media and seeded at the required density in the correct sized flask and media added (Table 2.13).

Tissue culture	Seeding density	PBS	Trypsin	Resuspension media	Volume of total media
6 well pallet	1.2×10^6	2	.25	1	2
T-25	2.8×10^6	5	1	4	5
T-75	8.4×10^6	10	2	8	15

T-175	18.4 x 10^6	15	4	11	25

Table 2.13 Proper quantity (ml) of PBS, TE, resuspension media and total volume of media needed for cell passaging.

Secondly, for suspension cells, cells were split when the quantity of cells extend approximately 70-80% and they were appeared in cluster shape. Cell passaging was performed by adding media to the flask, but if the media color appear yellowish the cells transferred into 15 ml or 50 ml tube and pelleted at 1000rpm for 5mins. The cell pellet were mixed with 1ml of media and seeded at the required density in the correct sized flask and media added (Table 2.14). Trypsin and TE were not used for suspension cell and the flask in the incubator should be in horizontal position.

Tissue culture	Volume of total media
T-25	5
T-75	15
T-175	25

Table 2.14 Recommended volumes (ml) media required for suspension cells according to flask size.

2.2.1.4 Freezing cells for long-term storage

Cells were grown to 80% confluence in a large flask (T-175). The cells were then trypsinised and re-suspended with freezing media which consisted of 80% of complete media in addition to 10% FBS and 10% Dimethyl Sulfoxide (DMSO). 1ml from suspension was liquated into individual cryo-vial and frozen at -80 °C for 24 hours and then stored in liquid nitrogen.

For suspension cell, 1 x 10^7 cells were pelleted by centrifugation at 1000 rpm in a Eppendorf centrifuge for 5 minutes and re-suspended in 1ml of freezing solution which contains higher concentration of FCS (95% FCS and 5% DMSO; Sigma). The

cells were then transferred to cryo-vials and placed in a freezing container at -80ºC freezer. A day later, the cells were moved to the liquid nitrogen freezer at -80ºC for long-term storage.

2.2.1.5 Cell count

Cells were re-suspended with complete medium after washing with PBS. 10µl of cell suspension were drawn up and placed in one chamber of hemocytometer gridlines. Cells were counted in all 4 sets of 16 corner squares and the average number of cells calculated multiplied by 10.000 to give a final concentration of cells/ml.

2.2.1.6 Cells treatment

2.2.1.6.1 Doxycycline (DOX) treatment

A431/ZEB2 cells express S100A4 protein in the presence of DOX. To induce S100A4 expression, cells were grown in the presence of DOX (2µg/ml) on the day of seeding and left for 48 or 72h before harvesting.

2.2.1.6.2 Cytokines treatment

Jurkat cells were cultured in T-25 flask in 5ml of RPMI-1640 media. After cell growth, the cells were washed twice with PBS and serum free media was added. The cells were incubated in the oven for a further 24h. 70µl of cytokines, including: IL-1 alpha, IL-6 and IL-11, was added to cells and incubated for 24h.

2.2.1.7 Transfection

2.2.1.7.1 Transfection via electroporation

This technique involves the use of electric shocks with a high voltage so as to insert DNA into the cells. Media (DMEM for HL-60 or RPMI for Jurkat and CLL cells) was added to the T-75 flask and incubated at 5% CO_2, 37^{O}C for 3 hours prior to transfection. Following the harvesting of cells by washing with PBS, the cell suspension was then centrifuged. The cell resuspension was suspended into 1ml of PBS. The cells were counted after that by using haemocytometer. Where the haemocytometer preparation was 10µl of cell suspension, it was loaded onto a haemocytometer by placing the pipette tip at the edge of the chambers prudently. It was ensured that around 3 million cells were used per transfection. The cell suspension was placed in Eppendorf tubes and centrifuged to form a pellet of cells. The supernatant was discarded and the cells were re-suspended in 60µl of Mirus buffer (electroporation buffer). The suspension was transferred to Eppendorf tubes containing DNA, diluted with DEPC-treated water. The suspension was mixed properly, ensuring no air bubbles were formed. It was then moved to 4mm electroporation cuvettes from GeneFlow and pulsed at 250V and 250µF with the Gene Pulser Xcell machine from BIO-RAD. 800µl of media was added to the cuvette and the cells were re-suspended. 400µl of cell suspension was added to the T-75 flask. Fresh media was supplied to the cells 24 hours after transfection and cells were lysed 48 hours later for protein analysis and RNA isolation.

2.2.1.7.2 Transfection with jetPRIME

A polyplus jetPRIME kit was used to transfect cells according to the manufacturer's protocol. Nucleic acids are negatively charged because of their polyphosphate backbone and are therefore able to interact with cationic transfection reagents (polymers or lipids) causing the formation of transfection complexes by which these nucleic acids are protected from nuclease degradation. The excess of cationic transfection reagent allows these complexes to be positively charged, which is

mandatory to allow them to interact with the negatively charged cell membrane. Briefly, one day prior to transfection, cells were cultured in a T-75 flask containing 4ml growth media. At the time of transfection, 4µl of target siRNA, 400ml of jetPRIME buffer and 8µl jetPRIME reagents were mixed thoroughly by pipetting, vortex for 10 sec, spun down quickly and incubated at RT for 10 mins. The transfection mixture was then added into the wells that contained cultured cells, drop wise, to be ready for the required experiment.

2.2.1.7.3 Optimization of the transfection protocol for suspension cells

Since S100A4 has been shown to be expressed in HL-60 cells, the expression of this protein was modulated by an RNAi approach so as to study its role in cell migration. A series of transfection protocols were checked to select the most efficient protocol of the transfection. For this purpose, HL-60 cells were transfected with pmaxGFP plasmid using Ingenio® Electroporation solution and Amaxa nucleofector II devices, as well as transfection with jetPRIME (see Materials and Methods chapter). Fluorescence and phase-contrast images were taken 48h after transfection in order to assess the level of the GFP-fluorescence as a measure of transfection efficiency.

Among all the used protocols, transfection with Ingenio® Electroporation and jetPRIME had shown the highest transfection efficiency, with a reasonable number of intact cells, in comparison with the other methods. Although transfection using Amaxa nucleofector II devices with different programs showed higher efficiency, the majority of cells were dead, which meant viability was insufficient for the required experiments (Figure 2.1).

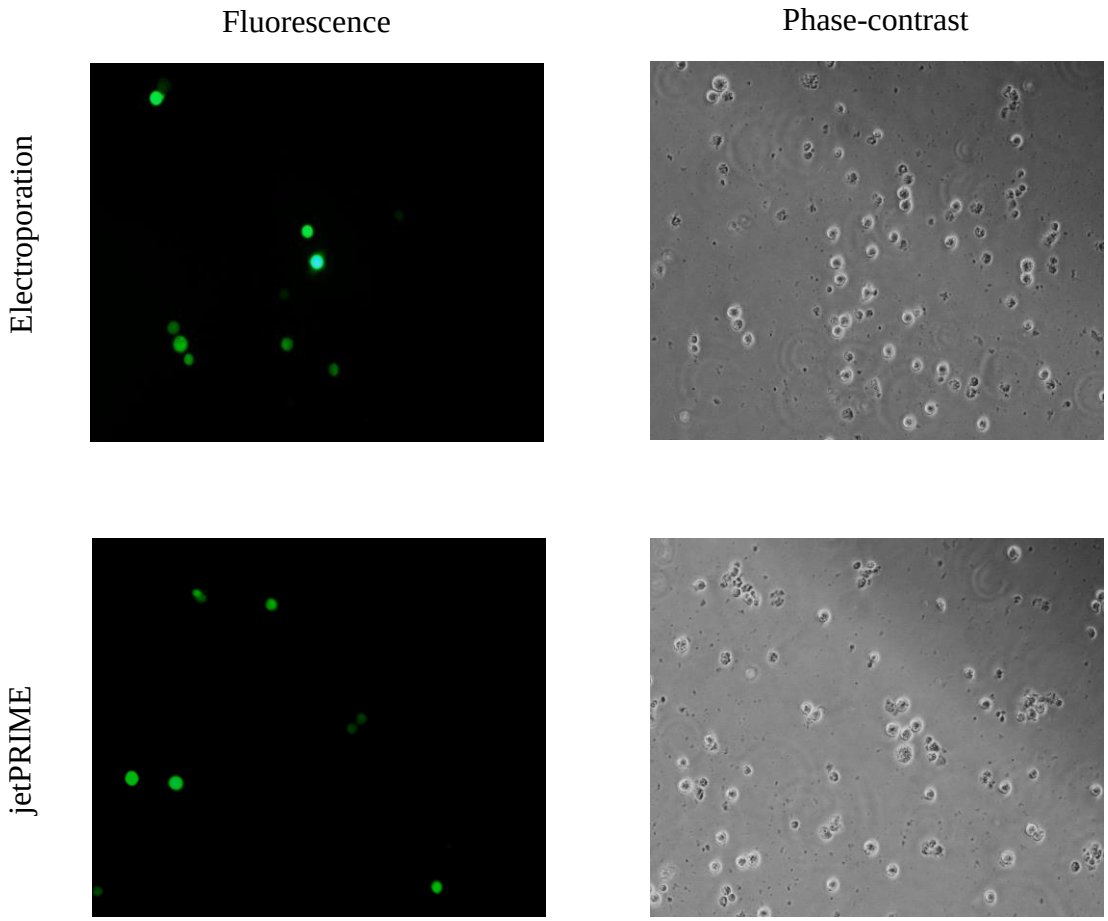

Figure 2.1 Optimization of the transfection protocol using HL-60 cells.
Fluorescence and phase-contrast images of cells were taken with a x20 objective after transfection with 1µg pmaxGFP plasmid using electroporation, a technique involves the use of electric shocks with high voltage so as to insert DNA into cells, and jetPRIME, where the transfection mixture was prepared according to the protocol then added into the wells that contained cultured cells to be ready for required experiment.

2.2.2 Manipulation of proteins

2.2.2.1 Sample preparation for Western blot

The cells were washed twice with PBS and lysed in appropriate volume of 1X Laemmli buffers for protein isolation, while in another tube lyzoil buffer was add for RNA isolation. Typically 150µl per 10^6 cells was used. Lysed cells were scrapped and the suspension was sonicated and boiled for 10 minutes at 94^{O}C. This was done to

disrupt DNA, to kill proteases and to homogenise the sample. The protein concentration of the lysates was then determined via Pierce™ BCA Protein Assay. In every 1ml of BCA Reagent A from the kit, 20µl of BCA Reagent B was added. 1ml of this working solution was then added to the standards and 4µl of each sample in Eppendorf tubes. After vortexing, the Eppendorf tubes with samples were incubated at $37^{O}C$ for a minimum of 30 minutes. The absorbance was then measured at 562nm. The samples were standardised to a final concentration of 1mg/ml. loading dye with a final concentration of 1% β-mercaptoethanol (v/v) and 0.005% bromophenol blue (w/v) was then added. The samples were heated at $94^{O}C$ for 5 minutes prior to loading into SDS-PAGE gels.

2.2.2.2 Western Blot

This process involves the separation of proteins via electrophoresis at constant voltage over time. The proteins are separated based on their molecular weight and migrated from a negative to positive charge. This is done through two types of gels. The stacking gel at pH 6.8 has a lower acryl amide concentration. This ensures the formation of thin and distinct bands. The second gel referred to as the resolving gel has a pH of 8.8 and a higher acrylamide concentration (Mahmood and Yang, 2012).

Glass plates consisting of an outer plate with spacers and a top short plate were assembled on top of each other and clamped together in the gel casting unit. The type of resolving gel, that is its percentage, was made according to the size of the protein of interest. The larger the molecular weight of the protein, the lower the gel percentage used. The percentage of resolving gel depends on the molecular weight of the antigen and ranges from 6 to 15% (Table 2.15). The appropriate volumes of distilled water, 30% Acrylamide solution, 1.5M Tris pH 8.8 and 10% SDS were mixed and N,N,N',N'-Tetramethylethylenediamine (TEMED) was added last as a catalyst to initiate polymerisation. The solution was loaded into the space between the glass plates immediately before the gel polymerises. A layer of butanol was added to form an air tight layer so that polymerisation could take place correctly. The butanol was washed off with distilled water once the resolving gel was set. Two types of stacking gel (8%

and 15%) were made which consist of adequate volumes of distilled water, 30% Acrylamide solution, 1.0M Tris pH 6.8 and 10% SDS and TEMED. It was loaded above the resolving gel and a loading comb was inserted to form the wells. The gel apparatus was set up and placed into the electrophoresis tank (Bio-Rad Quattro system). It was filled with 1X running buffer (0.3% (w/v) Tris, 1.4% (w/v) Glycine, 0.1% (w/v) SDS). The SDS-PAGE gels were loaded with 8µl of molecular marker (Fermentas Page Ruler prestained protein ladder PN26619) and 20µl of each sample. The gels were run at 170V for 1 hour. After separation, the proteins were transferred onto a polyvinylidene difluoride (PVDF) membrane overnight. This was carried out by applying a constant voltage perpendicular to the gel and membrane, leading to the proteins moving onto the membrane. (Mahmood and Yang, 2012) A transfer cassette consisting of a sandwich of a sponge, 2 filter papers, PVDF membrane (Immobilon–P, Millipore, IPVH 00010), 2 filter papers and sponge was set up. The PVDF membrane was activated in methanol and it was ensured that all the constituents of the sandwich were dampened in 1X transfer buffer (transfer buffer ((0.3% (w/v) Tris, 1.4% (w/v) Glycine, 20% (v/v) Methanol) prior to assembly. The cassette was placed into the transfer tank containing 1X transfer buffer. The transfer was completed overnight at 25V. The membrane was then blocked in 5% non-fat dried milk /TBS-T solution (50mM Tris pH7.65, 150mM NaCl, 0.1% (v/v) Tween-20, 5% (w/v) fat free milk powder) for 1 hour. This ensured the non-specific binding of antibodies to the membrane. The membrane was then washed twice with TBS-T (Mahmood and Yang, 2012). The protein of interest was stained with the appropriate primary antibody, diluted with BSA TBS-T (50mM Tris pH7.65, 150mM NaCl, 0.1% (v/v) Tween-20, 5% BSA) according to the manufacturer, to form a complex. The staining process was usually done over 1 hour but varied depending on the manufacturer's recommendation. The membrane was then washed 4 times with TBS-T for 15 minutes each. This ensured that unattached antibodies were removed and to minimise the background. The membrane was then stained for 1 hour with a secondary antibody: anti-Mouse HRP (P0447, DAKO) or anti-Rabbit HRP (P0448, DAKO) subject to the type of primary antibody used. The secondary antibody was diluted in 5% non-fat dried milk TBS-T solution with a dilution of 1:3000. The membrane was then washed with TBS-T 5 times 5 minutes each. The ECL reagent (prepared with solution A and B in 1:1) was then applied to the membrane. The membrane was transferred to a radiography cassette. An X-ray film was placed into the cassette, onto the membrane, and then placed into the

developer in the dark room. Varying the time the film was left in the cassette gave rise to different exposures. Table 2.7 shows the different antibodies used and their dilutions.

Gel (%)	Water	30% acrylamide mix	1.5 M Tris (Ph 8.8)	10% ammonium persulfate	TEMED
6	5.3	2	2.5	0.1	0.008
8	4.6	2.7	2.5	0.1	0.006
10	4.0	3.3	2.5	0.1	0.004
12	3.3	4	2.5	0.1	0.004
15	2.3	5	2.5	0.1	0.004

Table 2.15 Volume (ml) of components required to prepare 10ml of resolving gel with different concentrations.

2.2.3 PCR analysis

PCR analysis refers to polymerase chain reaction which is a technique that allows researchers to create millions of precise DNA replications from a single sample of DNA.

2.2.3.1 Designing Primers by Primer-BLAST

Primers were designed using Primer-Blast NCBI tool (National Centre for Biotechnology Information, **www.ncbi.nlm.nih.gov)**, an efficient program identifying sequencing for amplification of the gene of interest. Forward and reverse primers are short, temperature stable sequences with close melting points, complementary to the start and end of the amplified DNA fragment. Briefly, put the name of species in upper column and then click on search option.

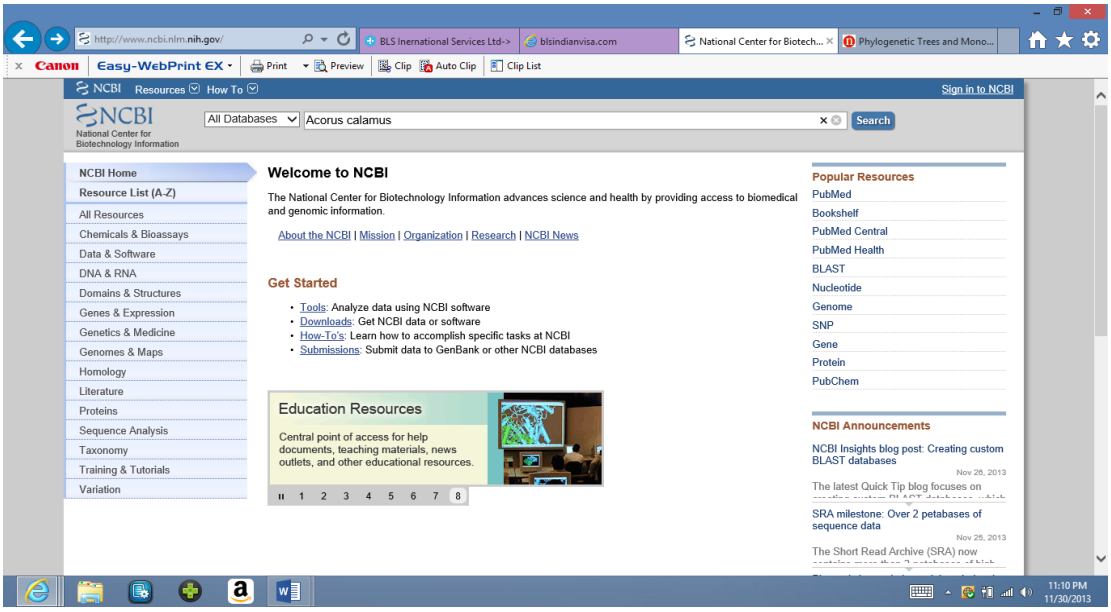

After that click on to the nucleotide sequences: Nucleotide (DNA and RNA sequences), Genome Survey Sequences and EST sequences, from which primer(s) has to be design.

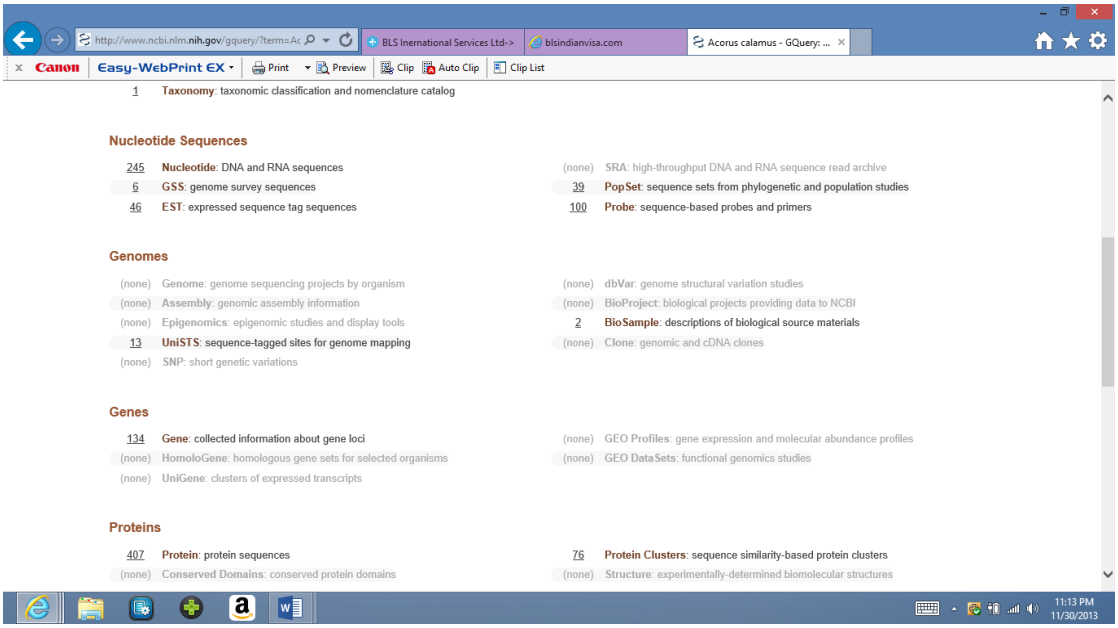

Then, click on the particular link of sequenced genome

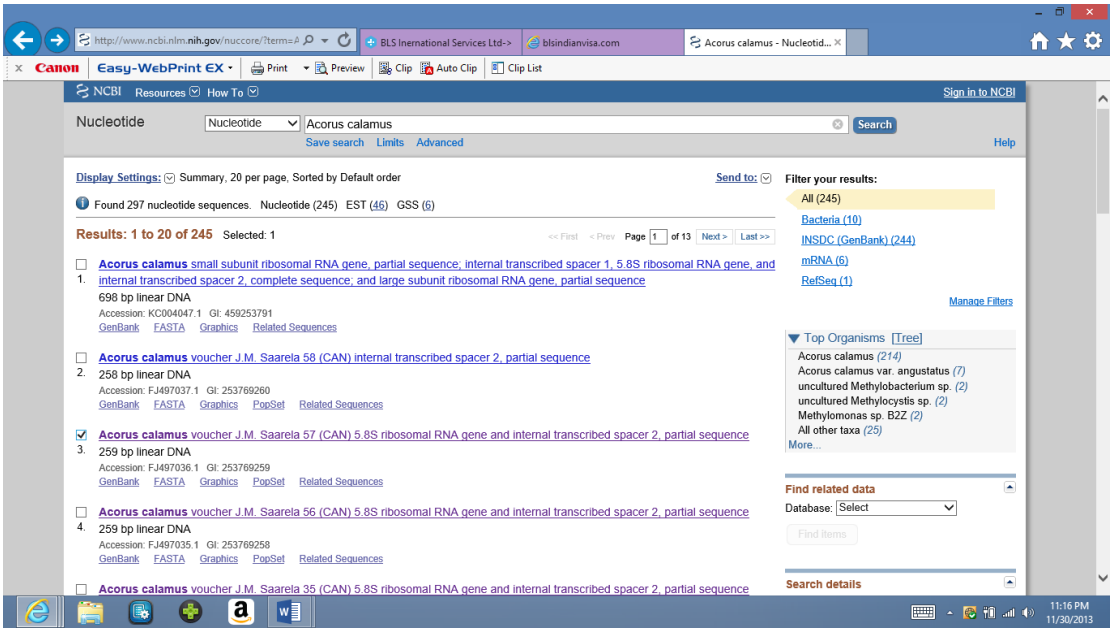

Click on the link and open the sequence and after that click on the option from right hand side bar: Analyze this sequence and pick up primers.

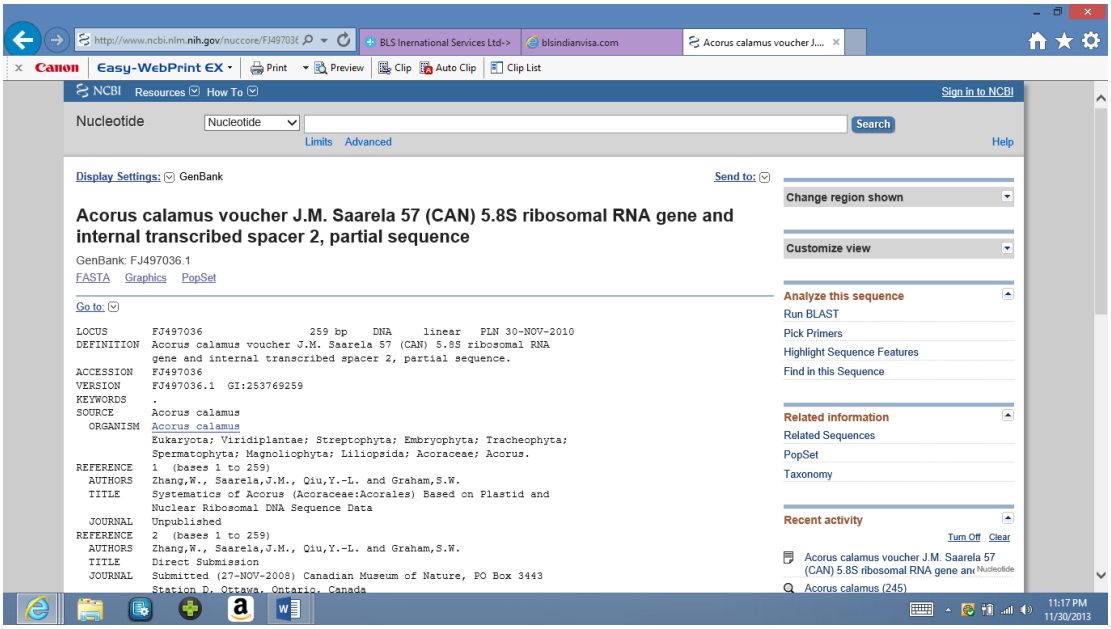

2.2.3.2 Trizol-RNeasy RNA extraction protocol

Cells grown on the 10 cm culture dish (75% confluence, 5-10 X 10^6) were washed twice with PBS. 1ml of trizol was then added to the 10cm dish and the cells were scraped. According to the procedure, the suspension was collected in Eppendorf tubes and 200µl of chloroform was added and mixed gently. After that the samples

were centrifuged at 12000g for 15min at 4^{O}C. This cause the formation of different layers, of which is the aqueous layer. 500µl of it was added to the gDNA eliminator and centrifuged for 30sec at 8000g. It is important to only collect the aqueous layer in order to prevent contamination of the sample. By using 70% Ethanol the RNA in the flow was precipitated. Then, 550µl was transferred to the RNeasy tube and centrifuged for 15 seconds at 8000g. The flow through was discarded. 550µl of RW1 buffer was added to the column and centrifuged for 15s at 8000g. The flow through was discarded. 500µl of RPE buffer was added and spun for 15 seconds at 8000g. This step was repeated (a second) time but centrifuged for 2 minutes. The column was placed in a new collection tube and in order to dry the membrane in the column the samples were centrifuged for 1 minute at maximum speed. Then, the column was transferred in to new collection tube and 50µl of RNase free water was added and centrifuged for 1min at 8000g. This was done to elute the RNA. The RNA concentration was then measured on the nanodrop.

2.2.3.3 cDNA synthesis

1µg of total RNA was used per cDNA synthesis. This was made up to 11µl by adding RNase free water according to the procedure. After that, 1µl of random hexamer primer, a mixture of oligonucleotides representing all possible hexamer sequences, was added and mixed, followed by centrifugation. The samples were boiled at 65^{O}C for 5 minutes. They were then spun down and placed on ice. The following solution in table 2.16 were added in order.

5X Reaction buffer	4µl
Riboblock RNase inhibitor	1µl
10mM dNTP mix	2µl
Revert Aid Reverse Transcriptase	1µl
Total	20µl

Table 2.16 Solutions used in DNA synthesis.

The reagents were mixed and spun down. Then, samples were incubated at 25^{O}C for 15 minutes followed by 42^{O}C for 45 minutes. The reaction was terminated by heating the samples at 70^{O}C for 5 minutes.

2.2.3.4 RT-PCR of synthesised cDNA

This procedure ensured that the cDNA made is of suitable quality. The following reagents (Table 2.17) were added to PCR tubes which provided from the kit.

2X Taq Master mix	10µl
Forward Primer	0.5µl
Reverse primer	0.5µl
Nuclease free water	7µl
cDNA	2µl
Total	20µl

Table 2.17 Reagents needed for synthesised cDNA

The samples were then run on the PCR machine using the following program (Table 2.18).

Step	**Temperature/^{O}C**	**Time/min**
Initial denaturation	95	5
Denaturation	95	0.5
Annealing	60	0.5

Extension	72	0.5
Termination	72	5

Table 2.18 Program used to run PCR

Following the completion of the PCR, the samples were run on a 1% agarose gel, which is the easiest and commonest way of separating and analyzing DNA, in 1X TBE buffer. To prepare 1% agarose gel, 0.5 g of agarose powder was mixed with 50 mL of 1X TBE, then placed in a microwave for about 1 minute to dissolve the agarose and after that the gel was leaved to cool on the bench for 5 minutes. 2µl of ethidium bromide solution was supplemented to the melted agarose. The samples were run with the 10µl ladder in TBE buffer at 85 V for 20 minutes. The gel was then analyzed under UV to ensure the presence of the required bands. Agarose gel electrophoresis is the easiest and commonest way of separating and analyzing DNA. The purpose of the gel was to look at the DNA, to quantify it or to isolate a particular band. The DNA is visualised in the gel by addition of ethidium bromide, which is mutagenic, or less-toxic proprietary dyes such as GelRed, GelGreen, and SYBR Safe. Ethidium bromide and the proprietary dyes bind to DNA and are fluorescent, meaning that they absorb invisible UV light and transmit the energy as visible light.

2.2.4 Tissue staining

2.2.4.1 Cell block preparation

The Shandon cytoblock system was used to prepare a paraffin-embedded suspension cell form with some cell lines such as HL-60 and Jurkat. Also, this system helps to produce paraffin block from cellular material, in this project we used it for CLL peripheral blood sample.

In this protocol, cells were placed into cytospin chambers in a cyto-centrifuge (Shandon, UK). Cells were spun at 800 rpm for 5 minutes. Upper fluid was decanted and 0.5ml of supernatant and re-suspend cells. After that, 10% formal saline was added to give approximately $2x10^6$ cells/ml. At RT, this mixture was mixed gently and

allowed to fix for minimum 30 minutes. Suspensions cells were centrifuged at 800rpm for 5 minutes. The supernatant was decanted and sufficient amount of reagent 2 was added to the cell concentrate to give a concentration of approximately $5x10^7$ cells per 100µl. After missing, each 100µl cell mixture produced one cytoblock. According to the kit instructions, the required number of cytoblock cassettes were prepared by applying 3 drops of reagent 1 to the well in the cytoblock board. Then, cytoblock cassettes were opened and cytofunnels were assembled in the cytospin clips, and loaded into the head. 100µl of the prepared cell mixture was added to the cytofunnels and spun for 5 minutes at 1500 rpm on 'Lo' acceleration. The clips were opened, and the cytoblock removed carefully, checking that the cell button was retained in the well. One drop of reagent 1 was added to the centre of the well and cassette was closed. The cytospin clips and cytofunnels were immersed in disinfectant and leaved overnight, then rinsed and allowed to dry. The cassettes were stored in 70% IMS prior to processing on a Leica ASP3000, using the overnight schedule. The cell buttons were embedded in paraffin wax and stored at RT.

2.2.4.2 Tissue sectioning

3-5 micrometre (µm) sections from paraffin-embedded tissues were cut by the model AS325 microtome (Thermo Electron Corporation, Basingstoke, UK). At all times the area used for cutting and the microtome blade (Surgipath Europe Ltd., Peterborough, UK) were sterilised and sharp. Tissue sections were collected from water bath containing distilled water at 50ºC and placed onto RNase-free adhesive-coated slides and incubated in a 60ºC incubator for 1-5 hours to allow tissue sections stick onto slides. All tissue sections were stored at room temperature in RNase-free conditions until further use in immunohistochemistry or immunofluorescence.

2.2.4.3 Haematoxylin and Eosin staining (H&E)

H&E was performed on all lymphoma samples. By so doing the state of each tissue was assessed. The protocol used was as follows: Tissue sections on adhesive-coated slides were dewaxed through xylene (Fisher Scientific UK Ltd., Loughborough,

UK) for 10 minutes and then through ethanol (Sigma-Aldrich Company Ltd., Gillingham, UK) for 10 minutes, and washed under running tap water for 5 minutes. Slides were then immersed in Mayer's haematoxylin (VWR International Ltd., Poole, UK) for 2 minutes before washing thoroughly in tap water. Scott's tap water (Surgipath Europe Ltd., Peterborough, UK) was then used to 'blue' the haematoxylin for 2 minutes and washed again in tap water. The slides were immersed in eosin (VWR International Ltd., Poole, UK) for 2 minutes before rinsing with tap water. Tissue sections were then dehydrated through ethanol twice, each time for 3 minutes and then through xylene for 15 minutes. Sections were mounted using coverslips with a drop of DPX (both Surgipath Europe Ltd., Peterborough, UK) and dried flat overnight.

2.2.4.4 Immunostaining

By using paraffin-embedded tissue of tonsil tissue slides, immunohistochemistry study was performed. Antibodies against the following antigens in different dilution were used: S100A4, S100A6, CD5, CD10, CD20, CD31, CD38, CD45, CD45RA, CD68, CD133 (Table 2.7). A negative control was included in each experiment.

In brief, 5µm section was cut and incubated at 37^{o}C overnight, de-paraffinised in xylene and hydrated through decreasing concentration of industrial methylated alcohol. Using a Pascal electric pressured cooker, sections were subjected to antigen retrieval in sodium citrate buffer (pH6.0) for 30 min at full pressure. According to the manufacture's instruction, the Novocaster Novolink Polymer detection system (Leica Biosystems, UK) was used. Endogenous peroxidase activity was neutralized by the Novocaster peroxidase block. Then, Novocaster protein block was applied to reduce non-specific binding of antibodies and polymer. This was followed by incubation the sections with optimally diluted S100A4, S100A6 and CDs at 4^{o}C overnight. After that, the sections were incubated with Novocaster post primary block, subsequently bound antibody complex detected by the Novolink polymer which can recognise mouse and rabbit immunoglobulin. In addition, sections were incubated with the substrate or chromogen, 3, 3' – diaminobenzidine (DAB, Novolink Polymer detection kit). Finally, the section were counterstained by using haematoxylin, dehydrated and mounted in DPX mount (mixture of Dibutyl Phthalate and Xylene isomers). For negative control

slides, primary antibody were replaced by TBS-T (50Mm Tris pH7.65, 150 Mm NaCl, 0.1% (v/v) Tween 20).

2.2.4.5 Single immunofluorescence staining

Five-micrometre paraffin-embedded sections were deparaffinised in xylene and hydrated through decreasing concentration of industrial methylated alcohol. Antigen retrieval was performed in sodium citrate buffer (pH 6.0) for 30 minutes at full pressure by using Pascal electric cooker. Tissue sections then incubated for 30 minutes with a blocking agent which is TBS-T (50Mm Tris pH 7.65, 150Mm NaCl, 0.1% (v/v Tween-20). Then, the sections were stained with primary antibodies which are rabbit anti-S100A4 polyclonal and rabbit anti-S100A6 polyclonal (Table 7) following by overnight incubation at 4^{o}C. After that, the sections were incubated with the secondary antibodies which are Alexa 488 or Alexa 568 (Table 8). Sections then were incubated with DAPI (4',6-diamidno-2phenyl-indole, dihydrochloride, 1:500). Finally, the sections were mounted using Fluromount-G mount agent.

2.2.4.6 Double immunofluorescence staining

In the double immunofluorescence labelling experiment, the primary antibody rabbit anti-S100A4 or rabbit anti-S100A6 polyclonal antibody was mixed with anti-CD5 (T lymphocytes and CLL marker), anti-CD10 (immature T- and B- precursor cells), anti-CD19 (B cell-specific marker), anti-CD20 (B-cell specific marker), anti-CD21 (B-cell specific marker), anti-CD23 (B-cell specific marker), anti CD45 (Leukocytes marker), antiCD45RA (B-cell marker), anti-CD68 (macrophage specific marker) and anti-CD133 (Hematopoietic stem cell marker) (Table 7). Moreover, the secondary antibodies was mix of are Alexa 488 and Alexa 568 (Table 8), in addition to DAPI (4',6-diamidno-2phenyl-indole, dihydrochloride, 1:1000). This experiment was done in tonsil tissue and bone marrow samples. Image processing and analysis for double immunofluorescence staining was by same microscope and camera of single immunofluorescence.

2.2.4.7 Four colour immunofluorescence

The first step was de-paraffinization and re-hydration. Slides were heated to 65°C for 10 minutes and placed in xylene for 3 minutes twice. Slides then were rehydrated by immersing in 99% industrial methylated spirits (IMS) for one minute twice. After that, they were placed in 95% IMS for 1 minute, once only, and moved in UP water and washed for 5 min. The second step was antigen retrieval. In this step, a working solution was prepared by diluting TE 1:100, 10 ml in 990 ml, and the slides were placed for retrieval in a 500 ml microwavable plastic container containing 1X TE buffer and microwave on 800W for 20 mins. The third step was immunofluorescence (IF) multiplexing. Slides were washed first in water then in PBS for 2 minutes twice. Three drops of OPAL blocking buffer were added to each slide and incubated for 10 min. 110 µl of S100A4 antibody (diluted in PBS 1:1000) was added to slides for 30 min at RT Incubate. Slides were washed in PBS twice and Incubated with 3 drops (or 110 µl) of OPAL HRP polymer for 30 min at RT. Slides were wash in PBS twice and incubated with 110 µl of OPAL 520 (diluted 1:100 in OPAL 1X Plus Amplification Diluent) for 10 min at RT. Slides were washed in PBS twice and unclipped from Sequenza and microwave in 1X TE for 5 min (until boiling) and then 5 min at 30% power. Then, slides were washed in water then in PBS for 2 minutes twice. Three drops of OPAL Blocking buffer were added to each slide and incubated for 10 min. after that, slides were incubated with 110 µl of CD3 antibody (diluted in PBS 1:200) for 30 min at RT. Slides then washed in PBS twice and incubated with 3 drops (110 µl) of OPAL HRP polymer for 30 min at RT. Slides were washed in PBS twice and incubated with 110 µl of OPAL 570 (diluted 1:100 in OPAL 1x Plus Amplification Diluent) for 10 min at RT. Slides were washed in PBS twice and unclipped from Sequenza and microwave in 1X TE for 5 min (until boiling) and then 5 min at 30% power. Slides were washed in water for 2 minutes twice, submerged in water and clipped into Sequenza. After washing slides with PBS twice 3 drops of blocking buffer were added to each slide and incubated for 10 min. Then, slides were incubated with 110 µl of CD20 antibody (diluted in PBS 1:200) for 30 min at RT. Slides were washed in PBS twice and incubated with 3 drops (110 µl) of OPAL HRP polymer for 30 min at RT. Slides were washed in PBS for 2 minutes twice and incubated with 110 µl of OPAL 690 (diluted 1:100 in OPAL 1x Plus Amplification Diluent) for 10 min at RT. Then, slides were

washed in PBS for 2 minutes twice and incubated with 100 µl DAPI (6µM of DAPI dilactate) for 5 min. Slides were washed in water for 2 minutes twice then, excess water was removed by shaking slides and drying and mounted in VectaShield. The edges was sealed with nail varnish and leaved at RT in the dark.

2.2.4.8 Image processing

2.2.4.8.1 Imaging slides of IHC, single immunofluorescence and double immunofluorescence staining

By using Epi-fluorescence attachment of Nikon E800 microscope (Nikon, Japan) which is equipped with ProgRes camera and ProgRes ImageJ driver software (JENOPTIC-Optical system, Germany) the tissue sections were analysed and imaged at 10x to 40x magnification. Hamamatsu Slide Scanner was used to scan some slides of IHC and scanned data can be viewed on a PC monitor by using the dedicated viewer software.

2.2.4.8.2 Imaging slides of four colour immunofluorescence

Hamamatsu Slide Scanner was used to scan slides. Scanned data can be viewed on a PC monitor by using the dedicated viewer software.

2.2.5 Isolation of human peripheral blood mononuclear cells from whole blood

Briefly, histopaque solution (17-1440-03, Ficoll-Paque PLUS) and RPMI 1640 (supplemented with 10%FCS, Glutamine and Pen/Strep) were warmed at room temperature. After labelling all tubes and lids with sample numbers, 15ml of histopaque was added into a 50ml falcon tube (Fisher Scientific, Hampton, New Hampshire, United States). Next, blood was loaded gently (up to 30 ml) onto histopaque and mixing blood with histopaque layer was avoided. The sample was centrifuged at 400 g without

acceleration or deceleration at 20ºC. The result after centrifugation was 4 layers, including: plasma, peripheral blood mononuclear cells (PBMCs), histopaque solution and erythrocytes (Figure 2.2). Then, WBCs were collected into a falcon tube using a pipette and added the re-warmed fresh culture media to make up to 30 ml. After that the mixture was spun down at 200g for 10 minutes, the supernatant was discarded and the cell pellet was re-suspended in about 10-50ml of media (depending on the pellet size). Finally, cells were counted using hemocytometer and TC20 automated cell counter-based trypan blue staining (BIO-RAD).

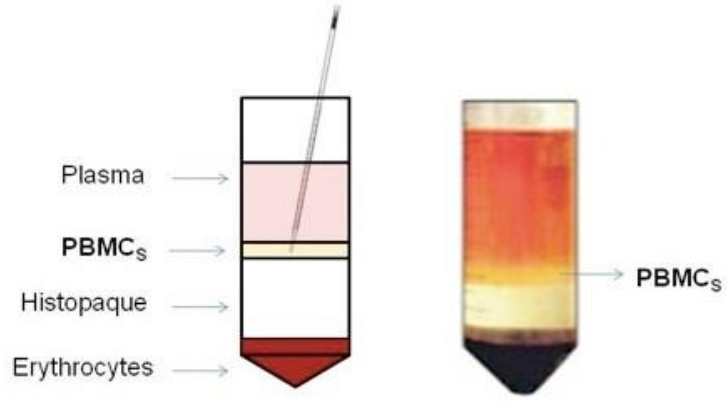

Figure 2.2 A schematic representation of the result of the density gradient stratification.

2.2.6 B-cell isolation

In order to compare normal B cell with B-cell from CLL Patient, B-cells were isolated using Dynabeads® Untouched™ Human B Cells kit. Summary of isolation of untouched B-cells protocol showed in figure 2.3. In brief, 500µl PBMC (5×10^7 cells) in the isolation buffer were transferred to a tube. Then, 100µl of antibody mix were added, mixed well and incubated for 20 min at 2°C to 8°C. The cells after that were washed by adding 4ml of isolation buffer and mixed well by tilting the tube several times and centrifuged at 350 × g for 8min at 2°C to 8°C. The supernatant was discarded. The cells were re-suspended in 500µl of isolation buffer and 500µl pre-washed Dynabeads® were added and incubated for 15min at 18°C to 25°C with gentle tilting and rotation. 4ml of isolation buffer were added. (When working with lower cell volumes, never use less than 1ml of isolation buffer). The bead-bound cells were re-suspended thoroughly by pipetting >10 times using a pipette with a narrow tip opening. Foaming was avoided.

The tube was place in the magnet for 2min and the supernatant, containing the untouched human B-cells, was transferred to a new larger tube. 4ml of isolation buffer was added to the tube containing the Dynabeads® and re-suspended the bead-bound cells by pipetting. The tube was placed in the magnet for 2min and the two supernatants were combine and used for analysis.

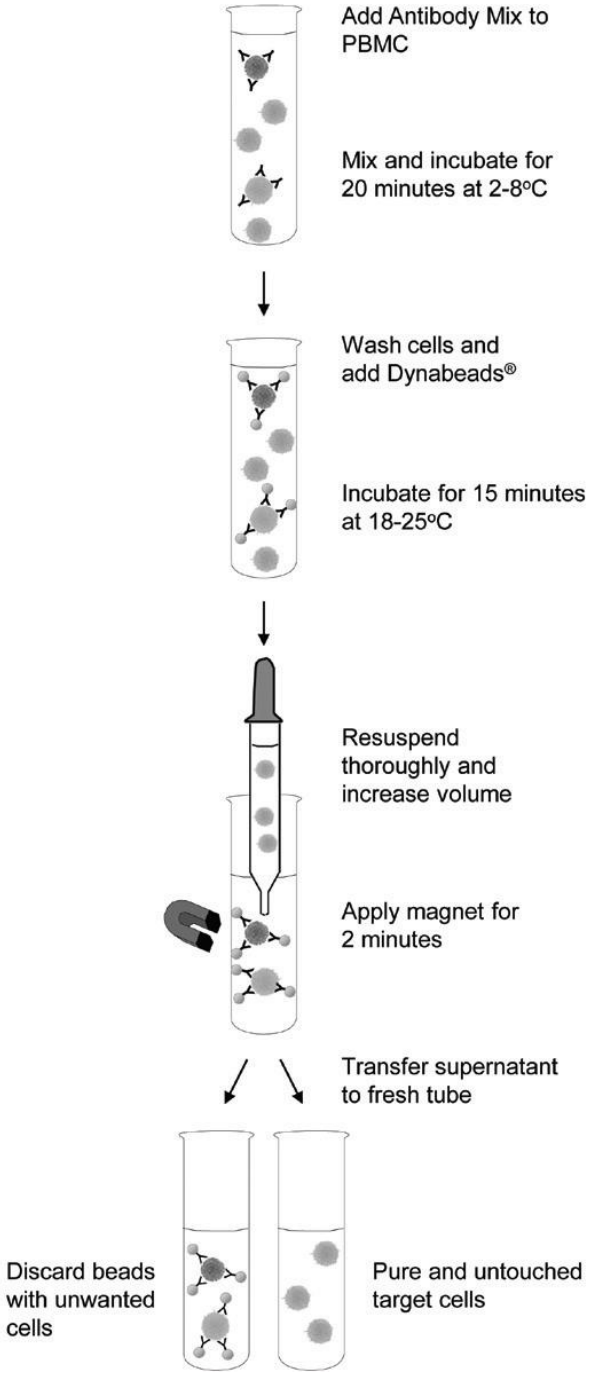

Figure 2.3 Isolation of untouched B Cells.

https://assets.thermofisher.com/TFS.Assets/LSG/manuals/Dyna_untouch_human_bcell_man.pdf

2.2.7 Chemotaxis assay

The study of cell migration is very important in order to understand many physiological and pathological conditions, including cancer metastasis. The cellular and molecular bases of cell migration have been thoroughly analyzed *in vitro*.

To summarize: the first step was preparation of 5 µm polycarbonate membrane by coating it with 600-700 µL, of 10 µg/mL fibronectin (fibronectin was reconstituted with 1ml sterile H_2O/mg of protein). This amount was sufficient to cover the entire wells. Then, the membrane was left at 4°C overnight. The membrane was washed twice with PBS and allowed to air dry for at least 45 min at RT. The chemotaxis (migration)/ binding medium (DMEM medium containing 1% BSA, 10 mM HEPES buffer, pH 6.7) with and without serum (we can use SDF-1α/CXCL12 or serum for lymphocytes activation) was placed in the lower chamber of trasnwells (Usually 600µl added to the well for 24-well plate). By sterile forceps transwells were inserted into 24-well plate (in Tissue Culture). 50-100 µl cell suspension in serum free medium was placed in the upper wells. After incubation of the apparatus at 37°C for 3 hours (this should be optimized based on cell types) in humidified air with 5% CO_2. Lastly, migrated cells were collected and counted using Trypan Blue Solution and Hemocytometer.

2.2.8 Statistical analysis

Most experiments were performed in triplicate. In order to compare data, GraphPad Prism Version 7.0 program was used. A t-test, one way ANOVA and two way ANOVA were used, and Statistical significance is indicated by asterisks $*P < 0.05$, $**P < 0.01$, $***P < 0.001$ and NS represents statistically non-significant.

All statistical analysis for immunohistochemical data was performed by Professor Kevin West (Department of Pathology, Leicester Royal Infirmary) using the Statistical Package for the Social Sciences 20.0® (SPSS, Chicago, Illinois, USA). Associations between different proteins were determined using pearson correlation coefficient. Results from this test produced a correlation coefficient, indicating the strength and direction of the association, and a *P* value, indicating the significance.

If the coefficient is positive, then both variables increase together. If the coefficient is negative then the variables are inversely related. The Chi-squared tests in GraphPad Prism Version 7.0 program were used to analyse significant associations and differences between subgroups within the cohort. Univariate prognostic significance of variables was analysed by means of univariate Cox regression analysis, Kaplan-Meier analysis and application of the log-rank test. Statistical significance was defined as $P < 0.05$.

Chapter 3. Expression of S100A4 in B-cell lymphomas

3.1 Introduction

Histological diagnosis of lymphoma is a challenging process that aims to characterise a type and a stage of the disease. Various biomarkers have been found to be clinically useful in building a diagnosis but there is still a need for new biomarkers. Comparative analysis of characterization of the gene and protein expression profiles of the lymphoma and normal samples is a traditional approach to search for new biomarkers.

The differential expression of S100 proteins in cancer and normal tissues was proposed to be associated with tumour progression, and can therefore be considered as an important diagnosis biomarker for patient stratification. Immunostaining analysis performed in different labs demonstrates that the expression of some S100 protein family members elevates in solid malignancies compared to the normal tissue (Bresnick et al., 2015b) but there is limited information about the expression of S100 proteins in haematological malignancies. However, according to our preliminary data, several members of the S100 family can be considered to be potential biomarkers in B-cell malignancies. A bioinformatics study showed that there was a different expression of S100 gene, up/down regulation, obtained from the dataset EGEO-2466 in CLL compared to normal cases. The results concluded that S100A4 and S100A6 could be considered as new biomarkers for CLL (G. Kaithakottil, MSc thesis, University of Leicester, 2010).

Several studies have shown a significant correlation between the EMT process and the S100 protein family. For instance, S100A4 has been detected as an active fibroblast-specific protein and its expression leads to EMT induction in renal fibrosis (Strutz et al., 1995). In addition, down regulation of S100A4 expression by RNA interference results in the inhibition of EMT induction in the epithelial cells of the proximal tube lining in the human kidney (Schneider et al., 2008). Also, it is found that EMT-inducing transcription factor ZEB1 has a critical role in haematological malignancy such as MCL (Sayan, 2014). Furthermore, experimental evidence demonstrated that EMT-related genes such as ZEB1 and ZEB2 could be used as potential markers for some types of cancer diagnosis and their expression is associated with higher histological grades and overall survival rates. Moreover, researchers found

that ZEB1 expression defines a differential response to chemotherapy drugs, thus also setting ZEB1 as a potential predictive biomarker and therapeutic target in mantle cells lymphoma (Sahasrabuddhe, 2016; Sánchez-Tilló et al., 2014).

In the quest to decrease mortality and morbidity from cancer, there is a continual effort to identify novel biomarkers to help in the early detection and the accurate prediction of tumor behavior. One group of proteins that is developing as a potentially important group of markers in multiple tumor types is the S100 family of calcium-binding proteins. There is an increasing suggestion that a different expression of S100 family members is seen in many cancers including breast, lung, bladder, kidney, thyroid, gastric, prostate and oral cancers. S100 proteins are commonly up-regulated in tumours and this is usually linked to tumor progression. There is no clear investigation which shows the expression of S100 genes in stem cells of lymphoma in general.

CLL is characterised by an accumulation of abnormal B-cells in the peripheral blood and bone marrow (Kuppers et al., 2005). A number of studies showed that CLL cases with mutated IgV genes are associated with an unfavourable clinical prognosis (Klein and Dalla-Favera, 2010). In spite of other prognostic markers, including CD38 and ZAP-70 that are in use to predict prognosis and requirements for early treatment of CLL patients, there are limitations in their clinical applications such as reproducibility of the CLL diagnosis. There is still an urgent need for new prognostic markers that can help in early detection of CLL. It was shown that the level of expression of S100 proteins is different between tightly controlled cells and is specific for particular cell types with some of S100s upregulated in epithelial cells, while others tend to be mesenchymal proteins. Transcription of S100 genes is orchestrated by multiple transcription factors and dependent on promoter methylation or chromosomal rearrangements in the locus 1q21 (Donato et al, 2013). A considerable amount of literature about S100 proteins in cancer particularly in solid malignancies has been published. It was shown that their expression was changed in cancer and could be used as a potential prognostic marker (Bresnick et al., 2015b). Historically, S100A4 has mainly been the focus of investigation and its involvement in cancer cell invasion is now proven. Many researchers consider that S100A4 expression in tumour cells is associated with reduced survival of cancer patients (Lee et al., 2004; Rudland et al., 2000). For example in breast cancer, detection of S100A4 in primary carcinoma cells was related to the poor patient survival and correlated with metastatic growth in the

axillary lymph nodes, positivity on c-erbB-2, c-erbB-3 and cathepsin D (Lee et al., 2004). In addition, it was found that there was a correlation between S100A4, osteopontin, vessel density and estrogen receptor alpha (ER alpha) presence in primary tumours and survival of patients (de Silva Rudland et al., 2006). Also, it was confirmed that the expression of S100A4 is associated with metastasis and survival of patients with bladder cancer (Davies et al., 2002; Matsumoto et al., 2007) or gastric cancer, where expression of S100A4 and down-regulation of E-cadherin were used to predict a metastatic potential of tumours (Yonemura et al., 2000). The suitability of S100 family members as prognostic markers is still under investigation. A recent study investigated the expression profile of 20 proteins of the S100 family in breast cancer using a multiomics approach, a combination of in silico analysis of all available databases. Gene/protein expression was found in the analyses tumour samples (Cancemi et al., 2018). The expression profile of S100 proteins associated with CLL development has not been investigated before. Identification of S100 proteins in CLL could impact on better understanding of the properties of CLL lymphocytes and might have value for the development of novel treatment options.

The aim of the chapter was to search for S100A4 and S100A6 as potential new biomarkers in B-cell lymphomas as was indicated by bioinformatics analysis of the publically available databases (G. Kaithakottil, MSc thesis, University of Leicester, 2010). The objective of the present work was to analyse S100A4, S100A6, ZEB1 and ZEB2 expression in normal lymphoid tissues, including: tonsil, spleen and thymus, and compare it with their expression in B-cell lymphoma tissues by immunohistochemistry (IHC). Also, this study was aimed to investigate a possible link between expressions of S100A4 and S100A6 and activation of the EMT transcriptional factors, ZEB1 and ZEB2. Moreover, in the current study a detailed analysis of S100A4 positive cells was performed using double immunofluorescence and four colour immunofluorescence staining. Sixty samples of CLL, MCL, DLBCL, MZL and FL were used to characterise and correlate the expression of S100 proteins and EMT transcription factors from ZEB family using IHC in parallel sections.

The second aim of this chapter was to characterize S100A4 expression in B-lymphocytes development with a special focus on haematopoietic stem cells. Pathological normal and CLL bone marrow samples were used to analyze S100A4 expression by IHC. Furthermore, it was important to characterize S100A4 in different

type of cells including pluripotent or precursors HSCs and other cells by double immunofluorescence using different markers including: CD5, CD10, CD34, CD45, CD31, CD45RA and CD68. In addition, we planned to perform 4-colour immunofluorescence to characterize expression of S100A4 in T and B-lymphocytes using CD3 and CD20, with the resulting evaluation of S100A4 as a marker of stemness in CLL.

The third aim of this chapter was to characterise the expression profile of *S100* genes and proteins in samples of the peripheral blood of CLL patients. Since the expression of EMT transcription factors of ZEB family was correlated with expression of S100 proteins, analysis of ZEB1 and ZEB2 expression was also included. An attempt to link expression of S100A4 protein with patients' survival was also made. Real time Q-PCR, Western blotting, immunohistochemistry and immunofluorescence were used for the analysis of *S100s* and *ZEB1* and *ZEB2* genes and proteins in CLL peripheral blood. 20 CLL samples of the peripheral blood and corresponding patients' survival data were kindly provided by The Ernest and Helen Scott Haematological Research Institute in the Leicester Cancer Research Centre, University of Leicester.

3.2 Results

3.2.1 S100A4 and S100A6 in B-cell lymphomas

3.2.1.1 Expression of S100A4, S100A6, ZEB1 and ZEB2 in normal lymphoid organs (tonsil, spleen and thymus) by IHC

In order to investigate the expression of S100A4, S100A6, ZEB1 and ZEB2 in tonsil, antibodies titration was performed. Optimization was done on tonsil tissue due to its availability and based on ThermoFisher Sientific reference (https://www.thermofisher.com/antibody/primary/query/S100a4%20antibodies). Rabbit polyclonal antibody from Proteintech against S100A4 was used in different concentrations and the dilution at 1:1000 given specific staining of cells in non-germinal centre and a few cells in germinal centre in paraffin embedded tonsil slides. Therefore rabbit polyclonal anti-S100A4 from Proteintech with 1:1000 dilution was used for immunostaining (Figure 3.1A). Also the specificity of S100A6 rabbit polyclonal antibody from Proteintech was tested in paraffin-embedded tonsil section at 1:200, 1:400, 1:1000 dilutions using immunohistochemistry technique. The results (Figure 3.1B) showed the dilution at 1:1000 to be most suitable dilution to be used in our research, which was very specific for group of cells in the peripheral zone cells. Anti-ZEB1 from Santa Cruz was optimized in the same way as anti-S100A4 and anti-S100A6 using ZEB1-positive pancreatic tumour slides. The result showed that the best dilution was 1:200. The anti-ZEB2 antibody was available in the lab and used in dilution 1:2000 after optimization.

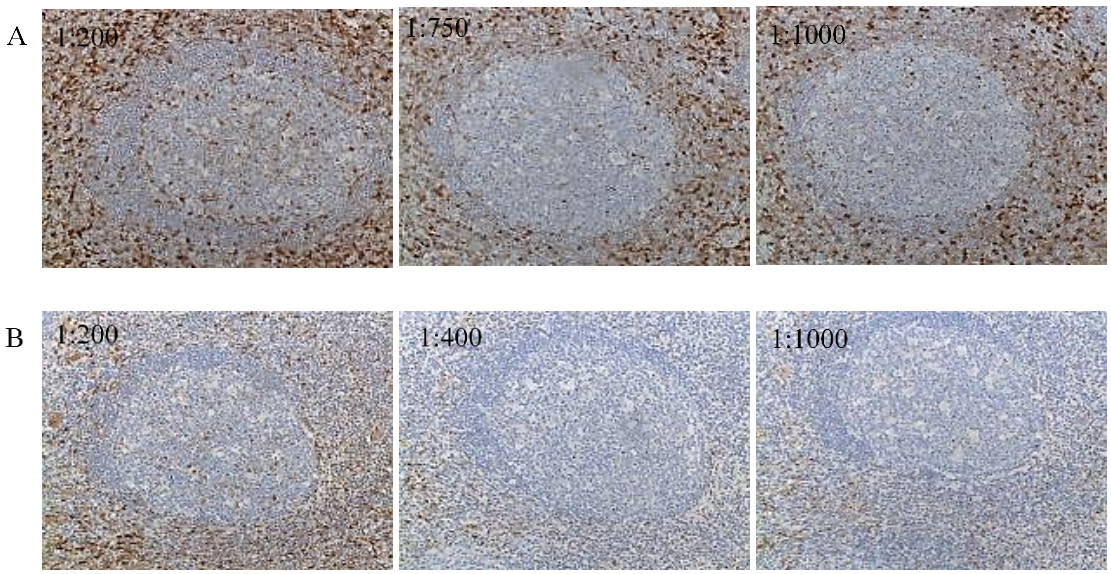

Figure 3.1 S100A4 and S100A6 antibodies optimization. Immunostaining of paraffin-embeded tonsil sections with different dilutions of the polyclonal anti-S100A4 and S100A6 antibodies.

Sections of tonsil tissue were cut to detect the expression of S100A4, S100A6, ZEB1 and ZEB2 by IHC. Staining was done in parallel sections for comparative analysis. The result of IHC examination of tonsil tissue revealed that S100A4 expression was detected in most areas of the section. S100A4 expressed T-lymphocytes mostly while S100A6 was expressed in macrophages and epithelial cells in addition to T-lymphocytes. A small number of fibroblasts showed low expression of S100A4 and S100A6. On the other hand, both proteins, S100A4 and S100A6, showed no expression in B-lymphocytes. Regarding the expression of ZEB1 in same tissue, the slides screening results showed that a high to medium expression was seen in T-lymphocytes in non-germinal centre while there was no expression in the germinal centre. Moreover, ZEB2 expression was obvious in T-lymphocytes present inside and outside of the germinal centres (Figure 3.2). Also, S100A4 and ZEB2 showed similarity in their distribution in tonsil tissue.

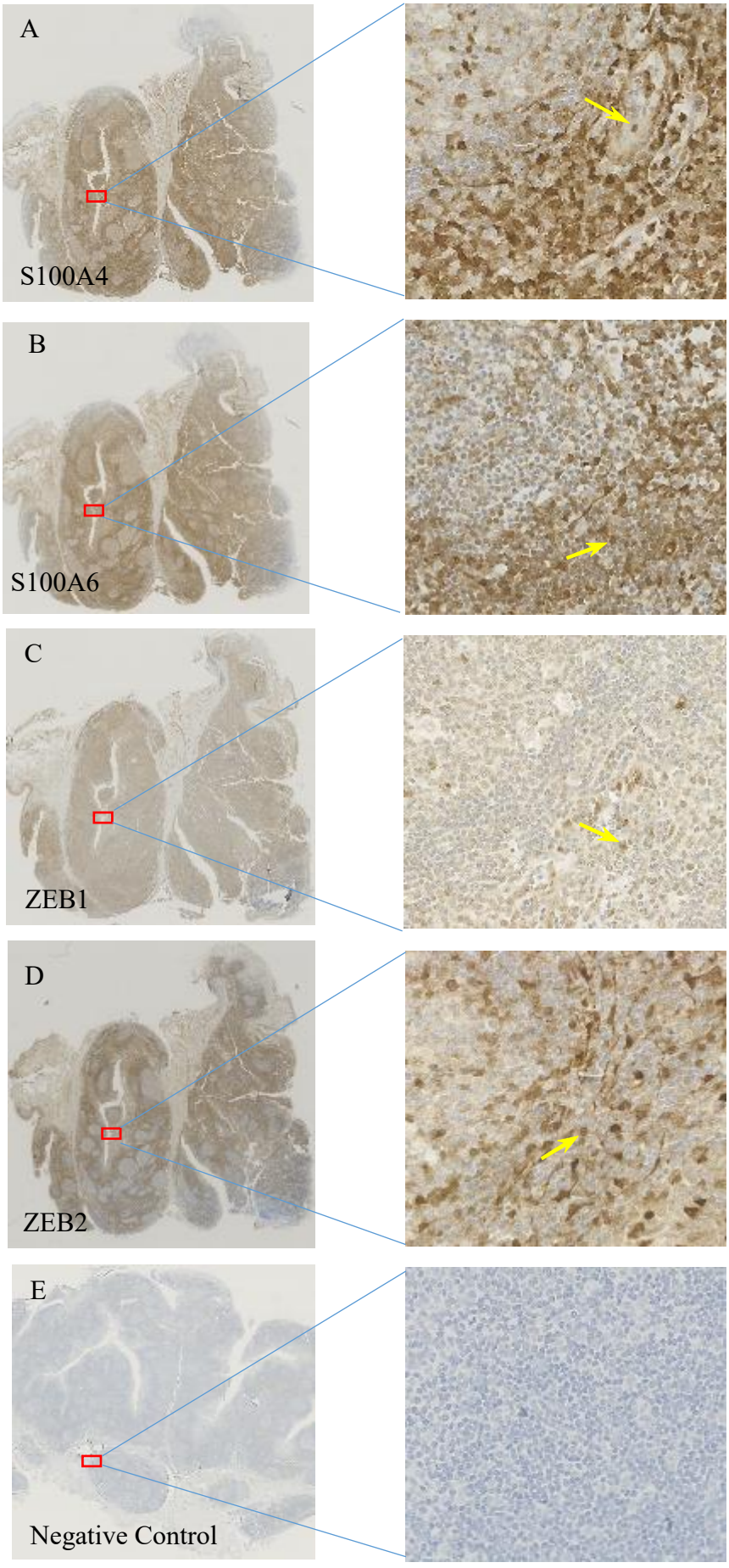
A
S100A4
B
S100A6
C
ZEB1
D
ZEB2
E
Negative Control

Figure 3.2 Immunohistochemical analysis of expression of (A) S100A4, (B) S100A6, (C) ZEB1 and (D) ZEB2 in tonsil tissue by IHC. (E) Negative control.

Immunohistochemical analysis of expressions of S100A4, S100A6, ZEB1 and ZEB2 in parallel tonsil sections was done using S100A4 (Proteintech, dilution 1:1000), S100A6 (Proteintech, dilution 1:1000), ZEB1 (Santa Cruz, dilution 1:200) and ZEB2 (Lab made, dilution 1:2000) antibodies as described in Materials and Methods. The arrows point to T-lymphocytes. Images were taken using a Hamamatsu Slide Scanner microscopy. Images presented with magnifications x1 and x40.

Expression of S100A4, S100A6, ZEB1 and ZEB2 was analysed by IHC in parallel sections of spleen tissue. Antibodies against S100A4, S100A6, ZEB1 and ZEB2 were used in the selected dilution as before in the analysis of tonsil staining. Of note, expression of S100A4 and S100A6 was detected in T-lymphocytes and macrophages mainly. ZEB1 showed a low to negative expression while ZEB2 showed expression in scattered cells such as T-lymphocytes, endothelial cells and fibroblasts. Similarity between S100A4 and ZEB2 distribution was also observed as in tonsil tissue (Figure 3.3).

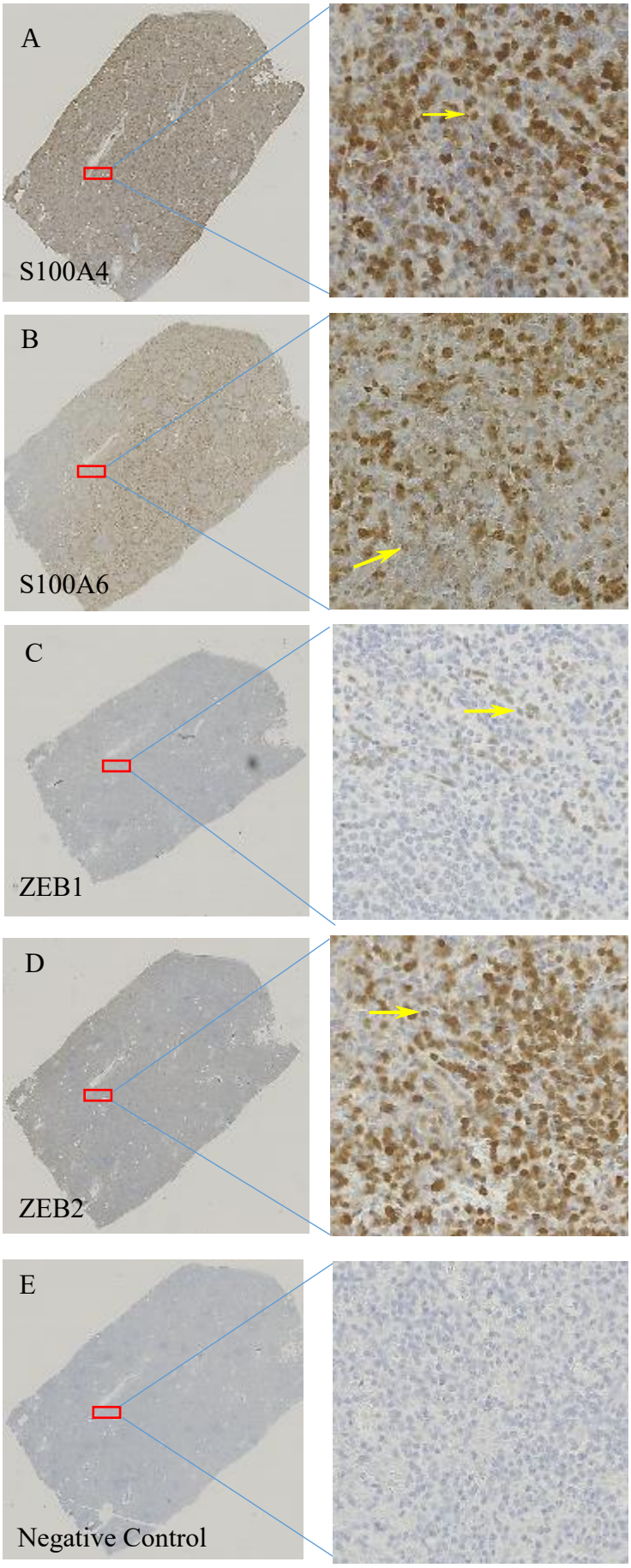
A
S100A4
B
S100A6
C
ZEB1
D
ZEB2
E
Negative Control

Figure 3.3 Immunohistochemical analysis of expression of (A) S100A4, (B) S100A6, (C) ZEB1 and (D) ZEB2 in spleen tissue by IHC. (E) Negative control.

Immunochemical analysis of S100A4, S100A6, ZEB1 and ZEB2 expression in parallel spleen sections was done using S100A4 (Proteintech, dilution 1:1000), S100A6 (Proteintech, dilution 1:1000), ZEB1 (Santa Cruz, dilution 1:200) and ZEB2 (Lab made, dilution 1:2000) antibodies as described in Materials and Methods. The arrows point to T-lymphocytes. Images were taken using a Hamamatsu Slide Scanner microscopy. Images presented with magnifications x1 and x40.

A block of thymus tissue was used to prepare parallel sections for IHC to study the expression of S100A4, S100A6, ZEB1 and ZEB2. IHC results found that S100A4 and S100A6 expressed in T-cells and other cells such as endothelial cells, monocytes and megakaryocytes. The degree of expression was low to moderate in most cells. Similar to spleen tissue, thymus tissue showed no expression of ZEB1 while ZEB2 expressed in a low to moderate level in some cells such as endothelial cells (Figure 3.4). The results showed that S100A4 and ZEB2 were expressed in T-lymphocytes during T-lymphocyte development in lymphoid organs, tonsil and spleen, but not thymus. This may be due to the fact that the tested thymus sample was taken from elderly people (post-mortem) but there was few T-lymphocytes in analysed tissue. Thus, in this sample T-lymphocytes practically few because the thymus shrinks by about 3% a year throughout middle age, as a result a fall in the thymus production of naïve T-lymphocytes occurred.

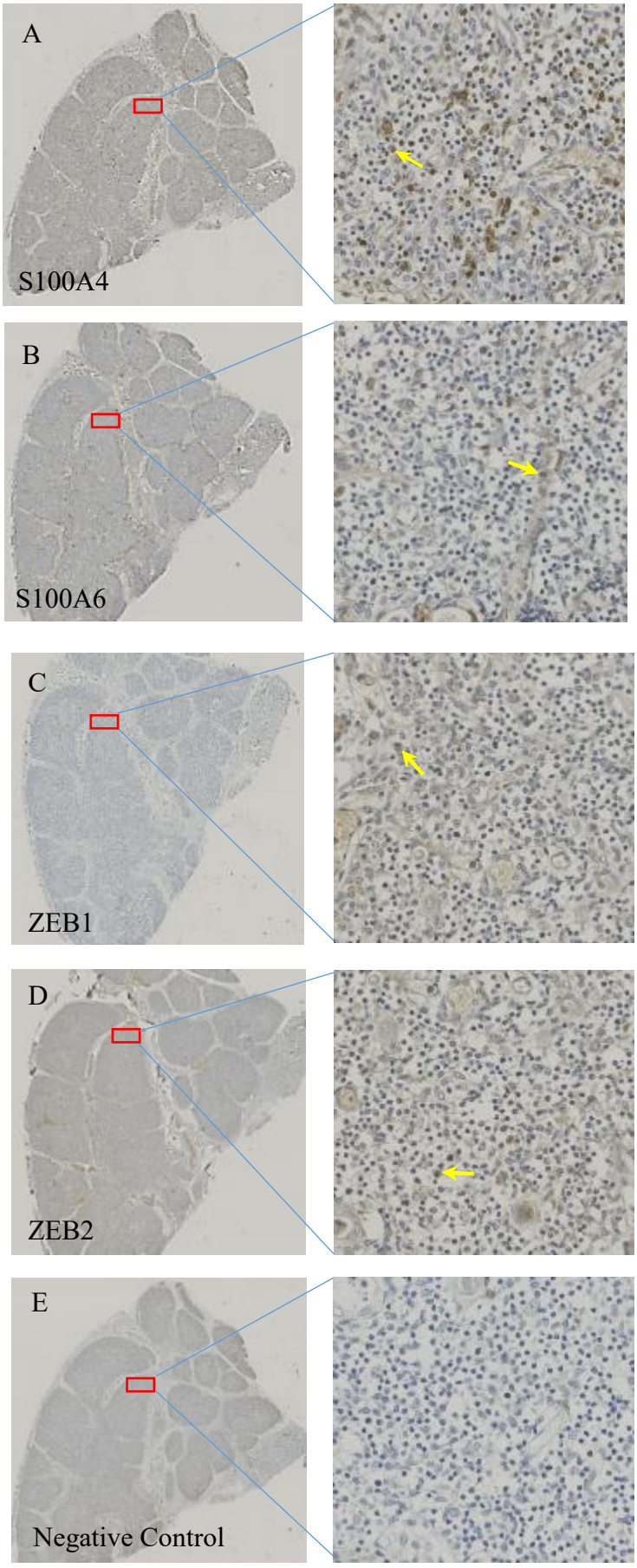
A
S100A4
B
S100A6
C
ZEB1
D
ZEB2
E
Negative Control

Figure 3.4 Immunohistochemical analysis of expression of (A) S100A4, (B) S100A6, (C) ZEB1 and (D) ZEB2 in thymus tissue by IHC. (E) Negative control.

Immunochemical analysis of expressions of S100A4, S100A6, ZEB1 and ZEB2 in parallel thymus sections was done using S100A4 (Proteintech, dilution 1:1000), S100A6 (Proteintech, dilution 1:1000), ZEB1 (Santa Cruz, dilution 1:200) and ZEB2 (Lab made, dilution 1:2000) antibodies as described in Materials and Methods. The arrows pointed to T-lymphocytes. Images were taken using a Hamamatsu Slide Scanner microscopy. Images presented with magnifications x1 and x40.

3.2.1.2 Study expression of S100A4, S100A6, ZEB1 and ZEB2 in B-cell lymphomas by IHC

Tissue samples from lymphoma patients were provided from the Department of Pathology of Leicester Royal Infirmary. Table 3.1 showed the number of lymphoma samples from patients diagnosed with B-cell lymphoma. Each tissue case was cut, stained and screened to study the expression level of S100A4, S100A6, ZEB1 and ZEB2 (in collaboration with Professor Kevin West, the Department of Pathology of Leicester Royal Infirmary) (Table 2).

Lymphoma types	Number of cases
Chronic Lymphocytic Leukaemia (CLL)	16
Diffuse Large B Cell Leukaemia (DLBCL)	26
Follicular Lymphoma (FL)	11
Mantle Cell Leukaemia (MCL)	6
Marginal Zone Leukaemia (MZL)	1
Total	60

Table 3.1 The number of B-cell lymphoma cases used throughout this study.

3.2.1.2.1 Expression of S100A4 in B-cell lymphomas

In this study, a set of 60 B-cell lymphoma cases were used. Lymphoma sections were cut and stained with S100A4 antibody (Proteintech, dilution 1:1000). A moderate level of expression of S100A4 was detected in B-lymphocytes of the CLL cases (Figure 3.5A). S100A4 immunostaining displayed a strong to moderate expression in some

case of DLBCL (16/26) (Figure 3.5B) whereas (6/26) of DLBCL cases showed a weak expression of S100A4. IHC results of 6 MCL cases showed a moderate-high level of expression in only one of them (Figure 3.5C), where a significant number of B-lymphocytes expressed S100A4 protein. In addition, weak expression was observed in one case of MZL (Figure 3.5E). Moreover, 11 lymphoma cases of FL did not express S100A4 protein in the cytoplasm or nucleus of B-lymphocytes while a strong signal was observed in a large number of infiltrating T-lymphocytes (Figure 3.5D). The overall results of IHC showed various degrees of staining in B-cells of the analysed lymphomas was summarised in the figure 3.6.

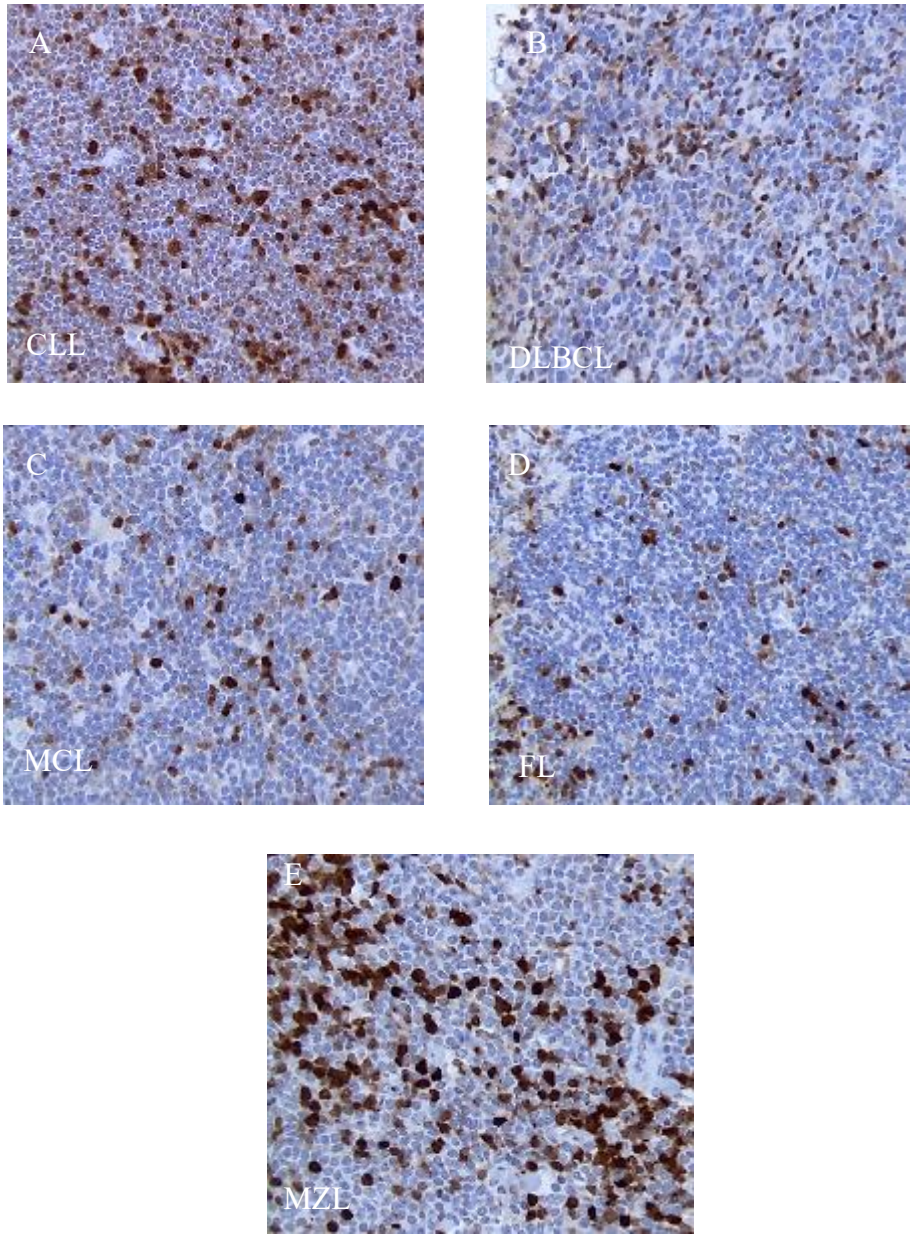

Figure 3.5 Selected images of immunohistochemical analysis of S100A4 expression in B-cell lymphomas.

Immunohistochemical analysis of expression of S100A4 in selected B-cell lymphoma cases (A) CLL, (B) DLBCL, (C) MCL, (D) FL and (E) MZL was done using S100A4 antibody (Proteintech, dilution 1:1000), as described in Materials and Methods. Images were captured using a Hamamatsu Slide Scanner microscopy. Images presented with magnification x40.

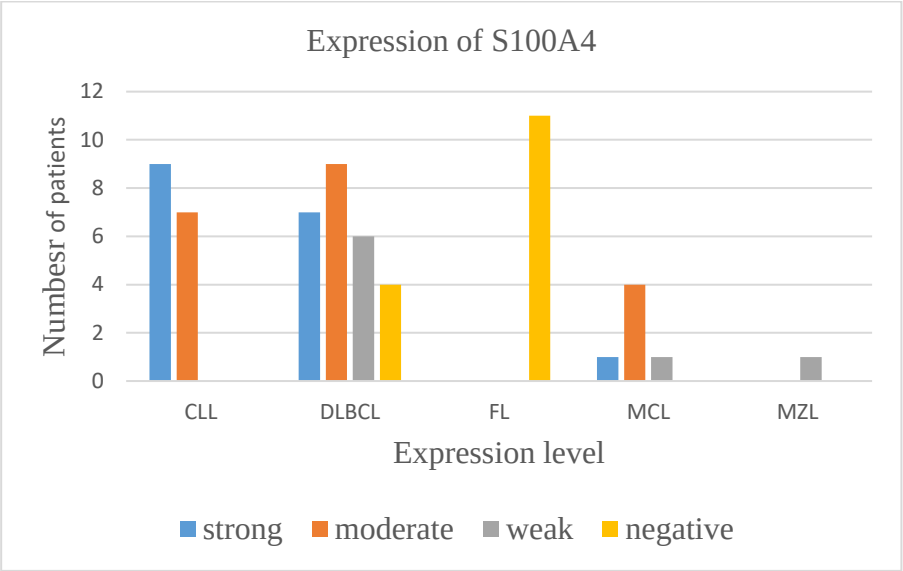

Figure 3.6 The number of analysed lymphoma cases that expressed S100A4 in different levels.

The number of the identified tumours with strong, moderate, weak or negative expression of S100A4 are presented on the Y axis. The level of expression (X axis) was measured as strong if there is > 70% B-lymphocytes positive, moderate if 70-30% B-lymphocytes positive, weak if there is B-lymphocytes positive < 30% or negative expression if <10% B-lymphocytes is positive.

3.2.1.2.2 Expression of S100A6 in B-cell lymphomas

The same set of 60 samples of B-cell lymphoma cases was tested for S100A6 expression by IHC using rabbit polyclonal anti-S100A6 antibody (Proteintech, dilution 1:1000). The result of S100A6 immunostaining revealed that no expression was detected in neoplastic B-lymphocytes in all 60 lymphoma samples. However, other cells such as T-lymphocytes, dendritic cells, and endothelial cells showed a strong expression of S100A6 protein (Figure 3.7).

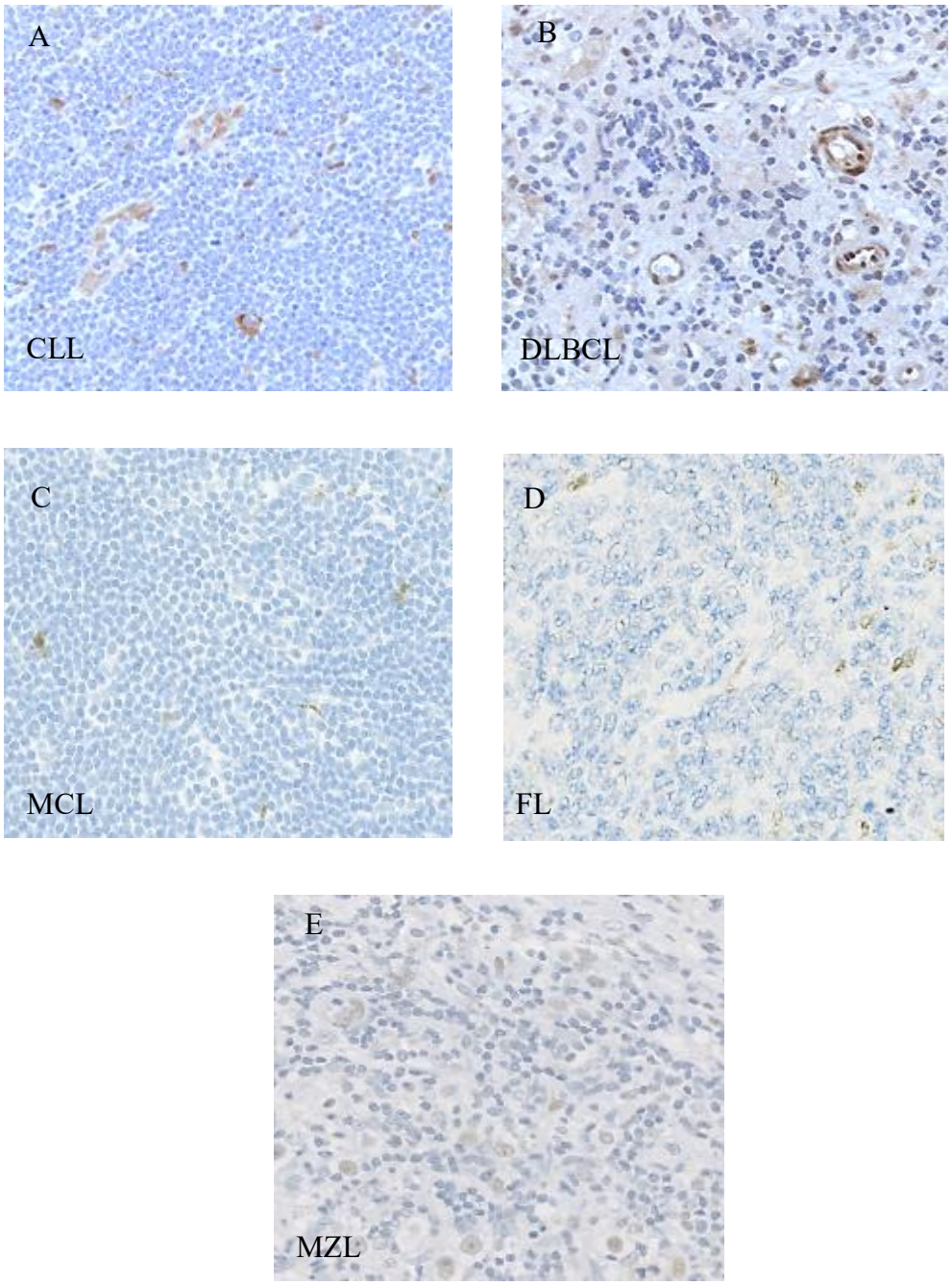

Figure 3.7 Selected images of immunohistochemical analysis of S100A6 expression in B-cell lymphoma cases.

Immunohistochemical analysis of expression of S100A4 in selected B-cell lymphomas cases (A) CLL, (B) DLBCL, (C) MCL, (D) FL and (E) MZL was done using S100A6 antibody, (Proteintech, dilution 1:1000) as described in Materials and Methods. Images were captured using a Hamamatsu Slide Scanner microscopy. Images presented with magnification x40.

3.2.1.2.3 Expression of ZEB1 in B-cell lymphomas

The expression of ZEB1 appeared in some B-cell lymphoma samples but the degree of expression was varied from moderate to low. Moreover, many samples showed negative expression of ZEB1 (Figure 3.8). The cells that expressed ZEB1 were T-lymphocyte, macrophages and endothelial cells.

Figure 3.9 showed the quantity of lymphoma cases that expressed ZEB1 and the level of expression. It was shown that out of 60 lymphoma cases only 3 showed moderate expression. However, all of them were DLBCL cases. On the other hand, 8 cases showed week expression, including: 1 case of CLL, 4 DLBCL and 3 MCL cases. 49/60 analysed lymphoma cases showed a negative expression of ZEB1.

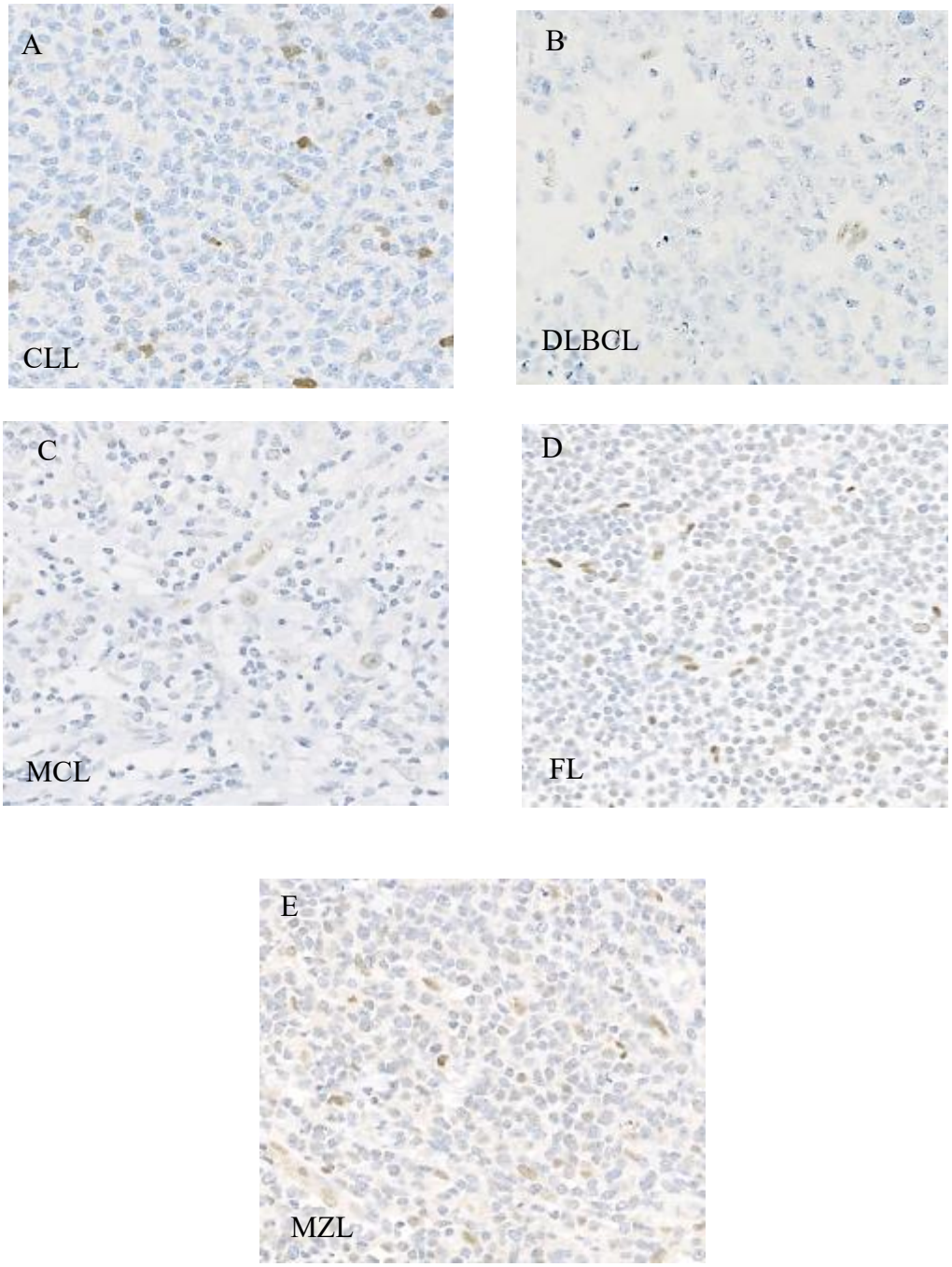

Figure 3.8 Selected images of immunohistochemical analysis of ZEB1 expression in B-cell lymphomas.

Immunohistochemical analysis of ZEB1 expression in selected B-cell lymphomas cases (A) CLL, (B) DLBCL, (C) MCL, (D) FL and (E) MZL was done using ZEB1 antibody (Santa Cruz, dilution 1:200), as described in Materials and Methods. Images were captured using a Hamamatsu Slide Scanner microscopy. Images presented with magnification x40.

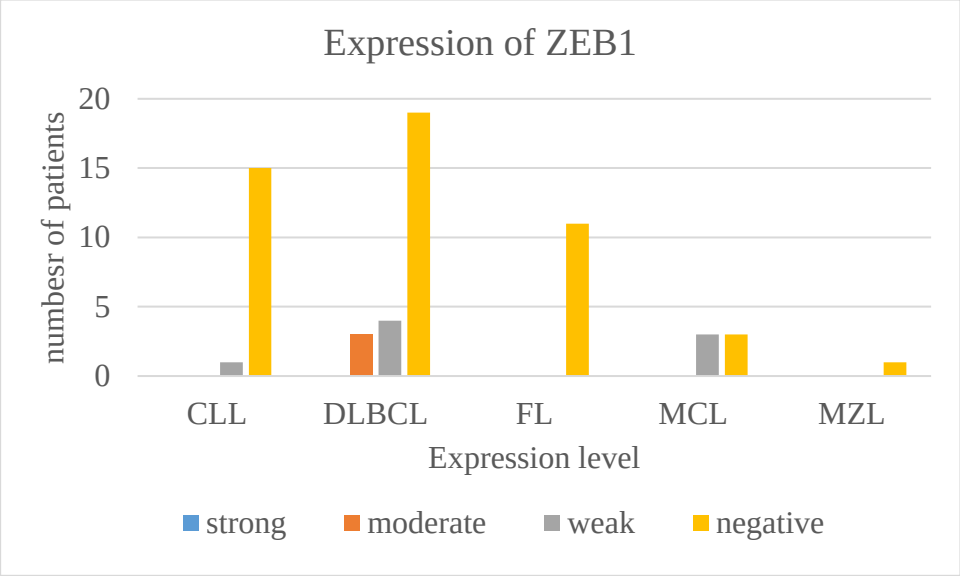

Figure 3.9 Expression of ZEB1 in B-cell lymphomas.
The number of the identified tumours with strong, moderate, weak or negative expression of ZEB1 are presented on the Y axis. The level of expression (X axis) was measured as strong if there is > 70% of B-lymphocytes positive, moderate if 70-30% B-lymphocytes positive, weak if there is B-lymphocytes positive < 30% or negative expression if <10% B-lymphocytes is positive.

3.2.1.2.4 Expression of ZEB2 in B-cell lymphomas

Screening results of IHC of lymphoma tissue showed that most lymphoma samples expressed ZEB2 in B-lymphocytes in different degrees, from weak to moderate, but there were a few negative cases. In addition, cells such as endothelial cells or macrophages were ZEB2 positive (Figure 3.10).

Figure 3.11 showed that out of 60 analysed cases, 9 revealed moderate expression, including: 2 CLL, 4 DLBCL, 2 FL and 1 case of MCL. On the other hand, 23 cases showed weak expression, including: 7 CLL, 6 DLBCL, 5 MCL and 1 case of MZL. 28/60 lymphoma cases showed negative expression.

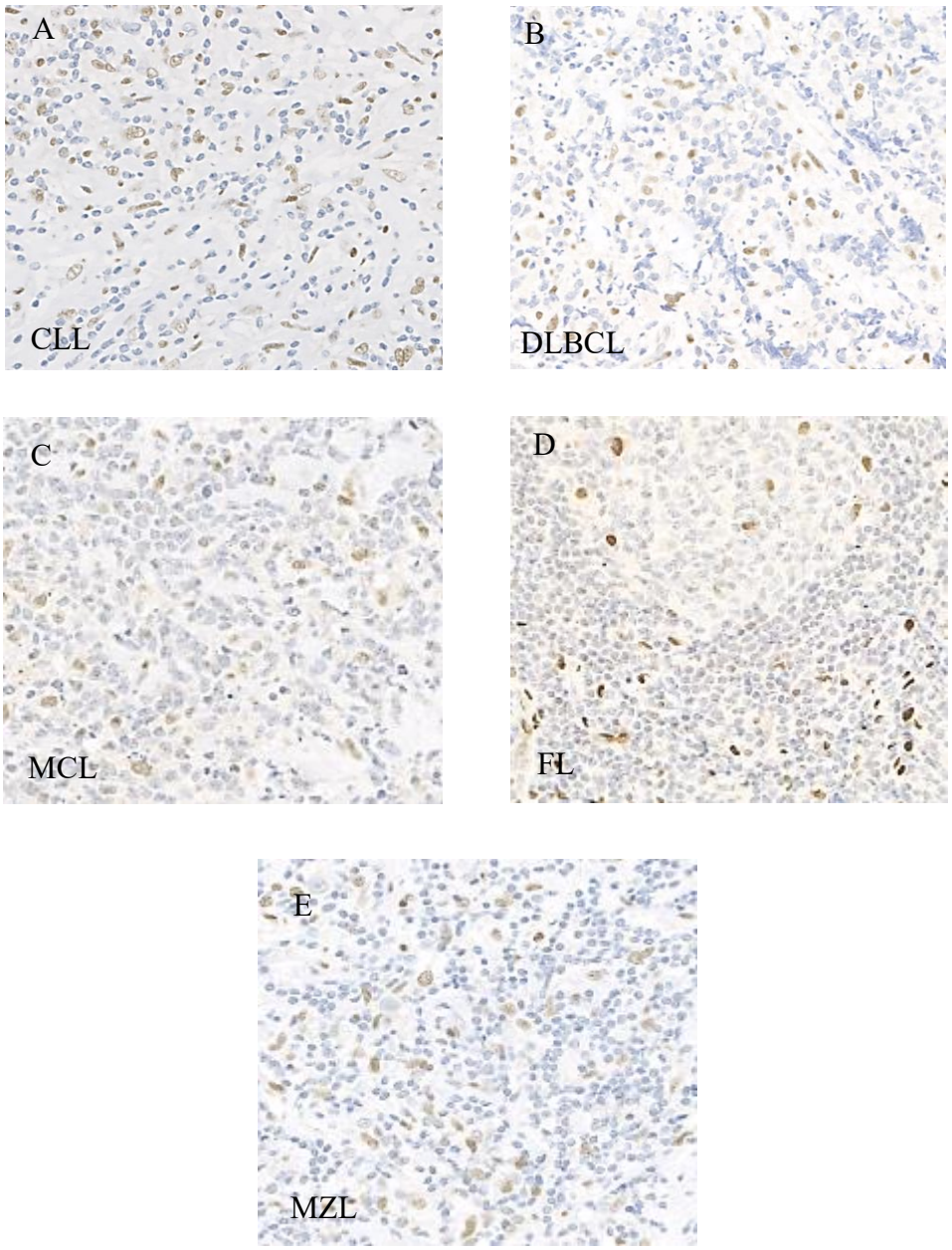

Figure 3.10 Selected images of immunohistochemical analysis of ZEB2 expression in B-cell lymphomas.

Immunohistochemical analysis of ZEB2 expression in selected B-cell lymphomas cases (A) CLL, (B) DLBCL, (C) MCL, (D) FL and (E) MZL was done using ZEB2 antibody (Lab made, dilution 1:2000), as described in Materials and Methods. Images were captured using a Hamamatsu Slide Scanner microscopy. Images presented with magnification x40.

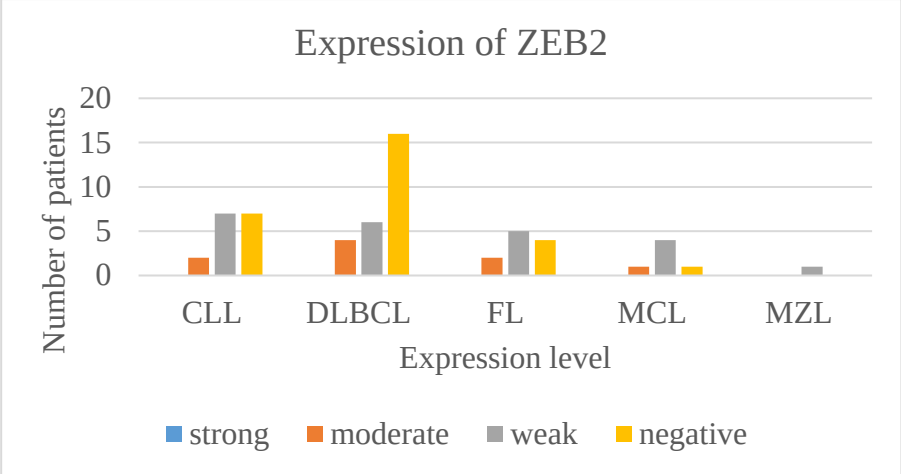

Figure 3.11 Expression of ZEB2 in analysed B-cell lymphomas.
The number of the identified tumours with strong, moderate, weak or negative expression of ZEB2 are presented on the Y axis. The level of expression (X axis) was measured as strong if there is > 70% positive B-lymphocytes, moderate if 70-30% B-lymphocytes are positive, weak if there is positive B- lymphocytes < 30% or negative expression if <10% B-lymphocytes is positive.

The level of expression S100A4, S100A6, ZEB1 and ZEB2 (in collaboration with Professor Kevin West, the Department of Pathology of Leicester Royal Infirmary) was summarized in table 3.2. In each IHC analysis, negative and positive controls were included (Figure 3.12)

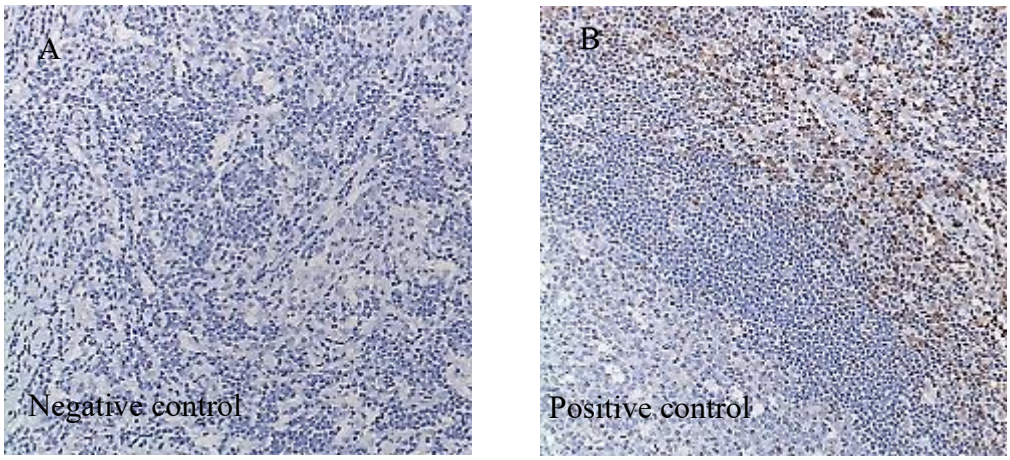

Figure 3.12 Examples of (A) the negative and (B) positive controls.

Negative and positive controls were run in each experiment of IHC to detect the expression of S100A4, S100A6, ZEB1 or ZEB2 in lymphoma cases. (A) Negative control, IHC staining of lymphoma tissue without application of the primary antibody. (B) Positive control of staining of the tonsil section against S100A6. Images were captured by using a Hamamatsu Slide Scanner microscopy. Images presented with magnification

	Lymphoma cases	Expression level of S100A4	Expression level of S100A6	Expression level of ZEB1	Expression level of ZEB2
1	CLL	***			*
2	CLL	***			
3	CLL	***			*
4	CLL	**			**
5	CLL	**		*	
6	CLL	***			*
7	CLL	***			
8	CLL	**			
9	CLL	**			
10	CLL	**			**
11	CLL	***			*
12	CLL	**			
13	CLL	***			*
14	CLL	***			
15	CLL	**			*
16	CLL	***			*
17	DLBCL	**			**
18	DLBCL	*		**	
19	DLBCL	***			*
20	DLBCL	***			**
21	DLBCL	**		*	
22	DLBCL				*
23	DLBCL	*			
24	DLBCL	**			
25	DLBCL				
26	DLBCL	***			*
27	DLBCL	**		**	
28	DLBCL	**			
29	DLBCL	*			**
30	DLBCL	***			*
31	DLBCL			*	
32	DLBCL	*			
33	DLBCL	***			
34	DLBCL				
35	DLBCL	**			*
36	DLBCL	*		*	
37	DLBCL	**			
38	DLBCL	***			
39	DLBCL	*		**	
40	DLBCL	**			**

41	DLBCL	***			
42	DLBCL	**		*	*
43	FL				
44	FL				*
45	FL				
46	FL				**
47	FL				*
48	FL				
49	FL				*
50	FL				**
51	FL				*
52	FL				
53	FL				*
54	MCL	**			*
55	MCL	**		*	
56	MCL	***			**
57	MCL	*		*	*
58	MCL	**		*	*
59	MCL	**			*
60	MZL	*			*

Table 3.2 Expression level analysis of S100A4, S100A6, ZEB1 and ZEB2 in tested B-cell lymphoma sections.

*** Strong expression > 70% of B-lymphocytes positive

** Moderate expression 70-30% of B-lymphocytes positive

* Weak expression < 30% of B-lymphocytes positive

Empty cells indicating negative expression

3.2.1.3 Characterization of cells that expressed S100A4 in B-cell malignancies by immunofluorescence.

3.2.1.3.1 Characterisation of S100A4 expression by immunofluorescence in tonsil.

The aim of this experiment was to characterize S100A4 expression in T-lymphocytes and/or B-lymphocytes in normal lymphoid tissue. Tonsil sections were used to set up the protocols and for analysis (Figure 3.13).

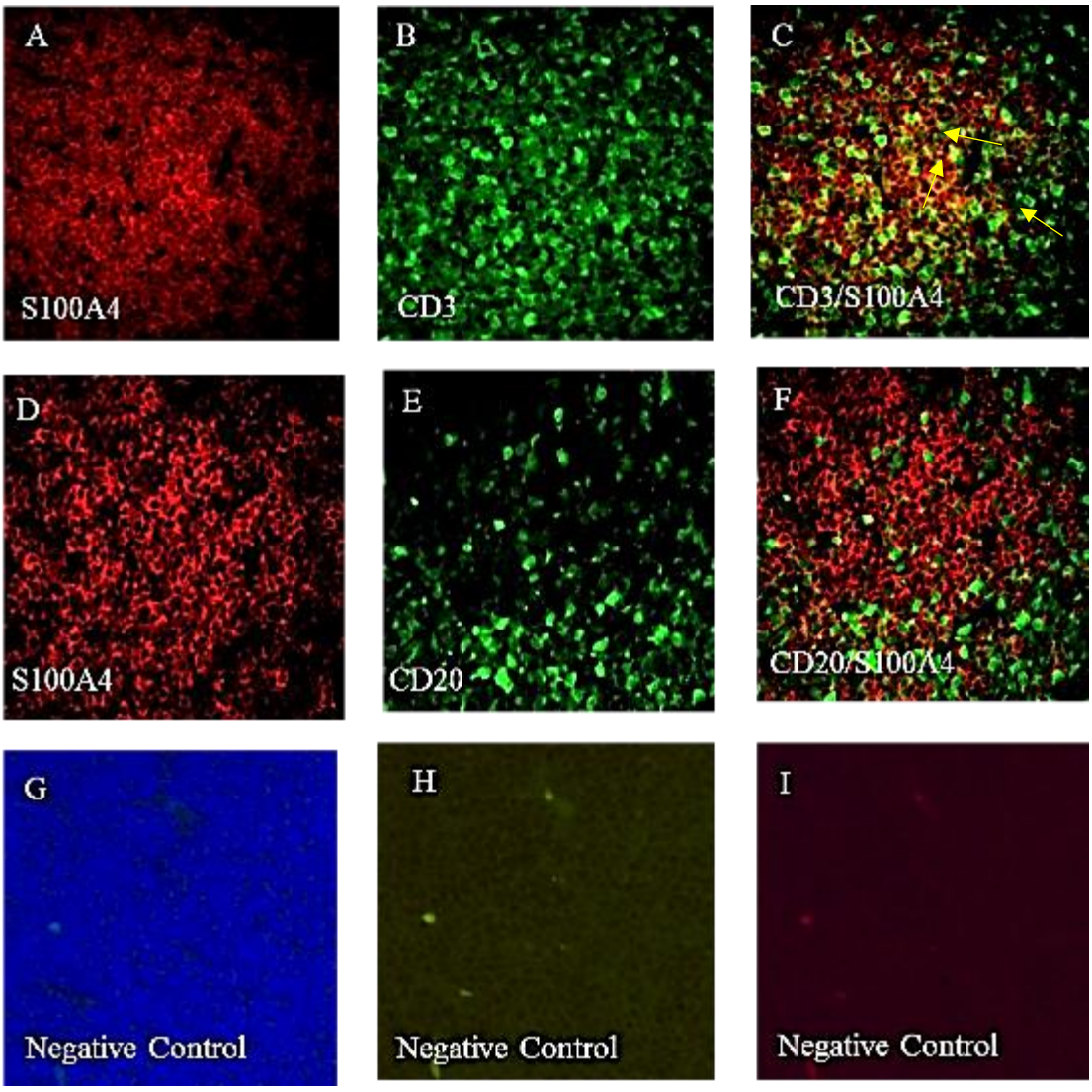

Figure 3.13 Double immunofluorescence staining of tonsil sections against S100A4, T and B-lymphocytes CD markers.

S100A4 expression in T/B-cells was analysed using anti-S100A4 rabbit polyclonal antibody in combination with mouse T or B-lymphocytes anti-CD markers as described

in Materials and Methods. As the secondary antibodies, anti-rabbit Alexa flour 568 antibody® (red colour, Invitrogen, dilution 1:1000) and anti-mouse Alexa flour 488 antibody® (green colour, Invitrogen, dilution 1:1000) were used. DAPI staining was used for nuclei identification. (A, B and C) refer to anti-S100A4 staining, T-cell specific anti-CD3 staining, and their merged image. (D, E and F) refer to anti-S100A4 staining, B-cell specific anti-CD20 staining, and their merged image. (G, H and I) refer to negative control images stained with DAPI, Alexa anti-mouse 488 flour® and Alexa anti-rabbit 568 flour® respectively. The arrows point to the stained cells showing co-expression of S100A4 and specific CD markers. Merged images were prepared using ImageJ software. Images were captured using Epi-fluorescence attachment of Nikon E800 microscope (Nikon, Japan) equipped with ProgRes camera and ProgRes ImageJ driver software (JENOPTIC-Optical system, Germany) using x20 objective.

Double immunofluorescence results explained IHC data showing expression of S100A4 in areas with the presence of T-cells. Results showed that S100A4 expression mainly in T-lymphocytes in germinal zone while there was no expression in B-lymphocytes. Four colour immunofluorescence is a more powerful technique that allows to characterise expression of 4 different proteins in a single cell of the tissue section. Thus, tonsil tissue was stained by four colour immunofluorescence using T-lymphocyte marker (Anti-CD3, mouse monoclonal, Dako 1:1000), B-lymphocyte marker (anti-CD20, mouse monoclonal, Dako 1:1000), anti-S100A4 (rabbit polyclonal, Proteintech, 1:1000) and DAPI that were visualized using OPAL HRP polymer following incubation with a specific detector OPAL 520 (green, 1:100), OPAL 570 (yellow, 1:100) and OPAL 690 (red, 1:100), respectively. Figure 3.14A showed the distribution of all cells in section using DAPI stain to differentiate the cells from artefact in the background. S100A4 expression was appeared in non-germinal zone mainly (Figure 3.14B) while CD3 and scattered CD20 positive cells were located in both germinal and non-germinal zone (Figures 3.14C and 3.14D, respectively). After merging all colours (Figure 3.15A), the section was screened to analyse the expression of S100A4 in T and B-lymphocytes of pathological normal tonsil tissue. The analysed selected section shown in figure 3.15B that was taken from area contained germinal and non-germinal zone. Figure 3.15C showed DAPI stain to confirm the specificity. The result showed that there was co-expression between S100A4 and CD3 positive cells (Figure 3.15D) while there was no expression between S100A4 and CD20 positive cells (Figure 3.15E). Thus, S100A4 expressed T-lymphocytes but not B-lymphocytes in pathological normal tissue of tonsil.

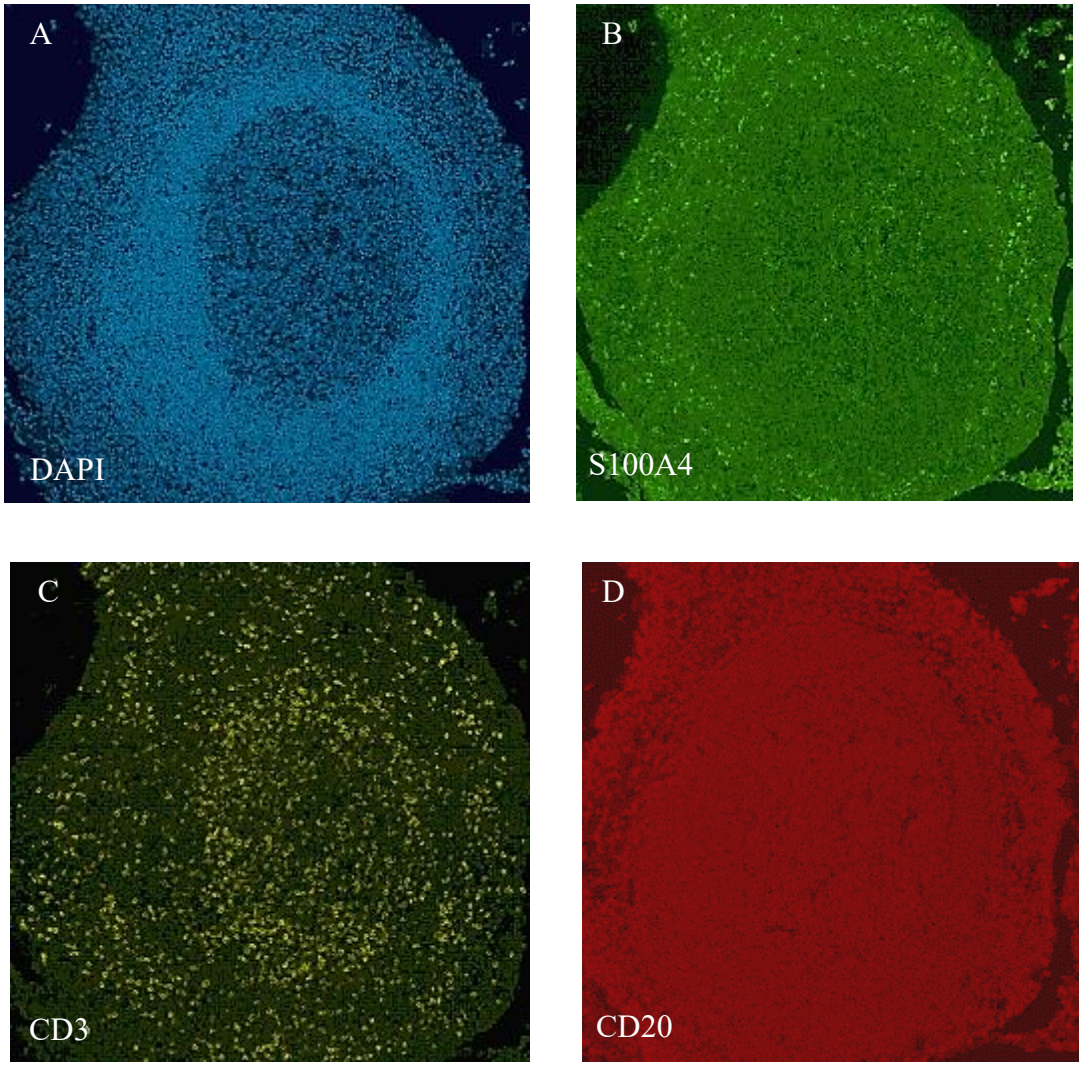

Figure 3.14 Four colour Opal multiplexed immunofluorescence of normal tonsil section.

Normal tonsil section was permeabilized and immunostained according to the Opal multiplexed protocol developed by PerkinElmer (Materials and Methods). (A) DAPI for nuclear detection, (B) for anti-S100A4 detection (rabbit polyclonal, Proteintech, 1:1000), (C) for T-lymphocyte marker (anti-CD3, mouse monoclonal, Dako 1:1000), (D) B-lymphocyte marker (anti-CD20, mouse monoclonal, Dako 1:1000) were visualized using OPAL reagents (A- blue for DAPI, B - green, OPAL 520, C - yellow, OPAL 570, D - red, OPAL 690). Images were captured using a Hamamatsu Slide Scanner microscopy. Images presented with magnification x10.

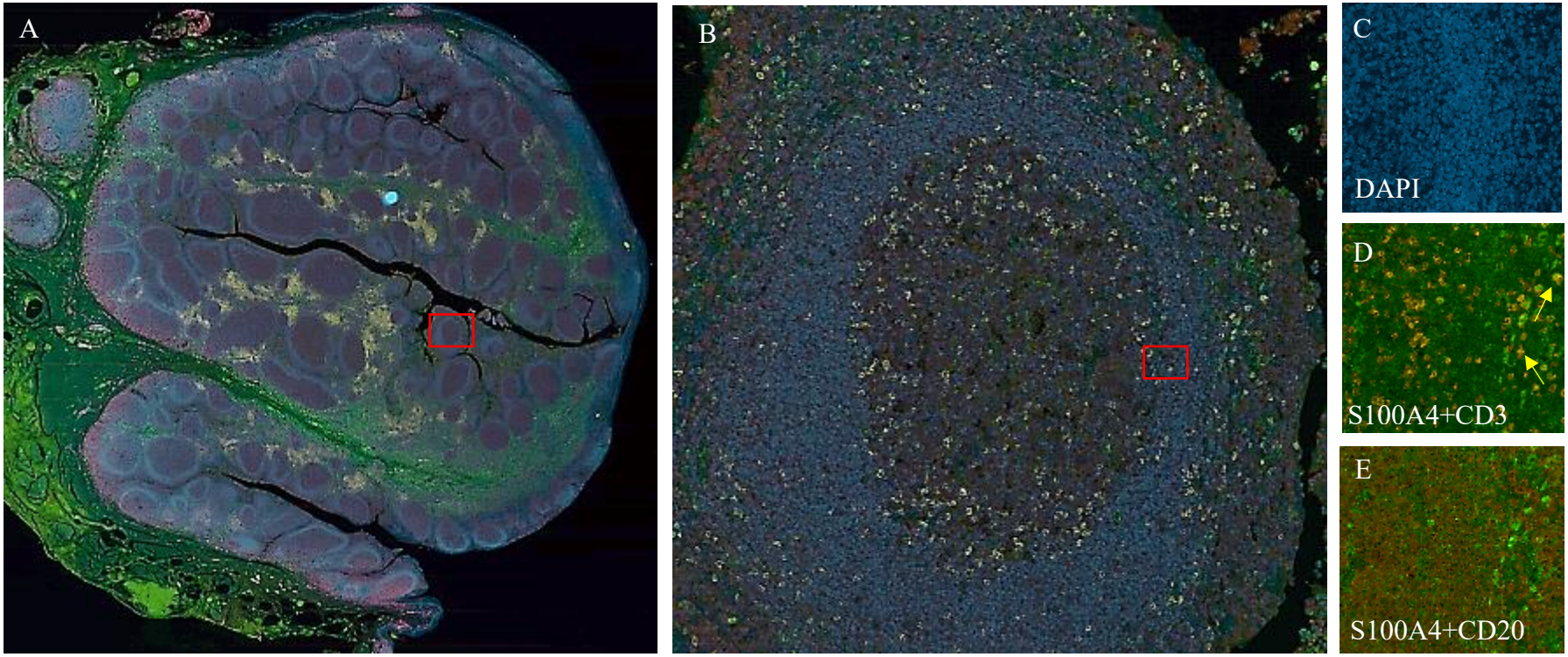

Figure 3.15 Merged images of S100A4 expression in T-lymphocytes in pathological normal tonsil tissue section by four-colour immunofluorescence.

Selected images of four-colour immunofluorescence of pathological normal tonsil section show the detection of S100A4 expression using anti-S100A4 antibody (rabbit polyclonal, Proteintech, 1:1000) in combination with antibody to T-lymphocyte marker (anti-CD3, mouse monoclonal, Dako 1:1000), B-lymphocyte marker (anti-CD20, mouse monoclonal, Dako 1:1000) which were visualized using OPAL reagents (OPAL 520 green, 1:100; OPAL 570, yellow, 1:100; OPAL 690, red, 1:100). Arrows point to cells expressing S100A4 in T-cells. Images were captured using a Hamamatsu Slide Scanner microscopy. Merge images were performed using NDP.view 2 software. Images presented with magnifications (A) x1, (B) x10 and (C, D and E) x40.

3.2.1.3.2 Expression of S100A4 in T & B-lymphocytes in B-cell lymphomas

Since four-colour immunofluorescence analysis confirmed the result of the standard double immunofluorescence staining, it was decided to use double immunofluorescence staining in analysis of B-cell lymphoma samples, including: CLL, DLBCL, MCL and MZL, using anti-S100A4 antibody in combination with antibodies to B-lymphocyte marker CD20 and T-lymphocyte markers CD3 or CD5, a marker of the B1-cells (Figure 3.16) to detect the expression of S100A4 in specific cell type.

Double immunofluorescence analysis of the CLL samples showed multiple CD20 positive cells and most of them were co-expressed S100A4 (Figure 3.16A). Simultaneously, a considerable number of cells were moderately expressed CD5, and significant number of them were S100A4 positive (Figure 3.16B). Notable fraction of CD3 positive T-lymphocytes that expressed S100A4, were also detected in the tumour sample (Figure 3.16C).

Additionally, staining of DLBCL tissue detected S100A4 positive cells, and most of them were CD20 and CD3 positive (Figures 3.16D & 3.16F, respectively), while only occasional cells co-expressed CD5 (Figure 3.16E).

Double immunofluorescence analysis also revealed that there was significant abundance of S100A4-positive cells in MCL section. However, immunofluorescence staining with CD3 and CD5 showed that most of the above-mentioned cells were T-lymphocytes (Figures 3.16H & 3.16I, respectively), whereas some cells showed co-expression of S100A4 with CD20 positive cells (Figure 3.16G).

Similarly, double immunofluorescence staining of MZL tissue showed that some S100A4 positive cells were CD20 positive (Figure 3.16J), however, significant fractions were CD3 positive (Figure 3.16L), but occasional co-expression with CD5 was also identified (Figure 3.16K).

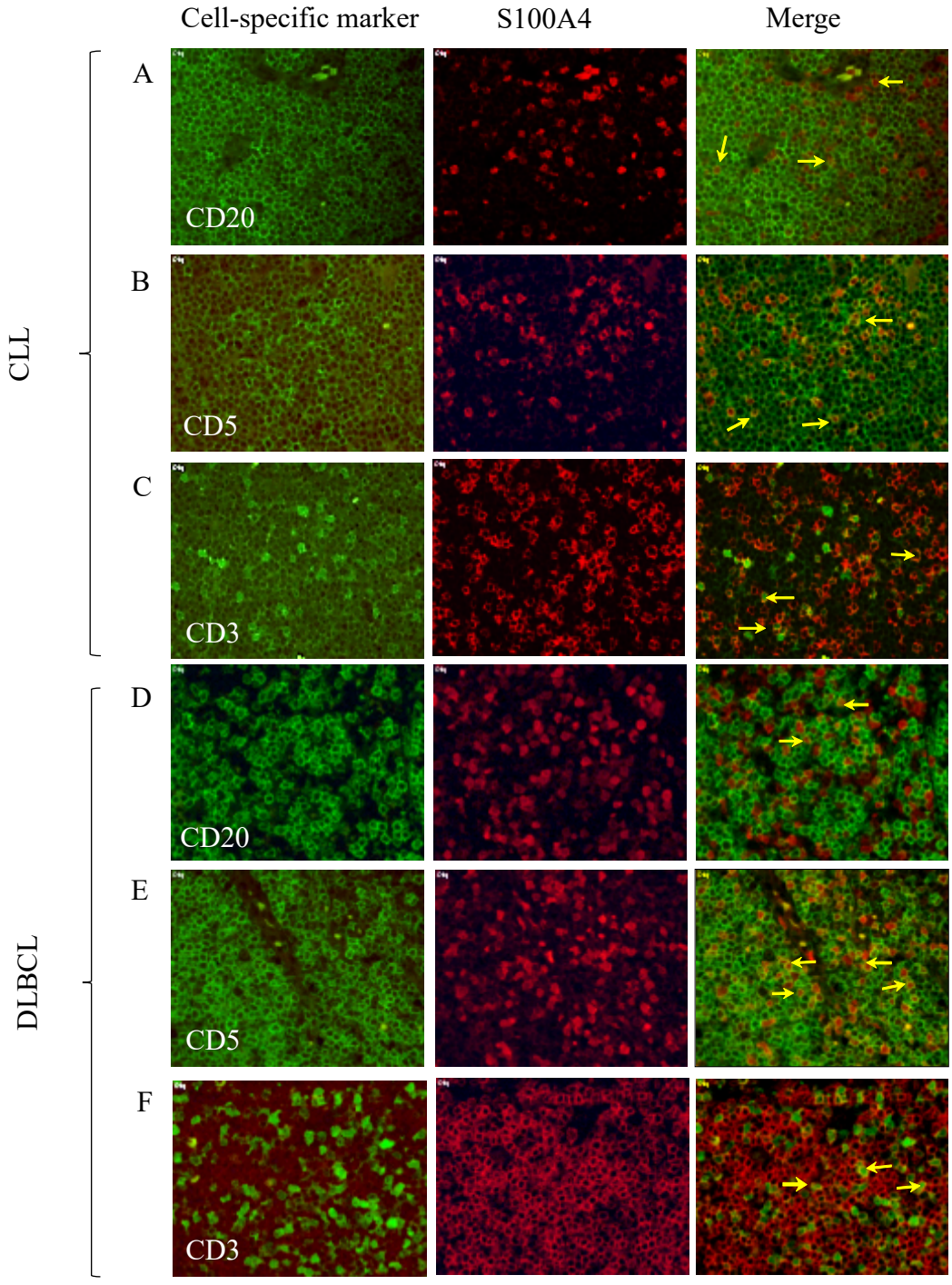
Cell-specific marker
S100A4
Merge
CLL
DLBCL
A
B
C
D
E
F
CD20
CD5
CD3
CD20
CD5
CD3

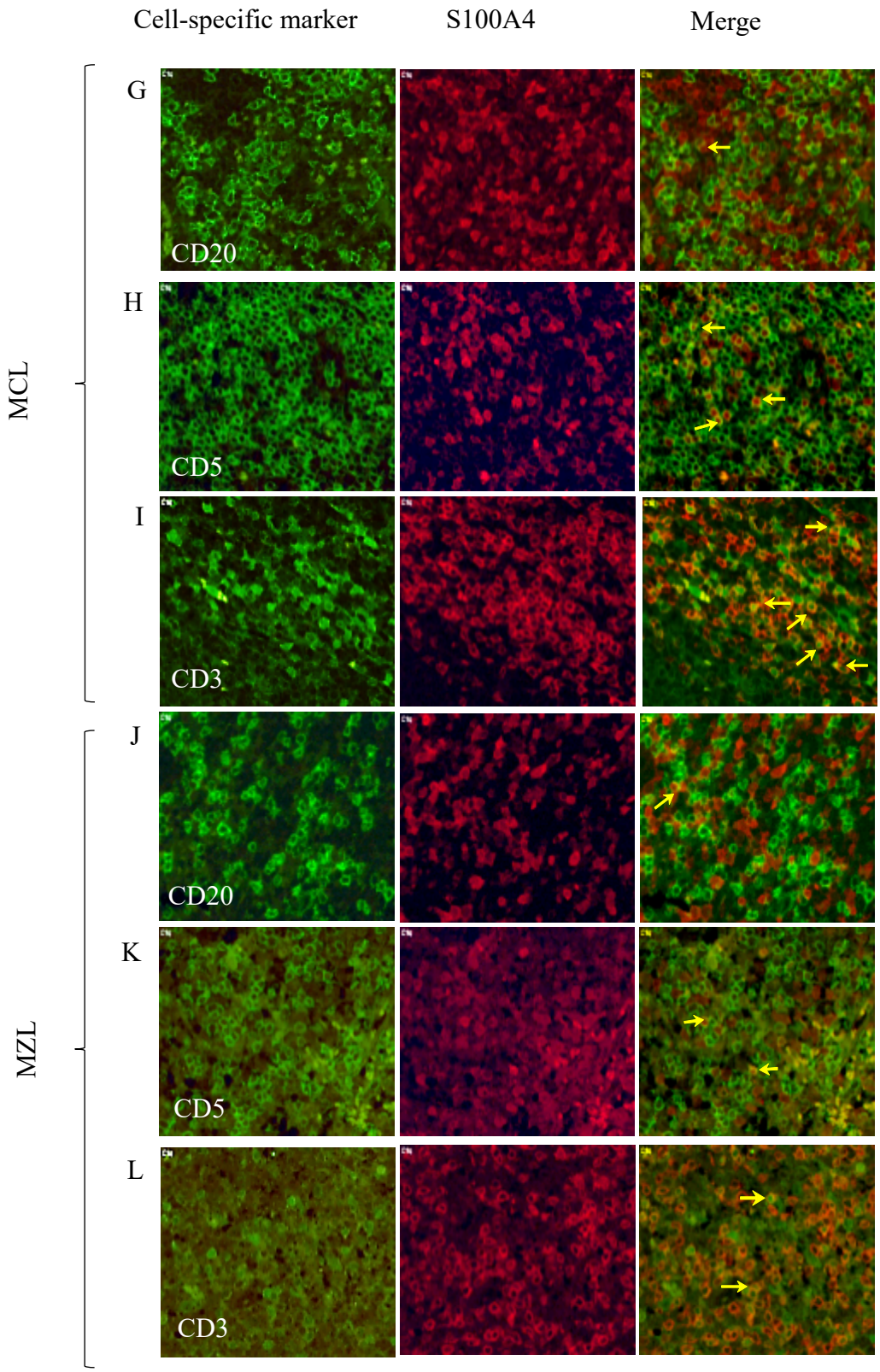
Cell-specific marker
S100A4
Merge
MCL
MZL
G
H
I
J
K
L
CD20
CD5
CD3
CD20
CD5
CD3

M 

Figure 3.16 Double immunofluorescence staining of B-cell lymphomas with anti-S100A4 antibody in combination with specific cell markers CD20, CD5 and CD3.

Double immunofluorescence detection of S100A4 using rabbit polyclonal antibody (Proteintech, 1:100) in combination with B-cell specific anti-CD20 (mouse monoclonal, Dako 1:1000), B1-cell specific anti-CD5 (mouse monoclonal, Abcam, 1:1000) and T-cell specific anti-CD3 (mouse monoclonal, Dako 1:1000) antibodies was performed as described in Materials and Methods using Alexa anti-rabbit 568 flour® (red colour, Invitrogen, dilution 1:100) and Alexa anti-mouse 488 flour® (green colour, Invitrogen, dilution 1:100) secondary antibodies. DAPI stain showed blue colour of nuclei for cell identification. (A, B and C) images present an example of CLL sample while (D, E, and F) refer to the case of DLBCL. (G, H and I) images present an example of MCL sample. (J, K, and L) refer to the case of MZL. Finally, (M) refers to negative controls. The arrows point to cells expressing S100A4 in the corresponding T/B-cell type. Merge images were prepared using ImageJ software. Images were captured by using the Epi-fluorescence attachment of Nikon E800 microscope (Nikon, Japan) which is equipped with ProgRes camera and ProgRes ImageJ software (JENOPTIC-Optical system, Germany) using 40x objective. In tested lymphoma cases, there was co-expression between S100A4 and CD20.

3.2.2 Expression of S100A4 in bone marrow mature and immature cells

3.2.2.1 Expression of S100A4 in pathological normal and CLL bone marrow samples by IHC

Pathological normal and CLL bone marrow tissue samples were used to study the expression of S100A4 protein. Paraffin-embedded sections of bone marrow samples were stained using rabbit polyclonal antibody against S100A4 as described in Materials and Methods (Figure 3.17). The staining of slides was evaluated by pathologist Professor Kevin West. Analysis of the samples showed cytoplasmic and partially nuclear localisation of S100A4 in a variety of cells in pathological normal BM cases (3.17A & 3.17B). However, in BM tissue of the CLL patients an increased number of S100A4 positive cells was observed. Of note, the expression level of S100A4 was higher in comparison with normal BM (Figure 3.17C & 3.17D).

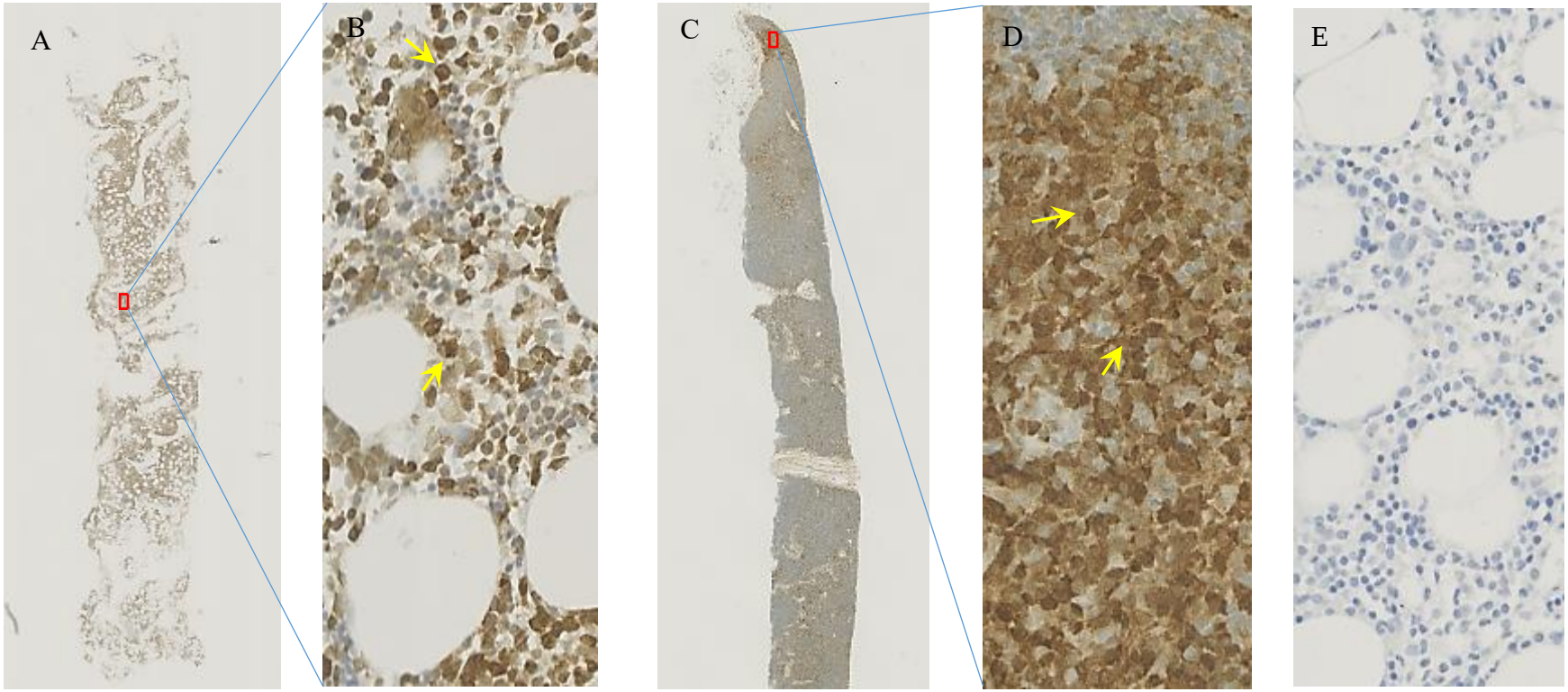

Figure 3.17 Distribution of S100A4 protein in control and CLL BM samples.
Immunohistochemical analysis of S100A4 expression in the selected control and CLL BM cases was done using anti-S100A4 antibody, (Proteintech, dilution 1:1000) as described in Materials and Methods. (A&B) represent an example of a normal bone marrow sample. (C&D) represent an example of bone marrow sample of the CLL patient. The arrows point to the cells that were positive for S100A4. (E) Refers to the negative control of a paraffin-embedded BM. Images were captured by using a Hamamatsu Slide Scanner microscopy. Images present with magnifications (A and C) x1 and (B, D and E) x20.

3.2.2.2 Characterization of cells expressing S100A4 by double and 4-colour immunofluorescence in pathological normal bone marrow tissue

In order to characterise S100A4 positive cells and to identify expression of S100A4 at different stages of lymphocytes development, double immunofluorescence and a 4-colour immunofluorescence approaches were applied. Bone marrow tissues from pathological normal and CLL patient samples were used.

For characterisation of the S100A4 positive cells, a double immunofluorescence approach was applied first. Mouse antibodies to the CD specific markers expressed by HSCs and progenitor cells in combination with rabbit anti-S100A4 antibody were used. Analysis of the stained samples identified a few number of cells positive on S100A4 and CD10, CD34 or CD45, HSCs markers (Figures 3.18A, 3.18B and 3.18C). In addition, a high level of S100A4 expression was observed in cells expressing CD31, an endothelial cell marker (Figure 3.18D). Also, there was occasional co-expression between S100A4 protein and CD45RA, a naive T cell marker (Figure 3.18E). A moderate expression of S100A4 in cells positive on CD68, a macrophage specific marker, was detected (Figure 3.18F). Negative control, where sections were proceeded in the absence of primary antibodies, was included in each experiment (Figure 3.18G).

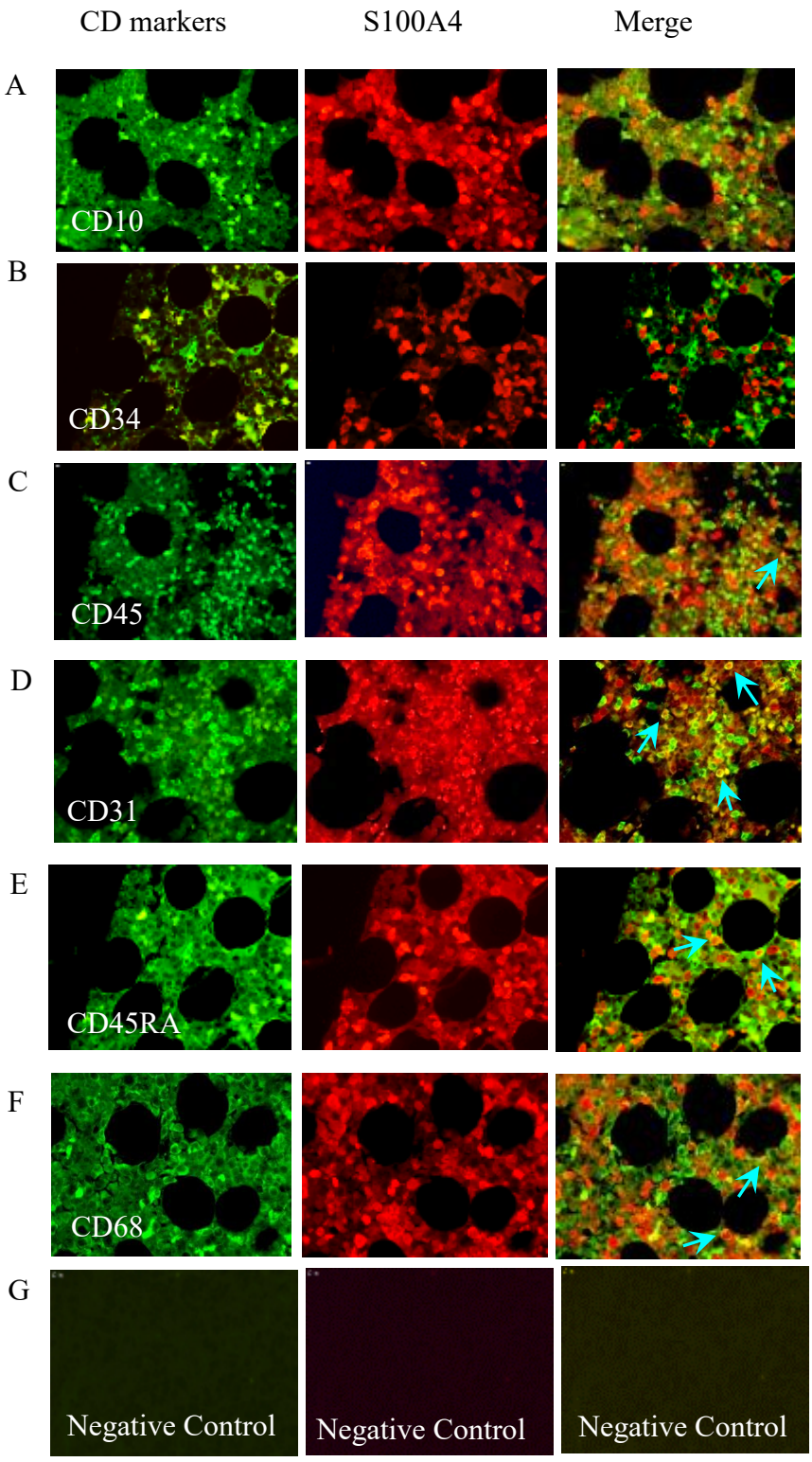

Figure 3.18 Double immunofluorescence staining of pathological normal bone marrow tissue with anti-S100A4 rabbit polyclonal antibody in combination with different haematopoietic and other cells CD markers.

Detection of S100A4 by rabbit polyclonal antibody in combination with mouse antibodies against CD markers was performed as described in Materials and Methods. A mixture of the secondary antibodies (anti-rabbit Alexa 568 flour®, red colour,

Invitrogen, dilution 1:100 and anti-mouse Alexa 488 flour® green colour, Invitrogen, dilution 1:100) were used. DAPI, blue stain, was used for nuclei detection. Tested CD markers included (A, B and C) HSC specific CD10, CD34 and CD45 markers; (D) CD31, endothelial cell marker; (E) CD45RA, naive T-cell marker; (F) CD68, macrophage specific marker. (G) Refers to negative control. Merged images were performed using ImageJ software. The arrows point to double-stained positive cells. Images were captured by using Epi-fluorescence attachment of a Nikon E800 microscope (Nikon, Japan) equipped with ProgRes camera and ProgRes ImageJ software (JENOPTIC-Optical system, Germany). Images were collected with a 20x objective.

In order to characterise the expression of S100A4 in T and B-lymphocytes, a 4-colour immunofluorescence was performed. Four colour immunofluorescence is a technique that was developed for detection of co-expression of three different antigens including DAPI stain in the same cell.

Thus, BM tissue was stained by four colour immunofluorescence using T-lymphocyte marker (Anti-CD3, mouse monoclonal, Dako 1:1000), B-lymphocyte marker (anti-CD20, mouse monoclonal, Dako 1:1000), anti-S100A4 (rabbit polyclonal, Proteintech, 1:1000) and DAPI that were visualized using OPAL HRP polymer following incubation with a specific detector OPAL 520 (green, 1:100), OPAL 570 (yellow, 1:100) and OPAL 690 (red, 1:100) (Figure 4.3).

Figure 3.19 shows staining of T, B and S100A4 positive cells with markers, including: S100A4 (Figure 3.19B), T-lymphocyte marker (Figure 3.19C) and B-lymphocyte (Figure 3.19D). DAPI stain was used to confirm the specificity (Figure 3.19A).

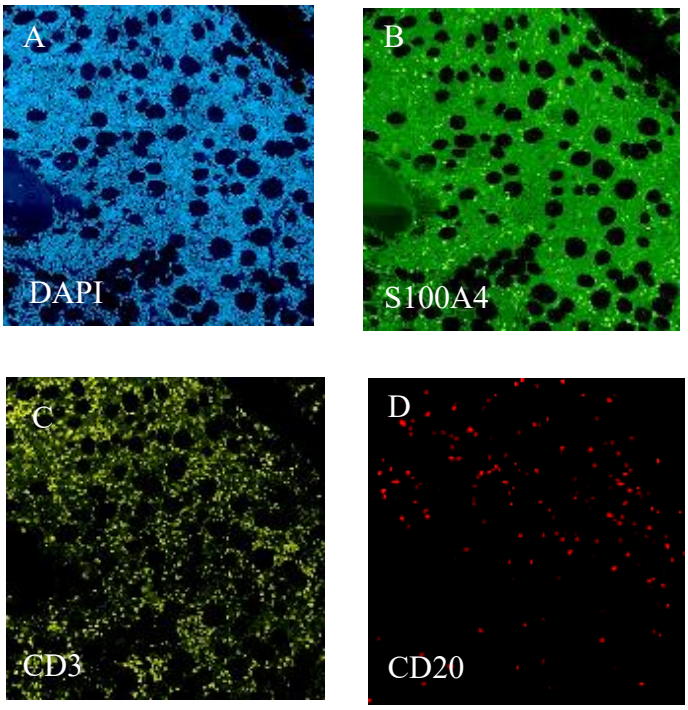

Figure 3.19 Four colour Opal multiplexed immunofluorescence of normal BM section.

Normal BM section was permeabilized and immunostained according to the Opal multiplexed protocol developed by PerkinElmer (Materials and Methods). (A) DAPI for nuclear detection, (B) for anti-S100A4 detection (rabbit polyclonal, Proteintech, 1:1000), (C) for T-lymphocyte marker (anti-CD3, mouse monoclonal, Dako 1:1000), (D) B-lymphocyte marker (anti-CD20, mouse monoclonal, Dako 1:1000) were visualized using OPAL reagents (A- blue for DAPI, B - green, OPAL 520, C - yellow, OPAL 570, D - red, OPAL 690). Images were captured by using a Hamamatsu Slide Scanner microscopy. Images presented with magnification x10.

After merging the colours (Figure 3.20A), the section was secreened to analyse the expression of S100A4 in T and B-lymphocytes of pathological normal BM tissue. A merged image is shown on figure 3.20B. Figure 3.20C showed DAPI stain to confirm cells. The result showed that there was a co-expression between S100A4 and CD3 positive cells (Figure 3.20D) while there was no expression between S100A4 and CD20 positive cells (Figure 3.20E). Thus, S100A4 expressed in T-lymphocytes but not B-lymphocytes of the pathological normal tissue of BM.

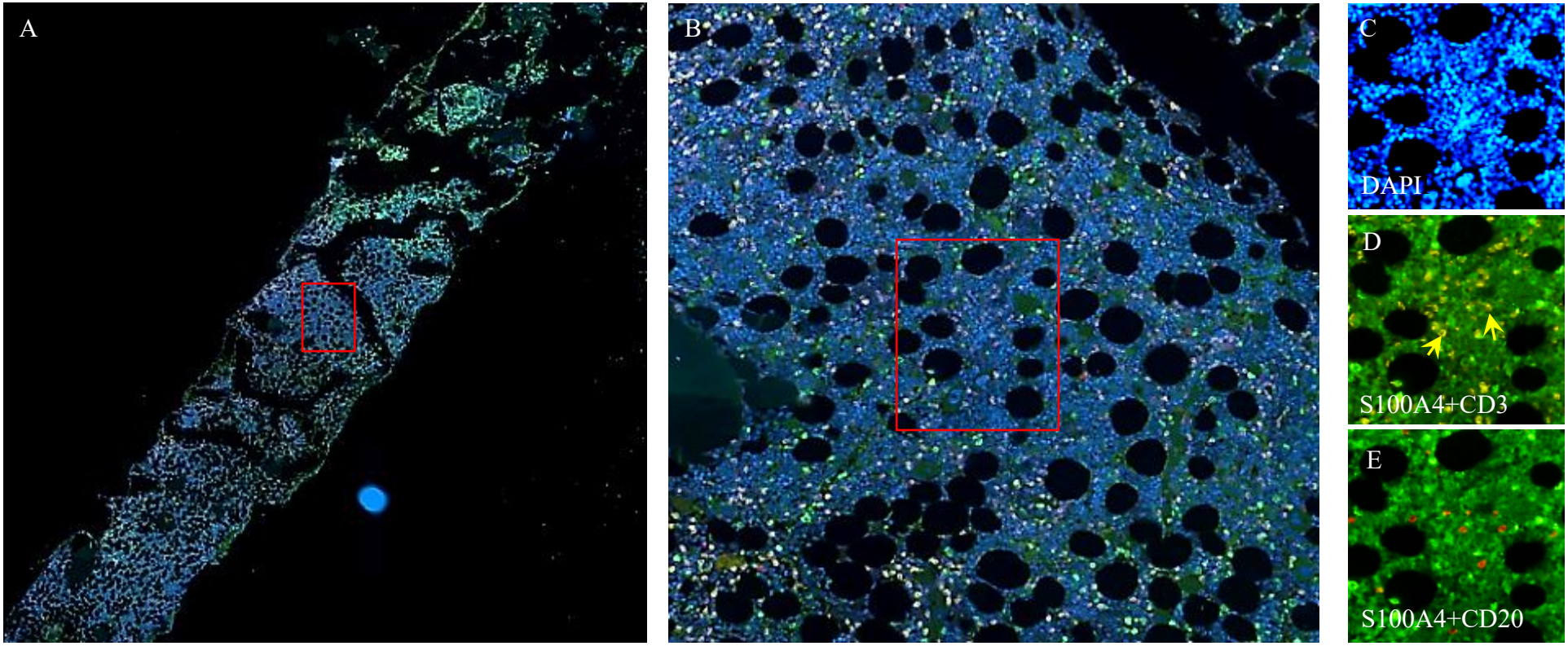

Figure 3.20 Merged images of S100A4 expression and T and B-lymphocytes in normal bone marrow sample.

Selected images of four-colour immunofluorescence of pathological normal BM section show the detection of S100A4 expression using anti-S100A4 antibody (rabbit polyclonal, Proteintech, 1:1000) in combination with antibody to T-lymphocyte marker (anti-CD3, mouse monoclonal, Dako 1:1000), B-lymphocyte marker (anti-CD20, mouse monoclonal, Dako 1:1000) which were visualized using OPAL reagents (OPAL 520 green, 1:100; OPAL 570, yellow, 1:100; OPAL 690, red, 1:100). The arrows point to cells expressing S100A4 in T-cells. Images were captured by using a Hamamatsu Slide Scanner microscopy. Images were merged using NDP.view 2 software. Images presented with magnifications (A) x1, (B) x10 and (C, D and E) x40.

3.2.2.3 Characterization of expression of S100A4 by double immunofluorescence in CLL bone marrow tissue

Following analysis of S100A4 expression in cells of the pathological normal bone marrow tissue, tissue sections of bone marrow from CLL patients from the Pathology Department in Leicester Royal Infirmary were processed by double immunofluorescence (Figure 3.21). The aim of the study was to compare the expression of S100A4 in haematopoietic stem cells and lymphocytes in pathological normal and CLL samples and to investigate suitability of S100A4 to be considered as a potential marker of BM cancer cells.

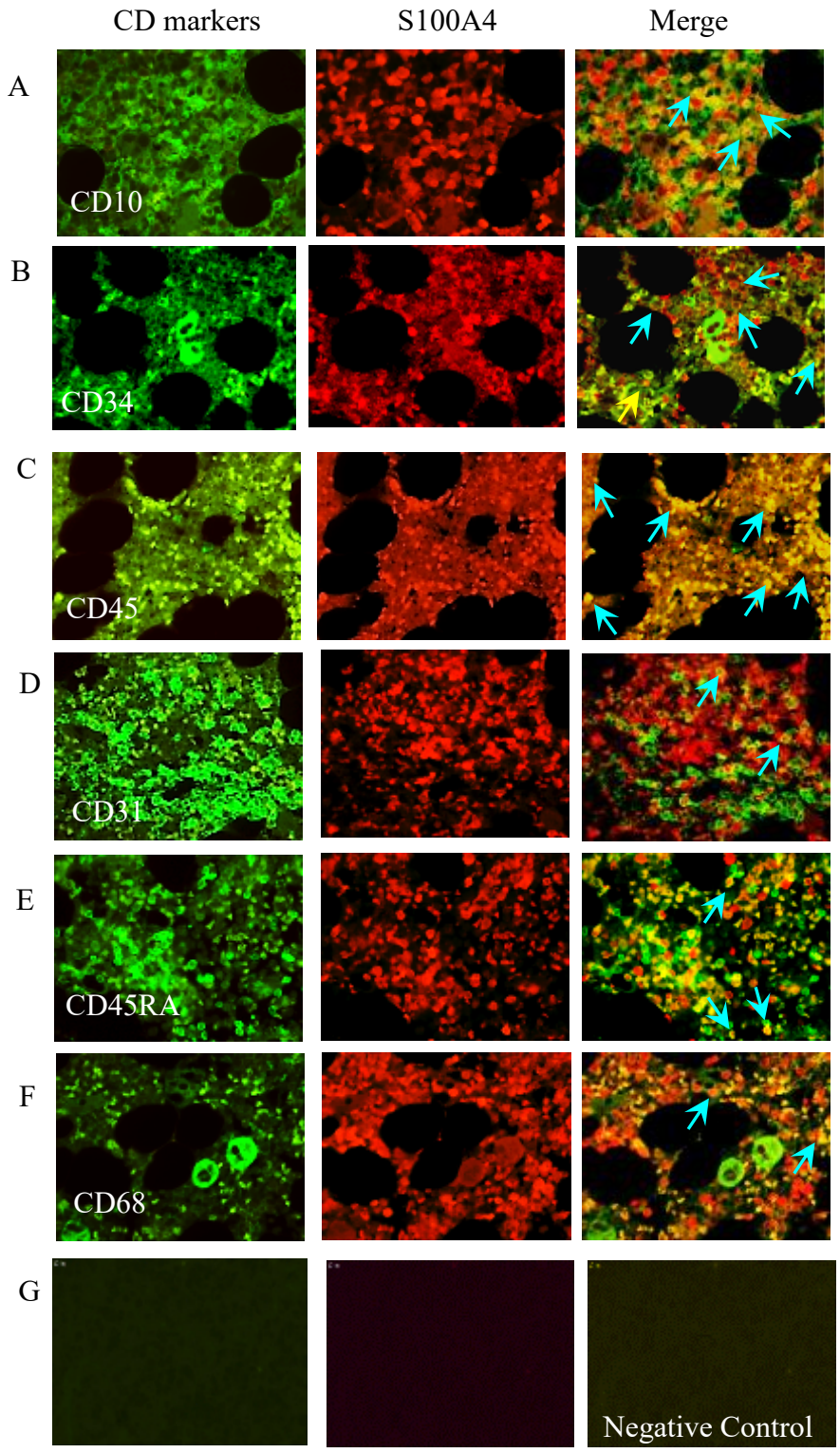

Figure 3.21 Double immunofluorescence staining of bone marrow tissue from patient with CLL for S100A4 and CD markers.

The detection of S100A4 by rabbit polyclonal antibody in combination with mouse antibodies against CD markers was performed as described in Materials and Methods. A mixture of the secondary antibodies (anti-rabbit Alexa 568 flour®, red colour, Invitrogen, dilution 1:100 and anti-mouse Alexa 488 flour® green colour, Invitrogen,

dilution 1:100) were used. DAPI, blue stain, was used for nuclear staining. Tested CD markers included (A, B and C) HSC specific CD10, CD34 and CD45 markers; (D) CD31, endothelial cell marker; (E) CD45RA, naive T-cell marker; (F) CD68, macrophage specific marker. (G) Refers to negative control. Merge images were performed using ImageJ software. The arrows pointed to double-stained positive cells. Images were captured by using an Epi-fluorescence attachment of a Nikon E800 microscope (Nikon, Japan) equipped with ProgRes camera and ProgRes ImageJ software (JENOPTIC-Optical system, Germany). Images were collected with a 20x objective.

In order to investigate expression of S100A4 in malignant B-lymphocytes, a 4-colour immunofluorescence of bone marrow tissue of CLL sample was applied as it was described in chapter 2. Briefly, a slide was sequentially stained against a T-lymphocyte marker (Anti-CD3, mouse monoclonal, Dako 1:1000), B-lymphocyte marker (Anti-CD20, mouse monoclonal, Dako 1:1000) and Anti-S100A4 (rabbit polyclonal, Proteintech, 1:1000) that were visualized using OPAL fluorophores.

Figure 3.22 shows the distribution of T and B-cells including: cells expressing S100A4 (Figure 3.22B), T-lymphocytes (Figure 3.22C) and B-lymphocytes (Figure 3.22D) and. DAPI stain was used for nuclear detection (Figure 3.22A).

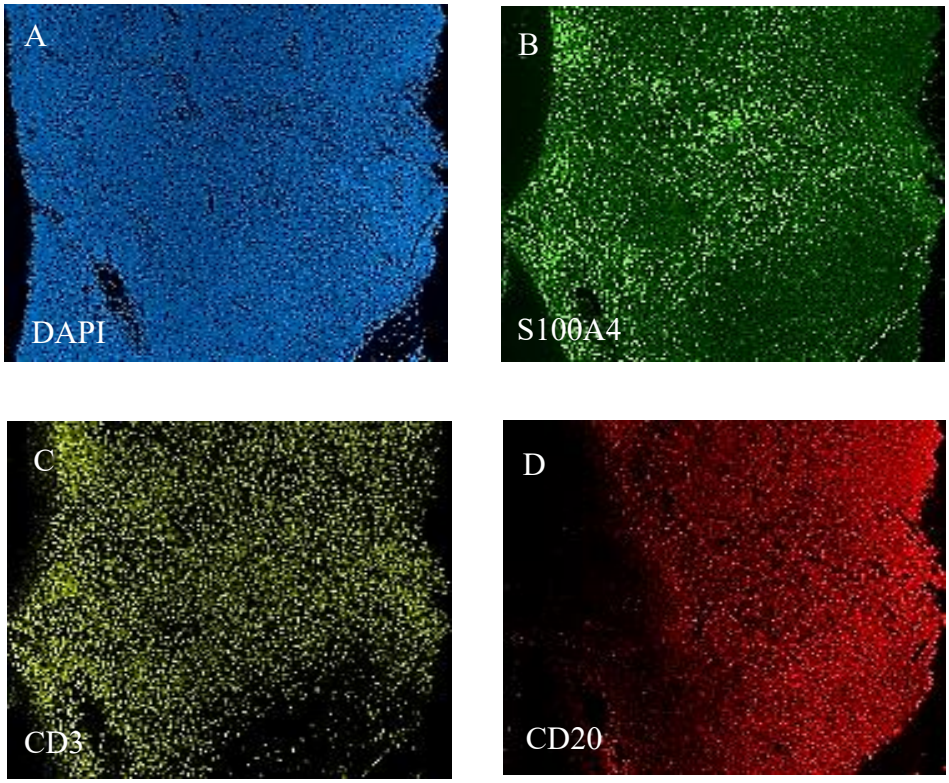

Figure 3.22 Four colour immunofluorescence Opal multiplexed of CLL BM section.

CLL BM section was permeabilized and immunostained according to the Opal multiplexed protocol developed by PerkinElmer (Materials and Methods). (A) DAPI for nuclear detection, (B) for anti-S100A4 detection (rabbit polyclonal, Proteintech, 1:1000), (C) for T-lymphocyte marker (anti-CD3, mouse monoclonal, Dako 1:1000), (D) B-lymphocyte marker (anti-CD20, mouse monoclonal, Dako 1:1000) were visualized using OPAL reagents (A- blue for DAPI, B - green, OPAL 520, C - yellow, OPAL 570, (D) - red, OPAL 690). Images were captured by using a Hamamatsu Slide Scanner microscopy. Images presented with magnification x10.

The expression of S100A4 in T and B-lymphocytes of the stained sample was analysed using NDP.view 2 driver software under different magnifications (Figure 3.23A). An analysed selected section is shown on figure 3.23B. DAPI stain was used for nuclear detection (Figure 3.23C). The result showed that there was co-expression between S100A4 and CD3 (Figure 3.23D) and CD20 positive cells (Figure 3.23E). Thus, expression of S100A4 in malignant B-lymphocytes of CLL patient was confirmed.

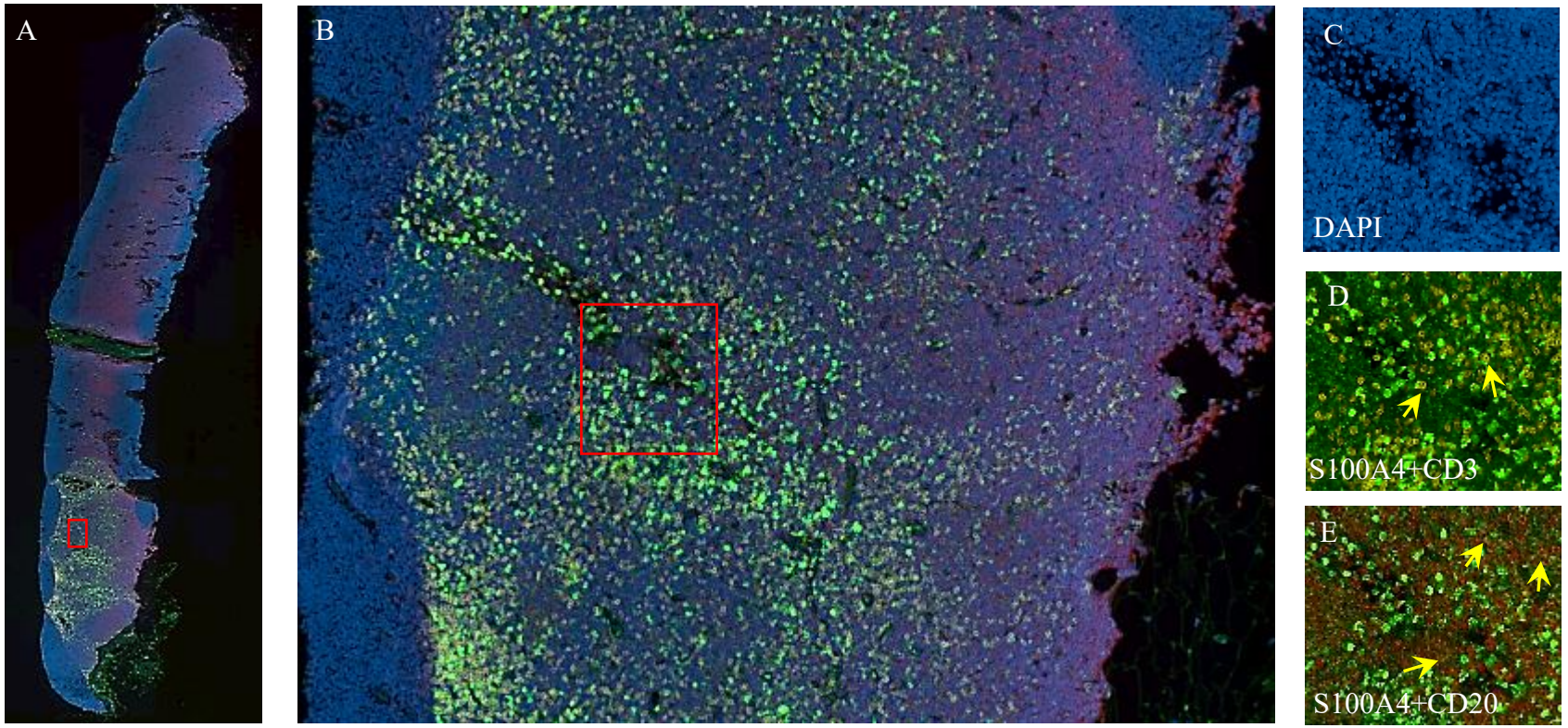

Figure 3.23 Merged images of S100A4 expression in T and B-lymphocytes in CLL BM tissue section by four-colour immunofluorescence.

Selected images of four-colour immunofluorescence of CLL section show the detection of S100A4 expression using anti-S100A4 antibody (rabbit polyclonal, Proteintech, 1:1000) in combination with antibody to T-lymphocyte marker (anti-CD3, mouse monoclonal, Dako 1:1000), B-lymphocyte marker (anti-CD20, mouse monoclonal, Dako 1:1000) which were visualized using OPAL reagents (OPAL 520 green, 1:100; OPAL 570, yellow, 1:100; OPAL 690, red, 1:100). Arrows point to cells expressing S100A4 in T and B-cells. Images were captured by using a Hamamatsu Slide Scanner microscopy. Merge image was performed using NDP.view 2 software. Images presented with magnifications (A) x1, (B) x10 and (C, D and E) x40.

3.2.3 S100A4 expression in the peripheral blood of CLL patients.

3.2.3.1 Gene expression profile of *S100A4* and ZEB family members in the peripheral blood of CLL patients.

Peripheral blood samples from healthy volunteers and CLL patients were collected and peripheral blood mononuclear cells (PBMC) suspension were prepared (see Chapter 2). Then, untouched human B cells were isolated by depletion of non-B cells (T cells, monocytes, NK-cells, macrophages, granulocytes, plasma cells, platelets and erythrocytes) from PBMCs. Thus, isolated B cells which were bead- and antibody free were suitable to analyse gene expression profile of S100 including: *S100A1, S100A2, S100A3, S100A4, S100A5, S100A6, S100A8, S100A9, S100A10, S100A11, S100A12, S100A13* and *S10014*, at the mRNA level. Additionally, mRNA expression level of the EMT-associated genes, *ZEB1* and *ZEB2*, were also analysed. The problem in this experiment was that the healthy volunteer's samples were not containing required amount of B-cells so, we combined the B-cells of 15 volunteer's samples and used them as one sample in this experiment.

RNA was normalised and summary of Nanodrop of analysed sampled appeared in table 3.3. qPCR data represented as a chart (Figure 3.24), showed that the mRNA expression level of *S100A4, S100A5, S100A6, S100A10, S100A11, S100A13 and S100A14* genes were upregulated in CLL B-cells compared to normal B-cells, and this expression was positively correlated with expression of EMT related genes, *ZEB1* and *ZEB2* according to statistic results of $-^{\Delta\Delta}$CT (for full statistical analysis see Appendix 3). Among differently expressed of S100 genes, the highest activation of expression was detected for *S100A4* and *S100A6.* Only inconsistent downregulation was shown in *S100A1, S100A2, S100A3, S100A8, S100A9* and *S100A12* genes.

Sample Name	RNA (ng/µl)	Absorption 260/280	Absorption 260/230
Control/B-cells from normal volunteers	70.05	2.095	2.22
CLL1	586.6	2.08	2.1
CLL2	1682.5	1.975	1.775
CLL3	1038	1.975	1.795
CLL4	192.85	2.13	2.23
CLL5	996.6	2.055	2.005

Table 3.3 Nanodrop summary of analysed samples.

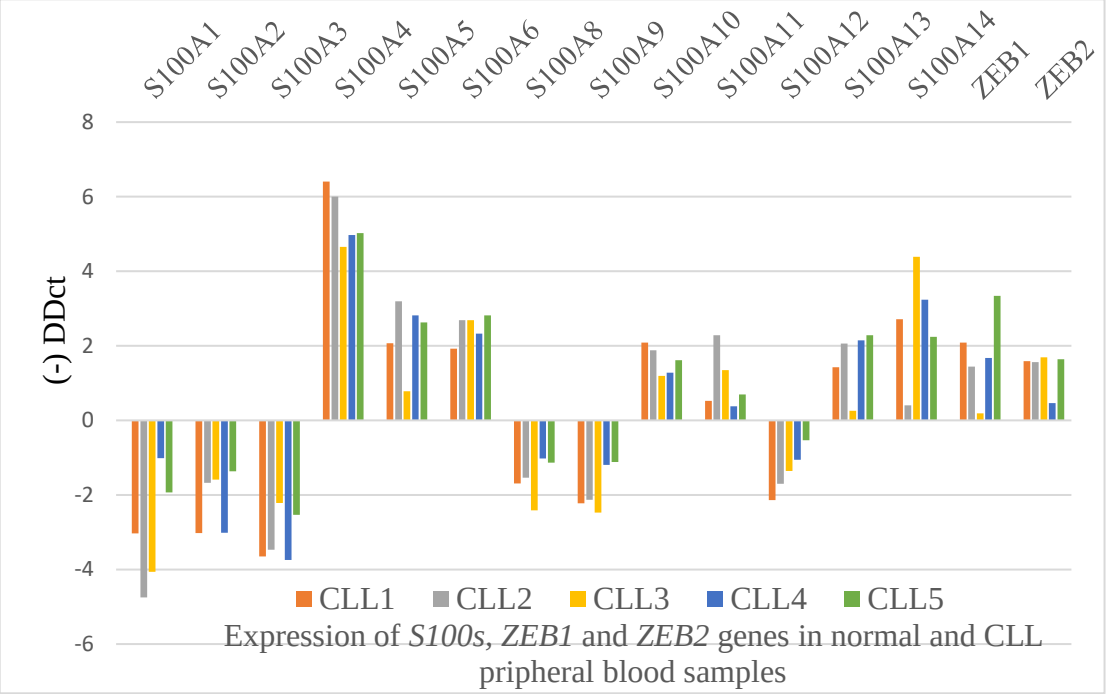

Figure 3.24 Comparative analysis of the expression of S100s, *ZEB1* and *ZEB2* genes in CLL samples relative to normal circulating B-cell control by real-time PCR.

Detection of the expression level of different members of S100 and EMT-related genes, *ZEB1* and *ZEB2*, was performed by Real-Time Quantitative PCR. qPCR, where a positive reaction is detected by the accumulation of a fluorescent signal, was quantified as $-^{\Delta\Delta}$Ct and calculated by normalizing expression level of gene of interest to a reference gene Beta-2 microglobulin (B2M). Where, Ct, cycle threshold, is the number of cycles required for the fluorescent signal to cross the threshold (exceeds background level). Ct levels are in reverse proportional to the amount of target nucleic acid in the sample (the lower Ct level the greater the amount of target nucleic acid in the sample). $^{\Delta}$CT = CT (a target gene) – CT (a reference gene (B2M)) and $^{\Delta\Delta}$CT = $^{\Delta}$CT (a target sample) – $^{\Delta}$CT (a reference sample (B2M)).

3.2.3.2 Expression of S100A4 by Western blotting

Lysates cells from 20 peripheral blood samples of CLL patients were prepared and used to study the expression of S100A4 by Western blotting. Figure 3.25 shows expression of S100A4 protein in CLL samples 1-20.

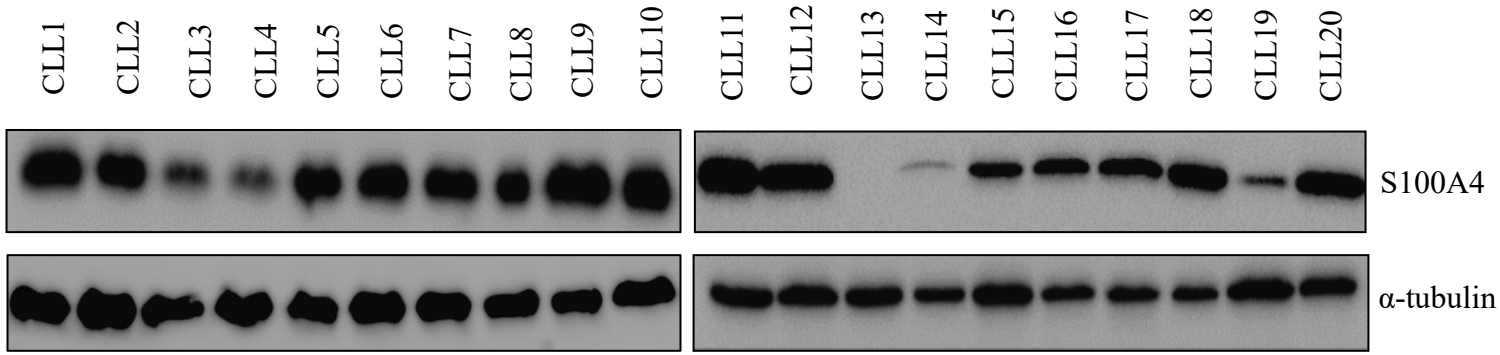

Figure 3.25 Expression of S100A4 in CLL samples.

Cells lysates were prepared and resolved into 15% SDS-polyacrylamide gel. Then proteins were transferred and the expression of S100A4 was detected using rabbit polyclonal anti-S100A4 from Proteintech (dilution 1:1000). Tubulin was used as a loading control.

The result showed that S100A4 expressed strongly in most samples apart from 4 samples which showed a weak expression, including: samples 3,4,13, and 19, compared to other samples. Sample 13 showed negative expression.

3.2.3.3 Expression of S100A4 in peripheral blood of chronic lymphocytic leukemia samples by IHC.

Cell blocks of most patient's lymphoma samples were made to analyse S100A4 expression by IHC. The results revealed that S100A4 showed a good level of expression in lymphocytes in most samples and this finding supported the Western blot result. Figure 3.26 shows immunostaining of sample two which was expressed strongly S100A4 (Figure 3.26A) and sample four which was weakly expressed S100A4 protein (Figure 3.26C). H&E stain was used to detect the quality of cell block (Figure 3.26B and 3.26D).

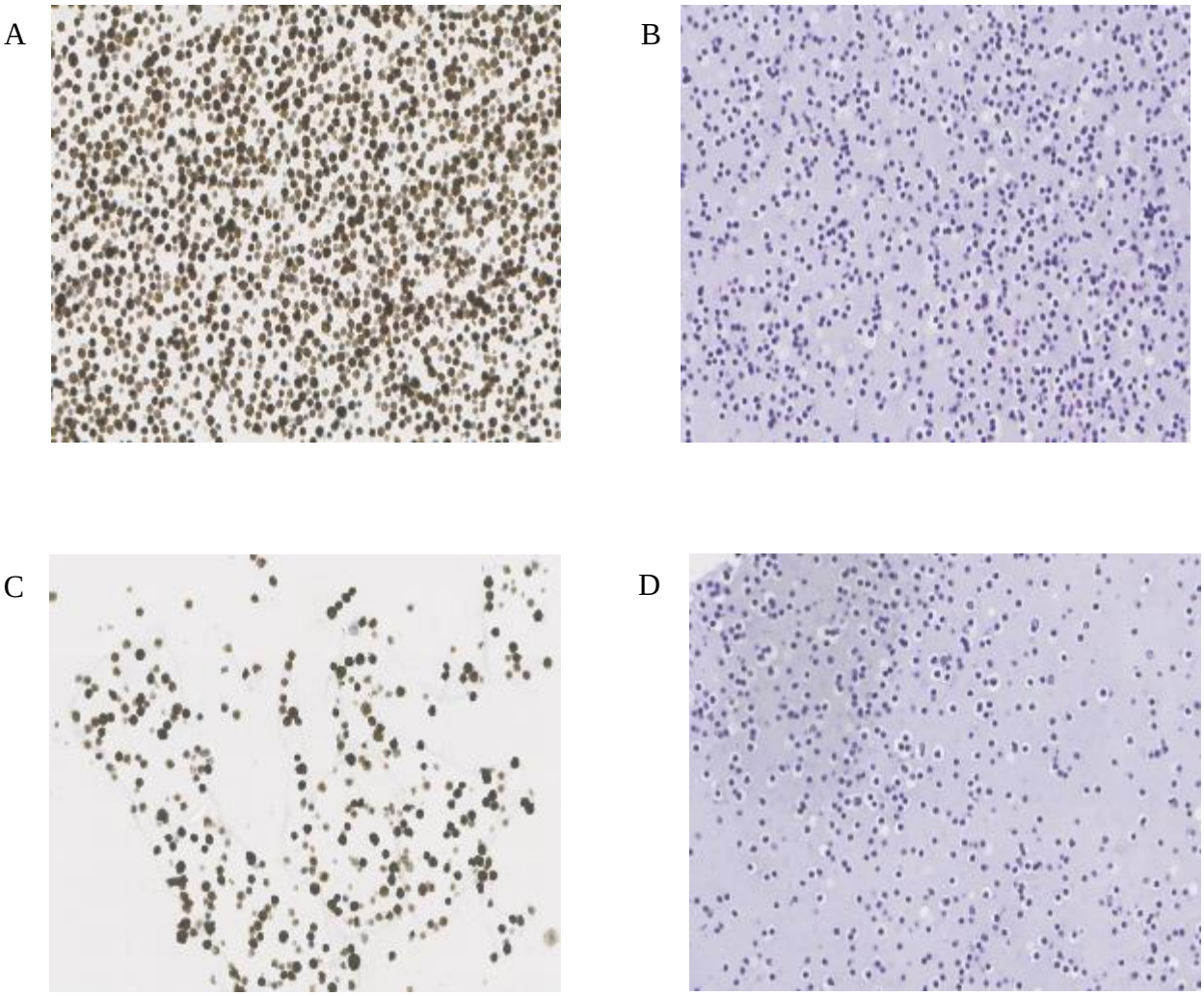

Figure 3.26 Expression of S100A4 in CLL peripheral blood samples, CLL2 and CLL4, by IHC.

Immunochemical analysis of S100A4expression in CLL samples, CLL2 (A) and CLL4 (C), was done using Anti-S100A4 (Proteintech, dilution 1:1000) antibody as described in Materials and Methods. H&E satin was used for CLL2 (B) and CLL4 (D). Images were taken using a Hamamatsu Slide Scanner microscopy. Images presented with magnifications x10 (H&E) and x20 (IHC).

3.2.3.4 Expression of S100A4 and CD markers in peripheral blood Samples of CLL by four colour immunofluorescence.

For further details to confirm S100A4 expression in B-cell, four colour immunofluorescence, which is an approach used to detect different antigens in the same cells, was used. The aim of this step was to study the characterization of the S100A4 positive cells. Thus, CLL2 and CLL4 cell blocks tissues were stained by four colour immunofluorescence using T-lymphocyte marker (Anti-CD3, mouse monoclonal, Dako 1:1000), B-lymphocyte marker (anti-CD20, mouse monoclonal, Dako 1:1000), anti-S100A4 (rabbit polyclonal, Proteintech, 1:1000) and DAPI that were visualized using OPAL HRP polymer following incubation with a specific detector OPAL 520 (green, 1:100), OPAL 570 (yellow, 1:100) and OPAL 690 (red, 1:100), respectively. Figure 3.27A showed the distribution of all cells in section using DAPI stain to differential the cells from artefact in the background. Figure 3.27B shows the selected section with all merged colours. DAPI stain to specify cells, expression of S100A4 in T-lymphocytes and in B-lymphocytes were shown in Figures 3.27C, 3.27D and 3.27E, respectively). Same procedures of staining and imaging were done for CLL4 to detect the difference of expression of S100A4 in T and B-lymphocytes (Figure 3.28).

The results of characterization of the S100A4 positive cells using NDP.view 2 driver software under different magnifications showed that most B-lymphocytes in sample CLL2 expressed while in sample CLL4 very few number of B-lymphocytes expressed S100A4.

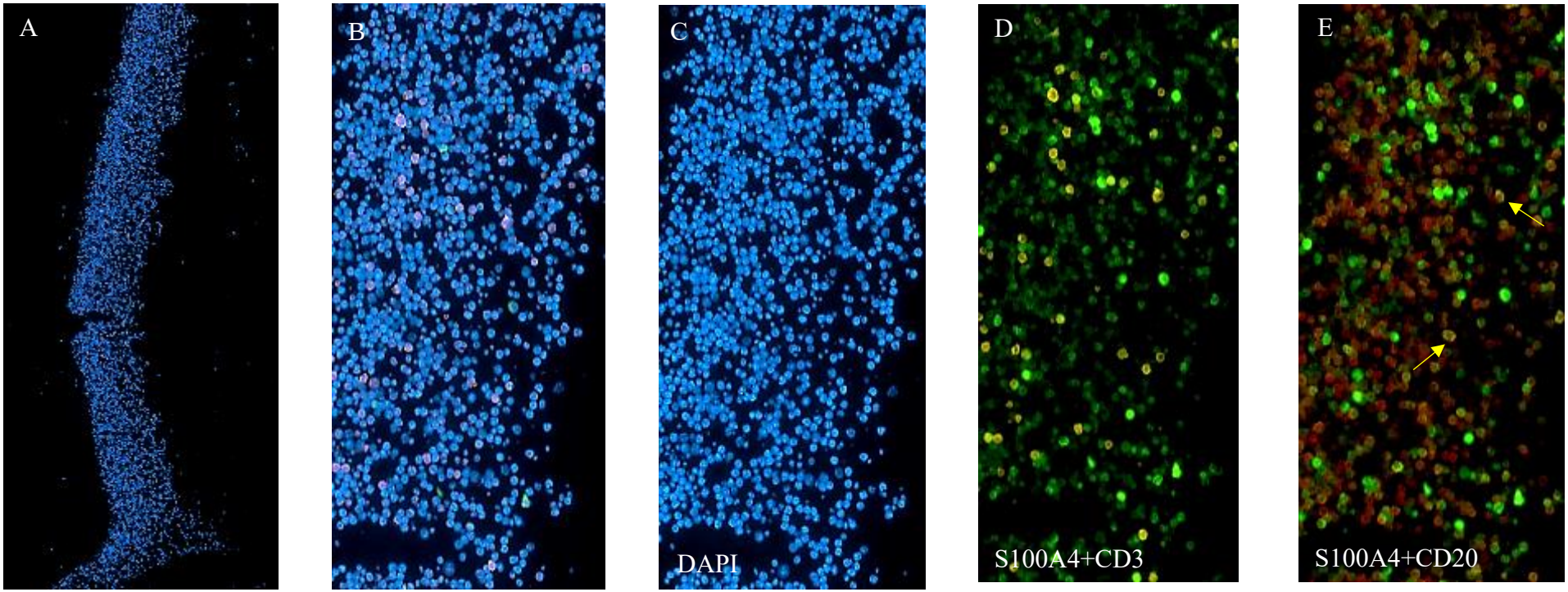

Figure 3.27 Merged images of S100A4 expression in T and B-lymphocytes in CLL2 cell block section by four-colour immunofluorescence.

Selected images of four-colours immunostaining of CLL2 sample section show the detection of S100A4 expression using anti-S100A4 antibody (rabbit polyclonal, Proteintech, 1:1000) in combination with antibody to T-lymphocyte marker (anti-CD3, mouse monoclonal, Dako 1:1000), B-lymphocyte marker (anti-CD20, mouse monoclonal, Dako 1:1000) which were visualized using OPAL reagents (OPAL 520 green, 1:100; OPAL 570, yellow, 1:100; OPAL 690, red, 1:100). The arrows point to cells expressing S100A4 in B-cells. Images were captured using a Hamamatsu Slide Scanner microscopy. Merged images were performed using NDP.view 2 software. Images presented with magnifications (A) x10 and (B, C, D and E) x20.

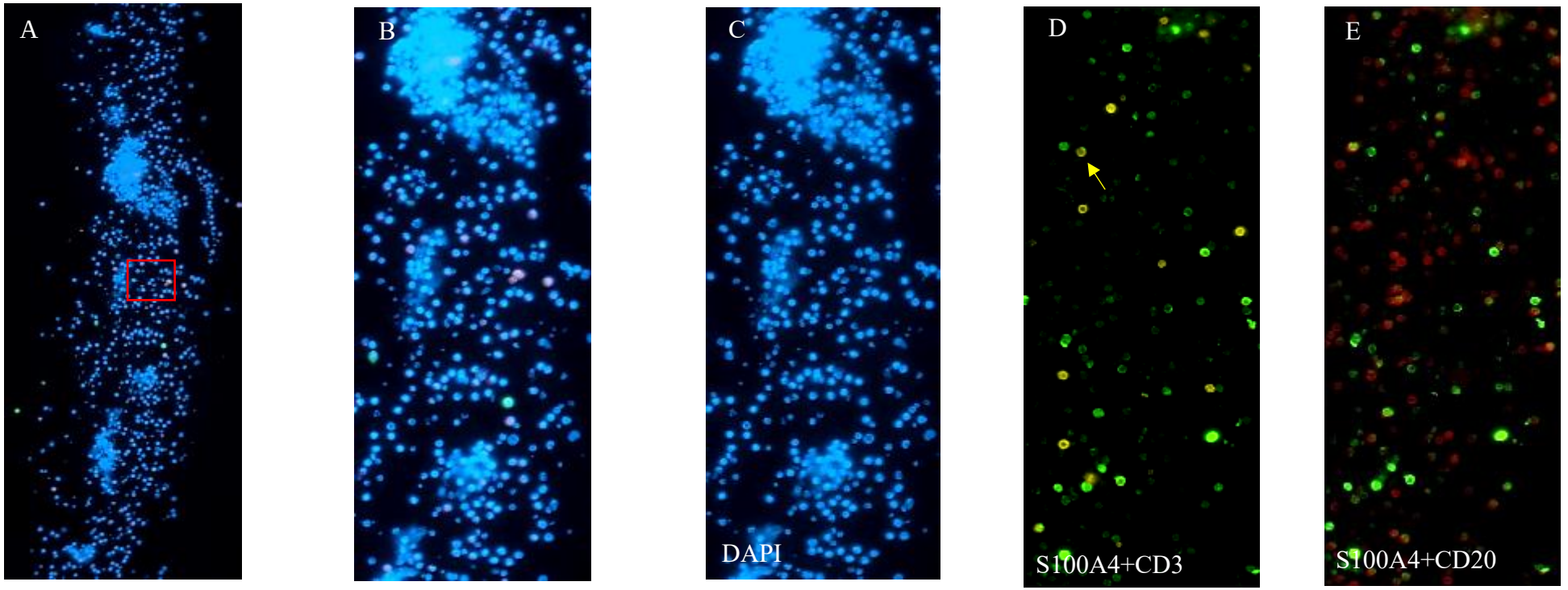

Figure 3.28 Merged images of S100A4 expression in T and B-lymphocytes in CLL4 cell block section by four-colour immunofluorescence.

Selected images of four-colour immunofluorescence of CLL4 sample section show the detection of S100A4 expression using anti-S100A4 antibody (rabbit polyclonal, Proteintech, 1:1000) in combination with antibody to T-lymphocyte marker (anti-CD3, mouse monoclonal, Dako 1:1000), B-lymphocyte marker (anti-CD20, mouse monoclonal, Dako 1:1000) which were visualized using OPAL reagents (OPAL 520 green, 1:100; OPAL 570, yellow, 1:100; OPAL 690, red, 1:100). The arrows point to cells expressing S100A4 in T-cells. Images were captured using a Hamamatsu Slide Scanner microscopy. Merged images were performed using NDP.view 2 software. Images presented with magnifications (A) x10 and (B, C, D and E) x20.

3.2.3.5 Statistical analysis of the survival of CLL patients with high and low S100A4 expression

A study of the correlation between S100A4 expression and the survival of patients with CLL by using 20 peripheral blood samples was undertaken. Samples were provided from The Ernest and Helen Scott Haematological Research Institute, Leicester Cancer Research Centre, University of Leicester. Patient's data was provided from same centre to compare survival of patient with high S100A4 expression and survival of those with low or negative expression (Table 3.4). Statistical analysis was carried out using the Statistical Package for the Social Sciences (SPSS Inc., Chicago, IL, USA), where P=0.0215 (<0.05) was considered to indicate statistical significance (Figure 3.29). This analysis was carried out in order to investigate if S100A4 expression has an effect on the survival of CLL patients.

CLL Patient #	sex	age diagnosis	date diagnosis	stage diagnosis	treatment	TTFT (days)	deceased	Vh	Fish	survival rate
1	M	59	01/04/1996	B	y	720	69	4-39 U	11q 13q	10
2	M	68	19/09/2001	B	y	222	75	1-69 U	11q 13q	7
3	M	63	25/11/2003	A0	y	2082	n(76)	7-81 M	tri12	13
4	M	76	12/12/1996	A0	y	4774	90	2-70 M	13q	14
5	M	78	17/04/2007	A	y	338	81	3-64 U	tri12	3
6	M	58	13/05/2008	A0	n		n(67)	3-07 M	13q 17q	9
7	M	69	22/04/2008	A0	y	1766	77	3-30 U	normal	8
8	M	83	14/10/2003	C	y	28	89	1-69 U	13q	6
9	F	62	12/04/2005	A0	0		68	3-23 M	normal	6
10	M	52	11/07/2006	B	y	27	n(62)	1-69 U	13q	10
11	F	78	22/02/2006	C	y	6	83	3-21 M	11q 13q	5
12	F	66	08/11/2004	A0	n		76	3-09 M	13q	10
13	F	66	05/11/1987	A	y	416	89	3-53 M	tri12	23
14	M	76	29/03/2005	A	n		n(88)	4-34 M	normal	12
15	M	64	25/11/2003	A	y	1202	72	2-05 U	13q	8
16	M	77	20/10/2011	B	y	509	79	3-21 M	t12, 13q	2
17	M	79	26/03/2014	B	y	116	n(82)	4 -39 U	17p, t12	3
18	M	61	29/04/2008	A	y	2612	n(70)	3-33 U	tri12	9
19	M	65	14/09/2004	A0	y	4182	n(77)	4-39 M	13q	12
20	F	77	06/01/2009	A	n		n85)	3-23 M	13q	8

Table 3.4 CLL patient's data.

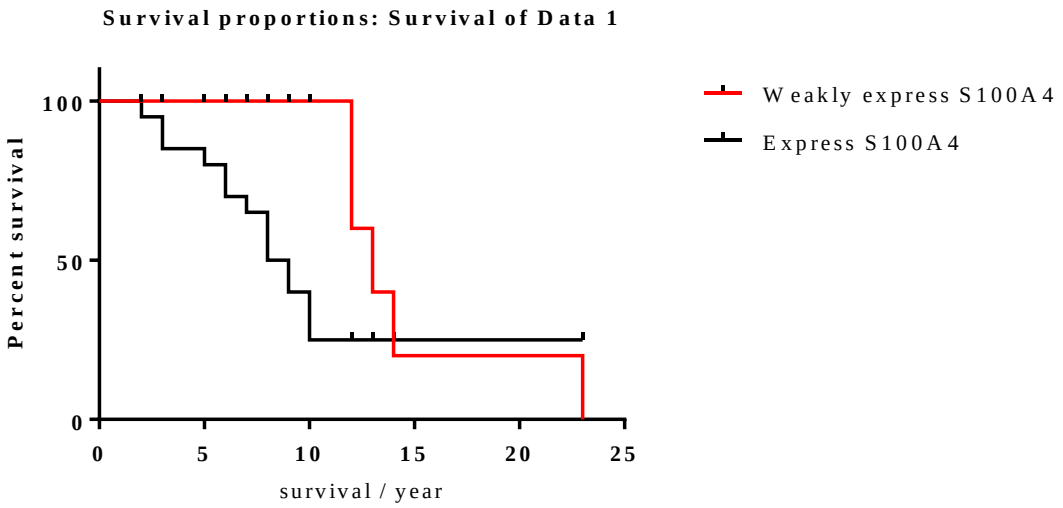

Figure 3.29 Survival analysis generated a Kaplan-Meier survival plot.

3.3 Discussion

Researchers found that some of the S100 proteins are expressed in different types of malignant cells (Donato, 2003; Marenholz et al., 2004) but the expression and function of these proteins in B-cell lymphomas is still unclear. Also, many studies have thoroughly investigated the S100 expression in cancer and most of these studies showed that the expression of S100 proteins played an important role in the metastasis formation and poor prognosis for many types of cancer (Ford et al., 1995; Jenkinson et al., 2004; Takenaga et al., 1994a). However, the correlation between these proteins expression and EMT factors such as ZEB1 and ZEB2 in B-cell lymphomas has not been confirmed.

Based on the bioinformatics study (G. Kaithakottil, MSc thesis, University of Leicester, 2010) and preliminary experimental data analysing expression of S100A4 in different lymphomas (Dr Karen Pulfard, Oxford University), it was indicated that S100A4 and S100A6 can be expressed in different type of blood cells, such as T-lymphocytes, macrophages or neutrophils, while not expressed in B-lymphocytes. On the other hand, in lymphomas, these proteins are probably expressed in B-lymphocytes.

3.3.1 Expression of S100A4 but not S100A6 in B-cell lymphomas

Immunohistochemistry, double immunofluorescence, and 4-colour immunofluorescence approaches were used to characterise the expression of S100A4 and S100A6 using single, double or quaternary immunofluorescence staining. The results showed that S100A4 was not expressed in normal B-lymphocytes of the tonsil, spleen or thymus, while it was expressed in T-lymphocytes, macrophages, and in a fraction of fibroblasts (Figures 3.2A, 3.3A, 3.4A, and 3.15).

Our results of S100A4 expression in normal tissue support early studies that showed that S100A4 expressed in different cells, such as fibroblasts, macrophages, T-lymphocytes, and neutrophils and was important for tumor stroma formation (Grigorian et al., 1994; Grigorian et al., 1993; Takenaga et al., 1994b).

Regarding the analysis of S100A4 expression in different lymphomas performed in this study, data was in accord with the earlier IHC analysis of the small number of B-lymphoma cases, when it was suggested that S100A4 protein is expressed in different types of B-cell lymphomas (Table 3.1). IHC analysis of 60 B-cell lymphoma samples with the antibody against S100A4 identified a differential pattern of expression (Figure 3.6). 75% of lymphoma cases showed positivity of S100A4 expression. With 62% of samples showed a strong to moderate expression. Among these cases were 16 CLL, 16 DLBCL and 5 MCL. Interestingly, all tested CLL samples showed good level of S100A4 expression. But 13% of lymphoma cases showed week level of S100A4 protein expression, including: 6 cases of DLBCL, one case of MCL and one case of MZL. Our results indicated that 25% of the analysed lymphoma cases were S100A4 negative, among them 4 cases of DLBCL and 11 of FL. We found that all of FL cases negatively expressed S100A4 (Figure 3.6). Thus, we excluded FL cases from further investigation. S100A4 is expressed in B-cell malignancies especially in CLL.

The next step was focused on the analysis of the co-expression between S100A4 protein and different CD markers, including: CD3, CD5 and CD20, in lymphoma cases, including: CLL, MZL, MCL and DLBCL. Double immunofluorescence analysis of the CLL samples showed that multiple CD20 positive cells co-expressed S100A4 (Figure 3.16A). Simultaneously, among high number of cells that moderately expressed CD5, a high proportion of them were S100A4 positive (Figure 3.16B). A notable fraction of CD3 positive T-lymphocytes were present in the tumour, also expressed S100A4 (Figure 3.16C). In DLBCL tissue, it was detected that there were many S100A4 positive cells, and most of them were CD20 but also CD3 positive as T-cells (Figures 3.16D & 3.16F, respectively), they also showed partial CD5 positivity (Figure 3.16E). It was revealed that there was a significant amount of S100A4 positive cells in MCL samples. However, immunofluorescence staining against CD3 and CD5 showed that most of them were T-cells (Figures 3.16H & 3.16I, respectively), whereas some co-expression of S100A4 in CD20 positive cells was detected (Figure 3.16G). Staining of MZL tissue showed that only a small amount of S100A4 positive cells were CD20 positive (Figure 3.16J), but majority of S100A4 positive cells were CD3 positive T-cells (Figure 3.16L). And occasional co-expression with CD5 was also identified (Figure 3.16K).

From the data obtained after analysis of the different lymphoma cases, it was confirmed that S100A4 was expressed in malignant B-cells. Since all CLL samples showed positivity of S100A4 expression in the majority of the CD20 positive cells, a further focus of this study was on analysis of the role of S100A4 protein in CLL development.

There is no publication analysing the expression of S100A4 in B-cell lymphomas, but a similar investigation was done on breast cancer which studied expression of S100A4 in stroma of breast cancer tumours and in the peripheral blood by double immunofluorescence. It was found that a major fraction of S100A4 positive cells in stroma were fibroblasts. Other blood cells such as macrophages (CD68 positive), mast cells (mast-cell tryptase positive) or neutrophils (neutrophil elastase positive) were also identified as S100A4 positive. Only a fraction of T-lymphocytes (CD3 positive) present in stroma expressed S100A4, while B-lymphocytes (CD20 positive) were negative. However, in normal breast sections, double immunofluorescence analysis showed that all of the above mentioned cells were also present, but S100A4 was expressed at a reduced level. The expression of S100A4 in a variety of immune cells circulating in the peripheral blood was also detected by double immunofluorescence. Around 90% of monocytes and granulocytes expressed S100A4, while only less than half of T-lymphocytes were S100A4 positive. Likewise, more than 60% of the NK cells expressed S100A4, while less than 10% of the B-lymphocytes were S100A4 positive (Cabezon et al., 2007). Thus, from this finding, we concluded that S100A4 expression in B-cell lymphomas was the opposite of the findings on breast cancer.

Regarding the expression of S100A6 protein in normal sections of tonsil, spleen and thymus detected by immunostaining (Figures 3.2B, 3.3B and 3.4B, respectively), a very strong expression in T-lymphocytes but not in B-lymphocytes was detected. In the analysed lymphoma samples the results revealed a lack of S100A6 expression in neoplastic B-lymphocytes in all of 60 samples. However, other cells such as T-lymphocytes, dendritic cells, and endothelial cells showed strong expression of S100A6 protein (Figure 3.7). On this point, we focused on the expression of S100A4 and not S100A6 protein as a potential prognostic marker of B-cell lymphomas.

It was suggested that S100A6 expressed in gastric adenocarcinomas and overexpression of S100A6 could be associated with poorly differentiated adenocarcinomas, lymph node metastasis and increase in tumour invasively (Zhang et al., 2014). Komatsu et al. (2000) found that there is a stronger expression in liver metastasis then in the primary tumours in colorectal cancer (Komatsu et al., 2000). This result indicates that an increased S100A6 level in tumour cells could be coupled with poor survival. The reason could be associated with the molecular and biologic factors that control the balance between cell proliferation and apoptosis in the development and progression of gastric cancers controlled by S100A6 expression.

In some studies, S100A6 protein has been involved in the regulation of cell growth and proliferation because its mRNA is preferentially expressed in the G1 phase of the cell cycle (Calabretta et al., 1985). The effect of S100A6 on the cell cycle control is probably mediated via interaction with various ligands such as calcyclin-binding protein (CacyBP/SIP), cyclin-dependent kinase 5 (CDK5), glyceraldehyde-3-phosphate dehydrogenase, and a 30 kDa protein present in Ehrlich ascites tumour cells (Li et al., 2013; Ning et al., 2012; Nowotny et al., 2003; Zeng et al., 1993). Thus, S100A6 protein was expressed and controlled metastasis in some cancers but not B-lymphomas.

3.3.2 ZEB1 and ZEB2 expression in B-cell lymphomas

In the current study, it was shown that a high to medium expression of ZEB1, a transcription factor better known for promoting metastasis in carcinomas, present in multiple cells of the germinal centre as well as in cells of the non-germinal centre but absent in squamous epithelial cells of the normal tonsil sections (Figure 3.1C). In spleen tissue, ZEB1 showed a low expression in scattered cells such as endothelial cells and fibroblasts (Figure 3.2C) but less in thymus tissue (Figure 3.3C).

Interestingly, a moderate to low expression of ZEB1 was found in a few B-cell lymphoma samples. Moreover, the majority of samples showed negative expression of ZEB1 (Figure 3.8). Cells that expressed ZEB1 was mainly T-lymphocytes, macrophages and endothelial cells but in 5 % of the analysed lymphomas a moderate ZEB1 expression was detected in B-cells. However, all of them were DLBCL cases. On

the other hand, 13% of the cases showed a weak expression, including: one case of CLL, 4 DLBCL and 3 MCL cases (Figure 3.9).

There is a study that shows different results to ours (Sánchez-Tilló et al., 2014). It shows that ZEB1 was expressed strongly in MCL. Probably, the discrepancy may due to the insufficient amount of the MCL samples in our study (6 samples). Authors found that that ZEB1 promoted cell proliferation, enhanced tumour growth and had an influence on the resistance to chemotherapy in MCL. Also, ZEB1 could be a predictive biomarker and a therapeutic target in this type of lymphoma. They showed that ZEB1 is overexpressed in MCLs with active Wnt signalling. Expression of ZEB1 was controlled by Wnt signalling, and being downregulated by *β*-catenin knockdown or blocking of Wnt signalling by salinomycin in MCL cells. Moreover, ZEB1 knockdown decreased *in vitro* cell viability and proliferation. Furthermore, they found that ZEB1 activated proliferation-associated factors, including: *HMGB2, UHRF1, CENPF*, *MYC, MKI67*, and *CCND1*, and anti-apoptotic, such as *MCL1*, *BCL2*, and *BIRC5*, genes and inhibited pro-apoptotic ones (*TP53*, *BBC3*, *PMAIP1*, and *BAX*). In addition, they showed that ZEB1 expression determined differential resistance to chemotherapy and controlled transporters involved in drug influx/efflux in MCL cells. ZEB1 downregulation by salinomycin raised the sensitivity of MCL cells to the cytotoxic effect of doxorubicin, cytarabine and gemcitabine. Finally, salinomycin and doxorubicin showed a synergistic effect in both established and primary MCL cultures (Sánchez-Tilló et al., 2014).

There is a study, that agrees with our finding and confirms that ZEB1 expression in B-lymphocytes in DLBCL cases. It was found that ZEB1, Slug and Twist were often expressed at different levels in DLBCL, and that ZEB1 is the only one of these EMT TFs expressed in small numbers of reactive lymphocytes, the intensity of expression varied from low to moderate and this is in line with our findings. In addition, it was found also in DLBCL, that nuclear expression of both ZEB1 and Slug was related to a poor prognosis. The effect of Slug might be linked to its ability to inhibit apoptosis, and ZEB1 to its effect through downregulation of BCL-6. These three TFs, which are usually linked with EMT in carcinomas, could potentially have a significant role in lymphomas, and their expression appeared to be upregulated during malignant transformation (Lemma et al., 2013).

Regarding ZEB2 expression, it was expressed in many cells such as T-lymphocytes in tonsil tissue (Figure 3.2D) and endothelial cells in thymus (Figure 3.4D) while it was weakly expressed in spleen tissue (Figure 3.3D). In addition, the results showed that 53% of lymphoma samples expressed ZEB2 in B-lymphocytes at different degrees ranged from weak to moderate expression. Moreover, some ZEB2 expression was detected in endothelial cells and macrophages (Figure 3.10). As a summary, out of 60 lymphoma cases 9 (15%) showed moderate expression, 2 CLL, 4 DLBCL, 2 FL and one cases of MCL. On the other hand, 38% of lymphoma cases showed weak expression, including: 7 CLL, 6 DLBCL, 5 MCL and one case of MZL, while around 47% showed negative expression (Figure 3.11).

There was no clear investigation showing correlation between ZEB2 expression and B-cell lymphoma development. In our study, the results show that ZEB2 is expressed in B-lymphocytes of different B-cell lymphomas mainly at the moderate level.

However, there is a study where the role of ZEB2 expression in T-cell acute lymphoblastic leukemia (T-ALL) was analyzed. It was demonstrated that ZEB2 was an oncogenic driver of immature T-ALL, a heterogenic subgroup of human leukemia characterized by a high incidence of reduction failure or hematological relapse after conventional chemotherapy. Authors showed that lysine-specific demethylase KDM1A was a novel interacting partner of ZEB2 and that in mouse and human T-ALL cultures ZEB2 activity critically depended on KDM1A in cells survival. So, targeting ZEB2 through direct disruption of the ZEB2-KDM1A complex by pharmacological inhibition of the KDM1A demethylase activity might be a novel therapeutic strategy in this aggressive subtype of human leukemia and possibly in other ZEB2-driven malignancies (Goossens et al., 2017).

Furthermore, a recent study demonstrated that expression of ZEB2 was upregulated in human lung cancer and knockdown of ZEB2 in lung cancer cell lines such as A549 or NCI-H292 inhibited cell proliferation, whereas overexpression of ZEB2 in lung cancer cell lines, H-125 and H1975, inhibited cell apoptosis (Guo et al., 2018).

Thus, ZEB2 may act as a prognostic factor for the diagnosis and treatment of patients with lung cancer (Guo et al., 2018) and T-ALL (Goossens et al., 2017) but not for patients with B-lymphomas.

3.3.3 S100A4 expressed in mature and immature bone marrow cells.

S100 proteins show a specific pattern of expression in various normal cell types and tumours (Bresnick et al., 2015b). A comparative assessment of their expression in both normal and tumour cells is an important approach that can be used in clinics. As a first step towards this goal, we examined samples of pathologic normal and CLL bone marrow tissues by immunostaining including immunohistochemistry, immunofluorescence and a 4-colour immunofluorescence using anti-S100A4 antibody.

In order to analyse early stages of S100A4 activation during lymphocyte development and in CLL, bone marrow samples of healthy individuals and CLL patients were used. Sections of bone marrow were stained with the antibody against S100A4. In pathological normal BM tissue, it was detected that all samples had the same pattern of staining and it was detected that S100A4 was expressed in different types of bone marrow cells including small immature lymphocytes showing occasional nuclear and cytoplasmic distribution (Figures 3.17A & 3.17B). While in CLL BM samples, there were multiple S100A4 positive cells. In general, the level of S100A4 expression was higher in CLL samples compare with normal BM cases (Figure 3.17C & 3.17D).

Further studies to analyse S100A4 protein expression in lymphocyte development and particularly in haematopoietic stem cells, double immunofluorescence was applied. Specific haematopoietic stem cell markers CD10, CD34, and CD45 were used for identification stem cells in bone marrow samples. Moreover, cells markers including: CD31, which is endothelial cells marker, CD45RA which is naive T-cell marker and antibody to macrophage specific marker CD68, were used. In normal bone marrow (Figure 3.18), it was observed that a proportion of S100A4 positive cells showed features of HSC or progenitor cells being positive for CD10, CD34, and CD45. Also, S100A4 expression was detected at high level in some proportion of cells expressing CD31. In addition, there was occasional matching between S100A4

positivity in cells expressing CD68 and CD45RA. Four colour immunofluorescence confirmed the expression of S100A4 in normal T cells (Figure 3.20).

In bone marrow samples of CLL patients, the result of double immunofluorescence showed that S100A4 positive cells were CD10, CD34, and CD45 positive, meaning that S100A4 expression was present in cancer stem cells. Also, it was found that there was a co-expression between S100A4 and CD68 and CD45RA (Figure 3.21). Four colour immunofluorescence confirmed the expression of S100A4 in T cells and in malignant B-lymphocytes (Figure 3.23).

Up to the present, there have been no studies relating to the expression of S100 protein in haematopoietic stem cells but it has been observed in solid malignancies that S100A4 was expressed in cancer stem cells. Our study for the first time showed that there was a significant level of S100A4 expression in haematopoietic cells in normal bone marrow and in cancer stem cells in samples of CLL patients.

3.3.4 Transcription of *S100A4* and *S100A6* in peripheral blood B-cells of CLL patients

This study focused on the analysis of the CLL peripheral blood samples available from The Ernest and Helen Scott Haematological Research Institute in the Leicester Cancer Research Centre, University of Leicester. The CLL clinical course is heterogeneous, with some patients experiencing an aggressive course that needed early treatment and others experiencing long term survival without disease-related symptoms or ever the requirement of treatment (Caligaris-Cappio and Dalla-Favera, 2005). Recent studies identified that EMT is one of the most common mechanisms contributing to metastatic progression and drug resistance in CLL (Chou and Yang, 2015; Yue et al., 2016). At the same time, it has been found that proteins of the S100 family play an active role in cancer progression, and the expression pattern of S100 genes is controlled by EMT programs (Buetti-Dinh et al., 2015). Although various studies have explored the expression of S100 proteins in cancer, up to date there is no investigation analysing their expression in CLL. The current study provides a clear picture of S100s expression in lymphocytes of the peripheral blood of the CLL patients.

Real time qPCR analysis, presented as a chart (Figure 3.24), revealed a differential expression of S100 genes in malignant B-lymphocytes of the CLL peripheral blood samples. The level of transcription of the majority of the analysed S100 genes, including, *S100A4*, *S100A5*, *S100A6*, *S100A10*, *S100A11*, *S100A13* and *S10014*, was found to be upregulated in the peripheral B-lymphocytes, and positively correlated with the expression of *ZEB1* and *ZEB2*. The expression of *S100A4* and *S100A6*, meanwhile, was found to be up-regulated more than other S100 genes. Conversely, *S100A1*, *S100A2*, *S100A3*, *S100A8*, *S100A9* and *S100A12* were downregulated in B-cells from blood of CLL patients.

Interestingly, the obtained data agreed with results from the analysis of the expression of S100s genes using the EBI ArrayExpress dataset EGEOD-2466. This showed a significant upregulation of *S100A4*, *S100A8*, *S100A9*, *S100A10* and *S100A11* genes (p value < 0.05) in B-lymphocytes of samples from the peripheral blood of CLL patients (G. Kaithakottil, MSc thesis, University of Leicester, 2010). Also, it predicted the expression of *S100A4* in normal blood cells such as T-lymphocytes, macrophages and platelets but not in B-lymphocytes as was shown before by (Cabezón et al., 2007).

It is a well-known the fact that the differential expression of individual members of the S100 family is a characteristic of the stage of cancer progression (Bresnick et al., 2015b). For instance, the expression of *S100A11* is upregulated in non-small cell lung carcinoma, but is downregulated in small cell lung cancer (Tian et al., 2007). *S100A7* is detected at early stages of oral squamous carcinoma but not later at poorly differentiated stages (Hunter et al., 2005). Thus, our results of activation of *S100A4* and *S100A6* genes in B-cell lymphomas, can be considered as an indicator of the disease progression.

3.3.5 The transcription of EMT regulators *ZEB1* and *ZEB2* in peripheral blood B-lymphocytes of CLL patients

Although various studies showed the expression of the individual S100s and EMT factors in cancer, so far there has been no investigation analysing expression of S100s and EMT regulators in CLL. The current study focused for the first time on the analysis of ZEB family and S100 genes expression in normal and malignant B-cells.

Our data showed an increased level of *ZEB1* and *ZEB2* expression in CLL B-lymphocytes and *S100A4* and *S100A6* that were mostly upregulated out of other S100s. For the first time, our results show that there is a strong association between expression of *S100A4* and *S100A6* genes and EMT transcription factors, *ZEB1* and *ZEB2*, in CLL at the transcriptional level. These observations raised the possibility that expression of these genes may link to the progression and drug resistance in CLL.

The correlation of the expression of S100s and EMT factors is not exclusive for lymphomas, as similar results were found in solid malignancies such as pancreatic cancer (Chen et al., 2015; Xu et al., 2014). Moreover, it has been proved that *S100A4* was an important mediator of EMT in breast cancer (Xu et al., 2016), hepatocellular carcinoma (Zhai et al., 2014), ovarian cancer (Yan et al., 2016), oesophageal squamous cell carcinoma (Jian et al., 2015) and endometrial cancer (Hua et al., 2016). Additionally, *S100A6* has also been found to be involved to a lesser extent in EMT in hepatocellular carcinoma (Li et al., 2014) and prostate cancer (Orr et al., 2012).

3.3.6 Expression of S100A4 protein in B-lymphocytes of CLL peripheral blood

It was shown that only S100A4 but not S100A6 was expressed in malignant B-cells of the most of the analysed tissue blocks of B-cell lymphomas. So further analysis was focused on the expression of S100A4 in the peripheral blood of the CLL patients provided by The Ernest and Helen Scott Haematological Research Institute in Leicester. Expression of S100A4 was analysed by Western blotting, IHC and 4-colours immunofluorescence of CLL B-lymphocytes.

Western blot analysis showed that the majority of peripheral blood samples among 20 analysed samples were S100A4 positive; in 75% of samples a high level of S100A4 expression was detected, and only 25% were with a moderate to negative S100A4 expression (Figure 3.25).

Since a low amount of S100A4 positive T-cells are present in the peripheral blood of CLL patients, a detailed analysis of S100A4 expression in T and B -cells was done. First CLL peripheral blood cytoblocks of most CLL samples were prepared and stained for S100A4 by IHC (Figure 3.26). After detection of S100A4 expression in

CLL peripheral blood cells, two blocks with a high and low level of S100A4 expression were selected for a detailed 4-colour immunofluorescence analysis using antibodies against S100A4 and CD3 and CD20, markers of T-cells and B-cells accordingly (Figures 3.27 and 3.28). Co-expression between S100A4 and CD20 was observed in a majority of B-cells but some proportion of CD3 and S100A4 positivity was detected as well. Therefore, IHC and immunofluorescence analysis confirmed Western blot data that showed a high level of S100A4 expression in the majority of the analysed CLL peripheral blood samples.

In spite of many studies showing S100A4 expression in different cancers (Ninomiya et al., 2001; Oida et al., 2006; Yonemura et al., 2000), for the first time we have shown that S100A4 was strongly expressed in CLL blood samples.

3.3.7 Expression of S100A4 is associated with unfavorable prognosis of CLL patients

The correlation between S100A4 expression and the survival of cancer patients diagnosed with breast cancer (de Silva Rudland et al., 2006; Lee et al., 2004), bladder cancer (Davies et al., 2002; Matsumoto et al., 2007), colorectal carcinoma (Lee et al., 2013a; Niu et al., 2015) has been investigated. However, the role S100A4 expression in the survival of patients diagnosed with B-cell lymphomas was unknown. For the first time, the correlation between S100A4 expression and the survival of CLL patients was demonstrated in this study.

Survival analysis was generated using a Kaplan-Meier survival plot that showed that low or negative expression of S100A4 was correlated with a statistically significant longer survival, P=0.0215 (<0.05) (Figure 3.29). It was demonstrated that S100A4 localized in the nucleus, cytoplasm, and secreted to the extracellular space and had a wide range of biological functions ranging from the regulation of angiogenesis to cell survival, motility, and invasion (Boye and Maelandsmo, 2010). Interestingly, S100A4 was also associated with lymphocyte infiltration that involved in tumour progression and destroyed tumour budding. In (Boye and Maelandsmo, 2010) study, S100A4 expression was detected in fibroblasts, monocytes, macrophages, T lymphocytes,

neutrophilic granulocytes, and endothelial cells and may be misinterpreted as a detection of S100A4 expression in cancer cells (Boye and Maelandsmo, 2010).

The critical point of our analysis was the limited number of used samples. In order to establish a prognostic significance of S100A4 expression in CLL, it is necessary to use more samples and have a longer follow-up investigation to prove that S100A4 expression is associated with the outcome of the disease. In the case of CLL lymphoma there is a requirement for a follow-up period of 10 years or longer. In spite of the fact that it was possible to demonstrate a link between S100A4 and CLL progression, it is important to investigate the mechanism behind. This current knowledge about S100A4 function points to its role in cell motility as the most likely target of the overexpressed S100A4, and more detailed examination of the molecular mechanisms involved in this process will undoubtedly shed light on the mechanism of S100A4 expression in B-cells lymphomas.

Accumulating evidence has demonstrated that the expression of S100A4 correlates with cancer metastasis and S100A4 plays an important role in mechanisms of tumour progression. Moreover, expression of S100A4 has a critical role in cell invasion and motility. Thus, in agreement with this study, we hypothesize that S100A4 expression has an impact on patient survival.

3.4 Conclusion

To sum up; the expression of S100A4, S100A6, ZEB1 and ZEB2 was analysed in normal and lymphoma cases. These proteins are mainly expressed in T-lymphocytes in normal lymphoid organs while some expressed B and T-lymphocytes in tested lymphoma cases except FL. In normal tonsil and spleen tissue, there is similarity in S100A4 and ZEB2 distribution. On the other hand, there is no correlation between the S100A4 and the ZEB family in lymphoma cases. In addition, S100A6 shows a negative expression in analysed lymphoma samples so, we focused on S100A4 expression and its role in B-cell lymphoma particularly CLL. In both normal and CLL BM samples S100A4 was expressed in stem cells but the level of expression is more in the case of BM of CLL. Detailed analysis of bone marrow HSC samples has shown a co-expression of S100A4 with CD10, CD34 and CD45 indicating that S100A4 expression can be considered as a potential biomarker of HSC in CLL. *S100A4* and *S100A6* genes express in CLL samples more than other S100 members while they do not express in normal samples. *ZEB1* and *ZEB2* are EMT factors shows a good level of expression in CLL samples. In addition, our results suggested that the expression of S100A4 in B-cell of CLL is well related to patient survival and S100A4 protein is a useful marker to predict prognosis.

Chapter 4. S100A4 is a modulator of B-cell migration

4.1 Introduction

S100A4 protein plays a critical role during cancer progression and metastasis since it is highly expressed in a vast repertoire of malignancies ranging from melanoma to non-small cell lung carcinoma and cancers of breast and stomach (Andersen et al., 2004; Kimura et al., 2000; Rudland et al., 2000; Yonemura et al., 2000). It is believed that S100A4 is a significant player regulating migration and invasion steps of the metastatic cascade. Hence, the overexpression of S100A4 increases the migratory abilities of transformed fibroblasts or metastatic adenocarcinoma cell line (Jenkinson et al., 2004; Li and Bresnick, 2006; Takenaga et al., 1994a). On the other hand, knockdown of S100A4 expression in tumour cells decreases cellular motility (Bjornland et al., 1999; Takenaga et al., 1997). S100A4 can stimulate cell migration in both tumour and normal cells; however, the underlying biological mechanism for such changes is still poorly understood. To shed more light on some of the mechanisms that could describe the increase of migratory properties, we used HL-60 cells (as a model system) and peripheral blood samples from CLL patients to analyse the role of S100A4 in cell migration. Expression of S100A4 was modulated by RNAi approach. Cells were transfected with the siRNA S100A4 and siControl 48 hours. To study the role of S100A4 in lymphocytes migration, chemotaxis assay was used as a tool for *in vitro* study of B-cell migration (Figure 4.1).

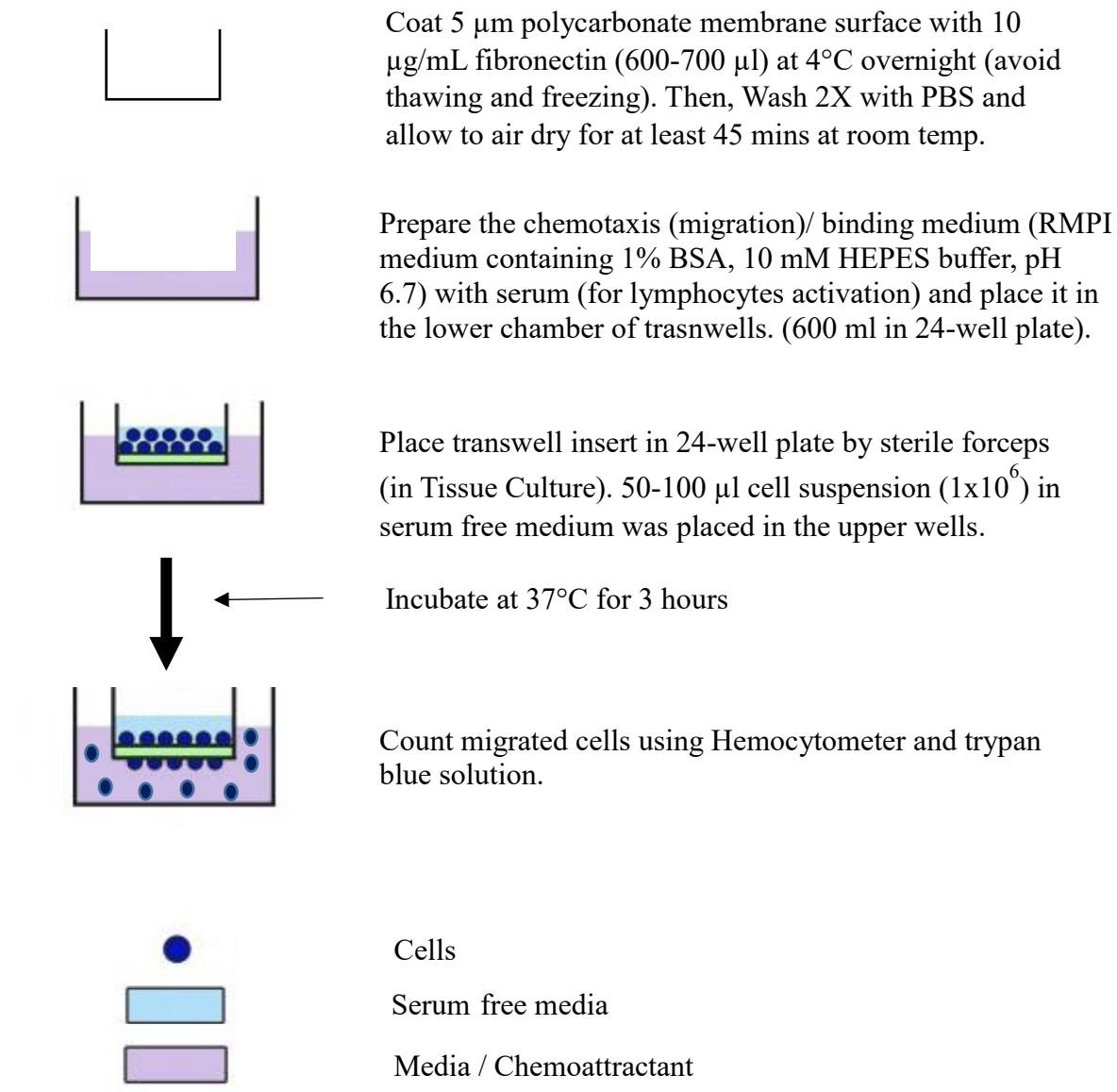

Figure 4.1 Chemotaxis assay.

4.2 Results

4.2.1 S100A4 role in HL-60 cells migration

It was shown that S100A4 is involved in stimulation of cell motility. Also, S100A4 expression in normal cell types is almost exclusively restricted to cells with a motile phenotype, such as leukocytes and fibroblasts (Stein et al., 2006). To support this finding, we aimed to investigate the role of S100A4 in HL-60 cells. S100A4 expressed in HL-60 cells in high level while it showed negative expression in Jurkat cells. This expression was detected by Western blotting, where +Dox A431 and –Dox A431 (the epidermoid carcinoma cell lines) were used as positive and negative controls, respectively (Figure 4.2). In order to correlate the expression of S100A4 and cell migration, a chemotaxis assay was performed using HL-60 cells. Cells were transfected with optimised amount (see Materials and Methods) of a non-targeting or S100A4-targeting siRNA (The amount of the used siS100A4 was optimized in advance and the control siRNA was used in the same concentration) for 48 hours and then seeded in the transwell inserts that were coated with 10 µg/ml fibronectin (usually in 600-700 µl which is good amount to cover the entire wells at 4°C overnight). After 3 hours of incubation, the average number of migrated cells was counted (Table 4.1). As was hypothesised, knockdown of S100A4 expression reduced the ability of cells to migrate significantly (Figure 4.3A; p =0.0108). The level of knockdown was confirmed by the Western blot (Figure 4.3B). The results represent the average of three independent experiments performed in triplicate. A Student's t-test was used to assess the statistical significance.

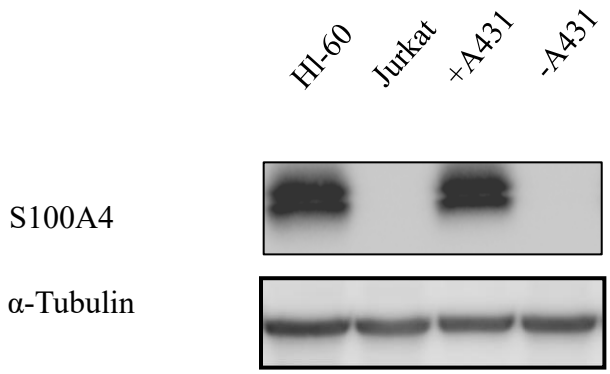

Figure 4.2 Expression of S100A4 in HL-60 and Jurkat cells lines.

HL-60 and Jurkat cells lysates were prepared and resolved into 15% SDS-polyacrylamide gel. Then proteins were transferred and the expression of S100A4 was detected using rabbit polyclonal anti-S100A4 from Proteintech (dilution 1:1000). + Dox A431 and – Dox A431 were used as positive and negative controls, respectively. Tubulin was used as a loading control.

HL-60 cells ($1x10^6$ cells)	% Migrated cells in experiment 1	% Migrated cells in experiment 2	% Migrated cells in experiment 3
siControl	7.28	8.41	5.96
siS100A4	4.13	4.08	3.5256

Table 4.1 An analysis of HL-60 cell migration.

Chemotaxis assay was performed using HL-60 cells that transfected with a non-targeting or S100A4-targeting siRNA 48hr to analyse cells migration. HL-60 cells were prepared at the concentration of 1 x 10^6 cells/100µl in the migration medium (DMEM and 0.1% BSA without serum). Medium DMEM containing 10% fetal bovine serum was used as the chemo-attractant. Prepared 100µl of HL-60 cells was added in the upper chamber and 600 µl of medium with serum as chemo-attractant was added to the lower chamber. After three hours of incubation, the average number of cells migrated through was counted.

A

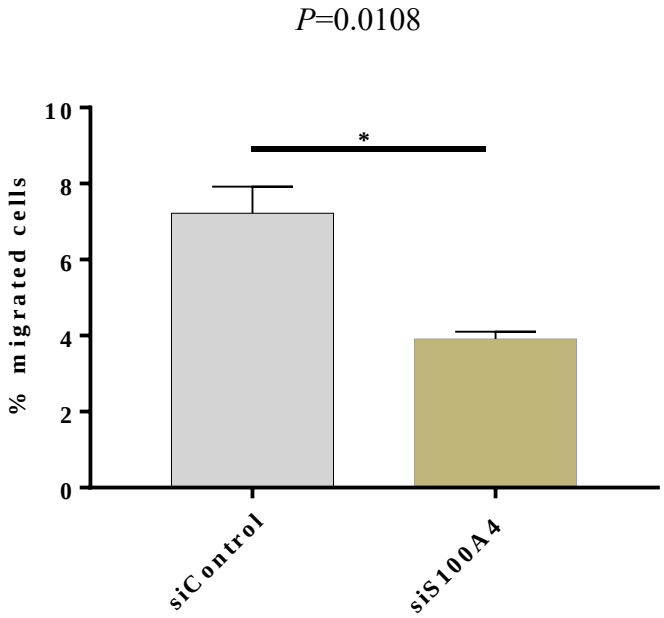

B

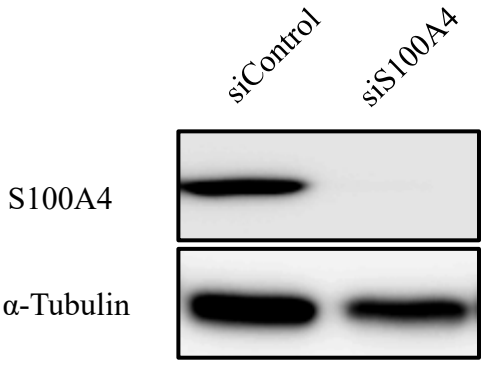

Figure 4.3 RNAi mediated knockdown of S100A4 reduced the ability of HL-60 cells to migrate.

(A) HL-60 cells that transfected (48 hours) with either a non-targeting or S100A4-targeting siRNA were used in chemotaxis assay. The results present the average of three independent experiments performed in triplicate. A Student's T-test was used to assess the statistical significance where *P*=0.0108. (B) In parallel, the efficiency of the S100A4 knockdown was evaluated by the Western blot. Cells lysates of the transfected cells were prepared and resolved into 15% SDS-polyacrylamide gel. Then, proteins were transferred and the expression of S100A4 was detected using rabbit polyclonal anti-S100A4 from Proteintech (dilution 1:1000). Tubulin was used as a loading control.

4.2.2 S100A4 role in regulation of lymphocytes migration in CLL patients

Samples of lymphocytes from CLL patients that were positive on S100A4 expression by Western blot (Figure 4.4) were used to investigate the role of S100A4 in lymphocytes migration. These samples were provided by The Ernest and Helen Scott Haematological Research Institute, Leicester Cancer Research Centre, University of Leicester. CLL cells were transfected with a non-targeting or S100A4-targeting siRNA, maintained for 48 hours and then seeded in a coated transwell insert (as described before). After three hours of incubation, the average number of migrated cells was counted (Table 4.2). As was assumed, knockdown of S100A4 expression decreased the ability of cells to migrate significantly (Figure 4.5A; $P < 0.05$ in all analysed samples). The level of knockdown was confirmed by Western blot (Figure 4.5B). The results represent the average of three independent experiments performed in triplicate. A Student's t-test was used to assess statistical significance.

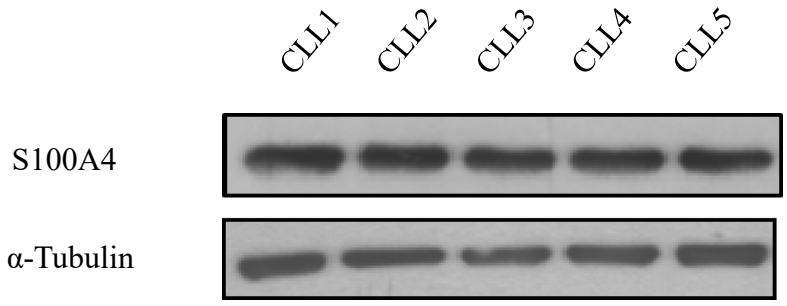

Figure 4.4 Analysis of S100A4 expression in CLL samples by Western blot.

Cells lysates from five CLL peripheral blood samples were prepared and resolved into 15% SDS-polyacrylamide gel. Then proteins were transferred and the expression of S100A4 was detected using rabbit polyclonal anti-S100A4 from Proteintech (dilution 1:1000). Tubulin was used as a loading control.

Sample #	Type of cells	% Migrated cells in experiment 1	% Migrated cells in experiment 2	% Migrated cells in experiment 3
Sample 1 (CLL1)	cells	11.31	11	11.52
	Transfected cells 48hr with siRNA S100A4	6.4	5.57	5.77
	Transfected cells 48hr with siControl	10.42	10.12	11.01
Sample 2 (CLL2)	cells	17.4	17.5	17. 9
	Transfected cells 48hr with siRNA S100A4	8.4	8.6	8.07
	Transfected cells 48hr with siControl	15.4	15.53	15.07
Sample 3 (CLL3)	cells	39.4	39	39.8
	Transfected cells 48hr with SiRNA S100A4	12.1	15	14.6
	Transfected cells 48hr with siControl	32.6	29.45	35.6
Sample 4 (CLL4)	cells	12	11.4	11.1
	Transfected cells 48hr with siRNA S100A4	7	6.3	6.97
	Transfected cells 48hr with siControl	10.95	9.5	10.1
Sample 5 (CLL5)	cells	23	19	24.5
	Transfected cells 48hr with siRNA S100A4	14	11	13
	Transfected cells 48hr with siControl	21	17	19.8

Table 4.2 S100A4 decreases migration ability of CLL B-cells.

Chemotaxis assay was performed using lymphoma cells isolated from the CLL patient's peripheral blood samples that transfected with a non-targeting or S100A4-targeting siRNA 48hr to analyse cells migration. Cells were prepared at the concentration of 1 x 10^6 cells/100µl in the migration medium RPMI and 0.1% BSA without serum. Medium RPMI containing 10% fetal bovine serum was used as the chemo-attractant. Prepared 100µl of lymphoma cells was added in the upper chamber and 600 µl of medium with serum as chemo-attractant was added to the lower chamber. After three hours of incubation, the average number of cells migrated through was counted.

A

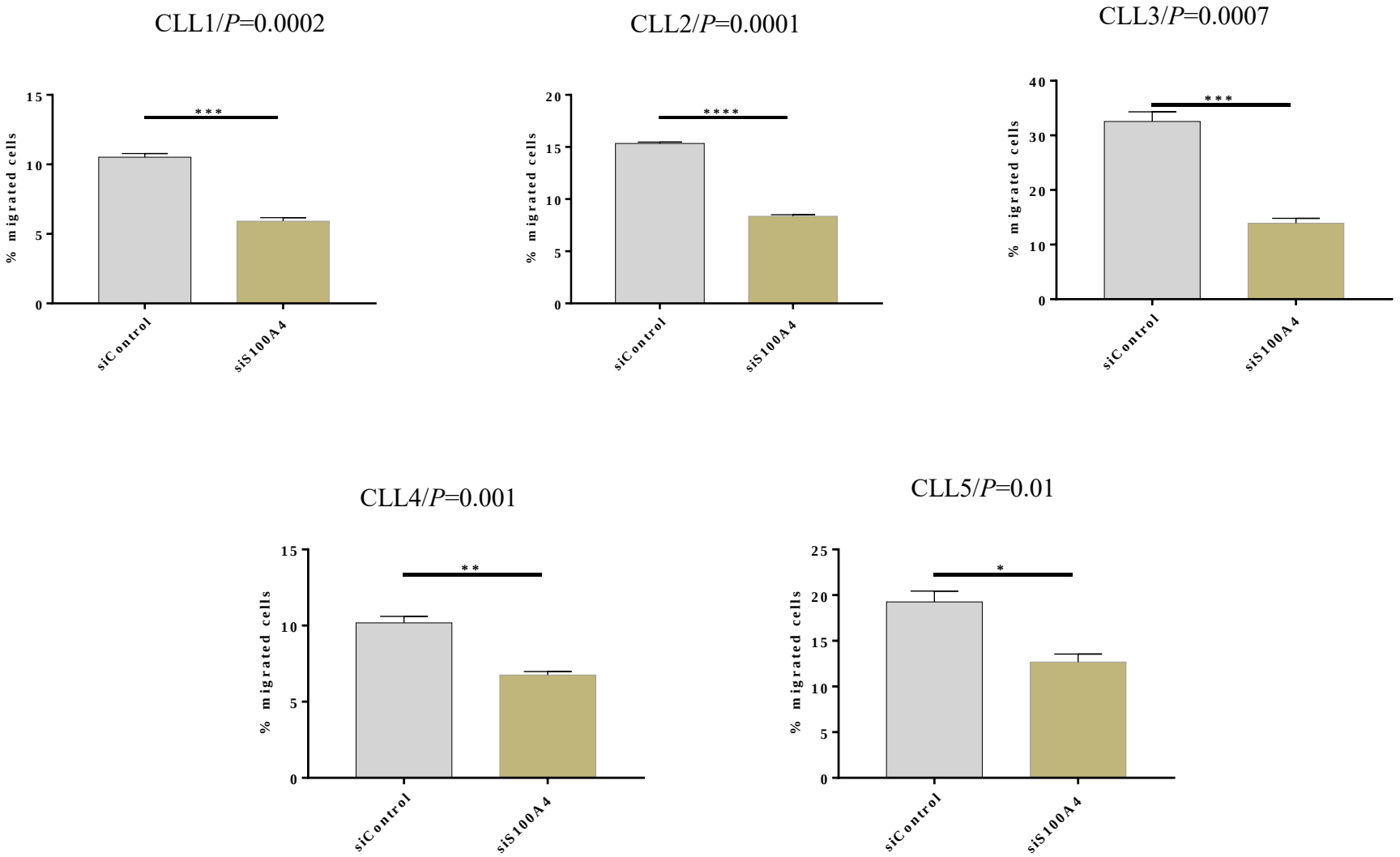
CLL1/P=0.0002
% migrated cells
15
10
5
0
***
siControl
siS100A4
CLL2/P=0.0001
% migrated cells
20
15
10
5
0
****
siControl
siS100A4
CLL3/P=0.0007
% migrated cells
40
30
20
10
0
***
siControl
siS100A4
CLL4/P=0.001
% migrated cells
15
10
5
0
**
siControl
siS100A4
CLL5/P=0.01
% migrated cells
25
20
15
10
5
0
*
siControl
siS100A4

B

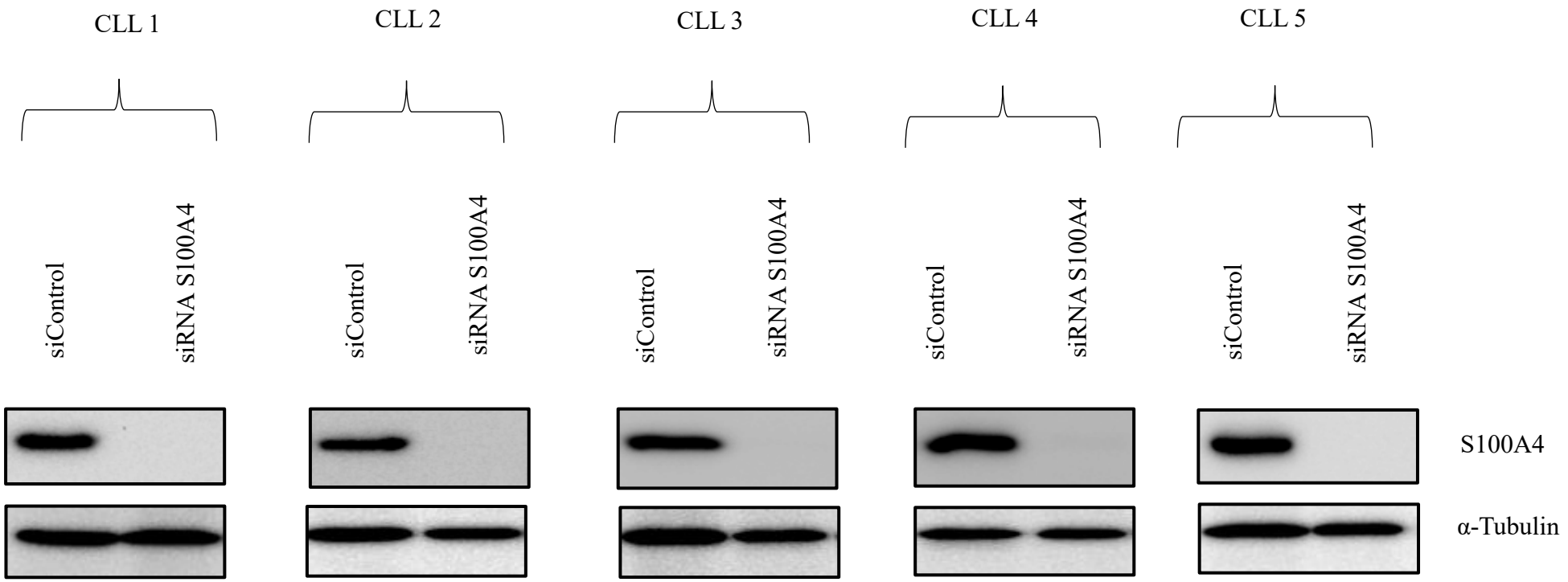

Figure 4.5 Effect of S100A4 expression in cell migration of CLL samples.

(A) Cells from CLL peripheral blood samples that were transfected (48 hours) with either a non-targeting or S100A4-targeting siRNA were used in chemotaxis assay. Results represented the average of three independent experiments performed in triplicate. A Student's T-test was used to assess the statistical significance, where $P<0.05$ in all analysed samples. (B) In parallel, the efficiency of the S100A4 knockdown was evaluated by the Western blot. Cells lysates of the transfected cells were prepared and resolved into 15% SDS-polyacrylamide gel. Then proteins were transferred and expression of S100A4 was detected using rabbit polyclonal anti-S100A4 from Proteintech (dilution 1:1000). Tubulin was used as a loading control.

4.3 Discussion

Migration is a key property of live cells and important for normal development, immune response, and disease processes including cancer metastasis and inflammation. Approaches to study cell migration are very useful and essential in a wide range of biomedical research such as cancer biology, vascular biology, immunology, cell biology and developmental biology. As described in the introduction, S100A4 has a critical role in coordination cells migration. It was shown that S100A4 stimulates metastasis in several experimental animal models, and S100A4 protein expression is related to patient outcome in a number of tumour types. S100A4 is localized in the nucleus, cytoplasm, and extracellular space and has different biological functions, such as regulation of angiogenesis, cell survival, motility, and invasion (Cohn et al., 2001; Flatmark et al., 2003; Stein et al., 2006). In this chapter, we analyze the role of S100A4 expression on lymphocyte migration.

4.3.1 Knockdown of S100A4 decreases cell migration in HL-60 cells

Transfection studies using several different cell systems have clearly shown that S100A4 is involved in stimulation of cell motility (Bjornland et al., 1999; Kikuchi et al., 2006; Stein et al., 2006; Takenaga et al., 1997). In support of this finding, we found that S100A4 expression associated with a motile phenotype of lymphoma cell line, HL-60. HL-60 cells that expressed S100A4 were transfected by siRNA and tested for migration. We found that downregulation of S100A4 protein leads to the suppression of the ability of cells to migrate while upregulation promotes it. This result supports researcher's finding (Cabezon et al., 2007; Tarabykina et al., 2007) that are shown that in highly motile cells, such as macrophages and neutrophils, S100A4 protein expresses in high level. In this study for the first time, we demonstrated that the presence of S100A4 was found to promote cell migration in lymphocytes by chemotaxis assays (Figures 4.3 and 4.5).

In agreement with a lot of research, high expression of S100A4 stimulates cell migration, while their downregulation reduces the number of migrated cells. For

example, in gastric cancer, Yuan et al., (2014) studied the functional role of S100A4 and they found that S100A4 overexpressed in two gastric cell lines, AGS and SCM-1. S100A4 expression significantly in these cell lines increased the invasive activity while knockdown of S100A4 expression caused in a decrease in the migration rate but without any effect on cells survival (Yuan et al., 2014).

4.3.2 S100A4 promotes CLL peripheral blood lymphocytes migration

S100A4 has been found to interact *in vitro* with actin filaments (Helfman et al., 2005), with non-muscle tropomyosin (Sheng et al., 1994) and possibly interacts with tubulin (Lakshmi et al., 1993). These results show indirect evidence of the possible involvement of S100A4 in the regulation of cell motility and cytoskeleton rearrangements. Up to the present there has been no investigation which shows the role of S100A4 in cell migration of lymphoma. In this study, B-cells from peripheral blood samples of CLL patients were tested for cell migration by chemotaxis assays to explore the effect of S100A4 protein on cell migration. It was found that all cells isolated from these samples expressed a high level of S100A4 (Figure 4.4). These cells were disseminated extensively through the pores and showed high migration ability (Table 4.2). In addition, it was found that siRNA mediated knockdown of S100A4 expression resulted in a decreased number of migrated cells *in vitro.* These results were significant, where *P* values were < 0.05 in all cells of analysed CLL samples (Figure 4.5).

Several publications support our results that S100A4 might contribute to the regulation of malignant cell migration (Ford et al., 1995; Jenkinson et al., 2004; Takenaga et al., 1994a; Takenaga et al., 1997).

4.4 Conclusion

In conclusion, our results show that S100A4 protein plays a significant role in lymphocytes migration in CLL.

Chapter 5. Therapeutic inhibition of CLL migration via S100A4 suppression

5.1 Introduction

B-cell malignancies are diagnosed in more than 10,000 new patients and cause >5,000 deaths a year in the UK (Cancer Statistics, Cancer Research, UK, 2017). Chronic Lymphocytic Leukaemia (CLL) accounted for 1% of all new cancer cases in the UK, and 37% of all leukaemia types, making it the most common blood cancer with growing number of patients requiring treatment and clinical care. CLL is a tumour of circulating CD5 positive B cells, variably stimulated and anergised following exposure to antigen in lymphoid tissue (proliferative centres, PC), which is essential for sustained proliferation and the survival of malignant CLL cells. CLL cells migration to the tissue sites where the activation and proliferation take place and subsequent exit into peripheral blood before next round of migration/activation/proliferation forming the life cycle of CLL cells. Most advanced treatments including anti-CD20 monoclonal antibody or inhibitors of B-cell receptor proximal kinases such as Ibrutinib and Idelalisib can prolong remission but do not prevent an inevitable relapse. Moreover, the risk of transformation into more aggressive forms remains high (Kipps et al., 2017).

We aimed at investigating an intracellular regulation of CLL migration and developing a novel approach to therapeutic inhibition of CLL migration. S100 proteins family of the intracellular regulators of migration recently came under the spotlight, e.g. S100A4 which in a healthy individual is expressed in T-cells and normally not found in mature B-cells. This Ca2+-dependent protein participates in control cell movement by direct interaction with cellular actin and non-muscle myosin thus facilitating cellular protrusions increasing cell migration and invasion.

We have demonstrated that CLL B-cells aberrantly express the proposed target S100A4 and that siRNA (a combination of three different siRNAs were used) interference with S100A4 expression leads to a complete knockdown of S100A4 and a strong decrease in migration of CLL cells. The GEO data analysis shows that S100A4 is increased expression in different B-cell malignancies (CLL, DLBCL, MZL, etc.). CLL cases with worse prognosis (prognostic markers Zap70 and CD38 high) express significantly higher level of S100A4 in comparison with less aggressive cases. Thus, our goal in this study was to analyse new highly specific inhibitors of S100A4 as potential inhibitors of CLL migration.

New small molecular inhibitors were identified in a protein - protein interaction assays based on AlphaScreen technology that was performed in Dr Oleg Fedorov laboratory (SGC/TDI Nuffield, Department of Clinical Medicine, University of Oxford). AlphaScreen™ is a tool that allows screening for a broad range of targets. The technology provides an easy and reliable means for determining the effect of compounds on biomolecular interactions and activities. AlphaScreen relies on the use of “Donor” and “Acceptor” beads coated with a layer of hydrogel providing. The preliminary screen of 10,000 compounds from SGC library identified BAY-11-7082 and BAY-11-7085 as effective inhibitors at low micromolar concentrations of S100A4 expression with a selectivity inside the family.

5.2 Results

5.2.1 Expression of S100A4 and NF-κB in CLL samples and HL-60 cells

As demonstrated before (see Chapter 4) S100A4 participates in regulation of migration of B-cells isolated from the peripheral blood of CLL patients. In order to characterise the role of specific anti-S100A4 small molecular inhibitors, three CLL samples were checked for S100A4 positivity. Thus, lysates of CLL patient's samples and HL-60 as a control cell line were analysed by Western blotting to detect the expression of S100A4 protein. However, the expression of p65 was also detected in same cells because BAY-11-7082 and BAY-11-7085 inhibitors were used to supress the NF-κB pathways (Pierce et al., 1997) (Figure 5.1).

The results showed that CLL samples were S100A4 and p65 positive but the level of expression was varies. CLL sample 1 (CLL1) and HL-60 cells were showed a high level of S100A4 expression in comparison with CLL sample 2 (CLL2) and CLL sample 3 (CLL3).

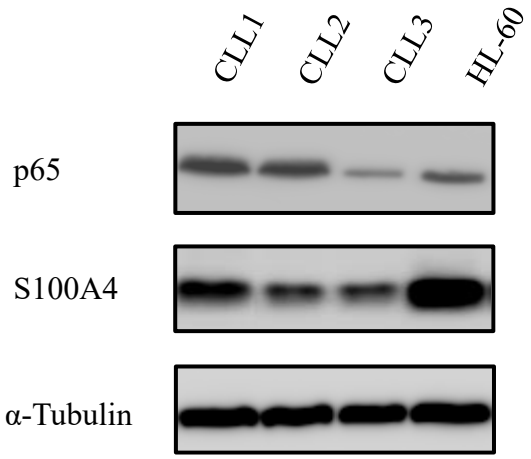

Figure 5.1 Expression of S100A4 and p65 in CLL samples and HL-60 lysates.

Cells lysates from peripheral blood samples of CLL patients and HL-60 cell line were prepared and resolved into 15% SDS-polyacrylamide gel. Then proteins were transferred and the expression of S100A4 and p65 was detected using rabbit polyclonal anti-S100A4 from Proteintech (dilution 1:1000) and rabbit polyclonal anti-p65 from Invitrogen (dilution 1:1000). Tubulin was used as a loading control.

5.2.2 Effect of small molecule inhibitors on migration of HL-60 cells

Before running migration assays, the toxicity of inhibitors was checked in HL-60 cells. Cells were treated in the presence of inhibitors (0.5 µM) or dimethyl sulfoxide (DMSO) that was used as a solvent. After 24 hours of treatment, cells were healthy and treated cells were similar to control cells. However, there was number of dead cells in flask of cells treated with BAY-11-7085. In addition, control and cells treated with 0.5 µM BAY-11-7082 were shown in clusters while cells treated with 0.5 µM BAY-11-7085 appeared single (Figure 5.2). In all group of cells, there was no significant changes in cells appearance.

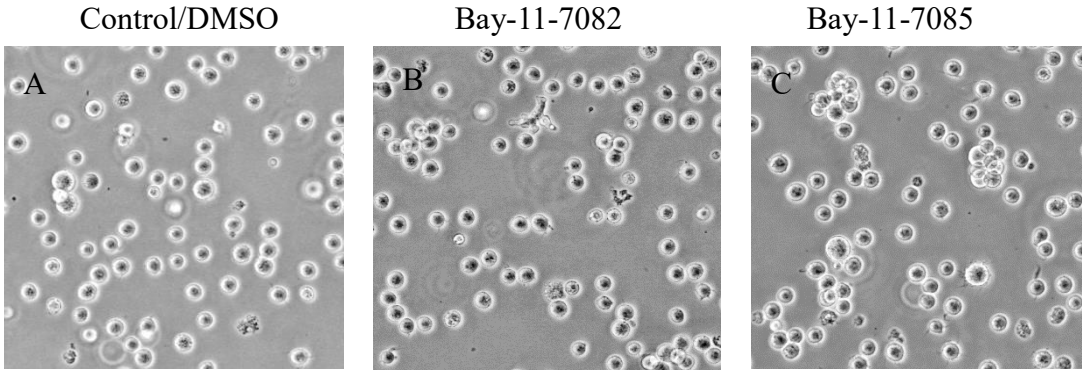

Figure 5.2 Effect of BAY-11-7082 and BAY-11-7085 inhibitors in HL-60 cells.

Phase-contrast images of (A) cells treated with 0.5 µM DMSO as a control, (B) cells treated with 0.5 µM BAY-11-7082 inhibitor and (C) cells treated with 0.5 µM BAY-11-7085 inhibitor. Images were taken with 20x objective.

5.2.3 BAY-11-7082 and BAY-11-7085 are new small molecule inhibitors of cell migration.

The effect of BAY-11-7082 and BAY-11-7085 of small molecule inhibitors on cell migration was studied using HL-60 and cells isolated from the peripheral blood of CLL patients. A chemotaxis assay protocol was used to study migration of lymphoma cells (see Materials and Methods chapter).

5.2.3.1 Effects of BAY-11-7082 and BAY-11-7085 inhibitors on HL-60 cells migration

After treating HL-60 with 0.5 µM of BAY-11-7082 or 0.5 µM of BAY-11-7085 inhibitors for 24 hours, migration test was performed to detect the effect of these inhibitors on cells motility (Table 5.1). Cells treated with 0.5 µM DMSO were used as a control. As was predicted, both inhibitors had a significant effect on cell migration by decreased their ability to migrate (Figure 5.3; $P < 0.05$). The results present the average of three independent experiments performed in triplicate. Ordinary one way ANOVA was used to assess the statistical significance.

HL-60 cells treated with	% of migrated cells in experiment 1	% of migrated cells in experiment 2	% of migrated cells in experiment 3
Control (0.5 µM DMSO)	8.4	7.9	8.0
0.5 µM Bay 11-7082	7.2	4.6	5.9
0.5 µM Bay 11-7085	4.0	3.6	3.8

Table 5.1 Migration analysis of HL-60 cells treated with Bay 11-7082 or Bay 11-7085.

Chemotaxis assay was performed using HL-60 cells treated with Bay 11-7082 or Bay 11-7085 for 24hr. HL-60 cells were prepared at the concentration of 1 x 10^6 cells/100µl in the migration medium (DMEM containing 0.1% BSA). DMEM containing 10% fetal bovine serum was used as the chemo-attractant medium. Prepared 100µl of HL-60 cells was added in the upper chamber and 600 µl of medium with serum as chemo-attractant was added to the lower chamber. After three hours of incubation, the average number of cells migrated through the fibronectin-coated inserts was counted.

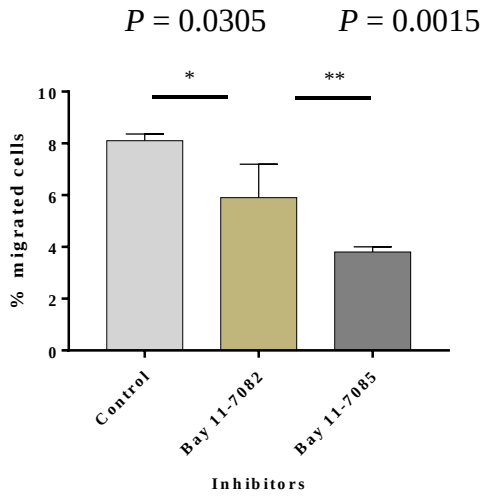

Figure 5.3 Effect of BAY-11-7082 and BAY-11-7085 inhibitors on migration of HL-60 cells.

HL-60 cells were treated with Bay 11-7082 or 11-7085 for 24hr and used in chemotaxis assay. The results presented the average of three independent experiments performed in triplicate. A student's T-test was used to assess the statistical significance where $P<0.05$.

5.2.3.2 Effect of BAY-11-7082 and BAY-11-7085 inhibitors on migration of cells from CLL samples

To investigate the effect of these inhibitors in migration of B-lymphocytes, the same approach was performed using preselected and S100A4 positive CLL samples. CLL samples were treated with 0.5 μM of BAY-11-7082 and BAY-11-7085 inhibitors for 24 hours. Then, migration test was performed to detect the effects of inhibitors on migration of B-lymphocytes (Table 5.2). Cells treated with 0.05 μM DMSO were used as a control. Significantly both inhibitors had a negative effect on cell migration and decreased the amount of migrated cells of CLL1 while there was no significant effect shown in CLL3. Regarding CLL2, Bay 11-7082 showed no significant effect but Bay 11-7085 was a negative regulator on cell migration (Figure 5.4). The results presented an average of three independent experiments performed in triplicate. Ordinary one way ANOVA was used to assess the statistical significance.

CLL Samples	cells treated with	% of migrated cells in experiment 1	% of migrated cells in experiment 2	% of migrated cells in experiment 3
Sample 1	Control (0.5 µM DMSO)	13	12	11.4
	0.5 µM Bay 11-7082	11	9	9.5
	0.5 µM Bay 11-7085	7	6.5	6.3
Sample 2	Control (0.5 µM DMSO)	27	22	25
	0.5 µM Bay 11-7082	23	19	21
	0.5 µM Bay 11-7085	16	10.5	13
Sample 3	Control (0.5 µM DMSO)	11	18	16
	0.5 µM Bay 11-7082	8.5	15.5	11.1
	0.5 µM Bay 11-7085	6.8	11	8.9

Table 5.2 Migration analysis of CLL cells treated with Bay 11-7082 or Bay 11-7085.

Chemotaxis assay was performed using CLL cells treated with Bay 11-7082 or Bay 11-7085 for 24hr. CLL cells were prepared at the concentration of 1 x 10^6 cells/100µl in the migration medium (RPMI containing 0.1% BSA). RPMI containing 10% fetal bovine serum was used as the chemo-attractant medium. Prepared 100µl of CLL cells was added in the upper chamber and 600 µl of medium with serum as chemo-attractant was added to the lower chamber. After three hours of incubation, the average number of cells migrated through the fibronectin-coated inserts was counted.

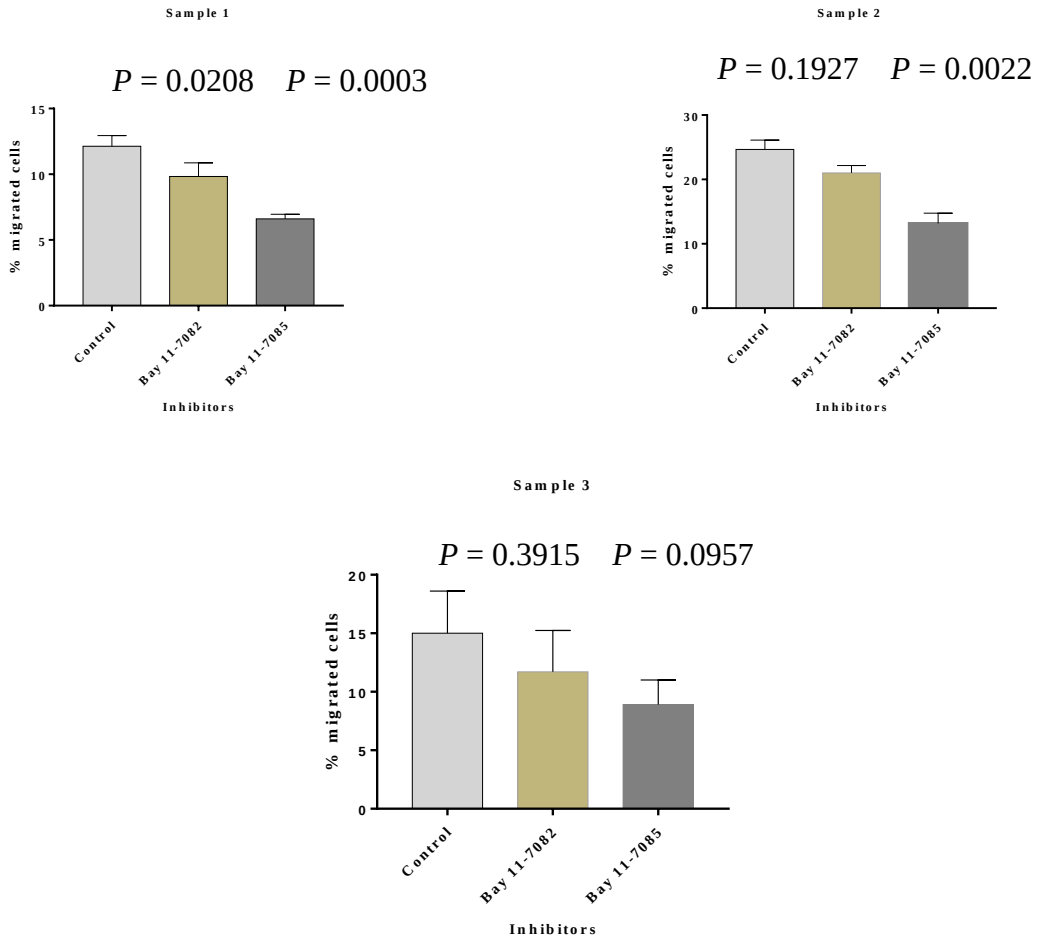

Figure 5.4 Effect of BAY-11-7082 and BAY-11-7085 inhibitors on CLL cells migration.

Cells from peripheral blood samples of CLL patients were treated for 24hr in the presence of Bay 11-7082 or Bay 11-7085 and used in chemotaxis assay. The results presented an average of three independent experiments performed in triplicate. A Student's T-test was used to assess the statistical significance, where *P* was <0.05 in CLL1 case.

5.2.4 BAY-11-7082 and BAY-11-7085 inhibit cell migration via S100A4 suppressing

As shown in figure 5.1 both S100A4 and p65 were expressed in HL-60 and CLL cells and both inhibitors downregulated migration of cells (Figures 5.3 and 5.4). So we decided to use siRNA protocol and test cells for migration assay to confirm that the effect of inhibitors was due to a specific compromise of S100A4 function.

Since S100A4 and p65 were mostly expressed in CLL1 and HL-60 cells in high level and not in CLL2 and CLL3. Chemotaxis assays was performed using HL-60 cells and cells from CLL1. Selected cells were transfected with either a non-targeting or S100A4-targeting siRNA which was maintained in medium for 48 hours. In parallel, cells were treated with either 0.5 μM BAY-11-7082 or BAY-11-7085 inhibitor for 24 hours. As a control, untreated cells were used. Following this, the cells were seeded in the transwell insert that was coated with 10 μg/ml fibronectin (see Materials and Methods chapter for details). After 3 hours of incubation, the number of migrated cells was counted (Table 5.3). As was hypothesised, knockdown of S100A4 expression reduced the ability of cells to migrate significantly (Figures 5.5A and 5.6A; $p< 0.05$). The level of knockdown was confirmed by Western blotting analysis (Figures 5.5B and 5.6B). The results are presented an average of three independent experiments performed in triplicate. Two way ANOVA was used to assess the statistical significance.

Cells	Used SiRNA	% Migrated cells in experiment 1	% Migrated cells in experiment 2	% Migrated cells in experiment 3	% Migrated cells in experiment 1	% Migrated cells in experiment 2	% Migrated cells in experiment 3	% Migrated cells in experiment 1	% Migrated cells in experiment 2	% Migrated cells in experiment 3
		Untreated cells (DMSO)			Treated with 0.5 µM BAY-11-7082			Treated with 0.5 µM BAY-11-7085		
HL-60 Cells ($1x10^6$)	siControl	9	8.8	10.5	8	7.2	7.06	7.5	8.4	6.9
	siS100A4	4	4	4.2	4.5	3.9	4.2	3.6	4.28	3.5
CLL1 cells ($1x10^6$)	siControl	13.2	11	12	11	9.5	11.3	9.78	10.8	9.9
	siS100A4	5.6	5.0	6.0	5.3	4.88	5.7	4.43	5.08	4.6

Table 5.3 Migration analysis of HL-60 and CLL1 cells transfected with a non-targeting or S100A4-targeting siRNA 48 hrs and treated with BAY-11-7082 or BAY-11-7085 inhibitors for 24 hrs.

Chemotaxis assay was performed using CLL1 and HL-60 cells that were transfected with a non-targeting or S100A4-targeting siRNA for 48hr and treated with BAY 11-7082 and BAY 11-7085 inhibitors for 24hr. Cells were prepared at the concentration of 1 x 10^6 cells/100µl in the migration medium (DMEM (for HL-60) or RPMI (for cells from CLL1) and 0.1% BSA). Medium containing 10% fetal bovine serum was used as a chemo-attractant. Prepared 100µl of cells was added in the upper chamber and 600 µl of medium with serum as chemo-attractant was added to the lower chamber. After three hours of incubation, the average number of cells migrated through was counted.

A

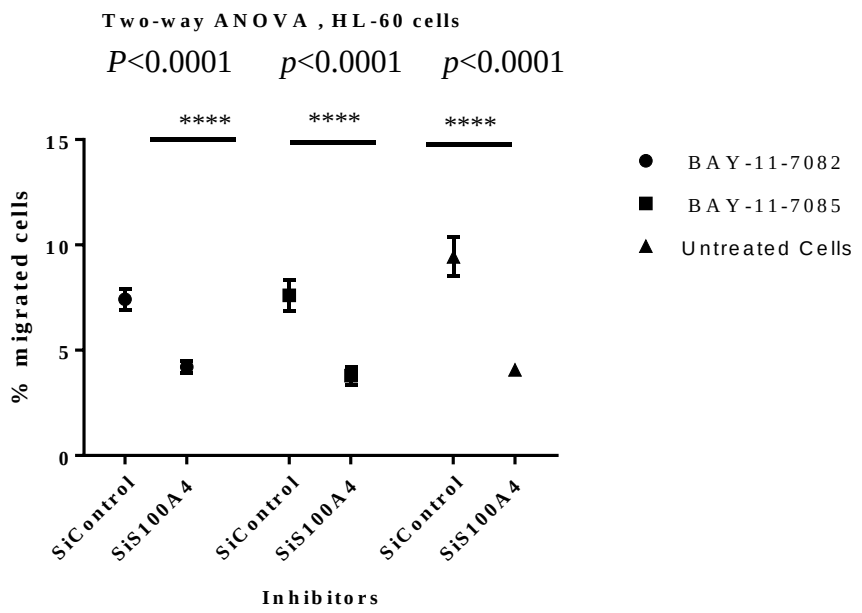

B

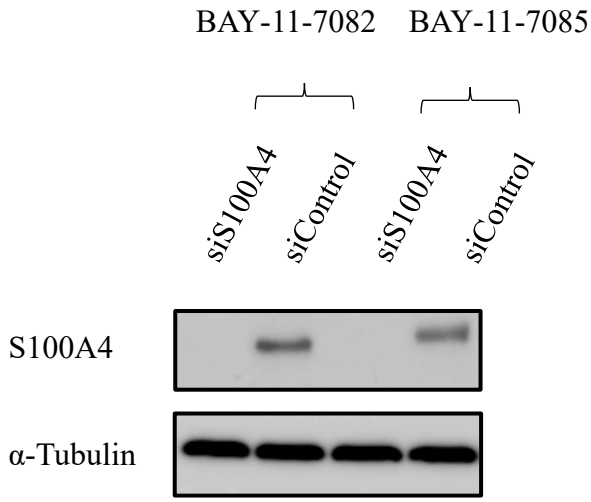

Figure 5.5 Effect of S100A4 on the migration ability of HL-60 cells treated with BAY-11-7082 or BAY-11-7085 inhibitor.

(A) HL-60 cells were transfected (48 hours) with either a non-targeting or S100A4-targeting siRNA and treated for 24hr in the presence of Bay 11-7082 or Bay 11-7085. These cells were used in chemotaxis assay. The results presented the average of three independent experiments performed in triplicate. A Student's T-test was used to assess the statistical significance where $P<0.05$. (B) In parallel, the efficiency of the S100A4 knockdown was evaluated by the Western blot. Cells lysates of the transfected and treated cells were prepared and resolved into 15% SDS-polyacrylamide gel. Then proteins were transferred and the expression of S100A4 was detected using rabbit polyclonal anti-S100A4 from Proteintech (dilution 1:1000). Tubulin was used as a loading control.

A

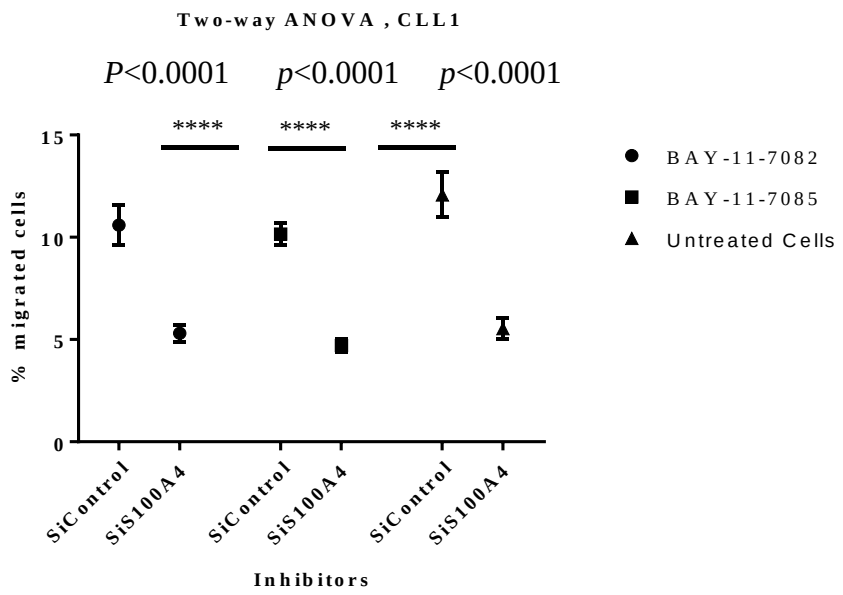

B

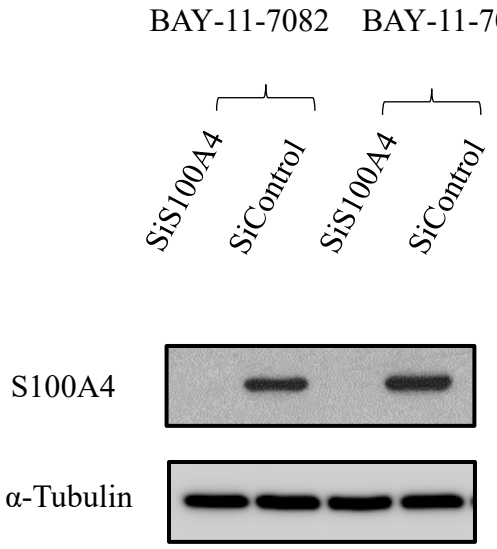

Figure 5.6 Effect of S100A4 on the migration ability of CLL1 cells treated with BAY-11-7082 or BAY-11-7085 inhibitor.

(A) CLL1 cells were transfected (48 hours) with either a non-targeting or S100A4-targeting siRNA and treated for 24hr in the presence of Bay 11-7082 or Bay 11-7085. These cells were used in chemotaxis assay. The results presented the average of three independent experiments performed in triplicate. A Student's T-test was used to assess the statistical significance where $P<0.05$. (B) In parallel, the efficiency of the S100A4 knockdown was evaluated by the Western blot. Cells lysates of the transfected and treated cells were prepared and resolved into 15% SDS-polyacrylamide gel. Then proteins were transferred and the expression of S100A4 was detected using rabbit polyclonal anti-S100A4 from Proteintech (dilution 1:1000). Tubulin was used as a loading control.

5.3 Discussion

S100 proteins have critical roles in inflammation, cytoskeleton dynamics, enzyme activity, in addition to cell growth and differentiation (Emberley et al., 2004; Heizmann et al., 2002; Roth et al., 2003). Various studies have shown that S100 proteins are involved in pathological conditions, especially with regard to tumour progression (Emberley et al., 2004). For example, S100A2, S100A4, S100A6, S100A7, and S100B were found to be differentially expressed in cancer cells, while S100A12 was detected at a high level in synovial tissues of arthritis patients (Foell et al., 2003). However, members of the S100 protein family are important, their function is specific but not always well characterised. Over the last decade, S100A4 has been associated with many cancer pathogenesis. S100A4 was shown to stimulate matrix metalloproteinase (MMP)-13 secretion through the receptor for advanced glycation end products (RAGE) in chondrocytes. Moreover, S100A4 plays critical roles in tumour progression by increasing tumour cell migration, invasion and MMPs secretion (Sherbet, 2009). Roles of S100A4 intracellularly and extracellularly have been studied. Intracellularly, S100A4 binds to the tumour suppressor protein p53, and promotes tumour survival; tumour cell migration that controlled through interactions with non-muscle myosin II. Extracellularly, S100A4 can interact with receptors such as RAGE, stimulating nuclear factor-kappaB (NF-κB) and mitogen-activated protein kinase pathways for tumour cell invasion and survival (Boye and Mælandsmo, 2010). Role of S100A4 in activation of NF-κB signalling via RAGE was characterised in many cells such as endothelial cells, macrophages, and lymphocytes (Yamazaki et al., 2009). Therefore, we postulated that inhibitors with a dual function against NF-κB signalling pathway and also S100A4 compromising S100A4 function could be used as a therapeutic inhibition of B-cell migration of HL-60 cell line and CLL samples. The present work demonstrated that two anti-S100A4 compounds, BAY-11-7082 and BAY-11-7085, were not cytotoxic for human HL-60 cell line and B-lymphocytes of CLL samples. Importantly, these inhibitors has a critical role in suppression of B-cell migration.

5.3.1 S100A4 and p65 are expressed in cells of HL-60 and CLL samples

BAY-11-7082 and BAY-11-7085 inhibitors are well-known as inhibitors of NF-κB signalling But their effect was detected only in high, millimolar concentrations. In the present study they were used as specific S100A4 inhibitors that interact with S100A4 in nanomolar concentrations and prevent interactions with known targets. Thus, in spite of the fact that NF-κB signalling is often activated in CLL, we decided to check expression of the transcription factor p65, a subunit of the nuclear factor NF-κB, in the selected samples of CLL. Western blot analysis was done using lysates of HL-60 cells and three different CLL cells. The results showed that both S100A4 and p65 were expressed in all samples but at different level of expression (Figure 5.1). Our results are in agreement with others that demonstrated positivity of p65 expression and S100A4 in a variety of cell systems (Hsieh et al., 2004; Pedersen et al., 2004; Schmidt-Hansen et al., 2004; Yammani et al., 2006).

5.3.2 BAY-11-7082 and BAY-11-7085 inhibitors are not toxic

The effect of BAY-11-7082 and BAY-11-7085 inhibitors on HL-60 cells was analysed. Cells viability was analysed after overnight treatment. Except clumping after treatment with BAY-11-7082, no any other effect were detected (Figure 5.2). In contrast to our finding, a study of Berger et al., 2007 showed that cell morphology is effected by Bay 11-7085 inhibitor but this may due to high concentration of inhibitors. They found that cells treated with 2μM (high concentration) BAY 11-7085 for one day were caused the dissolution of the cytoplasm and the appearance of condensed pyknotic nuclei (Berger et al., 2007).

5.3.3 BAY-11-7082 and BAY-11-7085 inhibitors slow down migration of HL-60 cells and CLL lymphocytes via blocking S100A4 effect

The present work demonstrated that two anti–S100A4 compounds, BAY-11-7082 and BAY-11-7085, were affecting migration of cells of HL-60 and CLL patient peripheral blood samples. However, BAY-11-7085 was more efficient than BAY-11-7082. Moreover, the significant effect on cell migration was confirmed using CLL samples too especially on one of the tested samples CLL1 (Figures 5.3 and 5.4). This may be due to the higher level of S100A4 expression in CLL1 cells in comparison with CLL2 and CLL3 (Figure 5.1).

Our study showed that the effect of inhibitors in cell migration was due to the suppression of S100A4 protein function (Figures 5.3 and 5.4). NF-κB may or may not has been involved. Thus, further studies are needed to understand the effect of NF-κB in parallel to S100A4 in cell migration. However, BAY-11-7082 and BAY-11-7085 are usually used as inhibitors for NF-κB signalling. Many researchers have linked S100A4 and NF-κB effects in cell migration. They found that activation of the NF-κB pathway by S1004 seems to involve RAGE which interacts with diverse ligands and binds to integrins, consequently stimulating some cellular functions as cell proliferation, motility and metastasis. Of note, the induction of cell migration by S100A4 is inhibited by the inhibition of RAGE using siRNA. This also inhibited the phosphorylation of ERK and MMP-2 (Spiekerkoetter et al., 2009).

Studies demonstrated that S100A4 is one of the regulators of tumour progression and metastasis. The role of S100A4 in cancer has been studied most widely in breast cancer models, in which they have demonstrated that overexpression of S100A4 in nonmetastatic mammary tumour cells associates with a metastatic phenotype (Davies et al., 1993; Grigorian et al., 1996). In a previous chapter, it was identified that S100A4 has a critical role in regulating migration of lymphocytes. Here, we showed that S100A4 could be used as therapeutic target in lymphoma treatment, especially in CLL via its effect on the CLL cycle. However, the mechanism responsible for S100A4 activation and function in lymphocytes is largely unknown and needs further investigation.

S100A4 is able to interact with multiple protein targets and can be considered as a regulator of different signalling systems and induce several biological activities highly significant in the context of cancer and that would make it an eminently valuable chemotherapeutic target. Some downstream effectors of S100A4 pathways might also provide themselves as targets of interest. It is now an indubitable fact that S100A4 expression is activated under certain circumstances and this leads to abnormal cell behaviour.

Recent studies have shown that S100A4 is important in the migration of many types of human cancers by its regulation of the NF-κB /MMP-2/9 signalling that activate cell invasion (Jia et al., 2013; Yang et al., 2013). In this study, we determined the effects of S100A4 in lymphocyte migration using chemotaxis assays.

5.4 Conclusion

Aberrant overexpression of S100A4 by CLL cells promotes migration of CLL cells into secondary tissue sites (especially in poor prognostic group) and is a promising novel target for developing therapeutic approaches in B-cell malignancies.

Chapter 6. General discussion and future directions

6.1 Discussion

Hematological B-cell malignancies include a large, heterogeneous group of lymphoproliferative disorders. These diseases range from less aggressive, indolent non-Hodgkin lymphomas (NHLs), for example follicular lymphoma (FL), to fast-growing or more aggressive NHL forms, such as diffuse large B-cell lymphoma (DLBCL) (Hallek, 2015). More than 85% of NHL cases are B-cell malignancies (National Cancer Institute, 2017). Statistics data from USA and UK show evidence that the annual rate has been increasing steadily since the 1970s (Fisher and Fisher, 2004) (Cancer Research UK, 2017). NHLs affect the elderly population more than the younger population, with NHL diagnoses commonly among patients aged 65–74 years (National Cancer Institute, 2017). In the USA, a projection of population dynamics for CLL patients expects that 199,000 patients will have the disease in 2025, partly driven by improved survival (Chen et al., 2017). In view of the aging population worldwide, B-cell haematologic malignancies diagnosis and treatment are to remain a significant focus for healthcare providers for the future.

The S100 protein family has been involved in different stages of tumourigenesis and progression. Among the *S100* genes, 22 are located at chromosome locus 1q21, a region commonly rearranged in cancers. S100 proteins have different intracellular and extracellular functions, including: calcium homeostasis regulation, proliferation, apoptosis, cell invasion and motility, cytoskeleton rearrangements, protein phosphorylation, transcription factors regulation, autoimmunity, chemotaxis and inflammation. Many studies suggest that changed S100 proteins expression is associated with tumour progression and prognosis. Hence, S100 proteins might also represent potential tumour biomarkers and therapeutic targets (Chen et al., 2014). Specific proteins of the S100 family, S100A4 and S100A6, are associated with different biological processes which are important in tumourgenesis and cancer progression. They exert their activity in stimulating metastasis through interaction with their target proteins (Bresnick et al., 2015a; Chen et al., 2014) that have a regulatory impact on cell migration and invasion (Gross et al., 2014).

In this study, we have summarized the evidence connecting S100A4 protein, as a new potential biomarker in B-cell lymphomas and discuss its function in cell migration. We found that S100A4 and S100A6 proteins were not expressed in normal B-lymphocytes of the tonsil, spleen or thymus, while they were expressed in T-lymphocytes, macrophages, and in a fraction of fibroblasts (in agreement with data from (Grigorian et al., 1994; Grigorian et al., 1993; Takenaga et al., 1994b)). Also, expression of S100A4 was observed in B-lymphocytes in cases of B-cell lymphomas (except FL) but not S100A6 by IHC using 60 blocks of different lymphoma cases. As an expression of S100A4 was present in the majority of the CD20 positive cells, further focus of this study was on the analysis of the role of S100A4 protein in CLL development.

S100A6 expression is directly correlated with the neoplastic phenotype in solid malignancies, for example being activated in pancreatic cancer (Vimalachandran et al., 2005), thyroid (Brown et al., 2006) and colorectal (Komatsu et al., 2000) cancers. However, no investigation was performed with regard to the expression of S100A6 in lymphomas. Furthermore, the clinicopathologic significance of S100A6 was not provided. The result of the current research suggested that S100A6 protein expression is strongly present in T-lymphocytes while not in B-lymphocytes. Regarding the expression of S100A4 in B-cell lymphomas, there is no publications, but a similar investigation was done on breast cancer. They found that a major fraction of S100A4 positive cells in stroma were fibroblasts. Other blood cells such as macrophages (CD68 positive), mast cells (mast-cell tryptase positive) or neutrophils (neutrophil elastase positive) were also identified as S100A4 positive. Only a fraction of T-lymphocytes (CD3 positive) present in stroma expressed S100A4, while B-lymphocytes (CD20 positive) were negative. Nevertheless, in normal breast sections, they found that all of the above mentioned cells were also present, but S100A4 was expressed at a reduced level. The expression of S100A4 in a variety of immune cells circulating in the peripheral blood was also detected by double immunofluorescence. Around 90% of monocytes and granulocytes expressed S100A4, while only less than half of T-lymphocytes were S100A4 positive. Also, more than 60% of the NK cells expressed S100A4, while less than 10% of the B-lymphocytes were S100A4 positive (Cabezon et al., 2007).

In the current study, the expression of S100 proteins was analysed in parallel with analysis expression of the EMT transcription factors, ZEB1 and ZEB2, which are important regulators of cancer progression. It was shown that a high to medium expression of ZEB1 was present in multiple cells of the germinal centre as well as in cells of the non-germinal centre but absent in squamous epithelial cells of the normal lymphoid organs. Cells that expressed ZEB1 were T-cells, endothelial cells and fibroblasts. On the other hand, in a few B-cell lymphoma samples, a moderate to low expression of ZEB1 was found. However, majority of samples showed a negative expression of ZEB1. The study of (Sánchez-Tilló et al., 2014) published contrary data. However, our data is supported by some published data (Lemma et al., 2013). There is a study that shows different results to ours (Sánchez-Tilló et al., 2014). It shows that ZEB1 was expressed strongly in MCL. Probably, the discrepancy may due to the insufficient amount of the MCL samples in our study (6 samples). Authors found that that ZEB1 promoted cell proliferation, enhanced tumour growth and an influence on the resistance to chemotherapy in MCL. Also, ZEB1 could be a predictive biomarker and a therapeutic target in this type of lymphoma. They showed that ZEB1 is overexpressed in MCLs with active Wnt signalling. Expression of ZEB1 was controlled by Wnt signalling, and being downregulated by β-catenin knockdown or blocking of Wnt signalling by salinomycin in MCL cells. Moreover, ZEB1 knockdown decreased *in vitro* cell viability and proliferation. In addition, they showed that ZEB1 expression determined differential resistance to chemotherapy and controlled transporters involved in drug influx/efflux in MCL cells. ZEB1 downregulation by salinomycin raised the sensitivity of MCL cells to the cytotoxic effect of doxorubicin, cytarabine and gemcitabine. Finally, salinomycin and doxorubicin showed a synergistic effect in both established and primary MCL cultures (Sánchez-Tilló et al., 2014). On the other hand, there is a study that agrees with our finding and confirms that ZEB1 expression in B-lymphocytes in DLBCL cases. They found that ZEB1, Slug and Twist were often expressed at different levels in DLBCL, and that ZEB1 is the only one of these EMT TFs expressed in small numbers of reactive lymphocytes. The intensity of expression was varying from low to moderate and this result is in line with our findings. In addition, it was found also in DLBCL, that nuclear expression of both ZEB1 and Slug was related to a poor prognosis (Lemma et al., 2013).

ZEB2 was expressed in mainly T-lymphocytes and endothelial cells in normal lymphoid tissues. However, in 53% of analysed lymphoma samples, it was expressed in B-lymphocytes and its expression was varied from moderate to weak. There was no clear investigation showing correlation between ZEB2 expression and B-cell lymphoma development. In our study, the results show that ZEB2 is expressed in B-lymphocytes of different B-cell lymphomas mainly at the moderate level. There is a study where the role of ZEB2 expression in T-cell acute lymphoblastic leukemia (T-ALL) was analyzed. It was demonstrated that ZEB2 was an oncogenic driver of immature T-ALL, a heterogenic subgroup of human leukemia characterized by a high incidence of reduction failure or hematological relapse after conventional chemotherapy. Authors showed that lysine-specific demethylase KDM1A was a novel interacting partner of ZEB2 and that in mouse and human T-ALL cultures ZEB2 activity critically depended on KDM1A in cells survival. So, targeting ZEB2 through direct disruption of the ZEB2-KDM1A complex by pharmacological inhibition of the KDM1A demethylase activity might be a novel therapeutic strategy in this aggressive subtype of human leukemia and possibly in other ZEB2-driven malignancies (Goossens et al., 2017). Furthermore, a recent study demonstrated that expression of ZEB2 was upregulated in human lung cancer and knockdown of ZEB2 in lung cancer cell lines such as A549 or NCI-H292 inhibited cell proliferation, whereas overexpression of ZEB2 in lung cancer cell lines, H-125 and H1975, inhibited cell apoptosis (Guo et al., 2018). Thus, ZEB2 may act as a prognostic factor for the diagnosis and treatment of patients with lung cancer (Guo et al., 2018) and T-ALL (Goossens et al., 2017) but not for patients with B-lymphoma.

In our study for the first time, the expression of S100A4 was analysed during lymphocyte development and was correlated with analysis of S100A4 positive cells in CLL bone marrow samples. In pathological normal BM tissue, it was shown that all samples had the same pattern of staining and it was detected that S100A4 was expressed in different types of bone marrow cells including small immature lymphocytes while in CLL BM samples, there were multiple S100A4 positive cells. In general, the level of S100A4 expression was higher in CLL samples compared to normal BM cases. Double immunofluorescence showed that specific haematopoietic stem cell markers CD10, CD34, and CD45 positivity overlapped with S100A4 expression. Moreover, four colour immunofluorescence confirmed the expression of

S100A4 in normal T-cells and CLL T and B-lymphocytes. Thus, there was a significant level of S100A4 expression in haematopoietic stem cells in normal bone marrow and in cancer stem cells in samples of CLL patients. Our results confirm the prediction based on bioinformatics analysis of publically available databases that identified a potential activation of S100A4 expression in B-cells present in bone marrow of CLL patients (G. Kaithakottil, MSc thesis, University of Leicester, 2010).

The current study provides a clear picture of the S100 gene expression in normal and malignant B-lymphocytes of CLL peripheral blood samples by qPCR that showed differential expression at mRNA levels of several members of *S100* genes. Among analysed members of *S100* genes, including, *S100A4*, *S100A5*, *S100A6*, *S100A10*, *S100A11*, *S100A13* and *S10014* genes, mRNA level was found to be upregulated in B-lymphocytes, and associated positively with *ZEB1* and *ZEB2*. The expression of *S100A4* and *S100A6*, meanwhile, was found to be up-regulated in malignant B-lymphocytes more than other S100 genes. As correlated with the absence of S100A4 expression in normal B-lymphocytes of healthy individual (Cabezón et al., 2007), it was strongly expressed in different B-lymphoma cell lines and the blood samples of patients diagnosed with CLL (G. Kaithakottil, MSc thesis, University of Leicester, 2010). Also, qPCR data showed that there was a strong association between *S100A4* and *S100A6* genes and EMT transcript factors, *ZEB1* and *ZEB2*, in CLL, and this association is not exclusive for lymphomas, same results were found but in pancreatic cancer (Chen et al., 2015; Xu et al., 2014). Moreover, it has been shown that S100A4 was an important key mediator of EMT in breast cancer (Xu et al., 2016), hepatocellular carcinoma (Zhai et al., 2014), ovarian cancer (Yan et al., 2016), oesophageal squamous cell carcinoma (Jian et al., 2015) and endometrial cancer (Hua et al., 2016). Additionally, S100A6 has also been found to be, to lesser extent, involved in EMT in hepatocellular carcinoma (Li et al., 2014) and prostate cancer (Orr et al., 2012).

The role S100A4 expression in the survival of patients diagnosed with B-cell lymphomas was unknown. For the first time, the correlation between S100A4 expression and the survival of CLL patients was demonstrated in this study. Survival analysis was generated using a Kaplan-Meier survival plot that showed that low or negative expression of S100A4 was correlated with a statistically significant longer survival, P=0.0215 (<0.05) (Figure 3.29). Thus, our results demonstrated that S100A4

expression correlated with the poorer rate of survival of CLL patients. So, this study confirmed that overexpression of S100A4 was associated with the recurrence and mortality of CLL patients. The present findings are supported by previous studies in other cancers (Boye et al., 2010; Flatmark et al., 2003; Kho et al., 2012; Lee et al., 2013b), which concluded that the expression of S100A4 was linked to a poor prognosis. Also, in the study by (Stein et al., 2006), it was shown that S100A4 was expressed at a high level in cell populations with a high proportion of cells with features of cancer stem cells, S100A4 expression was linked with Wnt/APC/β-catenin signalling pathway and S100A4 was characterised as β-catenin/TCF target gene (Stein et al., 2006). It was also demonstrated that S100A4 localized in the nucleus, cytoplasm, and secreted to the extracellular space and had a wide range of biological functions ranging from the regulation of angiogenesis to cell survival, motility, and invasion (Boye and Maelandsmo, 2010). Interestingly, S100A4 was also associated with lymphocyte infiltration that involved in tumour progression and destroyed tumour budding. In (Boye and Maelandsmo, 2010) study, S100A4 expression was detected in fibroblasts, monocytes, macrophages, T lymphocytes, neutrophilic granulocytes, and endothelial cells and may be misinterpreted as a detection of S100A4 expression in cancer cells (Boye and Maelandsmo, 2010).

In agreement with a lot of research, we found that a high expression of S100A4 stimulates cell migration in HL-60 and CLL cells, while their downregulation reduces the number of migrated cells. Researchers have found that the induction of cell migration by S100A4 is inhibited by the inhibition of RAGE, using siRNA, or/and by the phosphorylation of ERK and MMP-2 (Spiekerkoetter et al., 2009). As characterized before in different studies, S100A4 has a critical role in cell migration. For example, in gastric cancer, they found that S100A4 overexpressed in two gastric cell lines, AGS and SCM-1, and this expression significantly increased the invasive activity of these cells while knockdown of S100A4 expression in MKN-45 and TMK-1, which showed high levels of endogenous S100A4, caused in a decrease in the migration rate but without any effect on cell survival (Yuan et al., 2014). Therefore, novel treatment strategies targeting S100A4 could be developed. Several publications support our results that S100A4 might contribute to the regulation of malignant cells migration (Ford et al., 1995; Jenkinson et al., 2004; Takenaga et al., 1994a; Takenaga et al., 1997).

The result of our study showed that two anti–S100A4 compounds, BAY-11-7082 and BAY-11-7085, were efficient small molecule inhibitors of human lymphocyte migration isolated from HL-60 and CLL patient peripheral blood samples. Neither of the inhibitors were toxic. However, BAY-11-7085 was more potent than BAY-11-7082 but the cells were relatively resistant to both inhibitors. The effect of inhibitors in cell migration was due to a compromise of the function of S100A4 protein effect. However, the mechanism responsible for S100A4 activation and function in lymphocytes is largely unknown and needs further investigation. Rresearchers have linked S100A4 and NF-κB effects in cell migration. They found that activation of the NF-κB pathway by S1004 seems to involve RAGE which interacts with diverse ligands and binds to integrins, consequently stimulating some cellular functions as cell proliferation, motility and metastasis. Of note, the induction of cell migration by S100A4 is inhibited by the inhibition of RAGE using siRNA. This also inhibited the phosphorylation of ERK and MMP-2 (Spiekerkoetter et al., 2009). Studies demonstrated that S100A4 is one of the regulators of tumour progression and metastasis. The role of S100A4 in cancer has been studied most widely in breast cancer models, in which they have demonstrated that overexpression of S100A4 in nonmetastatic mammary tumour cells associates with a metastatic phenotype (Davies et al., 1993; Grigorian et al., 1996).

The present results identified that S100A4 induced the migration of lymphocytes in CLL. Transfection experiments using RNAi approach to downregulate expression of S100A4 following treatment with inhibitors showed that BAY-11-7082 and BAY-11-7085 inhibitors were interfering with migration via S100A4 supressing. However, (1) our observations were based on an *in vitro* experiments and not on the use of an animal model, and thus, the conclusions drawn may need to be confirmed by further experiments; (2) thus far, we do not know whether the down-regulation of S100A4 could inhibit NF-κB signalling and invasion *in vitro* and *vivo*. Therefore, the evidence suggests that S100A4 inhibitors can be used potentially as a treatment for CLL patients and further studies are needed to demonstrate the relation between the NF-κB activity, the nuclear translocation of NF-κB p65, as well as the MMP-9 regulation and S100A4 expression in lymphomas.

Other scientists have tried to use inhibitors to S100A4 but in solid cancers. Sack et al. have used experimental regime to show that the antihelminth drug (Niclosamide) is downregulated expression of S100A4 with parallel inhibition of cell functions,

including: proliferation, migration and metastatic spread, of colon cancer cells in xenograft tumour models (Sack et al., 2011).

The effect of the used compounds on CLL cells migration indicates that these inhibitors can be considered as dual inhibitors for treatment of CLL patients should be checked further based on the different range affinities with the target proteins (S100A4 and NF-κB).

6.2 Conclusion and future directions

S100A4 protein has a critical role in the development and progression of tumours based on its multifunctional properties and involvement in regulation of different intracellular and extracellular processes. Future studies on larger database of lymphoma cases are needed to further reveal molecular mechanisms and signaling pathways that describe many roles that S100A4 protein plays in tumour progression and metastasis, providing novel therapeutic targets and biomarkers.

Our study shows that the expression of S100A4, S100A6, ZEB1 and ZEB2 are mainly present in T-lymphocytes in normal lymphoid organs while some expressed B and T-lymphocytes in analysed B-cell lymphoma cases except FL. However, there is no significant correlation between S100A4 and ZEB family in B-cell lymphoma cases. In addition, S100A6 shows negative expression in analysed lymphoma samples so, we focused on analysis of S100A4 expression and its roles in B-cell lymphoma specially CLL. S100A4 was expressed in stem cells in both pathological normal and CLL BM samples but the level of expression was higher in BM of CLL case indicating that S100A4 expression can be considered as a potential biomarker of CLL. S100A4 has a critical role in cell migration and its overexpression promotes migration of CLL cells and is a promising novel target for (combinational) therapy.

Further studies are expected to investigate the role of S100A4 protein in the B-cell lymphomas and study the underlying mechanism, which may facilitate in cancer development, diagnosis, treatment and also prevention of cancer.

Finally, the clinical interest studying S100A4 protein is expected to expand. S100A4 protein not only provides important diagnostic and prognostic tools in management of B-cell lymphomas especially CLL, but also the inhibition of S100A4 activity may represent a possible means of controlling cancer development and progression.

Appendixes

Appendix 1. Updated classification of lymphoid neoplasms.

Mature B-cell neoplasms
Chronic lymphocytic leukemia
Monoclonal B-cell lymphocytosis*
B-cell prolymphocytic leukemia
Splenic marginal zone lymphoma
Hairy cell leukemia
Splenic B-cell lymphoma/leukemia, unclassifiable
Splenic diffuse red pulp small B-cell lymphoma
Hairy cell leukemia-variant
Lymphoplasmacytic lymphoma
Waldenström macroglobulinemia
Monoclonal gammopathy of undetermined significance (MGUS), IgM*
μ heavy-chain disease
γ heavy-chain disease
α heavy-chain disease
Monoclonal gammopathy of undetermined significance (MGUS), IgG/A*
Plasma cell myeloma
Solitary plasmacytoma of bone
Extraosseous plasmacytoma
Monoclonal immunoglobulin deposition diseases*
Extranodal marginal zone lymphoma of mucosa-associated lymphoid tissue (MALT lymphoma)
Nodal marginal zone lymphoma
Pediatric nodal marginal zone lymphoma
Follicular lymphoma
In situ follicular neoplasia*
Duodenal-type follicular lymphoma*
Pediatric-type follicular lymphoma*
Large B-cell lymphoma with IRF4 rearrangement*
Primary cutaneous follicle center lymphoma
Mantle cell lymphoma
In situ mantle cell neoplasia*
Diffuse large B-cell lymphoma (DLBCL), NOS
Germinal center B-cell type*
Activated B-cell type*
T-cell/histiocyte-rich large B-cell lymphoma
Primary DLBCL of the central nervous system (CNS)
Primary cutaneous DLBCL, leg type
EBV+ DLBCL, NOS*
EBV+ mucocutaneous ulcer*
DLBCL associated with chronic inflammation
Lymphomatoid granulomatosis
Primary mediastinal (thymic) large B-cell lymphoma

Intravascular large B-cell lymphoma
ALK+ large B-cell lymphoma
Plasmablastic lymphoma
Primary effusion lymphoma
HHV8+ DLBCL, NOS*
Burkitt lymphoma
Burkitt-like lymphoma with 11q aberration*
High-grade B-cell lymphoma, with MYC and BCL2 and/or BCL6 rearrangements*
High-grade B-cell lymphoma, NOS*
B-cell lymphoma, unclassifiable, with features intermediate between DLBCL and classical Hodgkin lymphoma
Mature T and NK neoplasms
T-cell prolymphocytic leukemia
T-cell large granular lymphocytic leukemia
Chronic lymphoproliferative disorder of NK cells
Aggressive NK-cell leukemia
Systemic EBV+ T-cell lymphoma of childhood*
Hydroa vacciniforme–like lymphoproliferative disorder*
Adult T-cell leukemia/lymphoma
Extranodal NK-/T-cell lymphoma, nasal type
Enteropathy-associated T-cell lymphoma
Monomorphic epitheliotropic intestinal T-cell lymphoma*
Indolent T-cell lymphoproliferative disorder of the GI tract*
Hepatosplenic T-cell lymphoma
Subcutaneous panniculitis-like T-cell lymphoma
Mycosis fungoides
Sézary syndrome
Primary cutaneous CD30+ T-cell lymphoproliferative disorders
Lymphomatoid papulosis
Primary cutaneous anaplastic large cell lymphoma
Primary cutaneous γδ T-cell lymphoma
Primary cutaneous CD8+ aggressive epidermotropic cytotoxic T-cell lymphoma
Primary cutaneous acral CD8+ T-cell lymphoma*
Primary cutaneous CD4+ small/medium T-cell lymphoproliferative disorder*
Peripheral T-cell lymphoma, NOS
Angioimmunoblastic T-cell lymphoma
Follicular T-cell lymphoma*
Nodal peripheral T-cell lymphoma with TFH phenotype*
Anaplastic large-cell lymphoma, ALK+
Anaplastic large-cell lymphoma, ALK−*
Breast implant–associated anaplastic large-cell lymphoma*
Hodgkin lymphoma
Nodular lymphocyte predominant Hodgkin lymphoma
Classical Hodgkin lymphoma
Nodular sclerosis classical Hodgkin lymphoma
Lymphocyte-rich classical Hodgkin lymphoma
Mixed cellularity classical Hodgkin lymphoma
Lymphocyte-depleted classical Hodgkin lymphoma

Posttransplant lymphoproliferative disorders (PTLD)
Plasmacytic hyperplasia PTLD
Infectious mononucleosis PTLD
Florid follicular hyperplasia PTLD*
Polymorphic PTLD
Monomorphic PTLD (B- and T-/NK-cell types)
Classical Hodgkin lymphoma PTLD
Histiocytic and dendritic cell neoplasms
Histiocytic sarcoma
Langerhans cell histiocytosis
Langerhans cell sarcoma
Indeterminate dendritic cell tumour
Interdigitating dendritic cell sarcoma
Follicular dendritic cell sarcoma
Fibroblastic reticular cell tumour
Disseminated juvenile xanthogranuloma
Erdheim-Chester disease*

Provisional entities are listed in italics.↵* Changes from the 2008 classification.
Copied from (Arber et al., 2016).

Appendix 2. *In vivo* cancer phenotypes of S100 family members.

Cancer	Family member	Model systems	Phenotype
Breast	S100A1	Xenograft	↑ Growth
	S100A4	Xenograft and GEMM	↑ Metastasis
	S100A7	Xenograft and GEMM	↑ ↓ Growth
	S100A8	Xenograft	↑ Metastasis
Osteosarcoma	S100A4	Xenograft	↑ Metastasis
Oral	S100A2	Xenograft	↓ Growth
	S100A7	Xenograft	↓ Proliferation and ↓ metastasis
Head and neck	S100A4	Xenograft	↑ ↓ Growth and ↑ metastasis
Lung	S100A2	Xenograft	↔ Growth and ↑ metastasis
	S100A4	Xenograft	↑ Metastasis
	S100A9	GEMM	↓ Inflammation
	S100A10	Xenograft	↑ Growth and ↑ immune evasion
	S100A11	Xenograft	↑ Growth
	S100P	Xenograft	↑ Angiogenesis and ↑ metastasis
Prostate	S100A3	Xenograft	↑ Growth
	S100A4	Xenograft and GEMM	↑ Growth, ↑ metastasis and ↑ angiogenesis
	S100A9	GEMM	↑ Growth, ↑ metastasis and ↑

Cancer	Family member	Model systems	Phenotype
			angiogenesis
	S100A8 and S100A9	Xenograft	↔ ↓ Growth, ↔ metastasis and ↓ inflammation
	S100P	Xenograft	↑ Growth
Colorectal	S100A4	Xenograft	↑ Metastasis
	S100A8 and S100A9	Xenograft	↑ Growth and ↑ metastasis
	S100P	Xenograft	↑ Growth and ↑ metastasis
Brain	S100A4	Xenograft	↑ Metastasis
	S100A9	Xenograft	↑ Growth
	S100B	Xenograft	↑ Growth, ↑ angiogenesis and ↑ inflammation
Gastric	S100A4	Xenograft	↑ Growth
	S100A6	Xenograft	↑ Growth and ↓ metastasis
Bladder	S100A4	Xenograft	↑ Metastasis
Lymphoma	S100A9	Xenograft	↑ Growth and ↑ immune evasion
Pancreas	S100A4	Xenograft	↑ Growth and ↑ angiogenesis
	S100P	Xenograft	↑ Growth and ↑ metastasis
Melanoma	S100A4	Xenograft	↑ Growth and ↑ angiogenesis
	S100A9	Xenograft	↑ Metastasis
	S100B	Xenograft and GEMM	↑ Growth
Renal	S100A4	Xenograft	↑ Growth and ↑ metastasis

Cancer	Family member	Model systems	Phenotype
Liver	S100A14	Xenograft	↑ Growth and ↑ metastasis
Thyroid	S100A4	Xenograft	↑ Growth and ↑ metastasis
	S100A8	Xenograft	↑ Growth and ↑ metastasis
	S100A11	Xenograft	↑ Growth
Thymus	S100A8 and S100A9	Xenograft	↑ Growth and ↑ immune evasion

***In vivo* cancer phenotypes of S100 family members.**

Copied from (Bresnick et al., 2015).

Appendix 3. Statistical tables of qPCR analysis.

ΔCt = (Average of gene - Average of housekeeping gene)
ΔΔCt= ΔCT gene-ΔCT control
RQ or npower= 2-ΔΔCt

B2M (housekeeping gene)				
	Cp1	Cp2	Cp3	Average
B-CELL NORMAL (blood samples from 5 volunteers)	19.74	19.85	20.04	19.87667
CCL-1	16.78	17.12	17.53	17.14333
CCL-2	17.46	17.89	18.24	17.86333
CCL-3	17.93	18.31	18.45	18.23
CCL-4	16.9	17.05	17.34	17.09667
CCL-5	17.71	17.76	17.86	17.77667

S100A1							
	Cp1	Cp2	Cp3	Average	dCt	ddCt	Fold change
B-CELL NORMAL (blood samples from 5 volunteers)	39.35	40.92		40.135	20.25833	0	1
CCL-1	40.93	39.93		40.43	23.28667	3.028333	8.158666
CCL-2	42.87			42.87	25.00667	4.748333	26.87762
CCL-3	42.34	41.91	43.41	42.55333	24.32333	4.065	16.73736
CCL-4	38.37			38.37	21.27333	1.015	2.020903
CCL-5	39.8	40.25	39.84	39.96333	22.18667	1.928333	3.806152

S100A2							
	Cp1	Cp2	Cp3	Average	dCt	ddCt	Fold change
B-CELL NORMAL (blood samples from 5 volunteers)	31.85	32.07	33.12	32.34667	12.47	0	1
CCL-1	32.65	32.61	32.65	32.63667	15.49333	3.023333	0.122995
CCL-2	32.15	31.88	31.99	32.00667	14.14333	1.673333	0.313528
CCL-3	32.42	32.48	31.97	32.29	14.06	1.59	0.332171
CCL-4	32.91	32.45	32.39	32.58333	15.48667	3.016667	0.123564
CCL-5	31.31	31.45	32.07	31.61	13.83333	1.363333	0.388683

S100A3							
	Cp1	Cp2	Cp3	Average	dCt	ddCt	Fold change
B-CELL NORMAL (blood samples from 5 volunteers)	30.64	31.21		30.925	11.04833	0	1
CCL-1	31.84			31.84	14.69667	3.648333	2.552068
CCL-2	32.17	32.6	32.14	32.385	14.52167	3.473333	2.419988
CCL-3	31.7	31.29		31.495	13.265	2.216667	0.215138
CCL-4		31.89		31.89	14.79333	3.745	1.193336
CCL-5		31.48	31.24	31.36	13.58333	2.535	1.380317

S100A4							
	Cp1	Cp2	Cp3	Average	dCt	ddCt	Fold change
B-CELL NORMAL (blood samples from 5 volunteers)	36.79	5.75	35.75	36.09667	16.22	0	1
CCL-1	24.44	27.91	28.53	26.96	9.816667	-6.40333	84.64385
CCL-2	25.46	28.74	30.04	28.08	10.21667	-6.00333	64.14804
CCL-3	26.73	30.96	31.69	29.79333	11.56333	-4.65667	25.22298
CCL-4	25.71	29.35	29.98	28.34667	11.25	-4.97	31.34145
CCL-5	26.33	29.89	30.69	28.97	11.19333	-5.02667	32.59699

S100A5							
	Cp1	Cp2	Cp3	Average	dCt	ddCt	Fold change
B-CELL NORMAL (blood samples from 5 volunteers)	38.08	35.34	36.83	36.75	16.87333	0	1
CCL-1	31.61	32.23	32.01	31.95	14.80667	-2.06667	4.189176
CCL-2	31.98	31.2	31.44	31.54	13.67667	-3.19667	9.168379
CCL-3	33.82	33.37	35.78	34.32333	16.09333	-0.78	1.717131
CCL-4	31.24	31.2	31.02	31.15333	14.05667	-2.81667	7.045327
CCL-5	31.35	32.19	32.53	32.02333	14.24667	-2.62667	6.175974

S100A6							
	Cp1	Cp2	Cp3	Average	dCt	ddCt	Fold change
B-CELL NORMAL (blood samples from 5 volunteers)	27.01	26.81	27.21	27.01	7.133333	0	1
CCL-1	22.21	22.42	22.44	22.35667	5.213333	-1.92	3.784231
CCL-2	22	22.41	22.53	22.31333	4.45	-2.68333	6.423383
CCL-3	22.51	22.78	22.75	22.68	4.45	-2.68333	6.423383
CCL-4	21.67	22.04	21.99	21.9	4.803333	-2.33	5.028053
CCL-5	21.97	22.15	22.17	22.09667	4.32	-2.81333	7.029068

S100A8							
	Cp1	Cp2	Cp3	Average	dCt	ddCt	Fold change
B-CELL NORMAL (blood samples from 5 volunteers)	29.47	28.94	29.22	29.21	9.333333	0	1
CCL-1	27.63	28.44	28.44	28.17	11.02667	1.693333	0.309212
CCL-2	28.09	28.94	29.18	28.73667	10.87333	1.54	0.343885
CCL-3	29.45	30.18	30.3	29.97667	11.74667	2.413333	0.187722
CCL-4	26.71	27.78	27.87	27.45333	10.35667	1.023333	0.491978
CCL-5	27.8	28.48	28.44	28.24	10.46333	1.13	0.456916

S100A9							
	Cp1	Cp2	Cp3	Average	dCt	ddCt	Fold change
B-CELL NORMAL (blood samples from 5 volunteers)	26.09	26.23	26.53	26.28333	6.406667	0	1
CCL-1	25.69	26.03	25.61	25.77667	8.633333	2.226667	0.213652
CCL-2	26.48	26.47	26.26	26.40333	8.54	2.133333	0.227931
CCL-3	26.83	27.36	27.15	27.11333	8.883333	2.476667	0.179659
CCL-4	24.47	25.01	24.62	24.7	7.603333	1.196667	0.436282
CCL-5	25.06	25.5	25.35	25.30333	7.526667	1.12	0.460094

S100A10							
	Cp1	Cp2	Cp3	Average	dCt	ddCt	Fold change
B-CELL NORMAL (blood samples from 5 volunteers)	26.93	27.06	27.64	27.21	7.333333	0	1
CCL-1	21.62	22.6	22.96	22.39333	5.25	-2.08333	0.235969
CCL-2	22.29	23.51	24.16	23.32	5.456667	-1.87667	0.272312
CCL-3	23.19	24.75	25.18	24.37333	6.143333	-1.19	0.438303
CCL-4	21.92	23.65	23.87	23.14667	6.05	-1.28333	0.410845
CCL-5	22.45	23.89	24.16	23.5	5.723333	-1.61	0.327598

S100A11							
	Cp1	Cp2	Cp3	Average	dCt	ddCt	Fold change
B-CELL NORMAL (blood samples from 5 volunteers)	28.47	28.39	28.28	28.38	8.503333	0	1
CCL-1	25.39	25.16	24.82	25.12333	7.98	-0.52333	0.695762
CCL-2	24.06	24.17	24.03	24.08667	6.223333	-2.28	0.205898
CCL-3	25.34	25.35	25.46	25.38333	7.153333	-1.35	0.392292
CCL-4	25.28	25.11	25.28	25.22333	8.126667	-0.37667	0.770215
CCL-5	25.56	25.58	25.61	25.58333	7.806667	-0.69667	0.616996

S100A12							
	Cp1	Cp2	Cp3	Average	dCt	ddCt	Fold change
B-CELL NORMAL (blood samples from 5 volunteers)	32.25	32.03	32.25	32.17667	12.3	0	1
CCL-1	31.54	31.31	31.89	31.58	14.43667	2.136667	0.227405
CCL-2	31.98	31.95	31.65	31.86	13.99667	1.696667	0.308498
CCL-3	32.1	31.85	31.72	31.89	13.66	1.36	0.389582
CCL-4	30.24	30.46	30.67	30.45667	13.36	1.06	0.479632
CCL-5	29.76	29.63	29.23	29.54	11.76333	0.53667	1.450617

S100A13							
	Cp1	Cp2	Cp3	Average	dCt	ddCt	Fold change
B-CELL NORMAL (blood samples from 5 volunteers)	30.72	30.69	31.04	30.81667	10.94	0	1
CCL-1	26.68	26.63	26.66	26.65667	9.513333	-1.42667	2.688249
CCL-2	26.76	26.72	26.74	26.74	8.876667	-2.06333	4.179509
CCL-3	29.62	29.26	29.39	29.42333	11.19333	0.253333	0.838956
CCL-4	26.05	25.71	25.91	25.89	8.793333	-2.14667	4.428035
CCL-5	26.38	26.33	26.58	26.43	8.653333	-2.28667	4.879275

S100A14							
	Cp1	Cp2	Cp3	Average	dCt	ddCt	Fold change
B-CELL NORMAL (blood samples from 5 volunteers)	42.85			42.85	22.97333	0	1
CCL-1		37.4		37.4	20.25667	-2.71667	0.152125
CCL-2	40.43			40.43	22.56667	-0.40667	0.754364
CCL-3	36.86	36.66	36.93	36.81667	18.58667	-4.38667	0.047806
CCL-4	37.52	36.14		36.83	19.73333	-3.24	0.105843
CCL-5	40.87	38.4	36.27	38.51333	20.73667	-2.23667	0.212176

ZEB1							
	Cp1	Cp2	Cp3	Average	dCt	ddCt	Fold change
B-CELL NORMAL (blood samples from 5 volunteers)	27.67	27.77	27.79	27.74333	7.866667	0	1
CCL-1	22.65	22.8	23.31	22.92	5.776667	-2.09	4.257481
CCL-2	23.94	24.32	24.61	24.29	6.426667	-1.44	2.713209
CCL-3	25.96	26.43	26.47	26.28667	8.056667	-0.19	0.876606
CCL-4	23.11	23.28	23.49	23.29333	6.196667	-1.67	3.182146
CCL-5	22.24	22.22	22.46	22.30667	4.53	-3.33667	10.10268

ZEB2							
	Cp1	Cp2	Cp3	Average	dCt	ddCt	Fold change
B-CELL NORMAL (blood samples from 5 volunteers)	27.64	28.58	29.54	28.58667	8.71	0	1
CCL-1	23.69	24.4	24.71	24.26667	7.123333	-1.58667	3.003546
CCL-2	24.55	25.29	25.19	25.01	7.146667	-1.56333	2.955359
CCL-3	27.93	29.05	28.92	28.63333	10.40333	-1.69333	0.309212
CCL-4	24.72	25.57	25.75	25.34667	8.25	-0.46	1.375542
CCL-5	24.34	25.01	25.19	24.84667	7.07	-1.64	3.116658

Appendix 4. The list of attended conferences

S100A4 & S100A6 Protein Expression in B-Cell Lymphomas

Zamzam Almutairi[1], Kevin West[2], Sandrine Jayne[1] and Marina Kriajevska[1]

[1] Department of Cancer Studies and Molecular Medicine, University of Leicester, Leicester, UK. [2] Department of Pathology in Leicester Royal Infirmary, Leicester, UK.

B-cell lymphomas are clinically, pathologically and molecularly heterogeneous disease. They are classified according to the morphologic, genotypic, and biologic features of the lymphoma cells present in the diagnostic samples. A variety of research was performed to develop prognostic markers to characterize the stages of disease. Studies have shown a link between some members of the S100 protein family expression and neoplastic disorders. Some of the S100 proteins are overexpressed in multiple cancers and has been shown to be correlated with poor prognosis. S100 proteins are important for metastatic development in different tumours. Until today there is no investigation about expression and the role of these proteins in B-cells lymphoma. In order to investigate the role of S100 proteins as prognostic markers in B-cell lymphoma we performed bioinformatics analysis. Two proteins from the S100 family, S100A4 and S100A6, were activated in DLBCL and CLL. An immunohistochemistry analysis of 60 blocks of different types of lymphomas has shown a positive expression of S100A4 in the majority of CLL, MCL, DLBCL cases and no expression was detected in the analysed follicular lymphoma cases. However, S100A6 expression was not detected in all analysed lymphoma cases. Detailed analysis of bone marrow haematopoietic stem cell (HSC) samples has shown a co-expression of S100A4 with CD34, CD133 and CD10 indicating that S100A4 expression can be considered as a potential biomarker of HSC in B-cells lymphoma.

Key words: B-cells lymphoma, DLBCL, CLL, S100A4 protein, S100A6 protein.

This abstract submitted to EMBO Conference: Advances in Stem Cells and Regenerative Medicine (23/05/2017 - 26/05/2017) Heidelberg, Germany.

S100A4 protein regulates cell trafficking in B-Cell Lymphomas

Zamzam Almutairi[1], Kevin West[2], Sandrine Jayne[1] and Marina Kriajevska[1]

[1] Department of Cancer Studies and Molecular Medicine, University of Leicester, Leicester, UK. [2] Department of Pathology in Leicester Royal Infirmary, Leicester, UK.

B-cell lymphomas are clinically, pathologically and molecularly heterogeneous disease. They are classified according to the morphologic, genotypic, and biologic features of the lymphoma cells present in the diagnostic samples. Various researches were performed to develop prognostic markers to characterize the stages of disease. Studies have shown a link between some members of the S100 protein family expression and neoplastic disorders. Some of the S100 proteins are overexpressed in multiple cancers and has been shown to be correlated with poor prognosis. S100 proteins are important for metastatic development in different tumours. Up to the present time there has been no investigation about expression and role of these proteins in B-cell lymphomas. In order to investigate the role of S100 proteins as prognostic markers in B-cell lymphoma we performed bioinformatics analysis. Two proteins from the S100 family, S100A4 and S100A6, were activated in DLBCL and CLL. An immunohistochemistry analysis of 60 blocks of different types of lymphomas has shown a positive expression of S100A4 in the majority of CLL, MCL, DLBCL cases and no expression was detected in the analysed follicular lymphoma cases. However, S100A6 expression was not detected in all analysed lymphoma cases. Western blotting analysis of the peripheral blood samples of CLL patients showed a high level of S100A4 expression in most samples. Low or negative expression of S100A4 correlated with a longer survival rate.

Key words: B-cells lymphoma, DLBCL, CLL, S100A4 protein, S100A6 protein, haematopoietic stem cells.

This abstract submitted to EMBO Conference: To-B or not to-B: B-cells in health and disease from 10 – 13 September 2017 in Girona, Spain

S100A4 protein in B-cell Lymphomas: expression and function

Zamzam Almutairi[1], Kevin West[2], Sandrine Jayne[1] and Marina Kriajevska[1]

[1]Leicester Cancer Research Centre, University of Leicester, Leicester, UK.

[2] Department of Pathology, Leicester Royal Infirmary, Leicester, UK

Introduction

B-cell lymphomas are biologically heterogeneous diseases and their classification is based on the morphological, genotypic, and biological features of the lymphoma cells present in the diagnostic samples. Numerous studies were aimed to identify prognostic markers characterizing stages of the disease.

Many S100 proteins are overexpressed in different cancers, and their expression correlates with poor prognosis1. Studies have revealed a link between expression of some members of the S100 family and metastatic spreading2.

A bioinformatics approach has identified two genes from the S100 family, S100A4 and S100A6, that are activated in DLBCL and CLL samples3, but protein expression and potential functions of these genes in the development of B-cell lymphomas have not been investigated.

Methods

60 paraffin tissue blocks of B-cell lymphomas (16 samples of Chronic Lymphocytic Leukaemia (CLL), 26 samples of Diffuse Large B-cell Lymphoma (DLBCL), 11 samples of Follicular Lymphoma (FL), 6 samples of Mantle Cell Lymphoma (MCL) and one sample of Marginal Zone Lymphoma (MZL) were collected from the Department of Pathology, Leicester Royal infirmary, and were used for IHC analysis of the S100A4 expression. Peripheral blood samples (PB) of the CLL patients were obtained from the Department of Haematology, Leicester Royal infirmary, and used for isolation of the PB lymphocytes. Expression of S100A4 in the PB samples were assessed by Western blotting. Correlation analysis of the S100A4 expression and patients' survival was performed by Kaplan-Meier test.

RNAi approach was used to modulate S100A4 expression in 5 PB lymphocyte samples of the CLL patients. Analysis of the S100A4 expression on the PB cells migration was evaluated in the chemotaxis transwell assay. One million of transfected cells with either a non-targeting or S100A4-targeting siRNA were maintained 48 hours and then seeded into coated 8.0μm transwell inserts. After 3 hours incubation, migrated cells were counted. 16 Bone Marrow (BM) blocks were used to analyse expression of S100A4 in haematopoietic stem cells by immunofluorescence.

Results

IHC analysis demonstrated the expression of S100A4 in the majority of CLL, MCL, DLBCL cases, while no expression has been detected in all analysed FL cases. Western blot analysis has revealed a high level of S100A4 expression in most PB samples of the CLL patients. Reduced expression of S100A4 was correlated with a longer survival rate, $p<0.0006$. RNAi-mediated knockdown of S100A4 expression had a strong negative effect on cell migration of PB lymphocytes obtained from 5 CLL patients (p values < 0.05 in all samples), Student's t-test analysis of three independent experiments. To confirm knockdown, lysates of CLL patient's samples were analysed by Western blot and membranes probed for S100A4 and α-tubulin. As hypothesis, double immunofluorescent showed co-expression of S100A4 and haematopoietic cells markers in BM tissue (CD133, CD10 and CD34).

Conclusions

S100A4 is a potential biomarker in B-cell lymphomas. It has a critical role in lymphocytes migration in CLL samples. S100A4 expressed in cells with features of the haematopoietic stem cells.

This abstract submitted to "9th International Conference on Leukaemia and Hematologic Oncology" held during October 05-06, 2017 in London, UK. In this conference I participated as oral speaker and presented the poster.

References

Abbas, A.K., Lichtman, A.H., and Pillai, S. (2012). Basic immunology: functions and disorders of the immune system (Elsevier Health Sciences).

Afanador, L., Roltsch, E.A., Holcomb, L., Campbell, K.S., Keeling, D.A., Zhang, Y., and Zimmer, D.B. (2014). The Ca2+ sensor S100A1 modulates neuroinflammation, histopathology and Akt activity in the PSAPP Alzheimer's disease mouse model. Cell Calcium 56, 68-80.

Aggarwal, N., Pongpruttipan, T., Patel, S., Bayerl, M.G., Alkan, S., Nathwani, B., Surti, U., Kitahara, S., Chinthammitr, Y., and Swerdlow, S.H. (2015). Expression of S100 Protein in CD4-positive T-cell Lymphomas Is Often Associated With T-cell Prolymphocytic Leukemia. The American journal of surgical pathology 39, 1679-1687.

Aigner, K., Dampier, B., Descovich, L., Mikula, M., Sultan, A., Schreiber, M., Mikulits, W., Brabletz, T., Strand, D., and Obrist, P. (2007). The transcription factor ZEB1 (δEF1) promotes tumour cell dedifferentiation by repressing master regulators of epithelial polarity. Oncogene 26, 6979-6988.

Al-Hamadani, M., Habermann, T.M., Cerhan, J.R., Macon, W.R., Maurer, M.J., and Go, R.S. (2015). Non-Hodgkin lymphoma subtype distribution, geodemographic patterns, and survival in the US: A longitudinal analysis of the National Cancer Data Base from 1998 to 2011. Am J Hematol 90, 790-795.

All, H., and Abd, H. (2007). Smooth muscle actin and s100p on non germinal centre diffuse large B cell lymphoma are adverse prognostic factors: pilot study. Diagnostic pathology 2, 9.

Almqvist, N., and Martensson, I.L. (2012). The pre-B cell receptor; selecting for or against autoreactivity. Scand J Immunol 76, 256-262.

Ambartsumian, N., and Grigorian, M. (2016). S100A4, a link between metastasis and inflammation. Molecular Biology 50, 510-520.

Andersen, K., Mori, H., Fata, J., Bascom, J., Oyjord, T., Maelandsmo, G.M., and Bissell, M. (2011). The metastasis-promoting protein S100A4 regulates mammary branching morphogenesis. Dev Biol 352, 181-190.

Andersen, K., Nesland, J.M., Holm, R., Florenes, V.A., Fodstad, O., and Maelandsmo, G.M. (2004). Expression of S100A4 combined with reduced E-cadherin expression predicts patient outcome in malignant melanoma. Mod Pathol 17, 990-997.

Arber, D.A., Orazi, A., Hasserjian, R., Thiele, J., Borowitz, M.J., Le Beau, M.M., Bloomfield, C.D., Cazzola, M., and Vardiman, J.W. (2016). The 2016 revision to the World Health Organization (WHO) classification of myeloid neoplasms and acute leukemia. Blood, blood-2016-2003-643544.

Arumugam, T., Ramachandran, V., Sun, D., Peng, Z., Pal, A., Maxwell, D.S., Bornmann, W.G., and Logsdon, C.D. (2013). Designing and developing S100P inhibitor 5-methyl cromolyn for pancreatic cancer therapy. Mol Cancer Ther 12, 654-662.

Attar, A. (2014). Changes in the cell surface markers during normal hematopoiesis: a guide to cell isolation. Global J Hematol Blood Transfu 1, 20-28.

Aukema, S.M., Siebert, R., Schuuring, E., van Imhoff, G.W., Kluin-Nelemans, H.C., Boerma, E.J., and Kluin, P.M. (2011). Double-hit B-cell lymphomas. Blood 117, 2319-2331.

Bagg, A. (2011). B cells behaving badly: a better basis to behold belligerence in B-cell lymphomas. ASH Education Program Book 2011, 330-335.

Baggiolini, M. (1998). Chemokines and leukocyte traffic. Nature 392, 565-568.

Bel Hadj Jrad, B., Chatti, A., Laatiri, A., Ahmed, S.B., Romdhane, A., Ajimi, S., and Chouchane, L. (2007). Tumour necrosis factor promoter gene polymorphism associated with increased susceptibility to non-Hodgkin's lymphomas. Eur J Haematol 78, 117-122.

Benito, C., Gomis, R., Fernandez-Alvarez, J., Usac, E.F., and Gallart, T. (2003). Transcript expression of two Iglambda rearrangements and RAG-1/RAG-2 in a mature human B cell producing IgMlambda islet cell autoantibody. J Clin Immunol 23, 107-118.

Berger, N., Ben Bassat, H., Klein, B.Y., and Laskov, R. (2007). Cytotoxicity of NF-kappaB inhibitors Bay 11-7085 and caffeic acid phenethyl ester to Ramos and other human B-lymphoma cell lines. Exp Hematol 35, 1495-1509.

Berridge, M.J., Bootman, M.D., and Roderick, H.L. (2003). Calcium signalling: dynamics, homeostasis and remodelling. Nat Rev Mol Cell Biol 4, 517-529.

Berridge, M.J., Lipp, P., and Bootman, M.D. (2000). The versatility and universality of calcium signalling. Nat Rev Mol Cell Biol 1, 11-21.

Bettum, I.J., Vasiliauskaite, K., Nygaard, V., Clancy, T., Pettersen, S.J., Tenstad, E., Maelandsmo, G.M., and Prasmickaite, L. (2014). Metastasis-associated protein S100A4 induces a network of inflammatory cytokines that activate stromal cells to acquire pro-tumourigenic properties. Cancer Lett 344, 28-39.

Bjork, P., Bjork, A., Vogl, T., Stenstrom, M., Liberg, D., Olsson, A., Roth, J., Ivars, F., and Leanderson, T. (2009). Identification of human S100A9 as a novel target for treatment of autoimmune disease via binding to quinoline-3-carboxamides. PLoS Biol 7, e97.

Bjornland, K., Winberg, J.O., Odegaard, O.T., Hovig, E., Loennechen, T., Aasen, A.O., Fodstad, O., and Maelandsmo, G.M. (1999). S100A4 involvement in metastasis: deregulation of matrix metalloproteinases and tissue inhibitors of matrix metalloproteinases in osteosarcoma cells transfected with an anti-S100A4 ribozyme. Cancer Res 59, 4702-4708.

Blum, K.A., Lozanski, G., and Byrd, J.C. (2004). Adult Burkitt leukemia and lymphoma. Blood 104, 3009-3020.

Bogenrieder, T., and Herlyn, M. (2003). Axis of evil: molecular mechanisms of cancer metastasis. Oncogene 22, 6524-6536.

Boye, K., and Mælandsmo, G.M. (2010). S100A4 and Metastasis : A Small Actor Playing Many Roles. The American Journal of Pathology 176, 528-535.

Boye, K., Nesland, J.M., Sandstad, B., Maelandsmo, G.M., and Flatmark, K. (2010). Nuclear S100A4 is a novel prognostic marker in colorectal cancer. Eur J Cancer 46, 2919-2925.

Bresnick, A.R., Weber, D.J., and Zimmer, D.B. (2015). S100 proteins in cancer. Nature reviews Cancer 15, 96-109.

Brown, L.M., Helmke, S.M., Hunsucker, S.W., Netea-Maier, R.T., Chiang, S.A., Heinz, D.E., Shroyer, K.R., Duncan, M.W., and Haugen, B.R. (2006). Quantitative and qualitative differences in protein expression between papillary thyroid carcinoma and normal thyroid tissue. Mol Carcinog 45, 613-626.

Broz, M.L., Binnewies, M., Boldajipour, B., Nelson, A.E., Pollack, J.L., Erle, D.J., Barczak, A., Rosenblum, M.D., Daud, A., Barber, D.L., et al. (2014). Dissecting the tumour myeloid compartment reveals rare activating antigen-presenting cells critical for T cell immunity. Cancer Cell 26, 638-652.

Buetti-Dinh, A., Pivkin, I.V., and Friedman, R. (2015). S100A4 and its role in metastasis - simulations of knockout and amplification of epithelial growth factor receptor and matrix metalloproteinases. Mol Biosyst 11, 2247-2254.

Buetti-Dinh, A., Pivkin, I.V., and Friedman, R. (2015). S100A4 and its role in metastasis - simulations of knockout and amplification of epithelial growth factor receptor and matrix metalloproteinases. Mol Biosyst 11, 2247-2254.

Bulk, E., Sargin, B., Krug, U., Hascher, A., Jun, Y., Knop, M., Kerkhoff, C., Gerke, V., Liersch, R., Mesters, R.M., et al. (2009). S100A2 induces metastasis in non-small cell lung cancer. Clin Cancer Res 15, 22-29.

Burkitt, D., and O'Conor, G.T. (1961). Malignant lymphoma in African children. I. A clinical syndrome. Cancer 14, 258-269.

Cabezon, T., Celis, J.E., Skibshoj, I., Klingelhofer, J., Grigorian, M., Gromov, P., Rank, F., Myklebust, J.H., Maelandsmo, G.M., Lukanidin, E., et al. (2007). Expression of S100A4 by a variety of cell types present in the tumour microenvironment of human breast cancer. Int J Cancer 121, 1433-1444.

Calabretta, B., Kaczmarek, L., Mars, W., Ochoa, D., Gibson, C.W., Hirschhorn, R.R., and Baserga, R. (1985). Cell-cycle-specific genes differentially expressed in human leukemias. Proc Natl Acad Sci U S A 82, 4463-4467.

Calado, D.P., Sasaki, Y., Godinho, S.A., Pellerin, A., Kochert, K., Sleckman, B.P., de Alboran, I.M., Janz, M., Rodig, S., and Rajewsky, K. (2012). The cell-cycle regulator c-Myc is essential for the formation and maintenance of germinal centers. Nat Immunol 13, 1092-1100.

Caligaris-Cappio, F., and Dalla-Favera, R. (2005). Chronic lymphocytic leukemia, Vol 294;294.; (New York;Berlin;: Springer).

Calis, J.J., and Rosenberg, B.R. (2014). Characterizing immune repertoires by high throughput sequencing: strategies and applications. Trends Immunol 35, 581-590.

Cancemi, P., Buttacavoli, M., Di Cara, G., Albanese, N.N., Bivona, S., Pucci-Minafra, I., and Feo, S. (2018). A multiomics analysis of S100 protein family in breast cancer. Oncotarget 9, 29064-29081.

Cancemi, P., Di Cara, G., Albanese, N., Costantini, F., Marabeti, M., Musso, R., Lupo, C., Roz, E., and Pucci-Minafra, I. (2010). Large-scale proteomic identification of S100 proteins in breast cancer tissues. BMC cancer 10, 476.

Cancer Research UK. Non-Hodgkin lymphoma (C82-C86): 1979-2013 European age-standardised incidence rates per 100,000 population, by sex, Great Britain. 2013.

Carafoli, E. (2002). Calcium signaling: a tale for all seasons. Proc Natl Acad Sci U S A 99, 1115-1122.

Chandramouli, A., Mercado-Pimentel, M.E., Hutchinson, A., Gibadulinova, A., Olson, E.R., Dickinson, S., Shanas, R., Davenport, J., Owens, J., Bhattacharyya, A.K., et al. (2010). The induction of S100p expression by the Prostaglandin E(2) (PGE(2))/EP4 receptor signaling pathway in colon cancer cells. Cancer Biol Ther 10, 1056-1066.

Chen, H., Xu, C., Jin, Q., and Liu, Z. (2014). S100 protein family in human cancer. Am J Cancer Res 4, 89-115.

Chen, M., Sastry, S.K., and O'Connor, K.L. (2011). Src kinase pathway is involved in NFAT5-mediated S100A4 induction by hyperosmotic stress in colon cancer cells. Am J Physiol Cell Physiol 300, C1155-1163.

Chen, M., Sinha, M., Luxon, B.A., Bresnick, A.R., and O'Connor, K.L. (2009). Integrin alpha6beta4 controls the expression of genes associated with cell motility, invasion, and metastasis, including S100A4/metastasin. J Biol Chem 284, 1484-1494.

Chen, Q., Jain, N., Ayer, T., Wierda, W.G., Flowers, C.R., O'Brien, S.M., Keating, M.J., Kantarjian, H.M., and Chhatwal, J. (2017). Economic Burden of Chronic Lymphocytic Leukemia in the Era of Oral Targeted Therapies in the United States. J Clin Oncol 35, 166-174.

Chen, X., Liu, X., Lang, H., Zhang, S., Luo, Y., and Zhang, J. (2015). S100 calcium-binding protein A6 promotes epithelial-mesenchymal transition through beta-catenin in pancreatic cancer cell line. PLoS One 10, e0121319.

Chong, P.P., Selvaratnam, L., Abbas, A.A., and Kamarul, T. (2012). Human peripheral blood derived mesenchymal stem cells demonstrate similar characteristics and chondrogenic differentiation potential to bone marrow derived mesenchymal stem cells. Journal of Orthopaedic Research 30, 634-642.

Chou, Y.S., and Yang, M.H. (2015). Epithelial-mesenchymal transition-related factors in solid tumour and hematological malignancy. J Chin Med Assoc 78, 438-445.

Chou, Y.S., and Yang, M.H. (2015). Epithelial-mesenchymal transition-related factors in solid tumor and hematological malignancy. J Chin Med Assoc 78, 438-445.

Chouchane, L., Ahmed, S.B., Baccouche, S., and Remadi, S. (1997). Polymorphism in the tumor necrosis factor-alpha promotor region and in the heat shock protein 70 genes associated with malignant tumours. Cancer 80, 1489-1496.

Chuang, S.-S., Ye, H., Du, M.-Q., Lu, C.-L., Dogan, A., Hsieh, P.-P., Huang, W.-T., and Jung, Y.-C. (2007). Histopathology and immunohistochemistry in distinguishing Burkitt lymphoma from diffuse large B-cell lymphoma with very high proliferation index and with or without a starry-sky pattern: a comparative study with EBER and FISH. American Journal of Clinical Pathology 128, 558-564.

Cohn, M.A., Hjelmso, I., Wu, L.C., Guldberg, P., Lukanidin, E.M., and Tulchinsky, E.M. (2001). Characterization of Sp1, AP-1, CBF and KRC binding sites and minisatellite DNA as functional elements of the metastasis-associated mts1/S100A4 gene intronic enhancer. Nucleic Acids Res 29, 3335-3346.

Compagno, M., Lim, W.K., Grunn, A., Nandula, S.V., Brahmachary, M., Shen, Q., Bertoni, F., Ponzoni, M., Scandurra, M., Califano, A., et al. (2009). Mutations of multiple genes cause deregulation of NF-kappaB in diffuse large B-cell lymphoma. Nature 459, 717-721.

Czuczman, M.S., Weaver, R., Alkuzweny, B., Berlfein, J., and Grillo-Lopez, A.J. (2004). Prolonged clinical and molecular remission in patients with low-grade or follicular non-Hodgkin's lymphoma treated with rituximab plus CHOP chemotherapy: 9-year follow-up. J Clin Oncol 22, 4711-4716.

Dakhel, S., Padilla, L., Adan, J., Masa, M., Martinez, J.M., Roque, L., Coll, T., Hervas, R., Calvis, C., Messeguer, R., et al. (2014). S100P antibody-mediated therapy as a new promising strategy for the treatment of pancreatic cancer. Oncogenesis 3, e92.

Davies, B.R., Davies, M.P., Gibbs, F.E., Barraclough, R., and Rudland, P.S. (1993). Induction of the metastatic phenotype by transfection of a benign rat mammary epithelial

cell line with the gene for p9Ka, a rat calcium-binding protein, but not with the oncogene EJ-ras-1. Oncogene 8, 999-1008.

Davies, B.R., O'Donnell, M., Durkan, G.C., Rudland, P.S., Barraclough, R., Neal, D.E., and Mellon, J.K. (2002). Expression of S100A4 protein is associated with metastasis and reduced survival in human bladder cancer. J Pathol 196, 292-299.

Day, T.K., and Bianco-Miotto, T. (2013). Common gene pathways and families altered by DNA methylation in breast and prostate cancers. Endocr Relat Cancer 20, R215-232.

de Silva Rudland, S., Martin, L., Roshanlall, C., Winstanley, J., Leinster, S., Platt-Higgins, A., Carroll, J., West, C., Barraclough, R., and Rudland, P. (2006). Association of S100A4 and osteopontin with specific prognostic factors and survival of patients with minimally invasive breast cancer. Clin Cancer Res 12, 1192-1200.

Deol, Y.S., Nasser, M.W., Yu, L., Zou, X., and Ganju, R.K. (2011). Tumor-suppressive effects of psoriasin (S100A7) are mediated through the beta-catenin/T cell factor 4 protein pathway in estrogen receptor-positive breast cancer cells. J Biol Chem 286, 44845-44854.

Dhar, A., Mallick, S., Ghosh, P., Maiti, A., Ahmed, I., Bhattacharya, S., Mandal, T., Manna, A., Roy, K., Singh, S., et al. (2014). Simultaneous inhibition of key growth pathways in melanoma cells and tumor regression by a designed bidentate constrained helical peptide. Biopolymers 102, 344-358.

Donato, R. (2001). S100: a multigenic family of calcium-modulated proteins of the EF-hand type with intracellular and extracellular functional roles. Int J Biochem Cell Biol 33, 637-668.

Donato, R. (2003). Intracellular and extracellular roles of S100 proteins. Microsc Res Tech 60, 540-551.

Dorosz, S.A., Ginolhac, A., Kahne, T., Naumann, M., Sauter, T., Salsmann, A., and Bueb, J.L. (2015). Role of Calprotectin as a Modulator of the IL27-Mediated Proinflammatory Effect on Endothelial Cells. Mediators Inflamm 2015, 737310.

Elenkov, I.J., Iezzoni, D.G., Daly, A., Harris, A.G., and Chrousos, G.P. (2005). Cytokine dysregulation, inflammation and well-being. Neuroimmunomodulation 12, 255-269.

Emberley, E.D., Murphy, L.C., and Watson, P.H. (2004). S100 proteins and their influence on pro-survival pathways in cancer. Biochem Cell Biol 82, 508-515.

Engels, E.A. (2007). Infectious agents as causes of non-Hodgkin lymphoma. Cancer Epidemiol Biomarkers Prev 16, 401-404.

Ernst, M., Najdovska, M., Grail, D., Lundgren-May, T., Buchert, M., Tye, H., Matthews, V.B., Armes, J., Bhathal, P.S., Hughes, N.R., et al. (2008). STAT3 and STAT1 mediate IL-11-dependent and inflammation-associated gastric tumorigenesis in gp130 receptor mutant mice. J Clin Invest 118, 1727-1738.

Federico, M., Bellei, M., Marcheselli, L., Luminari, S., Lopez-Guillermo, A., Vitolo, U., Pro, B., Pileri, S., Pulsoni, A., Soubeyran, P., et al. (2009). Follicular lymphoma international prognostic index 2: a new prognostic index for follicular lymphoma developed by the international follicular lymphoma prognostic factor project. J Clin Oncol 27, 4555-4562.

Fei, F., Qu, J., Zhang, M., Li, Y., and Zhang, S. (2017). S100A4 in cancer progression and metastasis: A systematic review. Oncotarget.

Fernandez, V., Salamero, O., Espinet, B., Sole, F., Royo, C., Navarro, A., Camacho, F., Bea, S., Hartmann, E., Amador, V., et al. (2010). Genomic and gene expression profiling defines indolent forms of mantle cell lymphoma. Cancer Res 70, 1408-1418.

Fisher, S.G., and Fisher, R.I. (2004). The epidemiology of non-Hodgkin's lymphoma. Oncogene 23, 6524-6534.

Flatmark, K., Pedersen, K.B., Nesland, J.M., Rasmussen, H., Aamodt, G., Mikalsen, S.O., Bjornland, K., Fodstad, O., and Maelandsmo, G.M. (2003). Nuclear localization of the metastasis-related protein S100A4 correlates with tumour stage in colorectal cancer. J Pathol 200, 589-595.

Foell, D., Kane, D., Bresnihan, B., Vogl, T., Nacken, W., Sorg, C., FitzGerald, O., and Roth, J. (2003). Expression of the pro-inflammatory protein S100A12 (EN-RAGE) in rheumatoid and psoriatic arthritis. Rheumatology 42, 1383-1389.

Ford, H.L., Salim, M.M., Chakravarty, R., Aluiddin, V., and Zain, S.B. (1995). Expression of Mts1, a metastasis-associated gene, increases motility but not invasion of a nonmetastatic mouse mammary adenocarcinoma cell line. Oncogene 11, 2067-2075.

Franco-Barraza, J., Valdivia-Silva, J.E., Zamudio-Meza, H., Castillo, A., Garcia-Zepeda, E.A., Benitez-Bribiesca, L., and Meza, I. (2010). Actin cytoskeleton participation in the onset of IL-1beta induction of an invasive mesenchymal-like phenotype in epithelial MCF-7 cells. Arch Med Res 41, 170-181.

Fujiwara, M., Kashima, T.G., Kunita, A., Kii, I., Komura, D., Grigoriadis, A.E., Kudo, A., Aburatani, H., and Fukayama, M. (2011). Stable knockdown of S100A4 suppresses cell migration and metastasis of osteosarcoma. Tumour Biol 32, 611-622.

Gaidano, G., and Dalla-Favera, R. (1993). Biologic and molecular characterization of non-Hodgkin's lymphoma. Curr Opin Oncol 5, 776-784.

Garrett, S.C., Hodgson, L., Rybin, A., Toutchkine, A., Hahn, K.M., Lawrence, D.S., and Bresnick, A.R. (2008). A biosensor of S100A4 metastasis factor activation: inhibitor screening and cellular activation dynamics. Biochemistry 47, 986-996.

Garrett, S.C., Varney, K.M., Weber, D.J., and Bresnick, A.R. (2006). S100A4, a mediator of metastasis. J Biol Chem 281, 677-680.

Gentilini, D., Busacca, M., Di Francesco, S., Vignali, M., Vigano, P., and Di Blasio, A.M. (2007). PI3K/Akt and ERK1/2 signalling pathways are involved in endometrial cell migration induced by 17beta-estradiol and growth factors. Mol Hum Reprod 13, 317-322.

Gemy G. Kaithakottil. Analysis of the expression and cluster analysis of the S100 genes in B-cell Chronic Lymphocytic Leukemia. MSc thesis, University of Leicester, 2010.

Glaser, R., Harder, J., Lange, H., Bartels, J., Christophers, E., and Schroder, J.M. (2005). Antimicrobial psoriasin (S100A7) protects human skin from Escherichia coli infection. Nat Immunol 6, 57-64.

Gogia, A., Raina, V., Kumar, L., Sharma, A., Sharma, M., and Mallick, S.R. (2017). Follicular lymphoma: an Institutional Analysis. Asian Pac J Cancer Prev 18, 681-685.

Golitsina, N.L., Kordowska, J., Wang, C.L., and Lehrer, S.S. (1996). Ca2+-dependent binding of calcyclin to muscle tropomyosin. Biochem Biophys Res Commun 220, 360-365.

Goossens, S., Peirs, S., Van Loocke, W., Wang, J., Takawy, M., Matthijssens, F., Sonderegger, S.E., Haigh, K., Nguyen, T., Vandamme, N., et al. (2017). Oncogenic ZEB2 activation drives sensitivity toward KDM1A inhibition in T-cell acute lymphoblastic leukemia. Blood 129, 981-990.

Grebhardt, S., Veltkamp, C., Strobel, P., and Mayer, D. (2012). Hypoxia and HIF-1 increase S100A8 and S100A9 expression in prostate cancer. Int J Cancer 131, 2785-2794.

Grigorian, M., Ambartsumian, N., Lykkesfeldt, A.E., Bastholm, L., Elling, F., Georgiev, G., and Lukanidin, E. (1996). Effect of mts1 (S100A4) expression on the progression of human breast cancer cells. Int J Cancer 67, 831-841.

Grigorian, M., Tulchinsky, E., Burrone, O., Tarabykina, S., Georgiev, G., and Lukanidin, E. (1994). Modulation of mts1 expression in mouse and human normal and tumor cells. Electrophoresis 15, 463-468.

Grigorian, M.S., Tulchinsky, E.M., Zain, S., Ebralidze, A.K., Kramerov, D.A., Kriajevska, M.V., Georgiev, G.P., and Lukanidin, E.M. (1993). The mts1 gene and control of tumor metastasis. Gene 135, 229-238.

Gross, S.R., Sin, C.G.T., Barraclough, R., and Rudland, P.S. (2014). Joining S100 proteins and migration: for better or for worse, in sickness and in health. Cellular and molecular life sciences 71, 1551-1579.

Grulich, A.E., Vajdic, C.M., and Cozen, W. (2007). Altered immunity as a risk factor for non-Hodgkin lymphoma. Cancer Epidemiol Biomarkers Prev 16, 405-408.

Guo, C., Chang, C.C., Wortham, M., Chen, L.H., Kernagis, D.N., Qin, X., Cho, Y.W., Chi, J.T., Grant, G.A., McLendon, R.E., et al. (2012). Global identification of MLL2-targeted loci reveals MLL2's role in diverse signaling pathways. Proc Natl Acad Sci U S A 109, 17603-17608.

Guo, J., Bian, Y., Wang, Y., Chen, L., Yu, A., and Sun, X. (2017). FAM107B is regulated by S100A4 and mediates the effect of S100A4 on the proliferation and migration of MGC803 gastric cancer cells. Cell Biol Int.

Guo, Y., Hu, Y., Hu, M., He, J., and Li, B. (2018). Long non-coding RNA ZEB2-AS1 promotes proliferation and inhibits apoptosis in human lung cancer cells. Oncol Lett 15, 5220-5226.

Guo, Y., Hu, Y., Hu, M., He, J., and Li, B. (2018). Long non-coding RNA ZEB2-AS1 promotes proliferation and inhibits apoptosis in human lung cancer cells. Oncol Lett 15, 5220-5226.

Gupta, G.P., and Massague, J. (2006). Cancer metastasis: building a framework. Cell 127, 679-695.

Hallek, M. (2015). Chronic lymphocytic leukemia: 2015 Update on diagnosis, risk stratification, and treatment. Am J Hematol 90, 446-460.

Heizmann, C.W., Fritz, G., and Schafer, B.W. (2002). S100 proteins: structure, functions and pathology. Front Biosci 7, d1356-1368.

Helfman, D.M., Kim, E.J., Lukanidin, E., and Grigorian, M. (2005). The metastasis associated protein S100A4: role in tumour progression and metastasis. Br J Cancer 92, 1955-1958.

Hernan, R., Fasheh, R., Calabrese, C., Frank, A.J., Maclean, K.H., Allard, D., Barraclough, R., and Gilbertson, R.J. (2003). ERBB2 up-regulates S100A4 and several other prometastatic genes in medulloblastoma. Cancer Res 63, 140-148.

Hernandez, J.L., Padilla, L., Dakhel, S., Coll, T., Hervas, R., Adan, J., Masa, M., Mitjans, F., Martinez, J.M., Coma, S., et al. (2013). Therapeutic targeting of tumor growth and angiogenesis with a novel anti-S100A4 monoclonal antibody. PLoS One 8, e72480.

Hiratsuka, S., Watanabe, A., Aburatani, H., and Maru, Y. (2006). Tumour-mediated upregulation of chemoattractants and recruitment of myeloid cells predetermines lung metastasis. Nat Cell Biol 8, 1369-1375.

Hock, H., Hamblen, M.J., Rooke, H.M., Schindler, J.W., Saleque, S., Fujiwara, Y., and Orkin, S.H. (2004). Gfi-1 restricts proliferation and preserves functional integrity of haematopoietic stem cells. Nature 431, 1002-1007.

Horiuchi, A., Hayashi, T., Kikuchi, N., Hayashi, A., Fuseya, C., Shiozawa, T., and Konishi, I. (2012). Hypoxia upregulates ovarian cancer invasiveness via the binding of HIF-1alpha to a hypoxia-induced, methylation-free hypoxia response element of S100A4 gene. Int J Cancer 131, 1755-1767.

Horn, H., Ziepert, M., Becher, C., Barth, T.F., Bernd, H.W., Feller, A.C., Klapper, W., Hummel, M., Stein, H., Hansmann, M.L., et al. (2013). MYC status in concert with BCL2 and BCL6 expression predicts outcome in diffuse large B-cell lymphoma. Blood 121, 2253-2263.

Horsman, D.E., Okamoto, I., Ludkovski, O., Le, N., Harder, L., Gesk, S., Siebert, R., Chhanabhai, M., Sehn, L., Connors, J.M., et al. (2003). Follicular lymphoma lacking the t(14;18)(q32;q21): identification of two disease subtypes. Br J Haematol 120, 424-433.

Houghton, A.M. (2010). The paradox of tumor-associated neutrophils: fueling tumor growth with cytotoxic substances. Cell Cycle 9, 1732-1737.

Hsi, E.D. (2012). Pathologic and molecular genetic features of chronic lymphocytic leukemia. Semin Oncol 39, 74-79.

Hsieh, H.L., Schafer, B.W., Weigle, B., and Heizmann, C.W. (2004). S100 protein translocation in response to extracellular S100 is mediated by receptor for advanced glycation endproducts in human endothelial cells. Biochem Biophys Res Commun 316, 949-959.

Hsu, K., Champaiboon, C., Guenther, B.D., Sorenson, B.S., Khammanivong, A., Ross, K.F., Geczy, C.L., and Herzberg, M.C. (2009). ANTI-INFECTIVE PROTECTIVE PROPERTIES OF S100 CALGRANULINS. Antiinflamm Antiallergy Agents Med Chem 8, 290-305.

Hua, T., Liu, S., Xin, X., Cai, L., Shi, R., Chi, S., Feng, D., and Wang, H. (2016). S100A4 promotes endometrial cancer progress through epithelial-mesenchymal transition regulation. Oncol Rep 35, 3419-3426.

Hugo, H.J., Wafai, R., Blick, T., Thompson, E.W., and Newgreen, D.F. (2009). Staurosporine augments EGF-mediated EMT in PMC42-LA cells through actin depolymerisation, focal contact size reduction and Snail1 induction - a model for cross-modulation. BMC Cancer 9, 235.

Hulkkonen, J., Vilpo, J., Vilpo, L., and Hurme, M. (1998). Diminished production of interleukin-6 in chronic lymphocytic leukaemia (B-CLL) cells from patients at advanced stages of disease. Tampere CLL Group. Br J Haematol 100, 478-483.

Hunter, K.D., Parkinson, E.K., and Harrison, P.R. (2005). Profiling early head and neck cancer. Nat Rev Cancer 5, 127-135.

Inamdar, A.A., Goy, A., Ayoub, N.M., Attia, C., Oton, L., Taruvai, V., Costales, M., Lin, Y.T., Pecora, A., and Suh, S.K. (2016). Mantle cell lymphoma in the era of precision medicine-diagnosis, biomarkers and therapeutic agents. Oncotarget 7, 48692-48731.

Jares, P., Colomer, D., and Campo, E. (2012). Molecular pathogenesis of mantle cell lymphoma. J Clin Invest 122, 3416-3423.

Jemal, A., Bray, F., Center, M.M., Ferlay, J., Ward, E., and Forman, D. (2011). Global cancer statistics. CA Cancer J Clin 61, 69-90.

Jenkinson, S.R., Barraclough, R., West, C.R., and Rudland, P.S. (2004). S100A4 regulates cell motility and invasion in an in vitro model for breast cancer metastasis. Br J Cancer 90, 253-262.

Jennbacken, K., Welen, K., Olsson, A., Axelsson, B., Torngren, M., Damber, J.E., and Leanderson, T. (2012). Inhibition of metastasis in a castration resistant prostate cancer model by the quinoline-3-carboxamide tasquinimod (ABR-215050). Prostate 72, 913-924.

Jia, W., Gao, X.J., Zhang, Z.D., Yang, Z.X., and Zhang, G. (2013). S100A4 silencing suppresses proliferation, angiogenesis and invasion of thyroid cancer cells through downregulation of MMP-9 and VEGF. Eur Rev Med Pharmacol Sci 17, 1495-1508.

Jian, L., Zhihong, W., Liuxing, W., and Qingxia, F. (2015). [Role of S100A4 in the epithelial-mesenchymal transition of esophageal squamous cell carcinoma and its molecular mechanism]. Zhonghua Zhong Liu Za Zhi 37, 258-265.

Jung, M.J., Murzik, U., Wehder, L., Hemmerich, P., and Melle, C. (2010). Regulation of cellular actin architecture by S100A10. Exp Cell Res 316, 1234-1240.

Kahn, H.J., Marks, A., Thom, H., and Baumal, R. (1983). Role of Antibody to S100 Protein in Diagnostic Pathology. American Journal of Clinical Pathology 79, 341-347.

Kallberg, E., Vogl, T., Liberg, D., Olsson, A., Bjork, P., Wikstrom, P., Bergh, A., Roth, J., Ivars, F., and Leanderson, T. (2012). S100A9 interaction with TLR4 promotes tumor growth. PLoS One 7, e34207.

Kalluri, R., and Weinberg, R.A. (2009). The basics of epithelial-mesenchymal transition. The Journal of clinical investigation 119, 1420-1428.

Karam, M., Ata, A., Irish, K., Feustel, P.J., Mottaghy, F.M., Stroobants, S.G., Verhoef, G.E., Chundru, S., Douglas-Nikitin, V., Oliver Wong, C.Y., et al. (2009). FDG positron emission tomography/computed tomography scan may identify mantle cell lymphoma patients with unusually favorable outcome. Nucl Med Commun 30, 770-778.

Karin, M. (2006). Nuclear factor-kappaB in cancer development and progression. Nature 441, 431-436.

Keirsebilck, A., Bonne, S., Bruyneel, E., Vermassen, P., Lukanidin, E., Mareel, M., and van Roy, F. (1998). E-cadherin and metastasin (mts-1/S100A4) expression levels are inversely regulated in two tumor cell families. Cancer Res 58, 4587-4591.

Kho, P.S., Jankova, L., Fung, C.L., Chan, C., Clarke, C., Lin, B.P., Robertson, G., Molloy, M., Chapuis, P.H., Bokey, E.L., et al. (2012). Overexpression of protein S100A4 is independently associated with overall survival in stage C colonic cancer but only in cytoplasm at the advancing tumour front. Int J Colorectal Dis 27, 1409-1417.

Kikuchi, N., Horiuchi, A., Osada, R., Imai, T., Wang, C., Chen, X., and Konishi, I. (2006). Nuclear expression of S100A4 is associated with aggressive behavior of epithelial ovarian carcinoma: an important autocrine/paracrine factor in tumor progression. Cancer Sci 97, 1061-1069.

Kim, C.E., Lim, S.K., and Kim, J.S. (2012). In vivo antitumor effect of cromolyn in PEGylated liposomes for pancreatic cancer. J Control Release 157, 190-195.

Kimura, K., Endo, Y., Yonemura, Y., Heizmann, C.W., Schafer, B.W., Watanabe, Y., and Sasaki, T. (2000). Clinical significance of S100A4 and E-cadherin-related adhesion molecules in non-small cell lung cancer. Int J Oncol 16, 1125-1131.

Kipps, T.J., Stevenson, F.K., Wu, C.J., Croce, C.M., Packham, G., Wierda, W.G., O'Brien, S., Gribben, J., and Rai, K. (2017). Chronic lymphocytic leukaemia. Nature Reviews Disease Primers 3, 17008.

Klein, U., and Dalla-Favera, R. (2008). Germinal centres: role in B-cell physiology and malignancy. Nat Rev Immunol 8, 22-33.

Klein, U., and Dalla-Favera, R. (2010). New insights into the pathogenesis of chronic lymphocytic leukemia. Semin Cancer Biol 20, 377-383.

Komatsu, K., Kobune-Fujiwara, Y., Andoh, A., Ishiguro, S., Hunai, H., Suzuki, N., Kameyama, M., Murata, K., Miyoshi, J., Akedo, H., et al. (2000). Increased expression of S100A6 at the invading fronts of the primary lesion and liver metastasis in patients with colorectal adenocarcinoma. Br J Cancer 83, 769-774.

Kriajevska, M., Bronstein, I.B., Scott, D.J., Tarabykina, S., Fischer-Larsen, M., Issinger, O., and Lukanidin, E. (2000). Metastasis-associated protein Mts1 (S100A4) inhibits CK2-mediated phosphorylation and self-assembly of the heavy chain of nonmuscle myosin. Biochim Biophys Acta 1498, 252-263.

Kube, D., Laser, H., von Knethen, A., and Tesch, H. (1999). The AT-rich region between -54 to -66 is important for the promoter activity of interleukin-10 in Epstein-Barr virus positive Burkitt's lymphoma cells. Genes Immun 1, 105-114.

Kuppers, R., and Dalla-Favera, R. (2001). Mechanisms of chromosomal translocations in B cell lymphomas. Oncogene 20, 5580-5594.

Kuppers, R., Schmitz, R., Distler, V., Renne, C., Brauninger, A., and Hansmann, M.L. (2005). Pathogenesis of Hodgkin's lymphoma. Eur J Haematol Suppl, 26-33.

Lagneaux, L., Delforge, A., Bron, D., Massy, M., Bernier, M., and Stryckmans, P. (1997). Heterogenous response of B lymphocytes to transforming growth factor-beta in B-cell chronic lymphocytic leukaemia: correlation with the expression of TGF-beta receptors. Br J Haematol 97, 612-620.

Lakshmi, M.S., Parker, C., and Sherbet, G.V. (1993). Metastasis associated MTS1 and NM23 genes affect tubulin polymerisation in B16 melanomas: a possible mechanism of their regulation of metastatic behaviour of tumours. Anticancer Res 13, 299-303.

Lan, Q., Zheng, T., Rothman, N., Zhang, Y., Wang, S.S., Shen, M., Berndt, S.I., Zahm, S.H., Holford, T.R., Leaderer, B., et al. (2006). Cytokine polymorphisms in the Th1/Th2 pathway and susceptibility to non-Hodgkin lymphoma. Blood 107, 4101-4108.

Landau, D.A., Carter, S.L., Stojanov, P., McKenna, A., Stevenson, K., Lawrence, M.S., Sougnez, C., Stewart, C., Sivachenko, A., Wang, L., et al. (2013). Evolution and impact of subclonal mutations in chronic lymphocytic leukemia. Cell 152, 714-726.

Lech-Maranda, E., Baseggio, L., Bienvenu, J., Charlot, C., Berger, F., Rigal, D., Warzocha, K., Coiffier, B., and Salles, G. (2004). Interleukin-10 gene promoter polymorphisms influence the clinical outcome of diffuse large B-cell lymphoma. Blood 103, 3529-3534.

Lee, S.-J., Choi, S.Y., Kim, W.-J., Ji, M., Lee, T.-G., Son, B.-R., Yoon, S.M., Sung, R., Lee, E.J., and Youn, S.J. (2013). Combined aberrant expression of E-cadherin and S100A4, but not beta-catenin is associated with disease-free survival and overall survival in colorectal cancer patients. Diagn Pathol 8, 99.

Lee, W.Y., Su, W.C., Lin, P.W., Guo, H.R., Chang, T.W., and Chen, H.H. (2004). Expression of S100A4 and Met: potential predictors for metastasis and survival in early-stage breast cancer. Oncology 66, 429-438.

Lemma, S., Karihtala, P., Haapasaari, K.M., Jantunen, E., Soini, Y., Bloigu, R., Pasanen, A.K., Turpeenniemi-Hujanen, T., and Kuittinen, O. (2013). Biological roles and prognostic values of the epithelial-mesenchymal transition-mediating transcription factors Twist, ZEB1 and Slug in diffuse large B-cell lymphoma. Histopathology 62, 326-333.

Lenz, G., Wright, G.W., Emre, N.T., Kohlhammer, H., Dave, S.S., Davis, R.E., Carty, S., Lam, L.T., Shaffer, A., and Xiao, W. (2008). Molecular subtypes of diffuse large B-cell lymphoma arise by distinct genetic pathways. Proceedings of the National Academy of Sciences 105, 13520-13525.

Lesniak, W., Slomnicki, L.P., and Filipek, A. (2009). S100A6 - new facts and features. Biochem Biophys Res Commun 390, 1087-1092.

Li, J., Wang, X.H., Li, Z.Y., Bu, Z.D., Wu, A.W., Zhang, L.H., Wu, X.J., Zong, X.L., and Ji, J.F. (2013). [Regulation mechanism study of S100A6 on invasion and metastasis in gastric cancer]. Zhonghua Wei Chang Wai Ke Za Zhi 16, 1096-1101.

Li, Z., Tang, M., Ling, B., Liu, S., Zheng, Y., Nie, C., Yuan, Z., Zhou, L., Guo, G., Tong, A., et al. (2014). Increased expression of S100A6 promotes cell proliferation and migration in human hepatocellular carcinoma. J Mol Med (Berl) 92, 291-303.

Li, Z.H., and Bresnick, A.R. (2006). The S100A4 metastasis factor regulates cellular motility via a direct interaction with myosin-IIA. Cancer Res 66, 5173-5180.

Lindsey, J.C., Lusher, M.E., Anderton, J.A., Gilbertson, R.J., Ellison, D.W., and Clifford, S.C. (2007). Epigenetic deregulation of multiple S100 gene family members by differential hypomethylation and hypermethylation events in medulloblastoma. Br J Cancer 97, 267-274.

Liriano, M.A., Varney, K.M., Wright, N.T., Hoffman, C.L., Toth, E.A., Ishima, R., and Weber, D.J. (2012). Target binding to S100B reduces dynamic properties and increases Ca(2+)-binding affinity for wild type and EF-hand mutant proteins. J Mol Biol 423, 365-385.

Lohr, J.G., Stojanov, P., Lawrence, M.S., Auclair, D., Chapuy, B., Sougnez, C., Cruz-Gordillo, P., Knoechel, B., Asmann, Y.W., Slager, S.L., et al. (2012). Discovery and prioritization of somatic mutations in diffuse large B-cell lymphoma (DLBCL) by whole-exome sequencing. Proc Natl Acad Sci U S A 109, 3879-3884.

Luu, H.H., Zhou, L., Haydon, R.C., Deyrup, A.T., Montag, A.G., Huo, D., Heck, R., Heizmann, C.W., Peabody, T.D., Simon, M.A., et al. (2005). Increased expression of S100A6 is associated with decreased metastasis and inhibition of cell migration and anchorage independent growth in human osteosarcoma. Cancer Lett 229, 135-148.

Mack, G.S., and Marshall, A. (2010). Lost in migration. Nat Biotechnol 28, 214-229.

Mahmood, T., and Yang, P.-C. (2012). Western Blot: Technique, Theory, and Trouble Shooting. North American Journal of Medical Sciences 4, 429-434.

Malashkevich, V.N., Dulyaninova, N.G., Ramagopal, U.A., Liriano, M.A., Varney, K.M., Knight, D., Brenowitz, M., Weber, D.J., Almo, S.C., and Bresnick, A.R. (2010). Phenothiazines inhibit S100A4 function by inducing protein oligomerization. Proc Natl Acad Sci U S A 107, 8605-8610.

Marenholz, I., Heizmann, C.W., and Fritz, G. (2004). S100 proteins in mouse and man: from evolution to function and pathology (including an update of the nomenclature). Biochem Biophys Res Commun 322, 1111-1122.

Mårtensson, I.-L., Almqvist, N., Grimsholm, O., and Bernardi, A.I. (2010). The pre-B cell receptor checkpoint. FEBS letters 584, 2572-2579.

Martin, V.G., Wu, Y.B., Townsend, C.L., Lu, G.H., O'Hare, J.S., Mozeika, A., Coolen, A.C., Kipling, D., Fraternali, F., and Dunn-Walters, D.K. (2016). Transitional B Cells in Early Human B Cell Development - Time to Revisit the Paradigm? Front Immunol 7, 546.

Martinez-Maza, O., and Breen, E.C. (2002). B-cell activation and lymphoma in patients with HIV. Curr Opin Oncol 14, 528-532.

Matsumoto, K., Irie, A., Satoh, T., Ishii, J., Iwabuchi, K., Iwamura, M., Egawa, S., and Baba, S. (2007). Expression of S100A2 and S100A4 predicts for disease progression and patient survival in bladder cancer. Urology 70, 602-607.

Melbye, M., Smedby, K.E., Lehtinen, T., Rostgaard, K., Glimelius, B., Munksgaard, L., Schollkopf, C., Sundstrom, C., Chang, E.T., Koskela, P., et al. (2007). Atopy and risk of non-Hodgkin lymphoma. J Natl Cancer Inst 99, 158-166.

Mercier, F.E., Ragu, C., and Scadden, D.T. (2011). The bone marrow at the crossroads of blood and immunity. Nat Rev Immunol 12, 49-60.

Miao, L., Grebhardt, S., Shi, J., Peipe, I., Zhang, J., and Mayer, D. (2012). Prostaglandin E2 stimulates S100A8 expression by activating protein kinase A and CCAAT/enhancer-binding-protein-beta in prostate cancer cells. Int J Biochem Cell Biol 44, 1919-1928.

Mishra, S.K., Siddique, H.R., and Saleem, M. (2012). S100A4 calcium-binding protein is key player in tumor progression and metastasis: preclinical and clinical evidence. Cancer Metastasis Rev 31, 163-172.

Molofsky, A.V., Pardal, R., Iwashita, T., Park, I.K., Clarke, M.F., and Morrison, S.J. (2003). Bmi-1 dependence distinguishes neural stem cell self-renewal from progenitor proliferation. Nature 425, 962-967.

Moody, S.E., Perez, D., Pan, T.C., Sarkisian, C.J., Portocarrero, C.P., Sterner, C.J., Notorfrancesco, K.L., Cardiff, R.D., and Chodosh, L.A. (2005). The transcriptional repressor Snail promotes mammary tumor recurrence. Cancer Cell 8, 197-209.

Morin, R.D., Mendez-Lago, M., Mungall, A.J., Goya, R., Mungall, K.L., Corbett, R.D., Johnson, N.A., Severson, T.M., Chiu, R., Field, M., et al. (2011). Frequent mutation of histone-modifying genes in non-Hodgkin lymphoma. Nature 476, 298-303.

Morton, L.M., Turner, J.J., Cerhan, J.R., Linet, M.S., Treseler, P.A., Clarke, C.A., Jack, A., Cozen, W., Maynadie, M., Spinelli, J.J., et al. (2007). Proposed classification of lymphoid neoplasms for epidemiologic research from the Pathology Working Group of the International Lymphoma Epidemiology Consortium (InterLymph). Blood 110, 695-708.

Murphy, K., Travers, P., Walport, M., and Janeway, C. (2012). Janeway's immunobiology (New York: Garland Science).

Nagasaki, T., Hara, M., Nakanishi, H., Takahashi, H., Sato, M., and Takeyama, H. (2014). Interleukin-6 released by colon cancer-associated fibroblasts is critical for tumour angiogenesis: anti-interleukin-6 receptor antibody suppressed angiogenesis and inhibited tumour-stroma interaction. Br J Cancer 110, 469-478.

National Cancer Institute. SEER cancer statistics review 1975–2013. Non-Hodgkin lymphoma. 2016. https://seer.cancer.gov/csr/1975_2013/results_merged/sect_19_nhl.pdf. Accessed 21 Jun 2017.

Naz, S., Bashir, M., Ranganathan, P., Bodapati, P., Santosh, V., and Kondaiah, P. (2014). Protumorigenic actions of S100A2 involve regulation of PI3/Akt signaling and functional interaction with Smad3. Carcinogenesis 35, 14-23.

Necula, L.G., Chivu-Economescu, M., Stanciulescu, E.L., Bleotu, C., Dima, S.O., Alexiu, I., Dumitru, A., Constantinescu, G., Popescu, I., and Diaconu, C.C. (2012). IL-6 and IL-11 as markers for tumor aggressiveness and prognosis in gastric adenocarcinoma patients without mutations in Gp130 subunits. J Gastrointestin Liver Dis 21, 23-29.

Nemeth, J., Stein, I., Haag, D., Riehl, A., Longerich, T., Horwitz, E., Breuhahn, K., Gebhardt, C., Schirmacher, P., Hahn, M., et al. (2009). S100A8 and S100A9 are novel nuclear factor kappa B target genes during malignant progression of murine and human liver carcinogenesis. Hepatology 50, 1251-1262.

Ngo, V.N., Young, R.M., Schmitz, R., Jhavar, S., Xiao, W., Lim, K.H., Kohlhammer, H., Xu, W., Yang, Y., Zhao, H., et al. (2011). Oncogenically active MYD88 mutations in human lymphoma. Nature 470, 115-119.

Nicolas, E., Ramus, C., Berthier, S., Arlotto, M., Bouamrani, A., Lefebvre, C., Morel, F., Garin, J., Ifrah, N., and Berger, F. (2011). Expression of S100A8 in leukemic cells predicts poor survival in de novo AML patients. Leukemia 25, 57-65.

Ning, X., Sun, S., Zhang, K., Liang, J., Chuai, Y., Li, Y., and Wang, X. (2012). S100A6 protein negatively regulates CacyBP/SIP-mediated inhibition of gastric cancer cell proliferation and tumorigenesis. PLoS One 7, e30185.

Ninomiya, I., Ohta, T., Fushida, S., Endo, Y., Hashimoto, T., Yagi, M., Fujimura, T., Nishimura, G., Tani, T., Shimizu, K., et al. (2001). Increased expression of S100A4 and its prognostic significance in esophageal squamous cell carcinoma. Int J Oncol 18, 715-720.

Niu, Y., Wang, L., Cheng, C., Du, C., Lu, X., Wang, G., and Liu, J. (2015). Increased expressions of SATB1 and S100A4 are associated with poor prognosis in human colorectal carcinoma. APMIS 123, 93-101.

Nowotny, M., Spiechowicz, M., Jastrzebska, B., Filipek, A., Kitagawa, K., and Kuznicki, J. (2003). Calcium-regulated interaction of Sgt1 with S100A6 (calcyclin) and other S100 proteins. J Biol Chem 278, 26923-26928.

Oida, Y., Yamazaki, H., Tobita, K., Mukai, M., Ohtani, Y., Miyazaki, N., Abe, Y., Imaizumi, T., Makuuchi, H., Ueyama, Y., et al. (2006). Increased S100A4 expression combined with decreased E-cadherin expression predicts a poor outcome of patients with pancreatic cancer. Oncol Rep 16, 457-463.

Okada, M., Tokumitsu, H., Kubota, Y., and Kobayashi, R. (2002). Interaction of S100 proteins with the antiallergic drugs, olopatadine, amlexanox, and cromolyn: identification of putative drug binding sites on S100A1 protein. Biochem Biophys Res Commun 292, 1023-1030.

Orazi, A., Du, X., Yang, Z., Kashai, M., and Williams, D.A. (1996). Interleukin-11 prevents apoptosis and accelerates recovery of small intestinal mucosa in mice treated with combined chemotherapy and radiation. Lab Invest 75, 33-42.

Orr, B., Riddick, A.C., Stewart, G.D., Anderson, R.A., Franco, O.E., Hayward, S.W., and Thomson, A.A. (2012). Identification of stromally expressed molecules in the prostate by tag-profiling of cancer-associated fibroblasts, normal fibroblasts and fetal prostate. Oncogene 31, 1130-1142.

Orre, L.M., Pernemalm, M., Lengqvist, J., Lewensohn, R., and Lehtio, J. (2007). Up-regulation, modification, and translocation of S100A6 induced by exposure to ionizing radiation revealed by proteomics profiling. Mol Cell Proteomics 6, 2122-2131.

O'Shea, J.J., Ma, A., and Lipsky, P. (2002). Cytokines and autoimmunity. Nat Rev Immunol 2, 37-45.

Osterreicher, C.H., Penz-Osterreicher, M., Grivennikov, S.I., Guma, M., Koltsova, E.K., Datz, C., Sasik, R., Hardiman, G., Karin, M., and Brenner, D.A. (2011). Fibroblast-specific protein 1 identifies an inflammatory subpopulation of macrophages in the liver. Proc Natl Acad Sci U S A 108, 308-313.

Paiva, P., Salamonsen, L.A., Manuelpillai, U., Walker, C., Tapia, A., Wallace, E.M., and Dimitriadis, E. (2007). Interleukin-11 promotes migration, but not proliferation, of human trophoblast cells, implying a role in placentation. Endocrinology 148, 5566-5572.

Pasqualucci, L., and Dalla-Favera, R. (2015). The Genetic Landscape of Diffuse Large B Cell Lymphoma. Seminars in hematology 52, 67-76.

Pasqualucci, L., Trifonov, V., Fabbri, G., Ma, J., Rossi, D., Chiarenza, A., Wells, V.A., Grunn, A., Messina, M., Elliot, O., et al. (2011). Analysis of the coding genome of diffuse large B-cell lymphoma. Nat Genet 43, 830-837.

Pedersen, K.B., Andersen, K., Fodstad, O., and Maelandsmo, G.M. (2004). Sensitization of interferon-gamma induced apoptosis in human osteosarcoma cells by extracellular S100A4. BMC Cancer 4, 52.

Pekarsky, Y., Zanesi, N., and Croce, C.M. (2010). Molecular basis of CLL. Semin Cancer Biol 20, 370-376.

Pierce, J.W., Schoenleber, R., Jesmok, G., Best, J., Moore, S.A., Collins, T., and Gerritsen, M.E. (1997). Novel inhibitors of cytokine-induced IkappaBalpha phosphorylation and endothelial cell adhesion molecule expression show anti-inflammatory effects in vivo. J Biol Chem 272, 21096-21103.

Pignatelli, M., Ansari, T.W., Gunter, P., Liu, D., Hirano, S., Takeichi, M., Kloppel, G., and Lemoine, N.R. (1994). Loss of membranous E-cadherin expression in pancreatic cancer: correlation with lymph node metastasis, high grade, and advanced stage. J Pathol 174, 243-248.

Pili, R., Haggman, M., Stadler, W.M., Gingrich, J.R., Assikis, V.J., Bjork, A., Nordle, O., Forsberg, G., Carducci, M.A., and Armstrong, A.J. (2011). Phase II randomized, double-blind, placebo-controlled study of tasquinimod in men with minimally symptomatic metastatic castrate-resistant prostate cancer. J Clin Oncol 29, 4022-4028.

Piris, M.A., Onaindia, A., and Mollejo, M. (2017). Splenic marginal zone lymphoma. Best Pract Res Clin Haematol 30, 56-64.

Purdue, M.P., Lan, Q., Kricker, A., Grulich, A.E., Vajdic, C.M., Turner, J., Whitby, D., Chanock, S., Rothman, N., and Armstrong, B.K. (2007). Polymorphisms in immune function genes and risk of non-Hodgkin lymphoma: findings from the New South Wales non-Hodgkin Lymphoma Study. Carcinogenesis 28, 704-712.

Putoczki, T.L., Thiem, S., Loving, A., Busuttil, R.A., Wilson, N.J., Ziegler, P.K., Nguyen, P.M., Preaudet, A., Farid, R., Edwards, K.M., et al. (2013). Interleukin-11 is the dominant IL-6 family cytokine during gastrointestinal tumorigenesis and can be targeted therapeutically. Cancer Cell 24, 257-271.

Qin, H., Lerman, B., Sakamaki, I., Wei, G., Cha, S.C., Rao, S.S., Qian, J., Hailemichael, Y., Nurieva, R., Dwyer, K.C., et al. (2014). Generation of a new therapeutic peptide that depletes myeloid-derived suppressor cells in tumor-bearing mice. Nat Med 20, 676-681.

Rafii, S., and Lyden, D. (2006). S100 chemokines mediate bookmarking of premetastatic niches. Nat Cell Biol 8, 1321-1323.

Rani, S.G., Mohan, S.K., and Yu, C. (2010). Molecular level interactions of S100A13 with amlexanox: inhibitor for formation of the multiprotein complex in the nonclassical pathway of acidic fibroblast growth factor. Biochemistry 49, 2585-2592.

Rivard, C.J., Brown, L.M., Almeida, N.E., Maunsbach, A.B., Pihakaski-Maunsbach, K., Andres-Hernando, A., Capasso, J.M., and Berl, T. (2007). Expression of the calcium-binding protein S100A4 is markedly up-regulated by osmotic stress and is involved in the renal osmoadaptive response. J Biol Chem 282, 6644-6652.

Robertson, K.D. (2005). DNA methylation and human disease. Nat Rev Genet 6, 597-610.

Rohde, D., Ritterhoff, J., Voelkers, M., Katus, H.A., Parker, T.G., and Most, P. (2010). S100A1: a multifaceted therapeutic target in cardiovascular disease. J Cardiovasc Transl Res 3, 525-537.

Roltsch, E., Holcomb, L., Young, K.A., Marks, A., and Zimmer, D.B. (2010). PSAPP mice exhibit regionally selective reductions in gliosis and plaque deposition in response to S100B ablation. J Neuroinflammation 7, 78.

Roos-Weil, D., Nguyen-Khac, F., and Bernard, O.A. (2016). Chronic lymphocytic leukemia: Time to go past genomics? American journal of hematology.

Roth, J., Vogl, T., Sorg, C., and Sunderkotter, C. (2003). Phagocyte-specific S100 proteins: a novel group of proinflammatory molecules. Trends Immunol 24, 155-158.

Rothman, N., Skibola, C.F., Wang, S.S., Morgan, G., Lan, Q., Smith, M.T., Spinelli, J.J., Willett, E., De Sanjose, S., Cocco, P., et al. (2006). Genetic variation in TNF and IL10 and risk of non-Hodgkin lymphoma: a report from the InterLymph Consortium. Lancet Oncol 7, 27-38.

Rudland, P.S., Platt-Higgins, A., Renshaw, C., West, C.R., Winstanley, J.H., Robertson, L., and Barraclough, R. (2000). Prognostic significance of the metastasis-inducing protein S100A4 (p9Ka) in human breast cancer. Cancer Res 60, 1595-1603.

Ryan, D.G., Taliana, L., Sun, L., Wei, Z.G., Masur, S.K., and Lavker, R.M. (2003). Involvement of S100A4 in stromal fibroblasts of the regenerating cornea. Invest Ophthalmol Vis Sci 44, 4255-4262.

Sabattini, E., Bacci, F., Sagramoso, C., and Pileri, S.A. (2010). WHO classification of tumours of haematopoietic and lymphoid tissues in 2008: an overview. Pathologica 102, 83-87.

Sack, U., and Stein, U. (2009). Wnt up your mind - intervention strategies for S100A4-induced metastasis in colon cancer. Gen Physiol Biophys 28 Spec No Focus, F55-64.

Sack, U., Walther, W., Scudiero, D., Selby, M., Aumann, J., Lemos, C., Fichtner, I., Schlag, P.M., Shoemaker, R.H., and Stein, U. (2011). S100A4-induced cell motility and metastasis is restricted by the Wnt/beta-catenin pathway inhibitor calcimycin in colon cancer cells. Mol Biol Cell 22, 3344-3354.

Sahasrabuddhe, A.A. (2016). BMI1: A Biomarker of Hematologic Malignancies. Biomarkers in Cancer 8, 65-75.

Sánchez-Tilló, E., Fanlo, L., Siles, L., Montes-Moreno, S., Moros, A., Chiva-Blanch, G., Estruch, R., Martinez, A., Colomer, D., Győrffy, B., et al. (2014). The EMT activator ZEB1 promotes tumor growth and determines differential response to chemotherapy in mantle cell lymphoma. Cell Death and Differentiation 21, 247-257.

Santamaria-Kisiel, L., Rintala-Dempsey, A.C., and Shaw, G.S. (2006). Calcium-dependent and -independent interactions of the S100 protein family. Biochem J 396, 201-214.

Santos, F.P., and O'Brien, S. (2012). Small lymphocytic lymphoma and chronic lymphocytic leukemia: are they the same disease? Cancer J 18, 396-403.

Sapkota, D., Bruland, O., Bøe, O.E., Bakeer, H., Elgindi, O.A.A., Vasstrand, E.N., and Ibrahim, S.O. (2008). Expression profile of the S100 gene family members in oral squamous cell carcinomas. Journal of Oral Pathology & Medicine 37, 607-615.

Sato, Y., Harada, K., Itatsu, K., Ikeda, H., Kakuda, Y., Shimomura, S., Shan Ren, X., Yoneda, N., Sasaki, M., and Nakanuma, Y. (2010). Epithelial-mesenchymal transition induced by transforming growth factor-beta1/Snail activation aggravates invasive growth of cholangiocarcinoma. Am J Pathol 177, 141-152.

Sayan, A.E. (2014). Tumour-promoting role of EMT-inducing transcription factor ZEB1 in mantle cell lymphoma. Cell Death Differ 21, 194-195.

Schmidt-Hansen, B., Örnås, D., Grigorian, M., Klingelhöfer, J., Tulchinsky, E., Lukanidin, E., and Ambartsumian, N. (2004). Extracellular S100A4(mts1) stimulates invasive growth of mouse endothelial cells and modulates MMP-13 matrix metalloproteinase activity. Oncogene 23, 5487.

Schneider, M., Hansen, J.L., and Sheikh, S.P. (2008). S100A4: a common mediator of epithelial-mesenchymal transition, fibrosis and regeneration in diseases? J Mol Med (Berl) 86, 507-522.

Sheng, J.G., Mrak, R.E., and Griffin, W.S. (1994). S100 beta protein expression in Alzheimer disease: potential role in the pathogenesis of neuritic plaques. J Neurosci Res 39, 398-404.

Sherbet, G.V. (2009). Metastasis promoter S100A4 is a potentially valuable molecular target for cancer therapy. Cancer Lett 280, 15-30.

Sherbet, G.V. (2014). Gene Section. http://AtlasGeneticsOncology org, 381.

Skibola, C.F., Curry, J.D., and Nieters, A. (2007). Genetic susceptibility to lymphoma. Haematologica 92, 960-969.

Soda, H., Raymond, E., Sharma, S., Lawrence, R., Cerna, C., Gomez, L., Schaub, R., Von Hoff, D.D., and Izbicka, E. (1999). Recombinant human interleukin-11 is unlikely to stimulate the growth of the most common solid tumours. Anticancer Drugs 10, 97-101.

Solal-Celigny, P., Roy, P., Colombat, P., White, J., Armitage, J.O., Arranz-Saez, R., Au, W.Y., Bellei, M., Brice, P., Caballero, D., et al. (2004). Follicular lymphoma international prognostic index. Blood 104, 1258-1265.

Sonderegger, S., Yap, J., Menkhorst, E., Weston, G., Stanton, P.G., and Dimitriadis, E. (2011). Interleukin (IL)11 mediates protein secretion and modification in human extravillous trophoblasts. Hum Reprod 26, 2841-2849.

Speiser, D.E., Utzschneider, D.T., Oberle, S.G., Munz, C., Romero, P., and Zehn, D. (2014). T cell differentiation in chronic infection and cancer: functional adaptation or exhaustion? Nat Rev Immunol 14, 768-774.

Spiekerkoetter, E., Guignabert, C., de Jesus Perez, V., Alastalo, T.-P., Powers, J.M., Wang, L., Lawrie, A., Ambartsumian, N., Schmidt, A.-M., Berryman, M., et al. (2009). S100A4 and BMP-2 Co-Dependently Induce Vascular Smooth Muscle Cell Migration via pERK and Chloride Intracellular Channel 4 (CLIC4). Circulation research 105, 639.

Spina, V., and Rossi, D. (2017). Molecular pathogenesis of splenic and nodal marginal zone lymphoma. Best Pract Res Clin Haematol 30, 5-12.

Spink, C.F., Keen, L.J., Mensah, F.K., Law, G.R., Bidwell, J.L., and Morgan, G.J. (2006). Association between non-Hodgkin lymphoma and haplotypes in the TNF region. Br J Haematol 133, 293-300.

Stein, U., Arlt, F., Smith, J., Sack, U., Herrmann, P., Walther, W., Lemm, M., Fichtner, I., Shoemaker, R.H., and Schlag, P.M. (2011). Intervening in beta-catenin signaling by sulindac inhibits S100A4-dependent colon cancer metastasis. Neoplasia 13, 131-144.

Stein, U., Arlt, F., Walther, W., Smith, J., Waldman, T., Harris, E.D., Mertins, S.D., Heizmann, C.W., Allard, D., Birchmeier, W., et al. (2006). The metastasis-associated gene S100A4 is a novel target of beta-catenin/T-cell factor signaling in colon cancer. Gastroenterology 131, 1486-1500.

Strutz, F., Okada, H., Lo, C.W., Danoff, T., Carone, R.L., Tomaszewski, J.E., and Neilson, E.G. (1995). Identification and characterization of a fibroblast marker: FSP1. J Cell Biol 130, 393-405.

Suda, T., Arai, F., and Hirao, A. (2005). Hematopoietic stem cells and their niche. Trends Immunol 26, 426-433.

Suman, P., Poehlmann, T.G., Prakash, G.J., Markert, U.R., and Gupta, S.K. (2009). Interleukin-11 increases invasiveness of JEG-3 choriocarcinoma cells by modulating STAT3 expression. J Reprod Immunol 82, 1-11.

Sweetenham, J.W., Goldman, B., LeBlanc, M.L., Cook, J.R., Tubbs, R.R., Press, O.W., Maloney, D.G., Fisher, R.I., Rimsza, L.M., Braziel, R.M., et al. (2010). Prognostic value of regulatory T cells, lymphoma-associated macrophages, and MUM-1 expression in follicular lymphoma treated before and after the introduction of monoclonal antibody therapy: a Southwest Oncology Group Study. Ann Oncol 21, 1196-1202.

Swerdlow, S.H., Campo, E., Pileri, S.A., Harris, N.L., Stein, H., Siebert, R., Advani, R., Ghielmini, M., Salles, G.A., and Zelenetz, A.D. (2016). The 2016 revision of the World Health Organization classification of lymphoid neoplasms. Blood 127, 2375-2390.

Tadmor, T., and Polliack, A. (2017). Nodal marginal zone lymphoma: Clinical features, diagnosis, management and treatment. Best Pract Res Clin Haematol 30, 92-98.

Takenaga, K., Nakamura, Y., and Sakiyama, S. (1994). Cellular localization of pEL98 protein, an S100-related calcium binding protein, in fibroblasts and its tissue distribution analyzed by monoclonal antibodies. Cell Struct Funct 19, 133-141.

Takenaga, K., Nakamura, Y., and Sakiyama, S. (1997). Expression of antisense RNA to S100A4 gene encoding an S100-related calcium-binding protein suppresses metastatic potential of high-metastatic Lewis lung carcinoma cells. Oncogene 14, 331-337.

Takenaga, K., Nakamura, Y., Endo, H., and Sakiyama, S. (1994). Involvement of S100-related calcium-binding protein pEL98 (or mts1) in cell motility and tumor cell invasion. Jpn J Cancer Res 85, 831-839.

Tang, W., Yang, L., Yang, Y.C., Leng, S.X., and Elias, J.A. (1998). Transforming growth factor-beta stimulates interleukin-11 transcription via complex activating protein-1-dependent pathways. J Biol Chem 273, 5506-5513.

Tarabykina, S., Griffiths, T.R., Tulchinsky, E., Mellon, J.K., Bronstein, I.B., and Kriajevska, M. (2007). Metastasis-associated protein S100A4: spotlight on its role in cell migration. Curr Cancer Drug Targets 7, 217-228.

Tarabykina, S., Griffiths, T.R., Tulchinsky, E., Mellon, J.K., Bronstein, I.B., and Kriajevska, M. (2007). Metastasis-associated protein S100A4: spotlight on its role in cell migration. Curr Cancer Drug Targets 7, 217-228.

Taylor, J., Xiao, W., and Abdel-Wahab, O. (2017). Diagnosis and classification of hematologic malignancies on the basis of genetics. Blood.

Terzic, J., Grivennikov, S., Karin, E., and Karin, M. (2010). Inflammation and colon cancer. Gastroenterology 138, 2101-2114 e2105.

Tesch, G.H., Lan, H.Y., and Nikolic-Paterson, D.J. (2006). Treatment of tissue sections for in situ hybridization. Methods Mol Biol 326, 1-7.

Thalmeier, K., Meissner, P., Reisbach, G., Hultner, L., Mortensen, B.T., Brechtel, A., Oostendorp, R.A., and Dormer, P. (1996). Constitutive and modulated cytokine expression in two permanent human bone marrow stromal cell lines. Exp Hematol 24, 1-10.

Thiery, J.P. (2002). Epithelial-mesenchymal transitions in tumour progression. Nat Rev Cancer 2, 442-454.

Tian, T., Hao, J., Xu, A., Hao, J., Luo, C., Liu, C., Huang, L., Xiao, X., and He, D. (2007). Determination of metastasis-associated proteins in non-small cell lung cancer by comparative proteomic analysis. Cancer Sci 98, 1265-1274.

Tothova, Z., and Gilliland, D.G. (2007). FoxO transcription factors and stem cell homeostasis: insights from the hematopoietic system. Cell Stem Cell 1, 140-152.

Tsimanis, A., Shvidel, L., Klepfish, A., Shtalrid, M., Kalinkovich, A., and Berrebi, A. (2001). Over-expression of the functional interleukin-11 alpha receptor in the development of B-cell chronic lymphocytic leukemia. Leuk Lymphoma 42, 195-205.

Tsoporis, J.N., Izhar, S., Leong-Poi, H., Desjardins, J.F., Huttunen, H.J., and Parker, T.G. (2010). S100B interaction with the receptor for advanced glycation end products (RAGE): a novel receptor-mediated mechanism for myocyte apoptosis postinfarction. Circ Res 106, 93-101.

Tsoporis, J.N., Marks, A., Haddad, A., Dawood, F., Liu, P.P., and Parker, T.G. (2005). S100B expression modulates left ventricular remodeling after myocardial infarction in mice. Circulation 111, 598-606.

Tsukasaki, K., and Tobinai, K. (2014). Adult T-cell leukemia-lymphoma. In Rare Lymphomas (Springer), pp. 99-110.

Tulchinsky, E., Grigorian, M., Tkatch, T., Georgiev, G., and Lukanidin, E. (1995). Transcriptional regulation of the mts1 gene in human lymphoma cells: the role of DNA-methylation. Biochim Biophys Acta 1261, 243-248.

Tuna, M., Machado, A.S., and Calin, G.A. (2016). Genetic and epigenetic alterations of microRNAs and implications for human cancers and other diseases. Genes, Chromosomes and Cancer 55, 193-214.

Van Den Berghe, H., Parloir, C., Gosseye, S., Englebienne, V., Cornu, G., and Sokal, G. (1979). Variant translocation in Burkitt lymphoma. Cancer Genetics and Cytogenetics 1, 9-14.

Vandewalle, C., Comijn, J., De Craene, B., Vermassen, P., Bruyneel, E., Andersen, H., Tulchinsky, E., Van Roy, F., and Berx, G. (2005). SIP1/ZEB2 induces EMT by repressing genes of different epithelial cell–cell junctions. Nucleic acids research 33, 6566-6578.

Venkov, C.D., Link, A.J., Jennings, J.L., Plieth, D., Inoue, T., Nagai, K., Xu, C., Dimitrova, Y.N., Rauscher, F.J., and Neilson, E.G. (2007). A proximal activator of transcription in epithelial-mesenchymal transition. J Clin Invest 117, 482-491.

Victora, G.D., and Nussenzweig, M.C. (2012). Germinal centers. Annu Rev Immunol 30, 429-457.

Vimalachandran, D., Greenhalf, W., Thompson, C., Luttges, J., Prime, W., Campbell, F., Dodson, A., Watson, R., Crnogorac-Jurcevic, T., Lemoine, N., et al. (2005). High nuclear S100A6 (Calcyclin) is significantly associated with poor survival in pancreatic cancer patients. Cancer Res 65, 3218-3225.

Vogl, T., Ludwig, S., Goebeler, M., Strey, A., Thorey, I.S., Reichelt, R., Foell, D., Gerke, V., Manitz, M.P., Nacken, W., et al. (2004). MRP8 and MRP14 control microtubule reorganization during transendothelial migration of phagocytes. Blood 104, 4260-4268.

Vollbrecht, C., Mairinger, F.D., Koitzsch, U., Peifer, M., Koenig, K., Heukamp, L.C., Crispatzu, G., Wilden, L., Kreuzer, K.A., Hallek, M., et al. (2015). Comprehensive Analysis of Disease-Related Genes in Chronic Lymphocytic Leukemia by Multiplex PCR-Based Next Generation Sequencing. PLoS One 10, e0129544.

Wang, J., Homer, R.J., Hong, L., Cohn, L., Lee, C.G., Jung, S., and Elias, J.A. (2000). IL-11 selectively inhibits aeroallergen-induced pulmonary eosinophilia and Th2 cytokine production. J Immunol 165, 2222-2231.

Wang, S.S., Cerhan, J.R., Hartge, P., Davis, S., Cozen, W., Severson, R.K., Chatterjee, N., Yeager, M., Chanock, S.J., and Rothman, N. (2006). Common genetic variants in proinflammatory and other immunoregulatory genes and risk for non-Hodgkin lymphoma. Cancer Res 66, 9771-9780.

Weber, C., Neacsu, I., Krautz, B., Schlegel, P., Sauer, S., Raake, P., Ritterhoff, J., Jungmann, A., Remppis, A.B., Stangassinger, M., et al. (2014). Therapeutic safety of high myocardial expression levels of the molecular inotrope S100A1 in a preclinical heart failure model. Gene Ther 21, 131-138.

Xie, R., Schlumbrecht, M.P., Shipley, G.L., Xie, S., Bassett, R.L., Jr., and Broaddus, R.R. (2009). S100A4 mediates endometrial cancer invasion and is a target of TGF-beta1 signaling. Lab Invest 89, 937-947.

Xu, H., Li, M., Zhou, Y., Wang, F., Li, X., Wang, L., and Fan, Q. (2016). S100A4 participates in epithelial-mesenchymal transition in breast cancer via targeting MMP2. Tumour Biol 37, 2925-2932.

Xu, P.P., Qian, Y., Chen, Q.S., Li, L.Q., Zhang, L., and Zhao, W.L. (2017). [Prognostic Significance of Follicular Lymphoma International Prognostic Index 2 (FLIPI2) in Follicular Lymphoma Patients Treated with Rituximab Maintenance]. Zhongguo Shi Yan Xue Ye Xue Za Zhi 25, 426-430.

Xu, X., Su, B., Xie, C., Wei, S., Zhou, Y., Liu, H., Dai, W., Cheng, P., Wang, F., Xu, X., et al. (2014). Sonic hedgehog-Gli1 signaling pathway regulates the epithelial mesenchymal transition (EMT) by mediating a new target gene, S100A4, in pancreatic cancer cells. PLoS One 9, e96441.

Yamaguchi, H., Hanawa, H., Uchida, N., Inamai, M., Sawaguchi, K., Mitamura, Y., Shimada, T., Dan, K., and Inokuchi, K. (2009). Multistep pathogenesis of leukemia via the MLL-AF4 chimeric gene/Flt3 gene tyrosine kinase domain (TKD) mutation-related enhancement of S100A6 expression. Experimental hematology 37, 701-714.

Yamazaki, M., Fukushima, H., Shin, M., Katagiri, T., Doi, T., Takahashi, T., and Jimi, E. (2009). Tumor necrosis factor alpha represses bone morphogenetic protein (BMP) signaling by interfering with the DNA binding of Smads through the activation of NF-kappaB. J Biol Chem 284, 35987-35995.

Yamazumi, K., Nakayama, T., Kusaba, T., Wen, C.Y., Yoshizaki, A., Yakata, Y., Nagayasu, T., and Sekine, I. (2006). Expression of interleukin-11 and interleukin-11 receptor alpha in human colorectal adenocarcinoma; immunohistochemical analyses and correlation with clinicopathological factors. World J Gastroenterol 12, 317-321.

Yammani, R.R., Carlson, C.S., Bresnick, A.R., and Loeser, R.F. (2006). Increase in production of matrix metalloproteinase 13 by human articular chondrocytes due to stimulation with S100A4: Role of the receptor for advanced glycation end products. Arthritis Rheum 54, 2901-2911.

Yan, W., Chen, J., Chen, Z., and Chen, H. (2016). Deregulated miR-296/S100A4 axis promotes tumor invasion by inducing epithelial-mesenchymal transition in human ovarian cancer. Am J Cancer Res 6, 260-269.

Yang, X.C., Wang, X., Luo, L., Dong, D.H., Yu, Q.C., Wang, X.S., and Zhao, K. (2013). RNA interference suppression of A100A4 reduces the growth and metastatic phenotype of human renal cancer cells via NF-kB-dependent MMP-2 and bcl-2 pathway. Eur Rev Med Pharmacol Sci 17, 1669-1680.

Yap, K.L., Ames, J.B., Swindells, M.B., and Ikura, M. (1999). Diversity of conformational states and changes within the EF-hand protein superfamily. Proteins 37, 499-507.

Yasui, T., Yamamoto, T., Sakai, N., Asano, K., Takai, T., Yoshitomi, Y., Davis, M., Takagi, T., Sakamoto, K., Sogabe, S., et al. (2017). Discovery of a novel B-cell lymphoma 6 (BCL6)-corepressor interaction inhibitor by utilizing structure-based drug design. Bioorg Med Chem 25, 4876-4886.

Yin, T., and Li, L. (2006). The stem cell niches in bone. J Clin Invest 116, 1195-1201.

Yonemura, Y., Endou, Y., Kimura, K., Fushida, S., Bandou, E., Taniguchi, K., Kinoshita, K., Ninomiya, I., Sugiyama, K., Heizmann, C.W., et al. (2000). Inverse expression of S100A4 and E-cadherin is associated with metastatic potential in gastric cancer. Clin Cancer Res 6, 4234-4242.

Yuan, T.M., Liang, R.Y., Hsiao, N.W., and Chuang, S.M. (2014). The S100A4 D10V polymorphism is related to cell migration ability but not drug resistance in gastric cancer cells. Oncol Rep 32, 2307-2318.

Yue, X., Zhao, Y., Zhang, C., Li, J., Liu, Z., Liu, J., and Hu, W. (2016). Leukemia inhibitory factor promotes EMT through STAT3-dependent miR-21 induction. Oncotarget 7, 3777-3790.

Zeng, D., Desai, A., Yan, F., Gong, T., Ye, H., Ahmed, M., Nomie, K., Romaguera, J., Champlin, R., Li, S., et al. (2018). Challenges and Opportunities for High-grade B-Cell

Lymphoma With MYC and BCL2 and/or BCL6 Rearrangement (Double-hit Lymphoma). Am J Clin Oncol.

Zeng, F.Y., Gerke, V., and Gabius, H.J. (1993). Identification of annexin II, annexin VI and glyceraldehyde-3-phosphate dehydrogenase as calcyclin-binding proteins in bovine heart. Int J Biochem 25, 1019-1027.

Zhai, X., Zhu, H., Wang, W., Zhang, S., Zhang, Y., and Mao, G. (2014). Abnormal expression of EMT-related proteins, S100A4, vimentin and E-cadherin, is correlated with clinicopathological features and prognosis in HCC. Med Oncol 31, 970.

Zhang, J., Grubor, V., Love, C.L., Banerjee, A., Richards, K.L., Mieczkowski, P.A., Dunphy, C., Choi, W., Au, W.Y., Srivastava, G., et al. (2013). Genetic heterogeneity of diffuse large B-cell lymphoma. Proc Natl Acad Sci U S A 110, 1398-1403.

Zhang, J., Zhang, K., Jiang, X., and Zhang, J. (2014). S100A6 as a potential serum prognostic biomarker and therapeutic target in gastric cancer. Dig Dis Sci 59, 2136-2144.

Zintzaras, E., Voulgarelis, M., and Moutsopoulos, H.M. (2005). The risk of lymphoma development in autoimmune diseases: a meta-analysis. Arch Intern Med 165, 2337-2344.

https://clinicalgate.com/cells-and-cellular-activities-of-the-immune-system-lymphocytes-and-plasma-cells/.

https://assets.thermofisher.com/TFS.
Assets/LSG/manuals/Dyna_untouch_human_bcell_man.pdf.

https://www.cancerresearchuk.org/health-professional/cancer-statistics-for-the-uk.

http://www.cancerresearchuk.org/sites/default/files/cstream-node/inc_asr_gb_nhl_1.pdf. Accessed 21 Jun 2017.

https://www.thermofisher.com/antibody/primary/query/S100a4%20antibodies)